Microbial Stoichiometric Traits: A Toolbox for Understanding and Predicting Responses of Microbial Decomposers to Global Changes

Ziming Wang

Thèse

Présentée et soutenue publiquement pour l'obtention du titre de

DOCTEUR DE L'UNIVERSITÉ DE LORRAINE

Mention : « Écotoxicologie, Biodiversité, Écosystèmes »

par **Ziming WANG**

Les Traits Stœchiométriques Microbiens : des Outils pour Comprendre et Prédire les Réponses des Décomposeurs Microbiens aux Changements Globaux

----- ----- ----- ----- ----- ----- -----

Microbial Stoichiometric Traits: A Toolbox for Understanding and Predicting Responses of Microbial Decomposers to Global Changes

Soutenance publique le 13 juillet 2023

Rapporteurs (Reviewers):	
Andreas BRUDER	Senior Scientist, Institute of Microbiology – SUPSI, Bellinzona, Switzerland
Julie LELOUP	Assist. Prof., HDR, iEES – Sorbonne Université, Paris, France
Examinateurs (Examinators):	
Pascale BAUDA (Jury President)	Professor, LIEC – CNRS – Université de Lorraine, Metz, France
Isabel FERNANDES	Researcher, CBMA – University of Minho, Braga, Portugal
Membre invité (Invited member):	
Marc BUÉE	Research Director, IAM – INRAE, Nancy, France
Directeurs de thèse (Supervisors):	
Michaël DANGER	Assist. Prof., HDR, LIEC – CNRS – Université de Lorraine, Metz, France
Aurélie CÉBRON (co-director)	Research Director, LIEC – CNRS– Université de Lorraine, Nancy, France

Acknowledgements

I would like to thank the jury members Pascale BAUDA, Andreas BRUDER, Isabel FERNANDES, Julie LELOUP, and Marc BUÉE who have kindly accepted the invitation to evaluate my work.

First, I would like to express my sincere and deepest gratitude to my thesis supervisors Aurélie CÉBRON and Michael DANGER. I thank them for their patience and valuable advice through this scientific adventure. Their mentorship has been instrumental in the successful completion of this research project. I often tell people around me about how lucky I feel to have them as my mentors. Other than their scientific knowledge, their human skills outside of the thesis supervision, their daily support and encouragement – especially during the COVID period – are just as important in keeping me on track and motivated. Without whom this thesis would certainly be a bumpier and more challenging journey.

Je tiens également à remercier Pascale BAUDA, Éric CHAUVET, Damien BLAUDEZ, et Gwenaelle LASHERMES d'avoir accepté de faire partie de mon comité de suivi individuel de thèse. Je leur remercie pour non seulement leurs commentaires constructifs et leurs suggestions qui ont grandement amélioré mes travaux de thèse, mais également pour leurs encouragements et soutiens.

Merci une fois de plus, à Pascale, et Michael — mes anciens professeurs de Licence, et à Aurélie et Damien — mes anciens professeurs de Master. De même pour tous mes autres anciens prof. Christophe, Delphine, Élise, Élisabeth, Florence, Marie L. J., Martin, Patrick, Sandrine, Simon, Vincent F., et Vincent R. de m'avoir supporté (oui, oui, je dis bien supporter) depuis ces années d'étude, et qui n'ont pas encore eu marre de me revoir tous les jours (au moins je l'espère).

Je remercie également tous les membres et les anciens membres du LIEC pour leur amitié, leur soutien et leur collaboration, en particulier Bénédicte, Clément, Étienne, Géraldine, Hélène L.C., Jean-François P, Marie Z., Maximilien, Thierry, Valérie, Jérémy J., Philippe R., Philippe V., et Quentin, qui m'ont porté de mains fortes dans les sorties de terrain, les manips., les analyses diverses et variées, les équipements et les matériels pour mes travaux de recherche. Catherine D, Catherine P et Nacim, pour leurs gestions de tous mes papiers administratifs. Merci à Céline, Danielle, Fanny, Laetitia, Justine, Sophie, et toutes les autres personnes que je n'ai pas pu

nommer, pour les coucous dans les couloirs de labyrinthe Bridoux, les discussions plus ou moins sérieuses, avec qui le temps passé au LIEC est rempli de bonne ambiance.

Special thanks to my old office colleagues Cláudia, Miriam, and Vincent, for their vibes and laughter. Especially to the girls with whom we had shared many afternoon teatimes, during which we had all sorts of interesting and mind opening discussions about almost everything. To Vincent who was my go-to for all my questions related to R, and who have kindly passed me his books about the scientific vocabulary and how to write papers in English which have been a great help for all the writings.

I thank aussi the rest of mes camarades de thèse: Alienor, Clara, Elsa, Eva, Hélène, Jérémie, Ludovic, Manon, Rafael, Samantha, Sarah, et enfin, Nicolas, Nicolas et Nicolas (But how many are they? Nobody knows…) for all the moments we shared in and en dehors du labo. I wish you all the best lucks for your travaux de recherche. Sans oublier of course Nicolas L (et oui, quand il y en a plus, there's more…). Je sais pas te mettre dans quelle case… Un ancien collègue du bureau ? But you're still here. A peer PhD fellow? Mais t'as déjà fini ta thèse… Peu importe, avec toi, on est les 2 seuls qui sont là depuis nos stages de M2, et mtn tu vas y rester encore un peu plus longtemps, je te souhaite donc une bonne continuation dans tes recherches et des bonnes chances en générale.

(ceci est un exemple de ce qui se passe dans mon cerveau, every single day…)

Une thèse n'est pas comme un petit ruisseau paisible, elle ressemble plutôt à une grande rivière profonde est souvent turbulente. Nul ne parviendra à traverser seul cette rivière. Je suis reconnaissant envers toutes les personnes qui m'ont aidé à atteindre mes objectifs et qui ont rendu cette thèse possible. Enfin, je voudrais exprimer ma gratitude envers ma famille et mes amis les plus proches qui m'ont soutenu dans cette traversée :

Amal, Mickaël, Perrine, Yoann & Sarah,

Yang (刘杨千格) & Ludo et toute la famille HOERNER.

Leur encouragement, leur soutien pendent la période de rédaction et leur amour ont été essentiels pour moi.

List of Figures

List of Tables

Table of Contents

Foreword

This thesis is part of the project "Stoichiometric Traits of Microbial Species and Communities for Predicting Freshwater Ecosystem Responses to Global Changes – StoichioMic". StoichioMic is a project for young researcher of the French National Research Agency (Agence Nationale de la Recherche, ANR 18 CE32 0003 01), leading by Assistant Professor, Dr Michaël Danger. The project aims to improve the understanding of microbial ecology by providing experimental and theoretical evidence of microbial stoichiometric plasticity on plant litter decomposition and gather valuable information about the potential consequences of global changes on microbial communities and their implications in nutrient cycles in freshwater ecosystems. This thesis gathers a selected part of the results I obtained on this project.

State of the Art

1. The Importance of Freshwater

Although 2/3 of the Earth's surface is covered with water, freshwater lakes, rivers, and streams make up only a tiny part of it. Freshwater is without a doubt one of the most valuable natural resources on Earth. It provides us, among other things, clean drinking water and habitats that support wildlife. However, the ever-intensifying human activities relying on freshwater have largely threatened this fragile resource (Dudgeon *et al.* 2006). From its source to the estuary, a typical waterway runs through areas with different types of land use, collecting water as it goes. Substances deriving from agriculture (pesticides, fertilisers), industrial wastes, or urban sanitation are major causes of water pollution. Some of the main pollutants contain high concentrations of nitrogen (N), phosphorous (P), metallic elements, to name a few, which are known for causing eutrophication and intoxication of water ecosystems. Freshwater quality may also be affected more indirectly, for example, from water discharges in riparian vegetation and temperature fluctuations. Water quality reduction could have huge impacts on aquatic organism communities and trophic structures, resulting in a degradation in freshwater ecosystem functioning (e.g. Amoatey and Baawain 2019). Among all ecological processes, primary production and the decomposition of detritus are certainly the two most important ones driving ecosystem functioning (Lindeman 1942, Odum 1956). Any impairment of one of these processes may have huge consequences on freshwater ecosystems, and all services rendered by these ecosystems to humanity.

2. Plant Litter Decomposition in Freshwater

In ecological sciences, decomposition is defined as the biological process which transforms and reduces the biomass of dead organic matter (Gessner *et al.* 2010). This dead organic matter, often referred as detritus, is primarily of plant origin, and only for a minor proportion of animal

origin (Moore *et al.* 2004). Primary producers (autotroph organisms) are indeed responsible for synthesising the bulk of biomass on Earth. More than 80 % of Earth's total biomass are plants (Bar-On, Phillips and Milo 2018). As initially conceptualised by Charles S. Elton (1927) followed by Raymond Lindeman (1942), all life on earth depends on this primary production directly (i.e. herbivores, also known as primary consumers, as well as plant litter decomposers and detritivores) or indirectly (i.e. carnivores, also known as secondary consumers), thus putting primary production at the base of most food webs on Earth. Because of its fundamental position and according to the modest ecological efficiency of plant consumption, plant-origin biomass is only weakly transferred to higher trophic levels, resulting in a large amount of this biomass not being consumed and ending up in a reservoir of dead organic matter. Once in this reservoir, as one step of the biogeochemical cycles of elements, there can be three major ways by which the energy and elements stocked in the organic matter can be transferred to other ecological compartments. First, there are the chemical (and the fastest) way, fire: burning releases heat and reduce organic matter to mineral molecules (e.g. CO_2). The second one is the geological and the slowest way where, under suitable conditions, organic matter will be slowly turning into coal or petroleum. And finally, the one we are interested in for this thesis, the biological way where organic matter will be decomposed by microorganisms and invertebrates, releasing nutrients and energy back into environment and into trophic chains. Under the scope of this thesis, we will not talk about the decomposition of dead animal-origin materials but focusing only on the decomposition of dead vegetal materials (or plant litter here after).

Plant litter is mostly made of cellulose, hemicellulose, lignin, and a variety of phenolic compounds, simple sugars, amino acids, and fatty acids (Berg and McClaugherty 2020a). Plant litter decomposition is a complex process controlled simultaneously by 3 characteristics: plant litter inner traits (e.g. lignin, cellulose, and nutrient content: Enríquez *et al.*, 1993; García-Palacios *et al.*, 2016; Jabiol *et al.*, 2019), physical environmental conditions (e.g. temperature:

Fierer *et al.*, 2005; Geraldes *et al.*, 2012; pH: Hopkins *et al.*, 1990; additional carbon sources and nutrient enrichment: Ferreira *et al.*, 2015; Fontaine *et al.*, 2003; Schindler *et al.*, 2009) and abundance and diversity of biological agents (Gessner *et al.* 2010; Bani *et al.* 2018). In a larger sense, the process of decomposition envelops 3 distinct mechanisms: leaching of soluble organic compounds, mechanical fragmentation, and microbial decomposition (Swift, Heal and Anderson 1979; Webster and Benfield 1986). Soluble compounds in plant litter dissolved rapidly into water during leaching. Mechanical fragmentation includes litter size reduction by both environmental forces and invertebrates feeding on litter. Microorganisms colonise litter, secrete enzymes to chemically break down the organic compounds.

The decomposition of plant litter is a main pathway of energy flow in the biogeochemical cycles of elements, it is a ubiquitous process and central for ecosystem functioning. For example, in terrestrial environments such as forest soils, plant litter decomposition allows nutrients to be recycled and reused by primary producers as their building material. However, this dead organic matter is not evenly distributed on Earth. Plant litter is only produced in ecosystems where photosynthesis and primary production occur. But plant detritus can be transferred to other ecosystems, becoming a major nutrient and energy source for the functioning of some ecosystems where primary production is reduced. In particular, numerous continental freshwater ecosystems are concave ecosystems (*sensu* Leroux and Loreau 2008) and are considered as major collectors of dead organic matter arising from adjacent ecosystems. Due to their small size relative to the size of their watershed, small rivers and headwater streams are among these kinds of ecosystems, receiving large amounts of plant detritus from terrestrial origin (ecosystems often referred as *Detritus-Based Ecosystems* in the literature, see Danger 2020). In these freshwater ecosystems, plant litter can represent the main energy and nutrient source at the basis of their functioning. This is especially true for forested headwater streams, where the main carbon and nutrient inputs come from the plant litter originating from riparian

forest (Fisher and Likens 1973; Vannote *et al.* 1980). In such environment, the decomposition of plant litter is the central functional process. A yearly estimation of 2×10^{18} t of terrestrial originated carbon passes through stream ecosystems, and estimations suggested that in forested headwater streams, more than 90 % of energy originates from allochthonous detritus decomposition, primary production being highly reduced in these light limited ecosystems (Rosenfeld and Roff 1991).

3. Decomposers

Numerous microorganisms occupy a central place in ecosystem functioning because of their role in decomposition, especially since they can free nutrients bounded in dead organic matter. These microorganisms are a functional group of fungi and heterotrophic bacteria able to produce particular exoenzymes (enzymes that are secreted outside of cells) that are capable of breaking down organic compounds, for example cellulases, hemicellulases, and peroxidases; but also enzymes used for ensuring nutrient uptake, such as ureases, phosphatases, and peptidases. It is important to understand that, from the viewpoint of decomposers, they do not decompose organic matter to ensure a functional process (in the sense of a purpose, a duty, or a special activity), but as a necessity for their survival and development (organic matter serves as their carbon and energy source, as well as their growth habitat). This way of seeing saprophytic microorganisms as "decomposers" was attributed to them by scientists from a human standard, which helps us to understand more easily the inner functioning of ecosystems, but also led to numerous misunderstandings. In particular, the mineralisation (i.e. the net release of nutrients through the decomposition process) is far from being direct and mandatory, and decomposers activity does not necessarily end up with a net release of mineral elements in ecosystems (see section *5. Stoichiometric Requirements of Decomposers*, below). With that said,

the rest of this manuscript will continue to refer the decomposition as the functional process ensured by decomposers.

The term *decomposer* is loosely employed in some studies to refer to both *true* decomposers and detritivores (or "*shredders*"), as they both reduce and transform the mass of dead organic matter. For this reason, some other studies use the term *microbial decomposers* to describe the *true* decomposers *sensu stricto* (e.g. Duarte, Cássio, *et al.*, 2016; Tlili *et al.*, 2017). In this manuscript, a decomposer is considered as a microorganism who absorb dissolved nutrients originated from dead organic matter, thanks to external chemical and biological processes. On the other hand, a detritivore is an animal who ingests then assimilates organic matter in their gut through an internal digestion process. From this strict sense, decomposers are fungi and heterotrophic bacteria, and detritivores are, for example, earth worms, insects, and other macroinvertebrates.

Fungi are eukaryote organisms including yeasts and moulds, which can be found in different habitats. Fungal taxonomy has been constantly evolving and was historically based on their morphology or physiology during the different stages of their life cycle (Whittaker 1969). Most fungi can produce spores either sexually or asexually (called conidia), when the conditions are favourable, spores grow into the threadlike, branching, and filamentous structure called hypha. The hyphae grow towards their substrates, secrete digestive enzymes, and absorb nutrients. A collection of hyphae is called mycelium, and these filamentous fungi are called hyphomycetes. In recent decades, advancement in genetics and molecular biology have started filling the gap in genomics and helped with fungal taxonomic classification (Hibbett *et al.* 2007). The current classification contains 9 fungal lineages including Ascomycota – the largest fungal phylum with around 2/3 of all described species (Esser, McLaughlin and Spatafora 2015), and Basidiomycota – the second-largest phylum with over 30 000 described species (Hibbett *et al.* 2007; Zhao *et al.* 2017). Fungi are often referred as the main decomposer because they are

better known for their ability to decompose dead organic matter (Kjøller, Struwe and Kjoller 1982).

Aquatic hyphomycetes (AH) represent a polyphyletic group of fungi that are commonly found in streams, rivers, and lakes (Bärlocher 1992). They are known as Ingoldian fungi, named after British mycologist Dr Cecil Terence Ingold. AH are thus an ecological group based on their lifestyle and morphology of their conidia. These conidia are usually tetraradiate or sigmoid in shape (Figure.1) and are able to attach to surfaces such as particulate organic matter (POM, e.g. dead leaves, or wood pieces) in running water (Dang, Gessner and Chauvet 2007; Kearns and Bärlocher 2008). Studies suggest that this morphological similarity is rather the result of a convergence of evolution due to adaptation to an aquatic lifestyle (Bärlocher *et al.* 1992). With molecular tools, researchers have been able to identify more than 600 different species of AH with the majority of which belong to Ascomycetes (e.g. *Tetracladium* spp., *Anguillospora* spp., *Clavariopsis* spp.), some belong to Basidiomycetes, and some yet to be phylogenetically classified (Shearer *et al.* 2007). AH are considered as the major decomposers in stream ecosystems (Hieber and Gessner 2002). Their biomass productions and their sporulation rates correlate with litter decomposition rate (Gessner and Chauvet 1994; Niyogi *et al.* 2009). Together with bacteria,

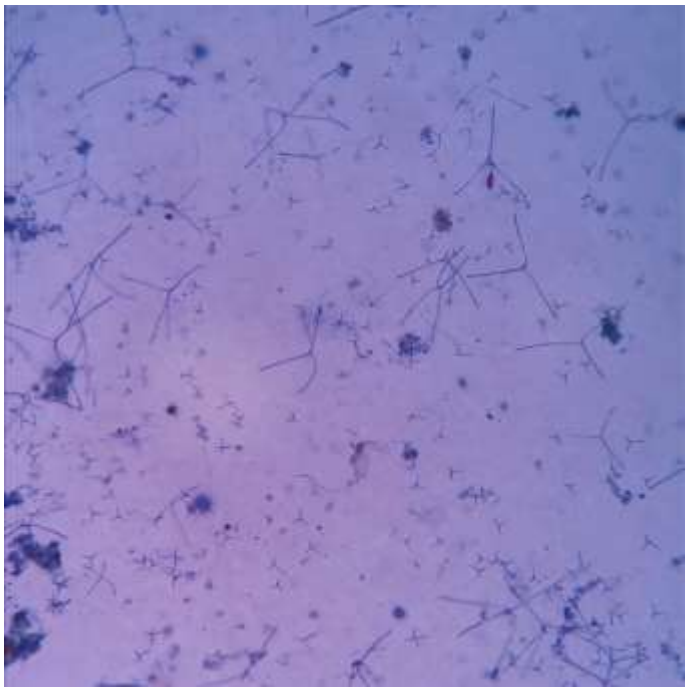

Figure 1. Conidia of aquatic hyphomycetes under optic microscope.

These conidia are naturally translucent in colour, the blue-violet shades are the result of colouration by blue Trypan. Size in picture is not to scale.

microbial biomass represents up to 99 % of total biomass associated with decomposing litter in streams (Baldy, Gessner and Chauvet 1995; Gulis and Suberkropp 2003a).

Bacteria are among the smallest and oldest unicellular organisms on earth, they are present in virtually all types of environments with various abundances (Flemming and Wuertz 2019), and have the second-largest estimated biomass on earth (Bar-On, Phillips and Milo 2018). Bacteria are abundant in freshwater ecosystems. They are able to directly assimilate dissolved organic matter (DOM) and break down simple organic compounds. Some of the main taxa involved in the litter decomposition process include *Actinobacteria*, *Bacteroidetes*, *Proteobacteria* and *Firmicutes*. Bacteria are shown to be actively involved in cellulose and hemicellulose decomposition (López-Mondéjar *et al.* 2016), under both aerobic and anaerobic conditions (Lynd *et al.* 2002; Kato *et al.* 2004). Bacteria are also believed to be the only cellulose decomposer in most anoxic environments (Leschine 1995). Although some bacteria possess ligninolytic enzymes (Crawford and Crawford 1980), lignin decomposition is often considered to be largely carried out by fungi (De Boer *et al.* 2005). In streams, due to water flows and bacteria relatively small size, planktonic bacteria prioritise utilisation of DOM, but highly diversified bacterial biofilm can also develop at the leaf litter surface (Besemer 2015). Plant litter decomposition is a dynamic process during which the bacteria would be active after fungal development, i.e. after the litter has been partially breakdown (Suberkropp and Klug 1976). Bacterial decomposer identification is rare and difficult in streams and did not receive as much attention as fungi, studies mostly rely on metabarcoding analyses from environmental samples since most bacteria are not cultivable in laboratory conditions (Pascoal *et al.* 2021).

Interactions between bacteria and AH in decomposition have been studied in the past decades and the results are conflicting (Gessner *et al.* 2010). Both fungi and bacteria have been shown to inhibit development of each other (Mille-Lindblom, Fischer and Tranvik 2006), alternately, bacteria were also shown to grow better with fungi (Romaní *et al.* 2006a), with faster metabolic

rate compared to fungi, bacteria can also take advantage of the more advanced fungal decomposition machinery, absorbing soluble compounds processed by fungal enzymes, and deprive fungi from its carbon and nutrient sources (De Boer *et al.* 2005). Bacteria may also detoxify molecules that may be toxic for fungal growth (Hendrickson 1991). One way to explain different fungi-bacteria ratio during organic matter decomposition is by looking into the stoichiometric requirements (often nitrogen and phosphorous) of both bacteria and AH (Gulis and Suberkropp 2003a). Enrichment of either N or P or both elements have been shown to affect litter decomposition (Ferreira *et al.* 2015b), but studies of nutrient enrichment did not necessarily look at which decomposer communities were involved, and directly comparing between studies are not feasible because of the differences in experimental setups.

4. Ecological Stoichiometry

Ecological stoichiometry is the study of the balance of chemical elements between different biotic and abiotic actors involved in trophic interactions (Sterner and Elser 2003a). By applying the law of conservation of matter, i.e. a chemical element can neither be created nor destroyed. Within a chain of biological interactions, elements which are present at the beginning of this chain can be traceable along the chain, which makes it predictable. Ecological stoichiometry enables us to study the effects and consequences of element flows on ecological processes and community structures. Schematically, an organism can be considered as a stock of chemical elements. To develop and ensure its biological functioning, an organism must therefore seek these chemical elements in a defined proportion. A limited supply of one or several elements could thus have a negative effect on the development of this organism. The elements most commonly studied in ecological stoichiometry are carbon (C), nitrogen (N) and phosphorus (P). These are the three major elements in the structure of biological molecules, C is the skeleton of all organic matter and carbon molecules, an energy source for heterotrophic organisms. N is

one of the main components of amino acids (building blocks for proteins) and P is a fundamental part of genetic materials (RNA and DNA) and energy molecule (ATP). The composition of these elements in the living organisms is usually expressed in terms of C:N:P ratios. For example, the Redfield ratio (C:N:P = 106:16:1) is an empirical ratio of marine phytoplankton (Redfield 1934).

Unlike a molecule in which the proportions of different elements are constant, the proportion of elements in an organism can vary, and the organism can regulate more or less its elemental composition according to the environmental availability of these elements (notion of homoeostasis at the organism level) and respecting the Liebig's law of minimum (the growth of an organism is limited only by the least available element in its environment, Odum 1959). Autotrophs are often considered as relatively non-homoeostatic, meaning their elemental ratios vary with that of their environment. Contrary to heterotrophs who present a more controlled homeostasis (Sterner and Elser 2003b). Nevertheless, at a community level, the strict application of the law of the minimum could be absurd since a community is most likely to adjust its global stoichiometry to that of the available resources through modification of the relative proportion of the species present. This adjustment ensures an optimal use of resources and often allows maximising biomass production. In other words, a community would rather have a less- or non-homoeostatic behaviour, whether for bacteria (Danger *et al.* 2008) or for fungi (Danger and Chauvet 2013).

In essence, differences in elemental compositions between resources and consumers can provide important information about how food quality and consumer requirements influence ecological processes (Hladyz *et al.* 2009). The composition and quality of resources in food webs vary considerably, while consumers often respect a more restricted homoeostasis than their resources (Sterner and Elser 2003a). Therefore, imbalances can arise when the elemental composition of the food resource does not meet the requirements of consumers. This has

implications in consumer growth, reproduction, and the efficiency of carbon assimilation, which in turn influences ecosystem processes, such as the decomposition of plant litter and element flows across trophic levels (Hladyz *et al.* 2009). The concept of ecological stoichiometry has been proven to be extremely useful in understanding a wide variety of processes and parts across the different levels of biological organisations. For many primary producers and metazoans, the elemental composition and its range of variation are relatively well studied, whereas for fungi and bacteria, the level and range of variation of their elemental compositions remains understudied (Danger, Gessner and Bärlocher 2016). Their ubiquitous presence and their essential role as decomposers underline the importance of studying their stoichiometry and characterising their elemental compositions and their elemental requirements.

The growth rate hypothesis is one of the principles of ecological stoichiometry. It states that the rapid development of an organism is positively correlated with its P demand (Elser *et al.* 2000, 2003; Isanta-Navarro *et al.* 2022). Therefore, organisms with a high growth rate should have low body N:P and C:P ratios. This is due to the fact that a rapid growth increases the production of proteins and thus generates a very high demand for RNA which is rich in P (Elser *et al.* 2000). The N:P ratio and the growth rate are thus linked by the allocation of P to ribosomes (rRNA) and the allocation of N to protein synthesis (Figure 2, Sterner and Elser 2003b; Hessen *et al.* 2007). Published studies either support or contradict this hypothesis (Sardans, Rivas-Ubach and Peñuelas 2012). One study about a bacterial strain have shown that the better competitor for P assimilation had faster growth rates but smaller size (Gounand *et al.* 2016). Another study focusing on five species of aquatic hyphomycetes at different stages of development have concluded that the relationship between growth and C:N:P ratios was not consistent. RNA and DNA concentrations, as well as RNA:DNA ratios were negatively correlated with culture age, but the concentration in RNA showed a positive linear correlation with growth rates (Grimmett *et al.* 2013). To explain this inconsistency, studies suggested that in fungi, the correlation

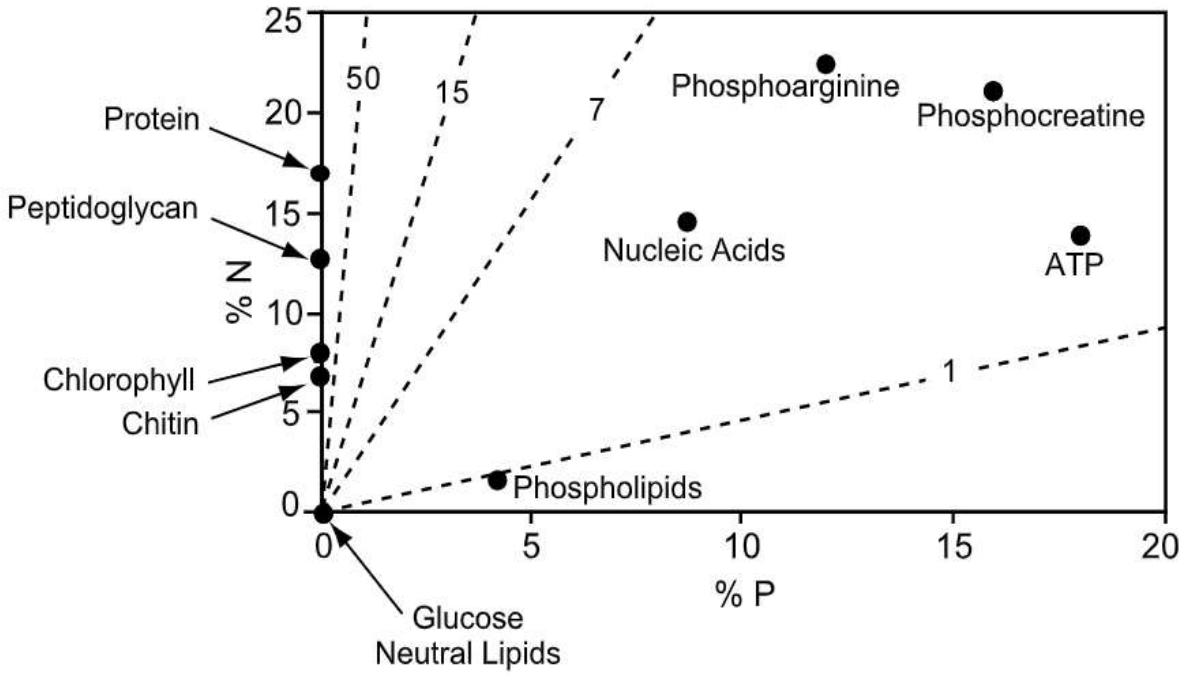

Figure 2. ***Biochemical stoichiometry.***

This diagram illustrates the % N and % P of important biomolecules. In most cases, estimates were made from the biochemical structure for each molecule. However, for proteins and phospholipids estimates were made by determining the average composition of the monomers (amino acids in the case of proteins) or of various types of the molecule (e.g. different kinds of phospholipid). (From Sterner and Elser 2003b)

between the amount of RNA and P content can be easily masked by P storage in fungal biomass when P was not limiting in the medium ("luxury consumption"). In addition, for filamentous fungi, growth takes place only at the tip of hyphae. These phenomena can lead to complexity in the strict application of the growth rate hypothesis in fungi (Grimmett *et al.* 2013; Danger, Gessner and Bärlocher 2016).

In freshwater ecosystems, N to P relative availability appears to be a factor that determines community structures (see review by Sardans, Rivas-Ubach and Peñuelas 2012). Low N:P ratios in the environment would favour organisms with a low body N:P ratio and a high growth rate. Conversely, higher N:P ratios would favour species with lower growth rates. Microbial decomposers have their own optimal ratios in these elements, i.e. ratios of elements which will maximise their growth, ensure their biological activity and their reproduction (Güsewell and Gessner 2009). The development of an individual is likely to be hampered by an imbalance

between the availability of elements and the demand for these elements (this imbalance is often referred to as “stoichiometric constraints”). Moreover, the N and P are most often the limiting elements in terrestrial and aquatic ecosystems (Elser *et al.* 2007), and particularly in headwater streams (Gibson *et al.* 2015).

5. Stoichiometric Requirements of Decomposers

Despite the fundamental importance of decomposition and the fact that this process has been studied for a long time, it remains difficult to predict the speed of microbial mineralisation of plant litter. This might be partly because decomposers also have to assimilate inorganic nutrient coming from their environment (i.e. water) to balance their stoichiometric requirements for their development (a process called “immobilisation”) before being able to break down organic compounds. It has indeed been shown that decomposers can assimilate dissolved organic carbon and inorganic nutrients from the water column to be able to start their development and decomposing activity (Cheever, Kratzer and Webster 2012; Cheever *et al.* 2013). When decomposers have enough nutrients to synthesis exoenzymes and break down plant litter, they will be ultimately able to release nutrients – most probably the less limiting ones for decomposer activity – back into their environment (the mineralisation process, Figure.3). Such imbalanced decomposition conditions might be especially common when decomposition takes place in oligotrophic and/or nutrient imbalanced environments and when either N or P is limiting decomposer activity. In such cases, nutrient enrichments have been shown as able to accelerate the decomposition process (Ferreira *et al.* 2015b).

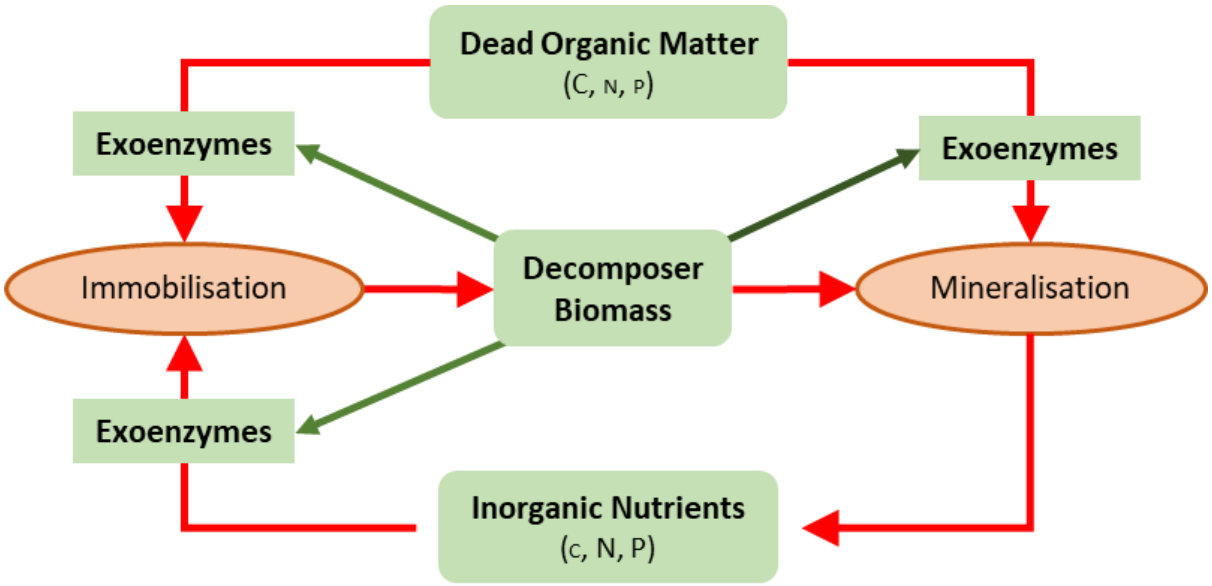

Figure 3. Schematic representation of nutrient immobilisation and mineralisation by decomposers.

Dead organic matter includes particulate organic matter (POM) and dissolved organic matter (DOM), it is the main carbon source and generally has high C:N and C:P ratios. Inorganic nutrients include dissolved nitrogen and phosphorus and are generally poor in carbon. Immobilisation of both organic matter and inorganic nutrients increases decomposer biomass and enables exoenzyme production. Exoenzymes catalyse nutrients immobilisation and mineralisation. Organic matter reduces in quantity as a result of microbial immobilisation and mineralisation.

Until now, most studies modelling nutrient cycling by decomposers have considered fixed values of microbial biomass elementary ratios for decomposers, whatever the environment and the type of microorganisms considered (Daufresne and Loreau 2001; Manzoni *et al.* 2021). However, we could expect that each species of decomposers, like all species, have their own optimal elemental ratio, i.e. ratios of elements that will maximise their growth, their reproduction, and/or their biological activity. In addition, it has been proven that many species involved in decomposition have fairly variable stoichiometric composition, providing them with a certain plasticity, i.e. each decomposer can develop in a more or less wide range of available nutrient ratios by varying its own elemental composition (Danger, Gessner and Bärlocher 2016). One study on terrestrial fungal stoichiometric ratios also found that individual strains showed high C:N and C:P flexibilities (Camenzind *et al.* 2021), as demonstrated for aquatic ones. Fungi can also store large amount of nutrients into their biomass, especially for P,

which result in highly variable stoichiometry (Danger and Chauvet 2013). For species assemblages and communities, one could expect a largely non-homoeostatic response of microbial biomass because the communities (at least bacterial) are likely to adjust their stoichiometry to that of their resources -at least partially – by adapting the diversity of species present, then altering the structure of the communities (Danger *et al.* 2008).

While the specific optimal elemental ratios have long been studied in plants (e.g. Tilman 1985, these ratios being key parameters of the "resource ratio theory") and more recently for animals (e.g. Frost *et al.* 2006; Ruiz *et al.* 2020), data are less available for microorganisms. Despite the possible nutrient stoichiometry flexibility for a decomposer community, nutrient ratios that maximise microbial activities and growth have already been shown. Using natural microbial inoculum, Güsewell and Gessner(2009) shown that cellulose and plant litter decomposition were maximised at N:P ratios ranged from 1.7 to 45, these ratios correspond to optimal N:P ratios for the decomposition process at the community level. Changes in the available N:P ratios also resulted in altered dominance between microbial decomposers. From a stoichiometric viewpoint, such changes in community structure could result from competitive exclusion and the selection of species based on their optimal nutrient requirements along the N:P availability gradient (Danger *et al.* 2008). Thus, based on microbial nutrient requirements, the relative N to P availability should, at least partly, determine community structure and microbial elemental composition but still need to be tested. Concerning the decomposition process, these species replacements are expected to maximise nutrient uptake and reduce variations in litter decomposition efficiency (Fanin *et al.* 2013). Further research is needed to better characterise the optimal elemental ratios of microbial decomposers and to understand the factors that influence these requirements and how they may be impacted by environmental changes such as nutrient pollution and climate change.

6. Litter Decomposition Facing Global Changes

With the development of human society, the intensification of human activities puts great pressure on Earth. As a fundamental component of the global environment, freshwater ecosystem is largely affected by global changes (Dudgeon *et al.* 2006). Factors such as changes in riparian land use type (e.g. urbanisation, conversion to monoculture), modifications of water channels (e.g. barriers, channels, and bank hardening with concrete), wastewater inputs, droughts, and floods, to name a few, can certainly cause disturbance on litter decomposition processes (Groffman *et al.* 2002, 2003; Nedeau, Merritt and Kaufman 2003; Hardison *et al.* 2009).

Giving the certain importance of microbial optimal nutrient ratios for the decomposition process and community structures, understanding the response of these optimal ratios to environmental stressors is of particular interest. If multiple environmental stressors impact microbial diversity, plant litter decomposition may be affected (Niyogi *et al.* 2009; Gessner *et al.* 2010; Ferreira *et al.* 2015a; Tolkkinen *et al.* 2015). Both nutrient availability (Falkowski *et al.* 2000) and ratios (Elser *et al.* 2009; Peñuelas *et al.* 2013) can be problematic for ecosystem functioning due to changes in nutrient balance. As introduced earlier, nutrient availability and balance in the decomposition resources and in the immediate environment of the microorganisms is essential for maintaining microbial diversity and intensity of microbial activities. Other global changes such as temperature increase and the presence of pollutants could alter microbial metabolic activities and therefore influence decomposition (Clarke and Fraser, 2004, Duarte *et al.* 2008, Gilbert *et al.* 2014, Cross *et al.* 2015, Jabiol *et al.* 2019). Although temperature is an environmental factor largely influencing the rate of organic matter decomposition, litter quality is also known to affect early-stage litter decomposition (Berg and McClaugherty 2020b), and in some conditions this parameter would even be more important than the effect of increasing temperature (Pérez *et al.* 2021; Monroy *et al.* 2022). Chemical stressors can cause a decrease

in microbial diversity and in turn reduce the intensity of litter decomposition (Beaumelle, De Laender and Eisenhauer 2020). Metal contamination is one of the major recurrent stressors potentially acting on plant litter decomposition. Metals have long been shown to reduce plant litter decomposition rates in lands (Berg *et al.* 1991) and in streams (Duarte *et al.* 2008). The number of litter-colonising fungal taxa decreases in presence of high metal concentrations (Solé *et al.* 2008). Microbial activity is lower in metal polluted environments (Niyogi *et al.* 2009). Among all metals, copper (Cu) and zinc (Zn), two essential elements for living organisms, become classical metallic contaminants in ecosystems impacted by human activities, these metals being often found in large quantities in both terrestrial and aquatic ecosystems. In particular, copper is still actively used in agriculture, even in organic contexts, resulting in its accumulation in soils and leaching into surface water ecosystems. Cu has been largely studied and is known to alter microbial community structures (Wakelin *et al.* 2010; Keiblinger *et al.* 2018) and affect litter decomposition (Pu *et al.* 2014; Fernández *et al.* 2015).

Freshwater ecosystems hold an essential position in global biogeochemical cycling of carbon and nutrients and plant litter decomposition makes up an important link in nutrient cycles and community structures. Assessing the decomposition process can give us valuable information in ecosystem functioning and health, since monitoring plant litter decomposition rates can be a useful tool to understand the potential impact of human activities on stream ecosystems (Gessner and Chauvet 2002). Understanding how all these stressors affect microbial optimal ratios might thus be an important step towards the prediction of the consequences of human-induced global changes on ecosystem functioning.

7. Objectives of the Thesis

This thesis focused on aquatic hyphomycetes and bacteria from freshwater ecosystems and their roles as plant litter decomposers. Attempting to develop a stoichiometric trait-based approach

to study the reactions of microorganisms facing global changes such as nutrient imbalances and other environmental stressors, our main objectives were the following (Figure.4):

- Characterise the elemental plasticity of decomposers from individual aquatic hyphomycetes strains to complex microbial communities (both bacteria and AH).
- Highlight the consequences of different stoichiometric requirements of decomposers on nutrient immobilisation and mineralisation dynamics.
- Identify the impact of selected parameters of global changes (copper pollution and temperature variations) on the plasticity of decomposers and their ecological consequences.

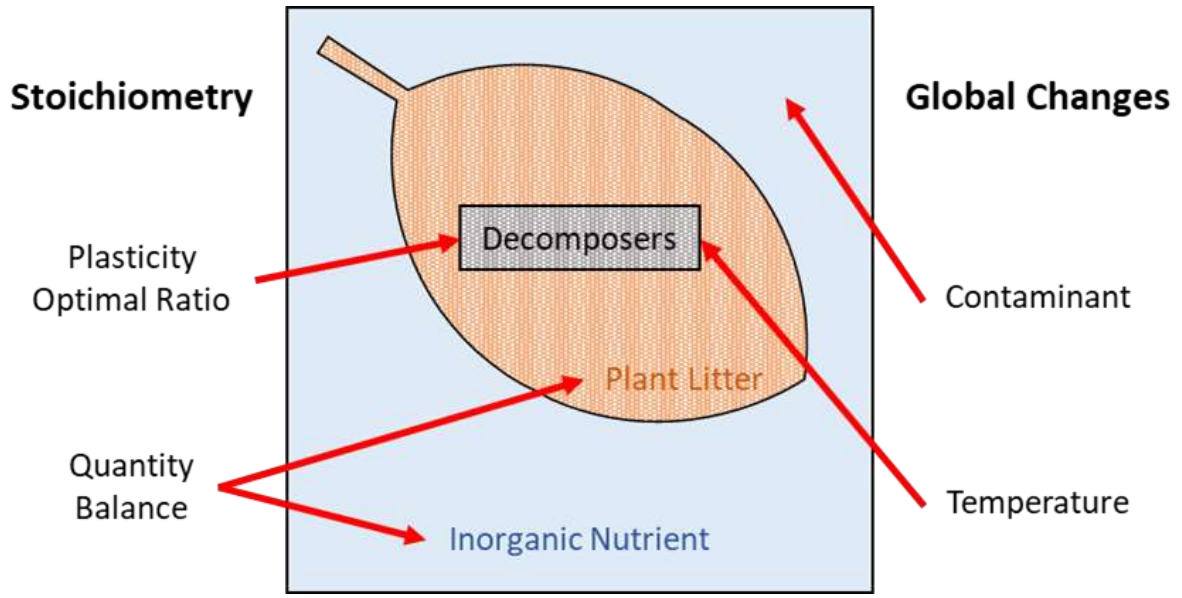

Figure 4. Visual representation of the objectives of the thesis.
Red arrows indicate the thesis main focuses.

Hypotheses were proposed around these objectives:

(1) Each species (strain) of decomposer has an optimal N:P ratio, which would make it possible to predict the structure of the community of decomposers at a given environmental N:P ratio. [H1]

(2) Above and below the optimal N:P ratio value, the microbial community in question will be limited by a single element, microbial activities (such as growth and decomposition) will be slowed, and there will be an accumulation of the element non-limiting in the microbial biomass and/or in the medium. [H2]

(3) Through a reduction in microbial diversity, the presence of a contaminant would alter the elemental plasticity of the community, leading to narrower ranges of N and P co-limitations of microbial processes and reduced nutrient immobilisation [H3]

(4) A rise in temperature would accelerate microbial growth rate, and therefore decrease the N:P ratio that optimises decomposition. [H4]

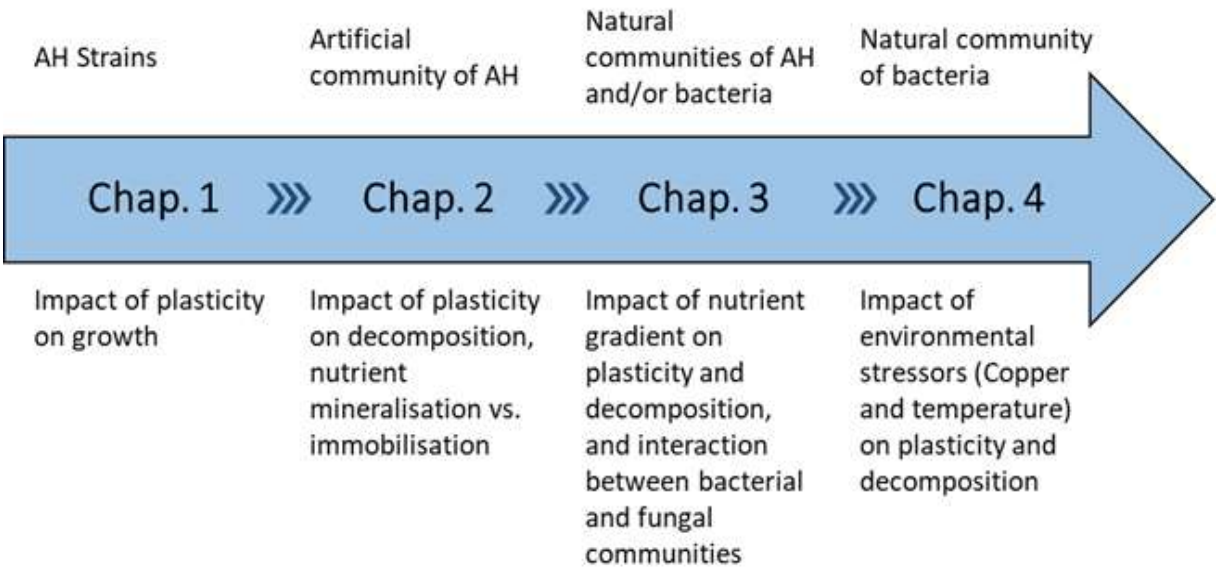

Figure 5. Organisation of the chapters in this thesis.

This manuscript will continue with firstly, a dedicated part of general methodologies and techniques applied for the different experiments. Then 4 chapters will be proposed, investigating the different hypotheses described above with increasing complexity of studied decomposer communities (Figure.5). In chapter I, we will characterise the stoichiometric trait and plasticity of four AH strains, focusing on variations depending on mycelium age, species, and the potential impacts of this plasticity on their growth. Chapter II will be focusing on

nutrient immobilisation and mineralisation during alder leaf decomposition on a range of several N:P ratios by an artificial AH community with only five strains. In chapter III, we will increase the complexity of decomposers by having both bacterial and fungal communities. We will investigate their cellulose decomposition capacity under 2 different nutrient gradients and compare differences between communities involved. Finally, in chapter IV, we will examine the effect of environmental stressors and nutrient balance on decomposition, questioning whether other stressors would cause similar effects and how decomposers evolution/adaptation may play a role in long-term.

Methodology

1. AH Collection, Isolation, and Identification

The main sampling areas for microorganisms were the La Maix Stream (latitude 48° 29'2.56″ N, longitude 7° 4'10.75″ E), an unpolluted second-order forested stream located in the Vosges Mountains (north-east France) and its neighbouring forest for leaf litter collection. AH strains were isolated from spores, using two methods – foam samples and leaf litter induction. These methods were described by Descals (2020) and were adapted by us accordingly.

Late winter and early spring are the high time for AH germination and sporulation. Thanks to snow melting, increased water volume, high flow velocity and turbulent conditions generate foam which traps AH spores. Foam sampling is a direct method which primarily allowed us to isolate individual strains of AH from its spores. We used 5 cm² fine nylon mesh (0.25 mm) to catch foam formed in the stream and transfer the foam into a fresh MAA plate (Malt Agar Antibiotic with 20 g L^{-1} of agar, 1 g L^{-1} of malt extract, 0.15 g L^{-1} of streptomycin sulphate, and 0.09 g L^{-1} of ampicillin sodium salt) then seal the plate with parafilm. We made sure to only open the plate rapidly to collect foam and close it right after to reduce chance of contamination. Plates were kept in a cooler during the field trip and transported back to the lab and kept at 15 °C. Foam containing plates were processed under 48 hours for easier identification, isolation, and transplantation of spores. Failed to do so would make it hard to morphologically identify spores as mycelium growth would mask their shapes.

The isolation of spores was done as soon as possible after sample collection. Under sterilised condition, MAA plate surface was gently washed with sterile water to remove excess liquid and particulate residue. Using a sterilised scalpel, a piece of 1 cm^2 of inseminated agar was cut and put onto an England Finder slide (Figure.6), then mounted under a microscope. Using 10× objective, spores were identified (based on their shape, using the key of Gulis *et al.* (2020) and those of Chauvet (1990)) and located on the slide to be isolated by their coordinate on the

England Finder. The slide was then transferred under a stereo microscope, where the spore was cut out carefully from the agar and deposited on a fresh MA plate (Malt Agar with 20 g L^{-1} of agar and 10 g L^{-1} of malt extract, without antibiotics). Plates with individual spores were then incubated at obscurity at 15 °C.

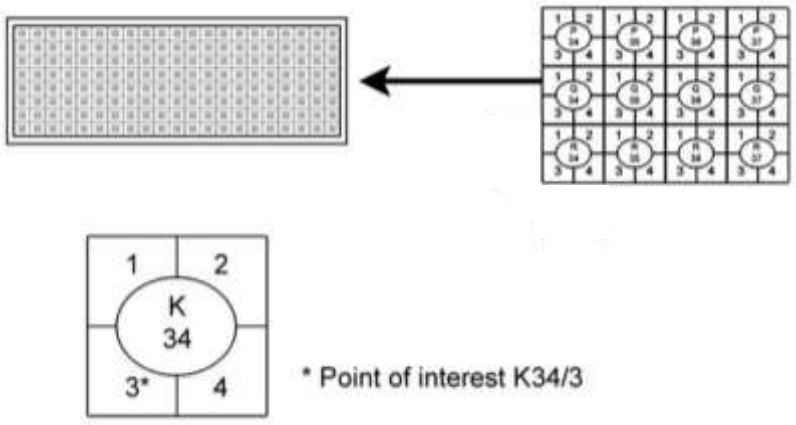

Figure 6. England Finder slide.

A glass slide with its surface divided into sections of 1 × 1 mm. Each section is subdivided into 4 smaller squares and each square can be identified with a unique code.

Leaf litter sampling was primarily used as a method to generate natural communities of AH (and bacteria depending on the experiment). Leaves were collected during autumn. Using nets suspended between trees (mixture of hazel *Corylus avellana*, alder *Alnus glutinosa*, and hornbeam *Carpinus betulus*) at about 1 m above ground (to avoid any contact between leaf litters and soil). After 1 to 2 weeks, leaves collected on nets were brought back to the lab, air dried then stored in plastic boxes. Prior to the launch of experiments, several leaf litter bags were prepared by putting a hand full (about 5 g) of dry leaves into nylon mesh (500 µm) bags and immerged in La Maix stream water. The fine mesh bags allow mostly AH and bacteria to enter the bags and colonise the leaves, excluding most invertebrates. The bags were then retrieved from the water after 2 to 4 weeks, along with some stream water. Back to the lab, partially decomposed leaves were gathered in a shallow basin and rinsed with distilled water to remove any dirt or other residues. To induce fungal spores and bacteria development, pieces of rinsed leaves were put into an Erlenmeyer flask, with either stream water or distilled water. We made sure not to stuff too many leaf pieces in the flask to ensure they were fully submerged and were able to flow freely in water without risking anoxia. The water volume was kept at a

maximum of 30 % of the flasks capacity to allow enough water-air interface for gas exchange. Flasks were gently agitated and kept at 15 °C for 48 h to 72 h. Fungal spores produced by AH growing on leaf litter as well as bacteria then accumulate in the water. Droplets of this suspension can then be spread on a MAA plate to proceed with the AH spore isolation step (as presented above), or the suspension can be used directly as a complex microbial inoculum (including both fungal conidia and bacteria) for experiments. The suspension can also be filtered with a glass fibre GF/C filter (1.2 µm cut off, Whatman) to get an inoculum with only bacteria.

For strain verification, we first induced spore production from isolated pure fungal colonies. Small pieces (25 mm^2) of agar with mycelium from the edge of growing colonies were cut from culture plates and put into 25 ml sterilised distilled water, in Erlenmeyer flasks. Flasks were incubated with gentle agitation at 15 °C to induce spore production. Typically, spores will be produced under 72 hours and can be visually verified by holding and gently shaking the flask against a bright background. They can appear as salt-crystal-like particles in suspension or congregated on the water surface forming a thin whitish layer. A certain volume (depending on the density, can also be diluted with water) of spore suspensions were then stained with several drops of Trypan blue (0.05 %, in 60 % lactic acid) before being filtered through nitrocellulose filters (Millipore MF™ 5.0 µm SMWP02500). Filters were then mounted on slides and observed under an optic microscope. The identification of strains was based on spore morphology, performed by referencing to the identification keys of Chauvet (1990) and (Gulis, Marvanová and Descals 2020).

For some strains of interest, this morphological identification was completed by sequencing of ITS region to determine their taxonomic affiliation. For this, REDExtract-N-Amp™ Plant PCR Kit protocol (Sigma Aldrich) was applied for each strain's DNA extraction individually from pieces of mycelium on malt-agar plate (25 mm^2) and PCR amplification using universal ITS1-

ITS4 primers (covering ITS1, 5.8S and ITS2). The amplification mix was prepared in 25 µl with: 0.5 µl of Dimethyl sulfoxide (DMSO); 0.25 µl of 0.3 % bovine serum albumin (BSA); 12.5 µl of REDExtract-N-Amp PCR ReadyMix; 0.6 µl of each primer (10 mM); 9.55 µl of DNA-free distilled water and 1 µl of template DNA (or distilled water for negative control). 35 cycles of amplification at 54 °C (annealing temperature) were performed. These PCR products were then sent to Eurofins Genomics for Sanger sequencing. Sequences obtained have been confirmed with BlastN (NCBI) for their taxonomic affiliation.

Specific PCR primers (ITS region) and TaqMan® probes (Eurofins Genomics) were then designed based on Baudy *et al.* (2019) with adaptations to our strains (see chapter 2). TaqMan® probes contain the fluorescent reporter dye 6-carboxyfluorescein (6-FAM) on the 5' end and the non-fluorescent quencher (MGBNFQ) on the 3' end. Primers and probes were tested for their specificity on each strain in a crossover manner for strain specific real-time quantitative PCR (qPCR). Total DNA was then extracted from samples of decomposing leaf litter using DNeasy PowerSoil Kit (Qiagen) and following the manufacturer's protocol. qPCR reactions were prepared in 20 µl volume consisted of 10 µl iTaq Universal Probe Supermix (BioRad), 2 µl of each primer (940nM final concentration), 0.5 µl of probe (260 nM final concentration), 0.4 µl of 3 % BSA, 0.2 µl of DMSO, 0.08 µl of T4gp32 (MP Biomedicals), 3.82 µl of sterile MilliQ water and 1 µl of template DNA, ten-time dilutions (from 10^8 to 10^2 copies μl^{-1}) of standard plasmids prepared as described in Cébron *et al.* (2008), or sterile DNA-free water for negative control. The qPCR assays were performed using CFX96 apparatus (BioRad) running a 2-step amplification protocol (50 cycles with denaturation for 30 s at 95 °C and hybridisation, extension, and fluorescence acquisition for 30 s at 60 °C).

2. Maintenance of AH Strains in Laboratory

The laboratory has a collection of 80 strains of AH isolated from French streams in which 50 strains were isolated by me at the beginning of this thesis. Plus 20 extra strains donated by colleagues from Portugal. In total, we have 20 identified species which are commonly found in west Europe. Strains are maintained in active growth at 15 °C, on MA plate with 20 g L^{-1} of agar and 10 g L^{-1} of malt extract. Each culture is transplanted into a fresh plate every 6 months. The transplantation is done inside a microbiology safety cabinet. A piece of 1 cm^2 mycelium is cut with a sterilise scalpel from the old plate and deposited in the centre of a new MA plate. Plates are then sealed with parafilm and put back at 15 °C.

3. Description of Some AH Strains

Here after is a brief description of the 5 AH strains used in various experiments for this thesis. These strains are among the most common strains that can be found in Europe, but also simply because in all of our AH collection in the lab, they were the most active in terms of growth and sporulation.

- *Articulospora tetracladia* Ingold (later named ARTE)

Synonym: *Hymenoscyphus tetracladius* Abdullah, Descals & J.Webster

Classification: Ascomycota (p.), Leotiomycetes (c.), Helotiales (o.), Discinellaceae (f.)

Description: Hyphae translucent, septate, and ramified. Conidia translucent, size 55–110 µm, with 4 or 5 septate branches of about 3 µm wide.

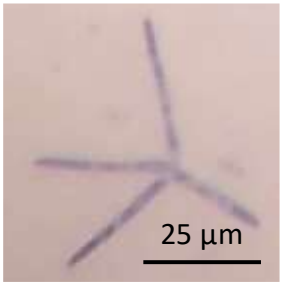

Reference: Ingold. In: Trans. Br. mycol. Soc. 25(4): 376 (1942)

- *Clavariopsis aquatica* De Wild (later named CLAQ)

Classification: Ascomycota (p.), Dothideomycetes (d.), Pleosporales (o.)

Description: Hyphae translucent, septate, and ramified. Conidia translucent, 50–200 µm long, 4 µm wide. Organised with 2 cells in the central axis with tapering toward the base and 3 thin arms symmetrically divergent.

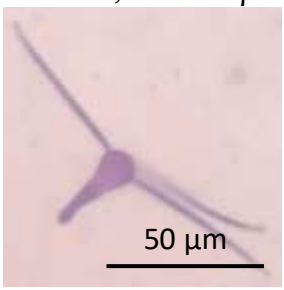

Reference: De Wild. In: Ann. Soc. Belge Microscop. 19:201 (1895)

- *Heliscus lugdunensis* Sacc. & Therry (HULU)

Synonym: *Neonectria lugdunensis* (Sacc. & Therry) L.Lombard & Crous

Classification: Ascomycota (p.), Sordariomycetes (c.), Hypocreales (o.), Nectriaceae (f.)

Description: Hyphae septate, ramified, translucent (young) and pale brown (old). Conidia 28–40 µm long, 4–5 µm wide. Organised in elongated ellipsoidal with 2–3 cells, sometimes with 3 small symmetrical apical bulges.

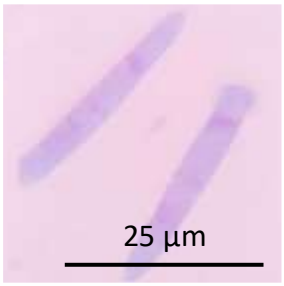

Reference: Sacc. & Therry. In: in Saccardo, Michelia 2(no. 6): 132 (1880)

Note: The name for this species currently recognised by the scientific community is *N. lugdunensis*, but throughout this thesis, this species.is still referred to as *H. lugdunensis*.

- *Tetracladium marchalianum* De Wild. (TEMA)

Synonym: *Tetrachaetum marchalianum* (De Wild.) Anon.

Classification: Ascomycota (p.), Leotiomycetes (c.), Rhytismatales (o.), Calloriaceae (f.)

Description: Hyphae septate and ramified. Conidia tetrahedral with 4 pointy arms of 20–40 µm long and 2–3 µm wide. Two smaller rod-like or spherical shaped bulges with one of them directly over the divergence point of the arms and the other not far from it on one of the arms.

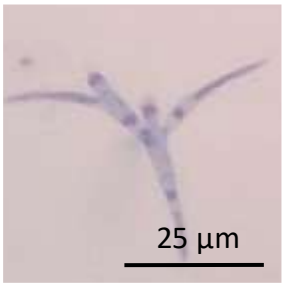

Reference: De Wild. In: Ann. Soc. Belge Microscop. 17:39 (1893)

- *Tricladium splendens* Ingold (TRSP)

Classification: Ascomycota (p.), Leotiomycetes (c.), Helotiales (o.), Solenopeziaceae (f.)

Description: Hyphae translucent, septate, and ramified. Conidia spindle-shaped septate 3–6 times, 60–120 µm long, 6–7 µm wide at the widest part. Two lateral arms 30–80 µm long, 6–7 µm wide at the widest part, tapering toward their apex, 2 µm wide at the junction with the main axis; the two arms separated by 10–20 µm on the main axis.

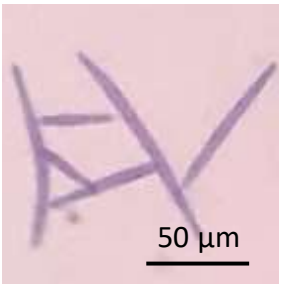

Reference: Ingold. In: Trans. Br. mycol. Soc. 25(4): 389 (1942)

4. Choice of N:P Gradient

N:P ratio is the main environmental variable manipulated in this thesis. We have used 2 types of N:P gradients (Figure.7): one with keeping either N or P at a constant quantity while varying the other element along a gradient, the other maintaining a global N and P quantity while varying simultaneously the individual quantity of both elements (as in Güsewell and Gessner 2009). More precisely:

- The first way to obtain an N:P gradient is by keeping a constant quantity of one element while varying the other. This method of setting up N:P ratios is the most straightforward

and the most used way in the literature to play with N and P quantities. By keeping one element in an intermediate quantity (relatively speaking), varying the other to form a gradient (Figure.7a 7b). The varying element would hopefully be the limited element at lower quantities and becomes excess at higher quantities. (Applied for chapter II and chapter III)

- As proposed by Güsewell and Gessner (2009), an N:P gradient can be obtained while maintaining constant a global quantity of nutrients by keeping constant the geometric mean of N and P inputs (Figure.7c). For example, a global quantity of 0.5 mg means $\sqrt{m_N \times m_P} = 0.5$, and by varying both m_N and m_P (mass in mg) we get a gradient of N:P ratios. The advantages of using geometric mean to define a series of N:P ratios are to give the smaller mass the same impact as the bigger one as opposite in maintaining a same arithmetic mean (average of the sum) in which the smaller value would be masked by the bigger one. (Applied for chapter IV)

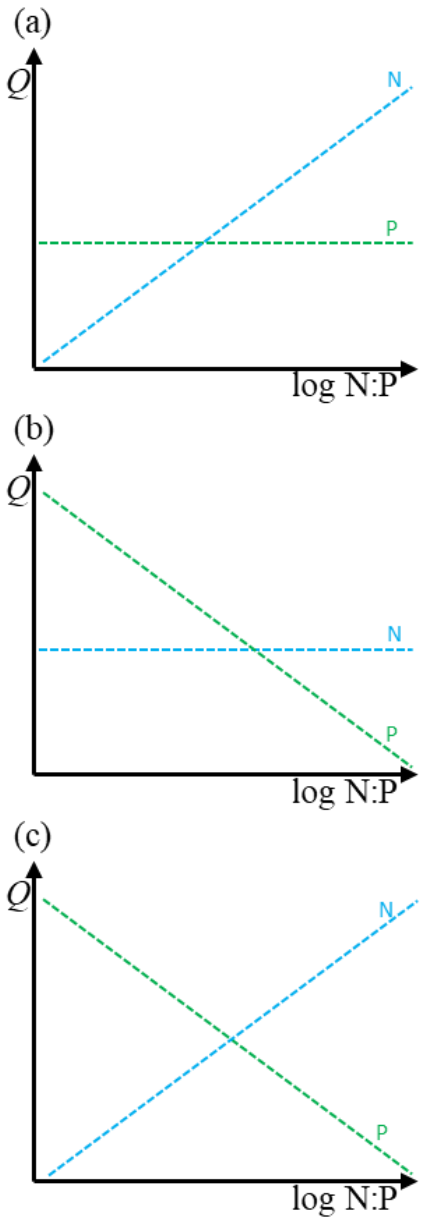

Figure 7. Representation of N:P gradients used in this thesis.

Q: quantity. **(a)** P-constant; **(b)** N-constant; **(c)** Global quantity of N and P constant.

Both gradients are totally different and impacts of these gradients on microbial decomposers and their activity are expected to vary much between these two different types of gradients. These differences will be discussed further in the different chapters presented in this thesis.

5. Culture Setups

5.1. Agar plates with cellophane membrane (in chapter I)

We first targeted a setup allowing us to grow pure fungal culture on a solid substrate with precisely controlled N and P quantities and being able to recover fungal biomass without agarose. To do so, we used 90 mm sterile plastic Petri dishes filled with a modified version of GMS (Glucose Mineral Solution, Gessner & Chauvet 1993) as the culture medium. The medium contains $Al(SO_4)_3 \cdot 18H_2O$ - 0.1 mg L^{-1}, KI – 0.1 mg L^{-1}, $CoCl_2 \cdot 6H_2O$ – 0.04 mg L^{-1}, $NiCl_2 \cdot 6H_2O$ – 0.25 mg L^{-1}, $FeCl_3$ – 2 mg L^{-1}, $MnSO_4 \cdot H_2O$ – 1 mg L^{-1}, H_3BO_3 – 1 mg L^{-1}, $ZnSO_4 \cdot 7H_2O$ – 1 mg L^{-1}, $Na_2MoO_4 \cdot 2H_2O$ – 0.1 mg L^{-1}, $MgSO_4 \cdot 7H_2O$ – 500 mg L^{-1}, $CaCl_2 \cdot 2H_2O$ – 150 mg L^{-1}, agarose – 20 g L^{-1}, and glucose – 5 g L^{-1}. N and P were added in various quantities to obtain diverse N:P ratios. Once the agar media was solidified, a cellophane membrane (regenerated cellulose) was placed on its surface. The membrane acts as a physical barrier, while allowing nutrient transfer to fungal biomass, it keeps fungal colonies separated from the culture media to facilitate later mycelium sample collection instead of what is traditionally done by melting the agar for extraction (which could alter microbial elemental composition). Another advantage is to allow us to collect mycelium of different ages depending on the position of the mycelium on the plate (the external edge of mycelium representing the youngest part of the fungi) and subsequently enable us to investigate the potential relationship between mycelium age and its nutrient content. However, since the membrane is made of cellulose, it can also be decomposed but at a slower rate than the colony growth rate. Incubation

time must thus be carefully controlled since fungi can eventually penetrate the membrane and starts developing inside the agar media.

5.2. Microcosm with cellulose discs (in chapter III and IV)

The microcosms were prepared in 90 mm Petri dishes, using a protocol adapted from Güsewell and Gessner (2009). Each Petri dish contains 50 g to 60 g of river sand or gravel and covered by a nylon mesh with 250 µm porosity. The sand or gravel is sieved (< 2 mm) to homogenise grains size, washed with tap water, and burned at 450 °C for four hours to sterilise and remove all traces of organic material. Cellulose discs (Whatman ashless) are then sterilised by autoclaving at 120 °C while wrapped in aluminium. Then cellulose discs are placed on top of the nylon mesh, this one avoiding the sand particles to stick on the cellulose discs and bias cellulose mass loss estimations. The number and the size of discs varied depending on the experiment, but it could cover almost all the surface of the plate if necessary. The cellulose is almost totally devoid of nutrients, and it represents a simplified form of leaf litter and the unique carbon source in the microcosms. Each microcosm was then filled with a sterilised mineral solution based on a modified version of COMBO mineral medium. The solution contains 36.8 mg L^{-1} $CaCl_2 \cdot 2H_2O$, 37.0 mg L^{-1} $MgSO_4 \cdot 7H_2O$, 12.6 mg L^{-1} $NaHCO_3$, 28.4 mg L^{-1} $Na_2SiO_3 \cdot 9H_2O$ and 24.0 mg L^{-1} H_3BO_3 (Kilham *et al.* 1998). N and P were added with different concentrations to create the desired N:P gradients.

5.3. Erlenmeyer flasks with alder leaf discs (in chapter II)

In this setup, we simply put discs of alder leaves in flasks with the COMBO mineral solution as described previously. Alder (*Alnus glutinosa*) leaves were collected during abscission in the Vosges mountains. They were air dried at room temperature and stored prior to use. For the experiment, leaves were moisturised with distilled water, then cut into discs (12 mm Ø) with a cork borer. Central veins sere avoided while cutting, and secondary veins were limited to one

(or two for smaller leaves) for each disc. The discs were then air dried and weighted to the nearest 0.1 mg for their initial dry weight. They were then sterilised by autoclave at 120 °C for 30 min while submerged in distilled water and then rinsed twice with sterilised water.

To ensure all discs were colonised equally for the experiment, they were incubated with the desired microbial inoculum prior to the main experiment. The colonisation took place in the COMBO mineral solution without N or P. The colonisation period lasted for 8 days, with agitation at 12 °C.

At the launch of experiments, a predefined number of discs were dispatched into sterilised 100 ml capacity Erlenmeyer flasks with 30 ml to 40 ml of fresh COMBO solution with predefined N and P concentrations. Flasks were covered with aluminium foil and incubated in the dark under agitation at 15 °C for the duration of the experiment.

6. Methods of Analyses

6.1. Mass loss measurement (in chapter II, III, and IV)

In the experiments where we measured decomposition rates, one type of solid carbon substrate was used as the only source of carbon. These substrates were either pure cellulose discs (as a simplified analogue of tree leaves) or alder leaf discs. Before starting each experiment, a set of discs were dried at 65 °C for two days, then weighted to the nearest 0.1 mg to determine the average starting dry mass per disc.

After the experiments, partially decomposed discs were collected with care to make sure they were retrieved in totality. Samples were kept frozen at – 80 °C before being freeze-dried. Each sample was then weighted to the nearest 0.1 mg to determine the final dry mass. The eventual mass lost from the discs through leaching in the control group was deduced to calculate the

mass loss of discs for each experimental setup. After being weighted, each disc can then be used for ergosterol analysis, or total N and P quantification.

6.2. Ergosterol extraction and quantification with HPLC (in chapter II and IV)

To avoid using a single conversion factor (5.5 mg of ergosterol per g of fungal biomass) from the literature (Gessner and Chauvet 1993; Brosed, Jabiol and Gessner 2017) and increase the accuracy of mycelium biomass estimations in our study, we choose to measure species specific conversion factors for each of AH used in our experiments. The method used for extraction and quantification of ergosterol content in samples was based and adapted from the description by Gessner (2020). Samples, whether they were cellulose discs, leaf discs or pure mycelium, were freeze-dried and weighed before extraction. The weighing step is crucial for later calculation of concentration. The extraction was carried out by series of 12 with 11 samples and 1 positive control (ergosterol, ACROS Organics, 98 %; in methanol, Chromasolv, for HPLC, ≤ 99.9 %. Sigma-Aldrich; at 200 µg ml^{-1}). The sample (or 100 µl of positive control) was placed into a glass tube with airtight screw cap, before adding 5 ml of KOH/methanol (8 g L^{-1}) solution and keeping it at 4 °C overnight. The next day, sample-containing-tubes were heated at 80 °C in a water bath under agitation for 30 minutes for extraction. The extracts were then let to cool down to room temperature (about 30 min) and 1 ml of HCl (0.65 M) was added into each tube (which makes the extract volume of each tube to 6 ml).

Extraction cartridges (HLB 3cc 60 mg Extraction Cartridges, Oasis)were placed onto a solid-phase extraction (SPE) vacuum manifold and conditioned by passing through 1 ml of methanol then 1 ml of conditioning solvent [methanol solution, KOH/methanol solution (8 g L^{-1}) and HCl (0.65 M) in 1:5:1 v/v/v]. Extra cares were taken to make sure cartridges were never dried out during and after this conditioning step.

Exactly 3 ml of extract was loaded and passed through the column with a low pressure (< -8 kPa). Each column was then washed with 1 ml of washing solution [KOH (0.4 M) in

methanol:H_2O (6:4 v/v)]. After washing, columns were dried under low pressure (between 0 and -5 kPa) for 1 hour. Before passing to the next step, columns were verified to be totally dried.

The last step of extraction was to elute ergosterol from columns. HPLC vials were numbered and weighted with their caps to the nearest 0.1 mg. Vials then placed in the vacuum manifold, and ergosterol was eluted with 4 times 350 µl of isopropanol (Chromasolv Plus, for HPLC, 99.9 %. Sigma-Aldrich) with a flow rate at about 1 ml min^{-1}. Vials were retrieved and tightly closed with corresponding caps and reweighted to the nearest 0.1 mg. Vials were kept at -20 °C before HPLC analysis. The volume of isopropanol in each vial was calculated with the density of isopropanol in the following equation:

$$V_{isopropanol}(ml) = \frac{M_{full\ vial}(g) - M_{empty\ vial}(g)}{0.786\ (g \cdot ml^{-1})}$$

For ergosterol quantification by HPLC. The programme used was with a mobile phase of methanol (1.4 ml min^{-1}), column temperature set at 33 °C using a thermostat. Pic detection wavelength was set at 282 nm, and with a sample injection volume of 10 µl. This analysis was carried out using Chromaster Hitachi (Pump 5110, autosampler 5210 and UV detector 5410) with a LiChrospher RP18 column (LiChroCART 250-4 HPLC cartridge, Merck). A standard curve with known concentrations of ergosterol (ACROS Organics, 98 %) in isopropanol (Chromasolv Plus, for HPLC, 99.9 %. Sigma-Aldrich) was prepared and ran on HPLC before each batch of analyses. The concentrations for the standard were 0, 1, 5, 10, 50 and 100 µg ml^{-1}. On the chromatograms, ergosterol peak started at 6.7 min and peaked at 7 min, the area of each peak was measured for ergosterol concentration calculation. A typical area to concentration conversion equation is:

$$C_{ergosterol} = 9E^{-5} \cdot x - 0.0152$$

Following the equations:

$$M_{ergosterol}(\mu g) = [ergosterol](\mu g \cdot ml^{-1}) \times V_{isopropanol}(ml) \times 2$$

$$M_{ergosterol\ in\ sample}(\mu g \cdot g^{-1}) = \frac{M_{ergosterol}(\mu g)}{M_{sample}(g)}$$

The final ergosterol quantity was obtained and expressed as micrograms (µg) of ergosterol per gram (g) of sample (cellulose disc or alder leaf disc).

6.3. Total N and P quantification (in all chapters)

Similarly to ergosterol extraction, samples were freeze-dried and weighed before analysis. Using clean grinding metallic balls and with the help of a bead beater (Mixer Mill, Retsch MM301), samples were reduced into fine powder. For cellulose discs, Ø 3 mm steel grinding balls were used, and for leaf discs, or mycelium, Ø 5 mm glass balls were used.

For total N analysis, between 1.5 and 2 mg of powder of each sample was put into a tin capsule (Säntis Analytical SA7698110), the masses were weighted to the nearest 1 µg using a microbalance (UYA 2.4Y, Radwag). The tin capsules were then folded carefully into compact cubes with tweezers and were made sure there was no powder leakage from each cube. Sample batches have then been entrusted to the chemical analysis department of the laboratory to be analysed using a CHN elementary analyser (Carlo Erba NA 2100). Briefly, the principle of the technique used is based on the Dumas method. Samples are burned in the presence of oxygen while in a helium current. All forms of organic nitrogen are turned into nitrogen oxides. The nitrogen oxides are then reduced into dinitrogen (N_2) in a reduction column containing copper. Gases are separated by a gas chromatography and detected by a thermal conductivity detector.

For total P quantification samples followed an alkaline digestion step to reduce all organic phosphates. Samples were previously reduced into powder. Between 1 to 2.5 mg of powder was measured to the nearest 0.01 mg and put in an Eppendorf microtube. The content of each

microtube then been transferred into a glass test tube with thread cap (washed with 0.1 % HCl to remove all traces of phosphorus, and dried). To make sure the transfer was quantitative, each microtube was rinsed carefully with ultrapure water (3 times 1 ml), and every drop of water was collected and transferred into the same glass test tube. And finally, in each glass tube, 1 ml of sodium hydroxide (NaOH, 1N), and 2.38 ml of sodium persulphate ($Na_2S_2O_8$, 125 g L^{-1}) were added, and the volume was completed to 10 ml with ultrapure water. Tubes were then closed loosely and autoclaved at 120 °C, 10^5 Pa (1 bar) for 2 hours. After autoclave, tubes were tightened and gently shook and left for decantation and cooling. P was measured from these digested fluids following the molybdate blue colorimetric method (NF EN ISO 6878). In 3 ml of digested samples, 300 µl of a combined reactive [3 g of $(NH_4)_6Mo_7O_{24}{\cdot}4H_2O$, 38 ml of H_2SO_4 (15 %) and 70 mg of $K_2Sb_2(C_4H_2O_6)_2$ complete with distilled water to 500 ml], and 150 µl of ascorbic acid [2 % (v/v), or 20 mg ml^{-1}] were added. Samples were homogenised and left for 30 min to allow reaction and development of a blue coloration. Using a spectrophotometer, sample absorbance was read at a wavelength of 880 nm. Samples P concentrations were calculated with a standard curve. The standard curve was prepared from either a K2HPO4 or KH2PO4 solution with five P concentrations at 0, 0.125, 0.25, 0.50,and 1 mg L^{-1}.

6.4. DNA extraction and Real-Time quantitative PCR (in chapter IV)

Total genomic DNA was extracted from either cellulose discs or alder leaf discs. Using a commercial extraction kit (DNeasy PowerSoil Kit, Qiagen), and following the manufacturer protocol. DNA concentrations were quantified with Nanodrop (NanoDrop One, ThermoScientific) and stored at -20 °C.

We used the number of bacterial 16S and fungal 18S rRNA gene copies for estimations of the relative abundance between bacteria and fungi. Real-Time qPCRs were performed as described

in Cébron *et al.* (2008) and Thion *et al.* (2012). For bacterial 16S rRNA gene, the primer pair used were 968F (5'-GAACGCGAAGAACCTTAC-3') and 1401R (5'-CGGTGTGTACAAGACCC-3')(Nübel *et al.* 1996). And for fungal 18S rRNA gene, they were Fung5F (5'-GTAAAAGTCCTGGTTCCCC-3') and FF390R (5'-CGATAACGAACGAGACCT-3')(Smit *et al.* 1999; Vainio and Hantula 2000). Amplification mix (20 µl) was prepared with 10 µl 2×iQ SyberGreen Supermix (BioRad), 0.8 µl of each primer (10 µM), 0.4 µl of BSA (Bovine serum albumin, 3 %), 0.2 µl of DMSO (dimethyl sulfoxide), 0.08 µl of T4 bacteriophage gene32 product (QBiogene), 6.72 µl of DNA-free distilled water and 1 µl of template DNA or water (for negative control) or standard plasmids from 10^1 to 10^8 copies μl^{-1}. The amplification programme used were as follows: starting with 5 min at 95 °C followed by 40 cycles with 20 s at 95 °C, 20 s at the primers specific annealing temperature (56 °C or 50 °C for 16S or 18S rRNA, respectively), 30 s at 72 °C and 5 s at 82 °C or 80 °C (for 16S or 18S rDNA respectively) to measure SYBR Green I Signal. Finally, a melting curve analysis from 50 °C to 95 °C with an increment of 0.5 °C per 5 s. The relative abundances between bacteria and fungi were calculated as a ratio with corresponding starting quantity or log stating quantity.

6.5. Bacterial Miseq NG-sequencing, diversity, and indicator species analyses (in chapter IV)

These methods were performed for analysing bacterial diversity, and attempt to identify indicator species for each experimental treatment.

For bacterial 16S rRNA gene amplicon-sequencing, the primer pair used for the first-step PCR were 341F (5'-CCTACGGGAGGCAGCAG-3'; Muyzer, de Waal and Uitterlinden 1993) and 787R (5'-GGACTACNVGGGTWTCTAAT-3'; Caporaso *et al.* 2011), each attached to an adaptor for a second-step PCR. The amplification mix was prepared for 50 µl final volume with:

10 µl 5× HF Buffer; 1 µl of dNTP (10 mM); 0.25 µl of dimethyl sulfoxide (DMSO); 0.1 µl of T4 bacteriophage gene32 product (QBiogene); 1.5 µl of $MgCl_2$ (50 mM); 1 µl of each primer (10 µM); 33.05 µl of DNA free distilled water; 0.1 µl of Phusion polymerase (Thermo Scientific) and 2 µl of DNA samples (or distilled water for negative control). 30 cycles of amplification at 56 °C annealing temperature were performed. Unpurified DNA collected from this first-step PCR was then sent to Microsynth (Next Generation Sequencing Department, Microsynth AG, Switzerland) for the second-step PCR and MiSeq 2 × 250 bp paired-end sequencing (Illumina).

Paired-end sequences obtained from the NG-sequencing were processed for quality filtering and clustered into operational taxonomic unit (OTU) at 97 % using Mothur (v1.44.3; Schloss *et al.* 2009) and following MiSeqSOP pipeline (first access date: 14 December 2020; Kozich *et al.* 2013). Taxonomy was assigned using SILVA ssu132 database. Singletons and sequences not affiliated to bacteria were removed. The final dataset was rarefied to the lowest number of sequences per sample to compare the diversity of OTUs present.

Alpha diversity was expressed by calculating Chao1 richness and Shannon diversity indices (Hill *et al.* 2003) using Mothur (v1.44.3; Schloss *et al.* 2009). Using R software (v4.1.0; R Core Team 2022), beta diversity based on Bray-Curtis dissimilarity was represented with non-metric multidimensional scaling (NMDS) analysis with two dimensions using the "metaMDS" function of the "vegan" R package (v2.5-7; Oksanen *et al.* 2020). The differences in community composition between each experimental treatment were tested by permutational multivariate analysis of variance (PerMANOVA) with 999 permutations using the "adonis2" function.

In an attempt to identify bacterial taxa that stand out the most under contrasted treatments, indicator species were analysed, also by using R software (v4.1.0; R Core Team 2022). The indicator values (IndVal < 1) of OTUs were calculated using the "multipatt" function of the "indicspecies" package (v1.7.9; de Cáceres, Legendre and Moretti 2010). We used the group-equalised IndVal (IndVal.g) index to find OTUs that were proportionally more likely to be

present at a group. By limiting the index between 0.7 and 1 as done previously by other studies (Demircan *et al.* 2018), we can focus on the most relevant OTUs. The higher the value, the more likely an OTU was abundant in that group. The indicator species analysis was performed with 9999 permutations on the rarefied dataset.

Chapter I

Characterising the Stoichiometric Plasticity of Some Aquatic Hyphomycetes

Aquatic hyphomycetes (AH) are shown to be rather flexible in their elemental requirements, and this stoichiometric plasticity makes it harder to study their role in plant litter decomposition and nutrient cycling. In this chapter, we looked directly at the implications of this plasticity in mycelial development of AH. The interspecific difference in growth strategy helps us to explain the outcomes of litter decomposition mediated by AH.

Abstract

Aquatic hyphomycetes (AH) are major decomposers of allochthonous plant litter in headwater streams and contribute to nutrient cycling in these ecosystems. Because AH are flexible in their stoichiometric requirements, predicting litter decomposition outcomes by AH under different conditions of nutrient availability remains a challenging task. This elemental plasticity of AH may influence their growth and the role they play in nutrient cycling, yet data on the plasticity of individuals AH taxon remain scarce. This chapter aims to characterise the degree of plasticity of 4 common AH species cultivated on solid nutrient media with contrasted nitrogen (N) and phosphorus (P) conditions. We compared N:P variations in fungal biomass between 3 age classes of mycelium (old, intermediate, young, based upon the distance to the centre of the culture dish). To investigate the role of this plasticity, we also tested whether nutrient storage in biomass would give any advantage for colonising new substrates.

Our results confirmed that AH are largely plastic for P, but plasticity for N might depend on taxa. Elemental plasticity of mycelium varied largely with mycelium age, young – , actively growing mycelium being stoichiometrically less plastic than older one. Finally, our results failed to demonstrate that nutrient storage gives any advantage in terms of growth when colonising a new, nutrient-poor substrate. This study stresses the need for future work on the characterisation of the stoichiometric traits for more AH taxa. Our results also underline that more data are required to fully understand the mechanisms and the consequences of such nutrient storage, not only for tackling questions on microbial community ecology but also for investigating the roles of fungi in ecosystem functioning and nutrient cycling.

Key words:

Aquatic hyphomycetes, elemental plasticity, stoichiometric traits, N:P ratios, mycelium age, nutrient storage, P storage, growth strategy, Growth Rate Hypothesis

1. Introduction

Aquatic hyphomycetes (AH) are a polyphyletic group of filamentous fungi that are commonly found in freshwater streams, rivers, and lakes (Bärlocher *et al.* 1992). Together with bacteria, they are one of the major decomposers of plant litter (dead wood, leaf litter) in stream ecosystems (Baldy, Gessner and Chauvet 1995; Gulis and Suberkropp 2003a). Thanks to their exoenzymatic activity (Chamier and Dixon 1982), these fungi are capable of breaking down complex organic compounds into simpler forms, building up their biomass but also releasing nutrients such as carbon, nitrogen (N), and phosphorus (P) into their environment. The ecological importance of AH in freshwater ecosystems has been widely recognised, and numerous studies have highlighted their contribution to nutrient cycling and ecosystem functioning (Ingold 1942; Gessner, Chauvet and Dobson 1999; Gulis, Kuehn and Suberkropp 2006; Findlay 2010). Yet, challenges remain in studying litter decomposition by AH when attempting to predict the outcome of the decomposition process under different environmental conditions, partially because AH are fairly flexible in their stoichiometric requirements (Danger, Gessner and Bärlocher 2016), and seem to be able to adapt their nutrient acquisition strategies to different environmental conditions.

The Growth Rate Hypothesis is one of the principles of ecological stoichiometry. It states that the rapid development of an organism is positively correlated with its P demand (Elser *et al.* 2000; Isanta-Navarro *et al.* 2022). Organisms with high growth rate are expected to exhibit low body N:P and C:P ratios, due to high requirements of protein production and thus a very high demand for RNA production, this kind of molecule being particularly rich in P (Elser *et al.* 2000). The N:P ratio and the growth rate are thus theoretically linked by the allocation of P to ribosomes (rRNA) and the allocation of N to protein synthesis (Sterner and Elser 2003a; Hessen *et al.* 2007). Studies have shown that AH exhibit plasticity in their elemental composition, which can vary depending on factors such as species and age of the mycelium (Danger and

Chauvet 2013; Danger, Gessner and Bärlocher 2016). In particular, a study focusing five AH strains at different development stages have concluded that the relationship between growth and N:P ratios in biomass was not consistent (Grimmett *et al.* 2013). Another study on AH also found flexible N:P ratios due to dissolved N concentrations affecting mycelial growth rate (Gulis *et al.* 2017). Similarly, a study on terrestrial fungal stoichiometric ratios also found that individual strains showed high C:N and C:P flexibilities (Camenzind *et al.* 2021). The correlation expected between the growth rate and P content can be easily hidden in fungi by P storage in fungal biomass ("luxury consumption") when P is not limiting in the environment (Danger and Chauvet 2013). In addition, contrary to bacteria, growth takes place only at the tip of hyphae for filamentous fungi. These phenomena can lead to complexity in the strict application of the Growth Rate Hypothesis in fungi (Grimmett *et al.* 2013; Danger, Gessner and Bärlocher 2016). Finally, one could expect large differences in response of fungi growing either on nutrient rich media – commonly done in previous studies dealing with fungal elemental plasticity (e.g. Danger and Chauvet 2013; Grimmett *et al.* 2013; Gulis *et al.* 2017), or fungi receiving a punctual, short-term pulse of nutrients as it may happen in aquatic ecosystems after a rainy event or a punctual pollution (Li *et al.* 2009; Danger *et al.* 2013).

This elemental plasticity of AH may have large ecological implications, such as influencing fungal growth rates but also their role in nutrient cycling. Decomposers, and AH in particular, are commonly described as nutrient mineralisers, i.e. organisms that participate to recycle plant detritus and release nutrients under forms available for sustaining primary production. High storage capacities of non-limiting nutrients could delay any nutrient release carried out by microbial decomposers activities. Also, this plasticity could represent species traits implied in species competitiveness and the abilities of some species to exclude others or to colonise nutrient poor media (Mason-Jones *et al.* 2022). Finally, this plasticity may also be important

for fungal consumers who largely benefit from nutrient-enriched mycelial resources (Danger *et al.* 2013).

Despite the recent acknowledgment of its potential ecological importance, the extent and causes of fungal elemental plasticity are still understudied. The goals of this study were to understand in more depth the degree of AH mycelial plasticity, their genericity, and test whether nutrient storage gives any advantage for colonising new substrates. To achieve these goals, we compared the N:P plasticity of 4 common AH strains cultivated on solid media representing diverse N:P conditions, and we compared N:P variations between different mycelium age classes. The obtained mycelia were then transferred to new media in order to test for any initial growth advantage acquired after storing some nutrients in fungal biomass. We mainly hypothesised that (H1) all AH strains are plastic in their elemental composition but (H2) the degree of elemental plasticity differs from one AH strain to another and (H3) the response of mycelium elemental content depends on the nature of the nutrient input (composition is expected to differ between mycelium grown on nutrient rich media and those receiving the same amount but punctual input of nutrients – pulse treatment). We also hypothesised that (H4) the elemental composition of mycelium is age-dependent, young-, fast-growing-mycelium being more stoichiometrically constrained than older mycelium, to ensure their growth activity. Finally, we expected that (H5) nutrient rich mycelium would be advantaged for colonising and developing in a new, nutrient-poor environment.

2. Materials and Methods

2.1. Fungal growth

The experiment was done in 90 mm plastic sterile Petri dishes. Nutritive culture medium was a modified version of GMS (Glucose Mineral Solution) medium for fungal culture (Gessner &

Chauvet 1993). The medium contains $Al(SO_4)_3 \cdot 18H_2O$ - 0.1 mg L^{-1}, KI – 0.1 mg L^{-1}, $CoCl_2 \cdot 6H_2O$ – 0.04 mg L^{-1}, $NiCl_2 \cdot 6H_2O$ – 0.25 mg L^{-1}, $FeCl_3$ – 2 mg L^{-1}, $MnSO_4 \cdot H_2O$ – 1 mg L^{-1}, H_3BO_3 – 1 mg L^{-1}, $ZnSO_4 \cdot 7H_2O$ – 1 mg L^{-1}, $Na_2MoO_4 \cdot 2H_2O$ – 0.1 mg L^{-1}, $MgSO_4 \cdot 7H_2O$ – 500 mg L^{-1}, $CaCl_2 \cdot 2H_2O$ – 150 mg L^{-1}, agarose – 20 g L^{-1}, and glucose – 5 g L^{-1}. $N\text{-}NO_3^-$ was added at either 0.93 mg L^{-1} or 9.3 mg L^{-1}, and $P\text{-}PO_4^{3-}$ at either 0.1 mg L^{-1} or 1 mg L^{-1} to form 4 nutrient combinations, as in Danger and Chauvet (2013). Those 4 nutrient combinations were named as *P-rich*, (NP-)*poor*, (NP-)*rich*, and *N-rich*. They represent 3 molar N:P ratios from *P-rich* (0.4, low N:P ratio) to both *poor* and *rich* (4.2, middle N:P ratio) and *N-rich* (42, high N:P ratio) and 2 different nutrient quantities (*poor* and *rich*). Petri dishes were poured with these media and the agar gel surfaces were covered with a cellophane membrane (regenerated cellulose, 8.5 cm Ø). The membrane facilitates later mycelium collection by keeping mycelium physically separated from the culture medium matrix while still allowing access to nutrients.

Four common AH strains were compared in this experiment, namely *Articulospora tetracladia* (ARTE), *Heliscus lugdunensis* (HULU), *Tetracladium marchalianum* (TEMA), and *Tricladium splendens* (TRSP). A 25 mm² square of agar with mycelium from the fringe of an active fungal culture was deposited on the centre of each newly prepared Petri dish, on top of the cellophane membrane. Each strain treatment was replicated 6 times for each of the 4 nutrient combinations.

An extra set of 6 replicates of each strain was grown on the *poor* medium for testing the effects of a punctual nutrient enrichment (hereafter referred to as the nutrient *pulse* treatment) on mycelium N and P content.

Each Petri dish was then sealed with Parafilm and incubated upside down (to prevent any water condensing on the Petri lid from dripping down on the fungal culture) at 15 °C in the dark. Fungal colony outlines were traced with a marker once a week until it covered the totality of

the dish surface. The experiment lasted 4 weeks for HULU and 5 weeks for the other 3 AH strains before mycelium collection.

2.2. Nutrient pulse

To be able to compare the effect of a long-term growth on a nutrient-rich media and the stoichiometric response of fungi exposed to a short-term nutrient input, the extra sets of strains grown on the *(NP-)poor* medium were opened under safety cabinet. Then, 10 ml of a sterile nutritive solution, bringing up enough N and P to reach the same N and P total content than in the (NP-)*rich* treatment, were dispensed directly over each colony. Colonies were submerged in this *pulse* solution for 18 hours, then drained out and rinsed twice with sterile ultrapure water before mycelium collection.

2.3. Mycelium collection

Once fungal colonies covered the whole Petri dish surface, and after nutrient pulse step for the nutrient pulse extra set, mycelia were collected into individual tubes. For each colony, the mycelia were divided equidistantly into 3 age categories (old, intermediate, young) from the centre to the fringe. Four 25 mm^2 of mycelium from each colony were kept for transplantation (see §2.5). Mycelium was separated from the cellophane membrane and gathered using a sterile scalpel by gently scraping the membrane surface. Extra care was taken to avoid cutting through the membrane, which would result in the pollution of mycelium with the culture medium. Mycelium samples were rinsed with sterile distilled water then immediately put to the freezer and subsequently freeze-dried before N, P measurements.

2.4. Mycelium N, P measurement

Freeze-dried mycelium samples were grinded into fine powder with glass beads (5 mm Ø) and a bead beater (Mixer Mill, Retsch MM301). Total N measurements were done by encapsulating between 0.01 mg to 2 mg (to the nearest 1 µg) of mycelium powder into tin capsules and passing through a CHN elementary analyser (Carlo Erba NA 2100). Total P analyses were done by weighing between 0.01 mg to 2.1 mg of powder (to the nearest 1 µg), followed by a step of alkaline digestion which reduces all organic P into inorganic one, as in Danger and Chauvet (2013). P was then measured spectrophotometrically using the molybdate blue colorimetric method (NF EN ISP 6878).

2.5. Transplantation

To answer our question whether growing previously on a medium with a certain nutrient level would give an advantage for starting a new colony on a new nutrient medium type, new 55 mm Petri dishes were prepared with the same 4 nutrient levels as described in §2.1 (*P-rich*, (NP-)*poor*, (NP-)*rich*, and *N-rich*), without cellophane membrane. Four squares (25 mm^2) of mycelium from each original colony was transplanted onto 4 new dishes with one of each nutrient type (6 replicates of the original colony from each of the 5 nutrient treatment to each of the 4 nutrient type, Figure.I.1). Each Petri dish was then sealed with Parafilm and incubated upside down at 15 °C in the dark. Fungal colony outlines were traced with a marker every 2 weeks until it covered the totality of the dish surface.

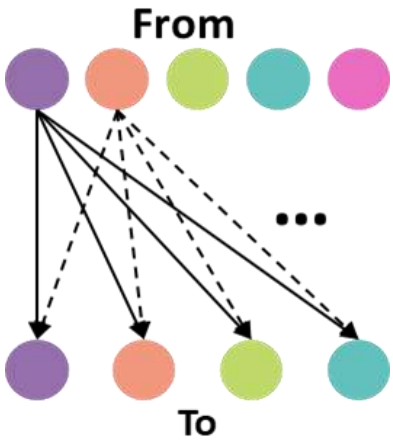

Figure I 1. Schematic representation for the crossed transplantation setup.

2.6. Colony size measurement

Pictures of each Petri dish (90 mm and 55 mm) were taken with a digital microscope (Keyence VHX-6000) using the same setup and software settings for each session of measurement. Measured size was calibrated with euro coins. Each marked ring of the colony was retraced using the software provided with the microscope to measure the colony size (Figure.I.2).

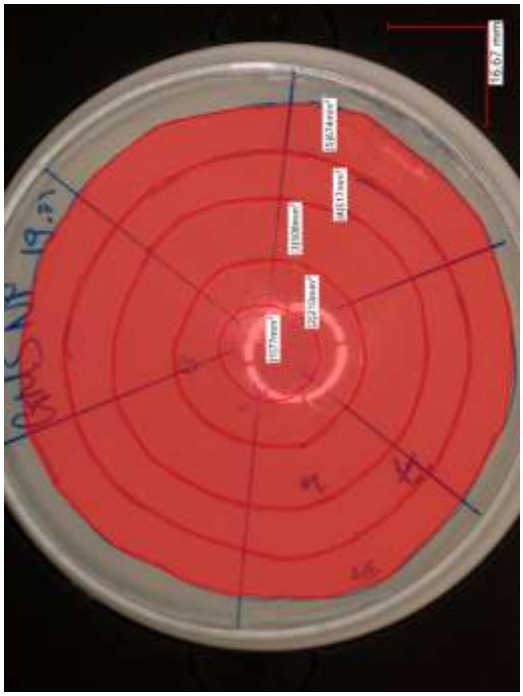

Figure I 2. Example of colony size retrace and measurement of a Petri dish.

Red circles marked each ring of colony.

2.7. Statistics

All statistical analyses were performed with R using RStudio (R Core Team 2022; RStudio Team 2022). For original cultures grown on top of cellophane membrane, supposing the growth only happened on the membrane surface and in a circular manner, the colony size would be: $S = \pi(tr)^2$, where *S* is the surface area of the colony in mm², *t* is time in days, and *r* is the growth rate in mm day^{-1}. This model gave us the growth rate with its confidence interval (CI) at 95 %. For subsequently transplanted cultures which grown directly on agar gel in 3 dimensions (growth on the surface as well as inside the gel), the growth was assumed to have followed a more linear model, so the colony's radius would be $R = tr$, where *R* is the radius in mm, *t* is the time in days, and *r* is the growth rate in mm day^{-1}. The growth rate was also given with its CI at 95 %, allowing to directly conclude on significant differences between parameters.

The degree of homoeostasis $(1/H)$ of each AH strain mycelium in all three ages were calculated as the slopes of the linear regression relationships between $ln(N{:}P_{mycelium})$ and

$ln(N{:}P_{medium})$ (Persson *et al.*, 2010). Following the classification proposed by Persson *et al.* (2010), $1/H$ values comprised between 0.75 and 1 signifies that the organisms considered are very plastic; organisms exhibiting $0.5 < 1/H < 0.75$ are considered as weakly plastic, those with $0.25 < 1/H < 0.5$ are considered as weakly homoeostatic, and those with $1/H$ values below 0.25 are considered as homoeostatic.

To consider the density of the mycelium and test the respective and interactive effects of nutrient levels and AH species on this parameter, we calculated the Biomass Size Ratio (BSR), i.e. the mass (mg) per unit of surface (cm^2). Data were then analysed using the nonparametric Kruskal-Wallis test and multiple comparison of treatments with "kruskal" function from the "agricolae" package (v1.3-5,Conover 1999). Note that this calculation was not possible for the transplantation test since cellophane was not used for this test and mycelium grown inside their substrates. Finally, effects of nutrient treatments, mycelium age, and species identity on mycelial elemental composition (%N, %P, and mycelium N:P) were also analysed using Kruskal-Wallis test described earlier. To simplify the reading of figures, *post-hoc* tests were performed for each species independently. Finally, to test for the Growth Rate Hypothesis theoretically relating organism growth rates and the N:P requirements, and due to data points distribution, we used Spearman's Rank correlation (with "stat_cor" function from the "ggpubr" package, v0.6.0, Kassambara 2023) to test for the presence of a correlation between fungal hyphae growth rate and mycelium N:P ratio. These tests were carried out on all data as well as independently on each of the three-age classes. For all analyses, the 0.05 *P-value* threshold was used.

3. Results

3.1. Colony growth and elemental plasticity of AHs

Out of the 4 tested AH strains, HULU was the first one to outgrow the Petri dish surface within only 3 weeks on the *rich* culture medium, and 4 weeks on the other 3 media. In contrast, for ARTE and TEMA, they took 5 weeks to cover the whole surface on all medium types. The incubation of TRSP was also stopped after 5 weeks despite not totally reaching the whole dish surface (Figure.I.3a). AH colony growth rates were thus different between strains and medium types (Figure.I.3b). The differences were more visible between strains than between media types of a strain: HULU exhibited the fastest growth within the range of 1.5 to around 1.9 mm day^{-1}. ARTE and TEMA shared similar growth rates which were between 1–1.25 mm day^{-1} depending on the culture medium. TRSP exhibited the slowest growth on all

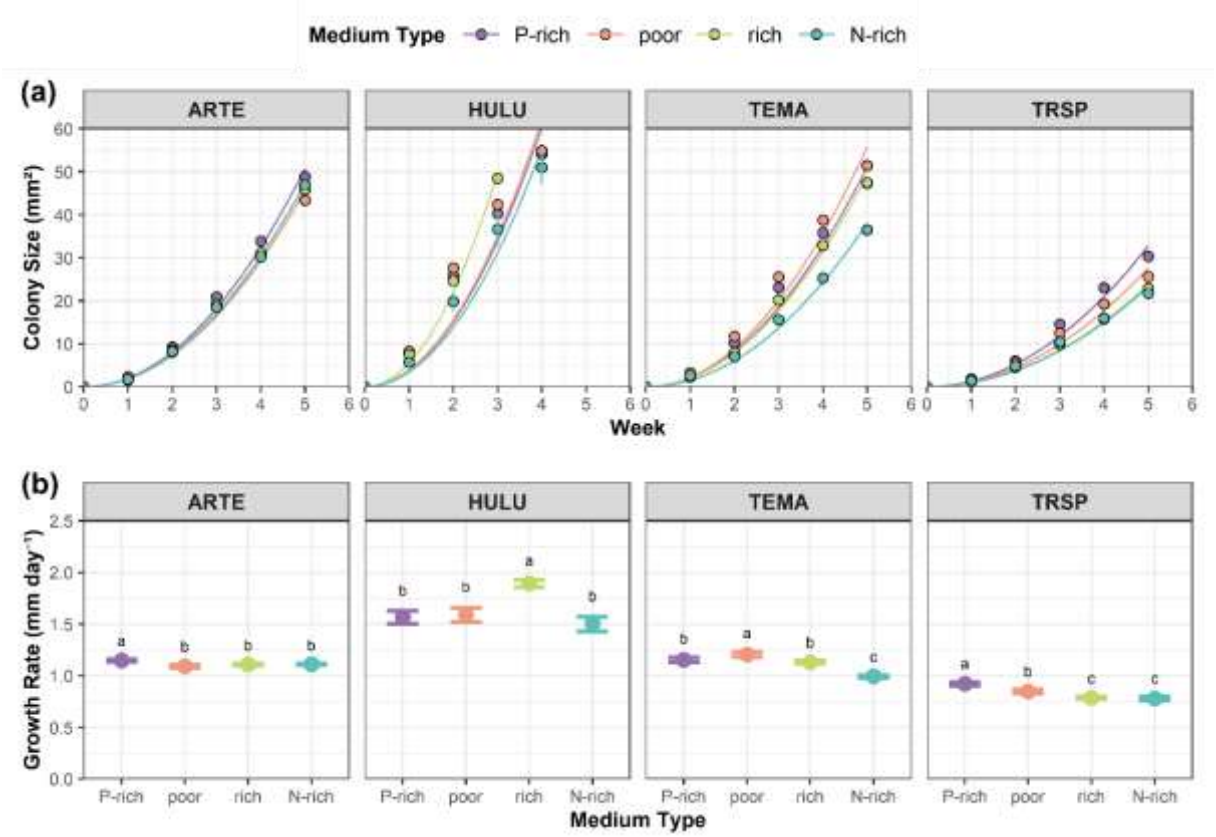

Figure I 3. (a) Colony size and (b) growth rate of each AH on different medium type.

Points in colony size shows the average value (n=6) ± SE. Curved lines show the fitted model. Growth rate shows the calculated rate by model ± CI (95 %). Letters of significance are directly concluded from CI and are grouped by strain.

media types reaching growth rates between 0.75–1 mm day^{-1}. In general, across all 4 strains, radial growth on *N-rich* medium was always the slowest. HULU exhibited its fastest radial growth on the *rich* medium while the fastest radial growth was reached on *P-rich* medium for ARTE and TRSP, and on the *poor* medium for TEMA (Figure.I.3b).

To consider potential differences in growth strategies between AH strains, i.e. radial growth and/or increase in mycelial density depending on the nutrient treatment, fungal biomass to colony size ratios (BSR) were also calculated (Figure 3). Whatever the strain tested, BSR showed a similar trend with the highest mycelium density on the *rich* medium, followed by *N-rich*, and finally with either *P-rich* or *poor* as the lowest. BSR profiles were also much more similar between ARTE, HULU, and TEMA, with values between 0.025–0.15 mg cm^{-2}, and the BSRs for *rich* medium were always around 0.1 mg cm^{-2}. In contrast to the three other AH strains,

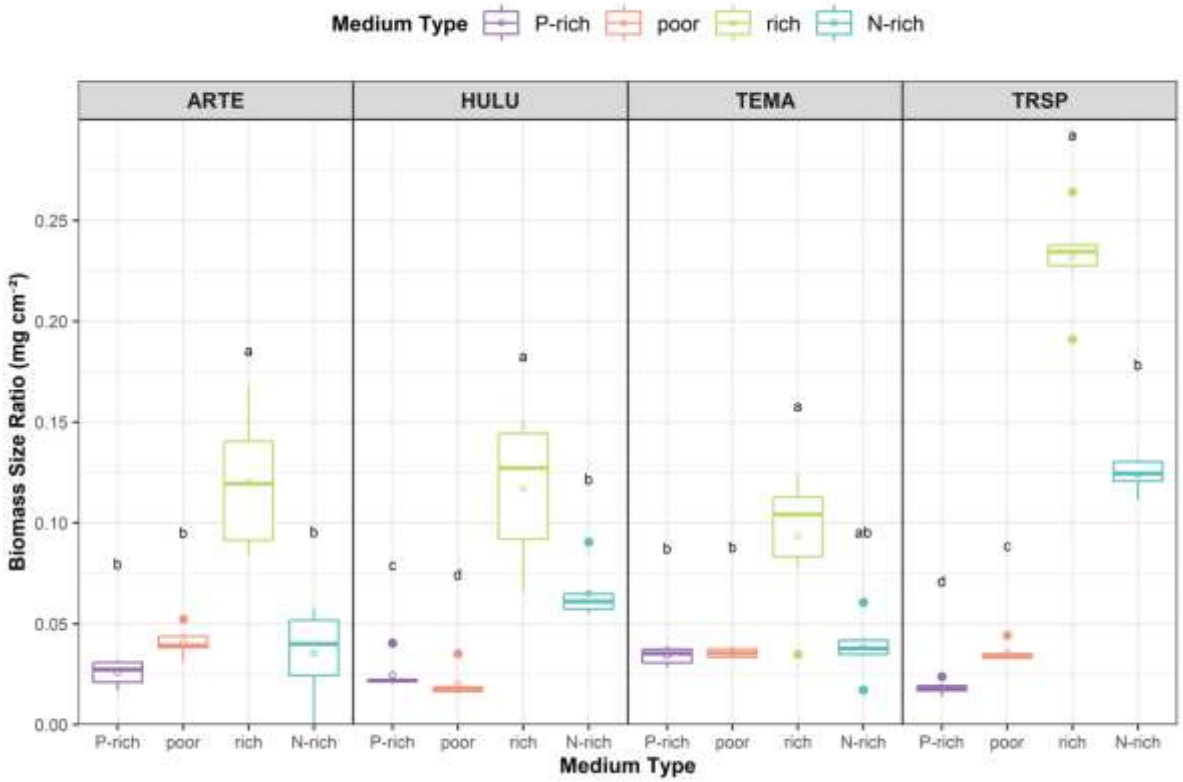

Figure I 4. Fungal Biomass Size Ratios (BSR) of each AH on different medium type. Significance letters (Kruskal-Wallis) are grouped by strain.

the BSR of TRSP growing on *rich* and *N-rich* media reached very high values, with BSR values about 2 times higher than those of the 3 other strains (Figure.I.4).

Mycelium N and P contents and N:P ratios were measured individually and calculated for old, intermediate (inter.), and young mycelium (Figure.I.5). Note that material was not always sufficient for carrying out multiple analyses, leading to a few missing (n = 2) or non-replicated

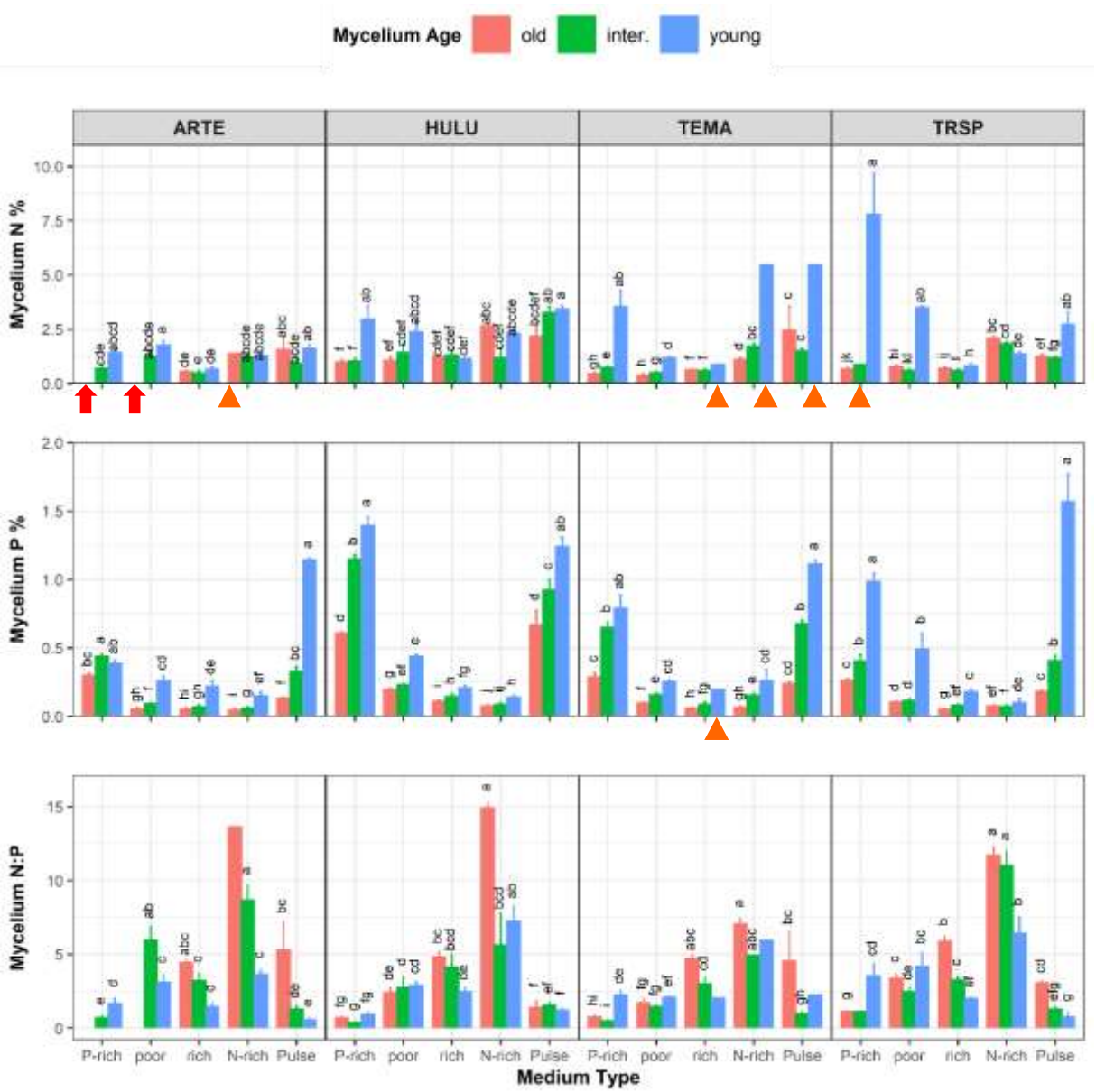

Figure I 5. Mycelium N (a) and P (b) contents, and N:P ratios (c) for the 4 AH strains (ARTE, HULU, TEMA and TRSP) and for each mycelium age (old, intermediate, and young) on different medium types.

Kruskal-Wallis test done for each panel individually. No data were acquired for N-old-ARTE (red arrows) due to analyse errors. Bars without error bars, nor significance letters were data without replicate due to the lack of material for statistical analyses (orange triangles).

(n = 5 for %N and n = 1 for %P) values. These data are shown on the Figure.I.5 as bars without error bars nor significance letters). Whatever the strain considered, for each medium type, N and P contents were about 2 times higher in young mycelia than in old ones, and mycelia N:P ratios were double in old mycelia than in young ones, with a few exceptions. When considering across all 4 media types (without the Pulse type), N contents were generally lower in mycelia grown in *P-rich* media (with N:P ratios of 0.4) then gradually went up, and higher in *N-rich* media (with N:P ratio of 42). In contrast, mycelium P contents across the 4 media types were significantly higher in *P-rich* media than in *N-rich* ones, and mycelia N:P ratios increased with increasing media N:P ratios (from *P-rich* to *N-rich*). For the *pulse* treatment, mycelia N content only rarely significantly differed from the values obtained on the *poor* treatment. In contrast, the 18 hours nutrient pulse largely impacted the P content and the N:P ratio.

Degree of homoeostasis $(1/H)$ of the mycelium of the four AH strain showed similar trends between the three mycelium age classes, with intermediate and old mycelium 1/H values > 0.48 – i.e. considered as weakly plastic following Persson *et al.* (2010), and young mycelium (except HULU) values < 0.17, i.e. considered as homoeostatic. However, note that linear regressions were not significant

Table I 1. Degree of homoeostasis of AH strains at different ages.

1/H was calculated as the slope of linear regressions between ln (N:P mycelium) and ln (N:P medium). 1/H close to 1 indicates organisms that are plastic in terms of elemental composition.

	1/H	r^2	P
Articulospora tetracladia			
young	0.17 [-0.03, 0.37]	0.33	0.085
inter.	0.53 [0.36, 0.7]	0.83	< 0.001
*old**	*0.49 [0.08, 0.89]*	*1*	*0.041*
mean	0.41 [0.27, 0.55]	0.61	< 0.001
Heliscus lugdunensis			
young	0.44 [0.36, 0.52]	0.95	< 0.001
inter.	0.53 [0.27, 0.79]	0.68	< 0.001
old	0.65 [0.53, 0.76]	0.94	< 0.001
mean	0.48 [0.44, 0.64]	0.76	< 0.001
Tetracladium marchalianum			
young	0.16 [-0.05, 0.37]	0.42	0.11
inter.	0.48 [0.35, 0.61]	0.88	< 0.001
old	0.48 [0.32, 0.64]	0.83	< 0.001
mean	0.36 [0.31, 0.51]	0.65	< 0.001
Tricladium splendens			
young	0.13 [-0.05, 0.32]	0.22	0.14
inter.	0.51 [0.41, 0.61]	0.95	< 0.001
old	0.5 [0.4, 0.6]	0.93	< 0.001
mean	0.36 [0.26, 0.45]	0.65	< 0.001

**: calculated with only 2 points.*

for young mycelium with also the exception of HULU (Table.I.1).

Finally, considering the test of the Growth Rate Hypothesis (Figure.I.6), no relationship between young mycelium N:P ratios and fungal growth rate was evidenced, whether analysed for each strain individually or all strains together (Figure.I.6a). However, there were significant negative relationships for both intermediate and old TEMA and TRSP mycelium, for which higher growth rates led to lower N:P ratios. A significant negative relationship for intermediate mycelium was also observed for all 4 strains analysed together (Figure.I.6b, 6c). The whole colonies – integrating the three-age classes of mycelium – of TEMA and TRSP conserved the significant negative relation between their mycelium N:P ratios and their growth rates (Figure.I.6d).

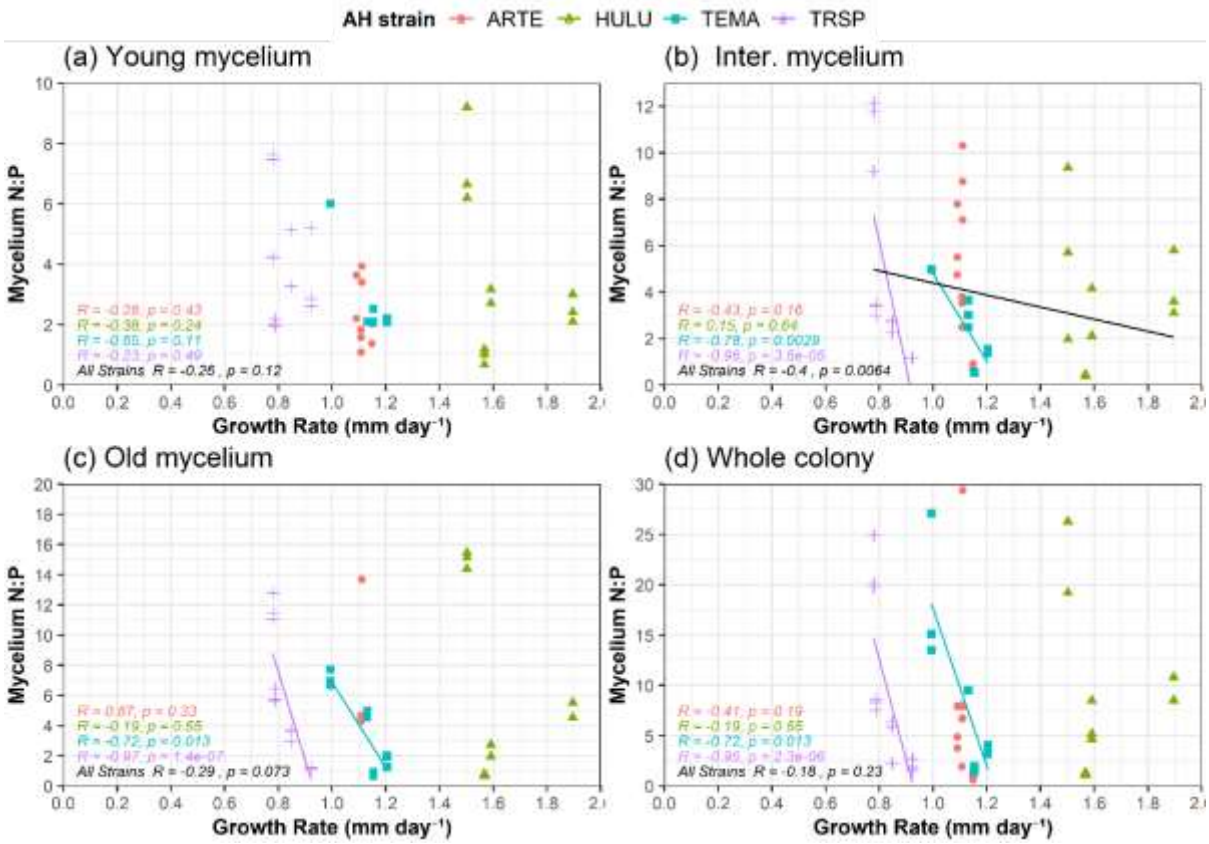

Figure I 6. Correlations between growth rates and mycelium N:P ratios.

Results of the Spearman's rank correlations of the three different aged mycelium and the whole colony are presented on each panel. When it is significant, the correlation line is drawn.

3.2. Transplantation experiment: testing the role of elemental plasticity for AH

Transplanted colony growth rates were dependent on fungal strain and the original culture medium type (one-way ANOVA, $P < 0.001$, Figure.I.7) and no general trend was observed across all tested strains. Original (donor) medium type did not significantly affect transplanted ARTE colony growth on any (receiver) medium type. All growth rates were between 0.5–0.75 mm day^{-1}. HULU had the highest growth rates (> 1 mm day^{-1}) among all strains. Colonies from *pulse* medium grown the fastest among all original medium types, followed by colonies from either *P-rich* or *poor* medium. For TEMA, colonies originating from *pulse* or *poor* medium grown significantly faster and colonies from *N-rich* medium significantly slower than those from the other original medium types. Transplanted TRSP grown on *N-rich* medium were the only transplanted TRSP that showed significantly different growth rates between different

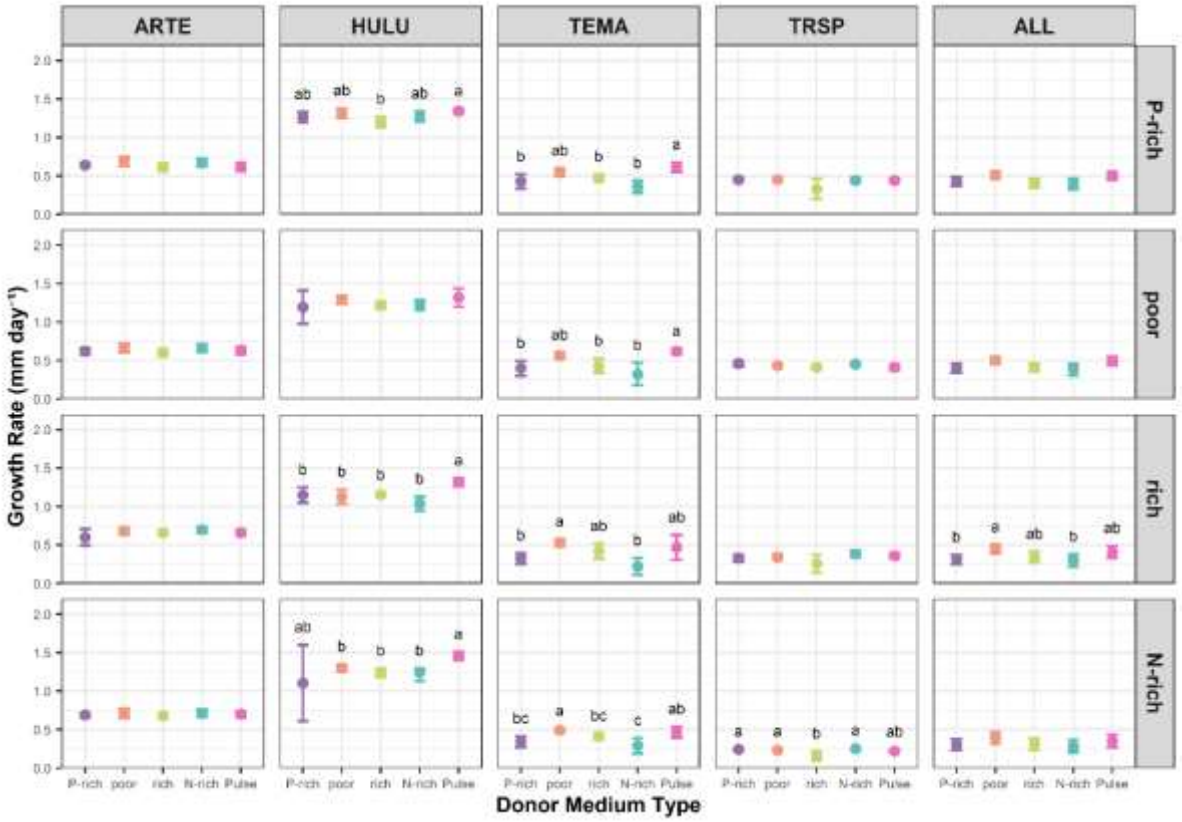

Figure I 7. Growth rate of transplanted cultures.

Columns show AH strains originating from the 5 nutrient treatments (donor treatments), rows show the four receiver-medium types. Growth rates are presented ± CI (95 %). Letters show differences between the five donor-(original)-medium types, each species being considered independently.

original medium type. TRSP growth rates were in general the lowest 0.25–0.5 mm day^{-1}) among all strains. The growth rates of all 4 strains mixed up were also different depending on the original medium type, but the differences were only significant when grown on *rich* medium with colonies came from *poor* medium grown faster.

4. Discussion

While a few studies have recently questioned the elemental plasticity of fungi, data are still scarce in the literature. Yet, storage capacities of microorganisms might be an important trait susceptible to largely impact ecosystem functioning, both in terrestrial and aquatic ecosystems (Mason-Jones *et al.* 2022). This study sheds new lights on the elemental plasticity of aquatic hyphomycetes and reveals different responses to N and P availabilities.

First of all, our results revealed several growth strategies (contrasting traits among AH species) when facing nutrient imbalanced conditions among the 4 AH species tested. Concerning the radial growth, HULU grew up to two times faster than TRSP. Also, only HULU exhibited a faster growth on the nutrient rich medium, which was unexpected since it should represent the best conditions with the most balanced N and P inputs. Interestingly, TRSP which exhibited the slowest radial growth had by far the highest mycelium density on both NP-rich and N-rich conditions, biomass to surface ratio being on average more than two times higher than those of the three other taxa. When facing a nutrient stress, some fungal taxa might thus respond by growing fast with a small mycelial density, in order to explore their environment and try to find a nutrient rich patch of resources, as already observed with terrestrial taxa (Camenzind *et al.* 2020). In contrast, other taxa, such as HULU, might adopt a similar strategy in nutrient-rich conditions probably to maximise the surface they colonise, as a pioneer strategy. This strategy would be similar to those commonly found in r-strategist that generally goes with a trade-off in the capacity to exploit complex resources (Arendt 1997). In that case, it is hard to evidence such

trade-off since most AH species exhibit large degradative abilities, at least in laboratory conditions (Suberkropp, Arsuffi and Anderson 1983). Studying fungi foraging strategies is a topic of interest in microbial ecology (Gilchrist, Sulsky and Pringle 2006; Veresoglou *et al.* 2018) but data are still scarce, and further studies would be required to explore this question in AH. In combination with other fungal traits (e.g. Crowther *et al.* 2014), it would give promising avenues to understand species successions in AH communities (Gessner *et al.* 1993) and predict plant litter decomposition in streams.

In the past decades, following the development of the Ecological Stoichiometry theory (Sterner and Elser 2003a), numerous studies questioned the elemental plasticity of organisms. Surprisingly, despite their central role in the functioning of numerous ecosystems, data concerning fungal stoichiometry are still scarce. Most available data indicate that fungi are quite plastic (Danger and Chauvet 2013; Camenzind *et al.* 2021), at least for their phosphorus content and there is no clear consensus for nitrogen (Gulis *et al.* 2017). Our study confirmed this plasticity (confirming our hypothesis H1) for the four AH taxa tested concerning phosphorus and at least for some species (especially TRSP) for nitrogen (confirming H2). Values varied in the same range as those reported in the literature review of Danger *et al.* (2016). However, the most interesting result certainly concerns the effect of mycelium age on fungal biomass elemental plasticity. As initially hypothesised (H4), young mycelium was close to strict homoeostasis for all taxa tested, and older biomass was by far more plastic than the young one (calculated 1/H being close or over 0.5, similar to values reported in Danger *et al.* 2016 but greater than those observed by Gulis *et al.* 2017). This result is quite similar to the observation made by Camenzind *et al.* (2021) on terrestrial fungi and comparing the elemental composition of the mycelium found at the edge and the centre of the fungal colony. Their results showed greater elemental variations for the inner part of the colony than for the margin. Such results might be explained by the fact that actively growing parts of fungi are more nutritionally

constrained since they must balance their elemental requirements to optimise their growth and new biomass production. This result has already been observed in other taxonomic groups, such as in phytoplankton where stoichiometric flexibility has been shown to decrease with population growth rates (Hillebrand *et al.* 2013) and might be generalised to actively growing mycelium. Depending on culture conditions and sampling strategies, considering whole fungal biomass (integrating young and old mycelium) or focusing only actively growing mycelium might largely change the plasticity patterns observed.

Another interesting result of the elemental plasticity is about nitrogen. Gulis *et al.* (2017) observed nearly strict homoeostasis for this element, while Danger and Chauvet (2013), Grimmett *et al.* (2013) or Camenzind *et al.* (2021) observed some significant variations. The strict control of fungal N composition might be strain dependent, since C:N plasticity was especially exacerbated in our study for one species, TRSP. This species was also the one that exhibited different growth patterns on culture dishes, growing more slowly in diameter but being able to increase more their hyphal density when N was available in larger amounts. This different growing strategy might be involved in the higher C:N plasticity patterns observed, either because young (homoeostatic) and old (plastic) mycelium are more in overlap in such conditions or because different growing strategies also correspond to different abilities of hyphae to acquire and/or to remobilise nutrients during their growth and their senescence (Tlalka *et al.* 2008; Mason-Jones *et al.* 2022). Studying foraging strategies in AH species might definitely help to solve these questions. For example, a recent study found that AH exhibit an inter- and intraspecific diversity in their nitrate reductase genes (Mariz *et al.* 2021) which could at least partially explain our findings.

One important tenet of Ecological Stoichiometry concerns the Growth Rate Hypothesis (GRH; Elser *et al.* 2003). Following this hypothesis, fast growing organisms should exhibit higher P requirements and lower N:P ratios than slow-growing ones due to higher cellular concentrations

of P-rich ribosomal RNA. In our study, growth rates could be compared either between species – some species growing faster than the other, as discussed above; or for each species individually – fast growing vs. slow growing mycelium parts (young vs. old mycelium) or mycelium growing on nutrient rich vs. on nutrient poor conditions. Our results revealed, for 2 AH species (TEMA and TRSP) over the 4 investigated, weak but significant negative relationships between mycelium N:P and fungal growth rate. These results were never observed on young mycelium, only on older ones. These results contrast with our expectations since the GRH was supposed to apply on the fast-growing, RNA-enriched parts of fungi, but are in line with Grimmett *et al.* (2013) and Gulis *et al.* (2017) who failed to evidence a similar relationship on AH. In particular, despite significant increases in cellular RNA contents with fungal growth rate, no significant reduction of mycelium N:P ratio was evidenced. In fungi, ribosomal RNA might thus not be the most important P source driving the elemental composition of mycelium and storage mechanisms (e.g. polyphosphate) could be more relevant in explaining these changes.

In this study, we also aimed at comparing the impacts of nutrient addition pulses to longer-term growth on nutrient rich media. In ecosystems, nutrient availability could indeed be quite stable through time or vary sharply after environmental changes, such as after heavy rains or punctual human-induced pollution (for example, use of fertilisers). We expected that short term inputs of both N and P on mycelium grown on poor media would lead to fast nutrient immobilisation and drastically change the elemental composition of fungal biomass (H3). This is precisely what was observed for P after an 18hr NP-rich solution addition, but not for N, which remained similar to the N concentrations observed in the mycelium grown on poor media. This result suggests that only P, not N, can be quickly stored in fungal biomass, in agreement with observations made by Gulis *et al.* (2017). N acquisition would take more time than P acquisition and would be more directly incorporated in new fungal biomass in comparison with P which

could certainly remain under storage forms for a longer time. Polyphosphates have been hypothesised as one form used by fungi to store P (Beever and Burns 1981). Yet, after a short-term pulse, one could question the feasibility to produce these storage forms in such a short-term period. It would then be interesting to investigate in AH under which form this extra P is stored in fungal cells, and if these forms are stable through time and how – and for which purpose – they are remobilised in the cell. This would be especially important since fungi are major actors of the P biological cycle in ecosystems.

Finally, after observing fungal elemental plasticity, one remaining question concerns the ecological and evolutionary interest of being plastic. As revealed by our study, AHs are especially plastic for their P content, either when growing on P rich resources or when receiving short-term P inputs. Recently, Mason Jones *et al.* (2021) suggested that this storage might be essential for mitigating against stoichiometric imbalances frequent in nature, these constraints being especially strong for decomposers decomposing litters with generally extremely high C:nutrient ratios. In our study, we wanted to verify if nutrient storage could give a competitive advantage by increasing fungal growth rates when colonising a new, nutrient poor medium (H5). Contrary to our expectations, mycelium transplanted from a nutrient rich media did not grow faster on nutrient poor media than mycelia coming from the other treatments. Only systematic differences between AH species were found, confirming what was observed in the main experiment. This observation must be taken cautiously since we did not use exactly the same protocol for measuring fungal growth rates between the initial cultures and the transplantation test (with and without cellophane, respectively), and absence of radial growth rate differences does not mean that fungal biomass growth rate was unaffected. However, even if it was not quantified, we did not observe any strong difference in mycelium density between the different treatments. Also, since different growth strategies were observed in the 4 AH taxa used in this experiment, the absence of such an effect on all tested taxa seems to confirm that nutrient stored

were not sufficient to provoke large differences in fungal growth rates. Only TEMA and HULU seemed to have slightly but significantly higher growth rates when mycelia came from the nutrient pulse treatment, and this whatever the receptor media type. This observation questions again the form of nutrient stored by fungi and its influence on the temporal dynamic of their remobilisation when required by fungi. Also, since no clear advantage on growth has been evidenced, alternative hypotheses may be proposed. In particular, would it be possible that storage of nutrients in excess allows reducing toxicity risks for some compounds? Or could it be involved in the reduction of the competition with other taxa requiring more nutrients? This would be particularly the case for outcompeting bacterial decomposers which have higher P-requirements than fungi (Danger, Gessner and Bärlocher 2016). This way of outcompeting bacteria – or other fungal taxa requiring more nutrients than they do – through nutrient immobilisation would be a complementary strategy to antibiotic production. Even if it has, to our knowledge, never been tested on microorganisms, this strategy has already been proposed theoretically as a strategy used by organisms to outcompete taxa with higher nutrient demands (de Mazancourt and Schwartz 2012). These hypotheses would deserve further investigations to understand in more details what are the real costs of nutrient storage and what advantages they bring to organisms using this strategy?

5. Conclusion

To conclude, our study has provided evidence supporting that aquatic hyphomycetes are largely plastic for phosphorus, and that plasticity in N content might be dependent on taxa. Also, elemental plasticity of mycelium may largely vary depending on its age, actively growing mycelium being stoichiometrically more constrained than older one. Finally, our study failed to demonstrate that nutrient storage – at least P that varied more than N – gives any advantage in terms of growth when colonising a new, nutrient depleted medium. This study should

encourage future works on characterisations of the stoichiometric traits for more AH taxa. All our results underline that more data are required to fully understand the mechanisms and the consequences of such nutrient storage, not only for tackling questions on microbial community ecology but also for investigating the roles of fungi in ecosystem functioning and nutrient cycles in interaction with bacteria.

CHAPTER II

Dissolved N:P Ratios Control the Nutrient Immobilisation vs. Mineralisation Balance During Leaf Litter Decomposition by Aquatic Hyphomycetes

In the last chapter, we have learned that aquatic hyphomycetes are more plastic for P than for N when it comes to their growth, and their plasticity depends on the taxa considered. In this chapter, instead of measuring fungal growth on culture plates with solid culture media with different N:P ratios, we looked at fungal growth and activity through an experiment of leaf litter decomposition along a gradient of N:P ratios. Following the nutrient dynamics during decomposition also allowed to test if dissolved N:P ratio was an important determinant of nutrient immobilisation vs. mineralisation balance.

Abstract

Inorganic nutrient enrichment stimulates plant litter decomposition by aquatic hyphomycetes (AH), but AH are rather flexible in their nutrient requirements. Studying the outcome of litter decomposition by AH under different nutrient availabilities can thus be challenging. Effects of internal N:P ratios on plant litter and those of dissolved inorganic nutrients on the decomposition of plant litter could thus be modulated by the elemental plasticity of decomposers present on the litter and the diversity of decomposers communities.

In this study, we tested the effects of N:P ratios and fungal diversity on the amounts and temporal dynamics (after 13, 26 and 40 days) of N and P immobilisation and mineralisation during alder leaves decomposition. Five common AH species and their assemblage were compared along a gradient of 8 dissolved N:P ratios with varying P quantity. Leaf litter mass loss remained unaffected by N:P ratios but it was significantly different between AH species. Mixing the 5 AH species did not increase leaf litter decomposition. Response of fungal biomass to N:P ratios were also significantly different between AH species and also between species and their assemblage. N and P immobilisation followed our expectations along the N:P ratios. Net N uptake on leaf litter was significantly affected by both AH species and by the N:P ratio. The decomposition speed of litter by the AH assemblage significantly slowed down after 26 days, while fungal biomass significantly increased between each sampling date but only for the lowest N:P ratios. Finally, single species stoichiometric traits partly explained species dominance in the AH assemblage, but other traits should be accounted for further understanding of the determinism of fungal community structure on decomposing leaf litter.

Key words:

Aquatic hyphomycetes, nutrient availability, N:P ratios, nutrient immobilisation, nutrient mineralisation, leaf litter, decomposition, temporal dynamic, fungal diversity

1. Introduction

Over 80 % of earth's biomass is composed of plant (Bar-On, Phillips and Milo 2018). Despite its huge quantity and basal position in numerous trophic chains, plant-origin living biomass is only weakly transferred up to higher levels (herbivores), resulting in a large portion of this biomass ending up in a reservoir of dead vegetal organic matter (Cebrian 1999). Microbial decomposers come into play at this stage to break down the plant litter and recycle organic nutrients back into environment under inorganic form. This is especially important since a large proportion of primary producers rely on ammonium (NH_4^+) and/or nitrate (NO_3^-) to meet their N demands (Waring and Running 2007) —although some plants can also depend on nitrogen-fixing-bacteria to satisfy part of their N demand. For this reason, plant litter decomposition is considered as a crucial process in ecosystems (Lindeman 1942). Moreover, plant detritus is particularly important and known as the dominant energy and nutrient source for numerous aquatic ecosystems (Leroux and Loreau 2008).

One of the primary locations for plant litter breakdown and nutrient cycling among aquatic systems are forested headwater streams. Situated at the upper part of watersheds, these ecosystems are essential for maintaining the functions of whole river networks (Alexander *et al.* 2007). For forested headwater streams, leaf litter originating from riparian forests is the main carbon input in the water column (Fisher and Likens 1973; Vannote *et al.* 1980). Plant litter is also a main food source for aquatic detritivores, but since plant litter is generally nutrient poor (Moore *et al.* 2004; Martinson *et al.* 2008), detritivores often prefer partially decomposed litter by microbial decomposers (Bärlocher 1985). Microbial conditioning indeed improves leaf litter nutritional quality for detritivores, leading to nutrient content improvements (Bärlocher 1985; Danger *et al.* 2013). Exoenzymes secreted by microorganisms can also help to facilitate digestion of recalcitrant organic carbon (Bärlocher 1982; Sinsabaugh *et al.* 1985; Graça and Cressa 2010).

Plant litter decomposition in freshwater has long been studied and this process is known to be controlled by multiple factors, such as temperature, diversity of decomposers or nutrient availability (Schindler *et al.* 2009; Gessner *et al.* 2010; Geraldes, Pascoal and Cássio 2012; Jabiol *et al.* 2019). In particular, a metanalysis on nutrient enrichments stimulate plant litter decomposition by microorganisms showed that the input of both nitrogen (N) and phosphorus (P) has stronger effects than the input of either N or P alone (Ferreira *et al.* 2015b). Interestingly, the impact of available N:P ratios on this process is still not well understood (but see Güsewell and Gessner 2009). One reason could be that microbial decomposers have highly flexible nutrient requirements, as much at the species level (bacteria: Makino *et al.* 2003; fungi: Danger and Chauvet 2013) than at the community level, at least partially contributed by species replacements along N:P gradients (Danger *et al.* 2008). Despite these observations, most models studying decomposition and microbial nutrient recycling have assumed that decomposers elemental ratios were constant (e.g. Daufresne and Loreau 2001). Effects of internal N:P ratios on plant litter and those of dissolved inorganic nutrients on the decomposition of plant litter could thus be modulated by the elemental plasticity of decomposers present on the litter and the diversity of decomposers communities.

Among microbial decomposers, fungi are known for their abilities to decompose dead organic matter. As all living organisms, these decomposers must acquire nutrients in definite proportions to ensure their optimal growth and activity (Güsewell and Gessner 2009). For this reason, while breaking down organic matter, fungi incorporate simultaneously elements present in the material they decompose and dissolved inorganic nutrients from their environment to meet their elemental requirements (e.g. N and P). This incorporation of dissolved inorganic nutrients is generally referred to as microbial immobilisation (*sensu* Daufresne and Loreau 2001, see Figure.II.1). These nutrients are then used to build fungal biomass and synthesise exoenzymes which are subsequently secreted to decompose litter detritus. In contrast

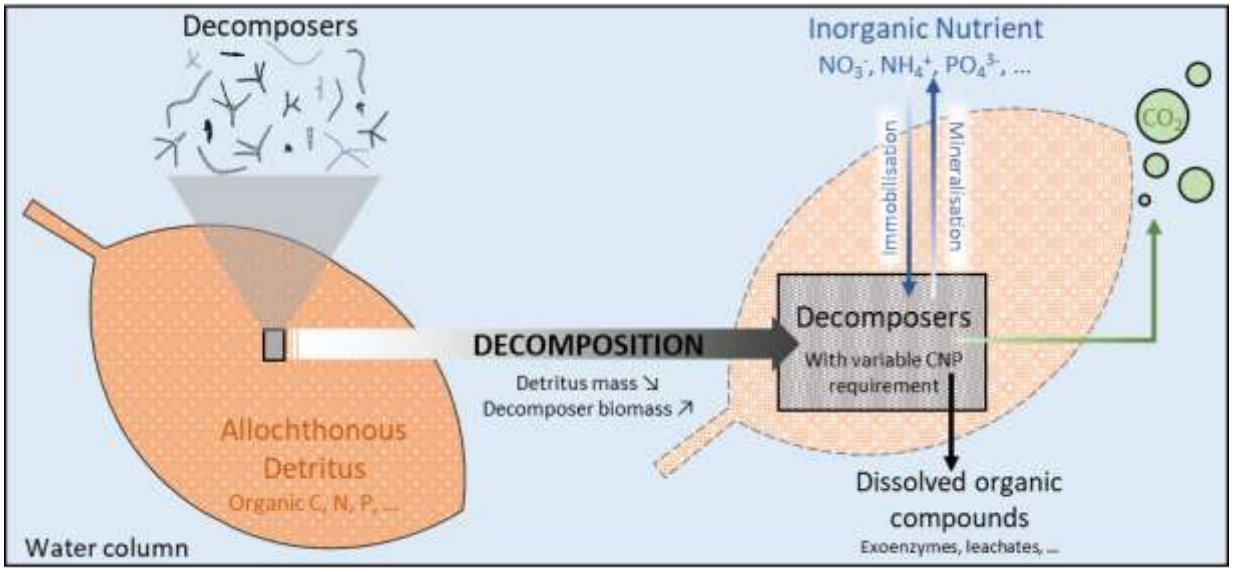

Figure II 1. Schematic representation of litter decomposition and nutrient cycles in freshwater streams.

Decomposers colonise leaf litter (allochthonous detritus) in streams and start the decomposition process. While reducing litter mass, decomposers gain in biomass by simultaneously breaking down organic matter and incorporating dissolved nutrients (nutrient immobilisation) to meet their elemental requirements. During decomposition, nutrients in sufficient amounts are released back into the stream under inorganic forms and/or simpler dissolved organic forms.

with immobilisation, mineralisation is the process where nutrients in organic compounds breaks down into soluble inorganic forms and returns to the environment (Figure.II.1). Leaf litters generally have higher C:N and C:P ratios than fungi (Cross *et al.* 2015; Danger, Gessner and Bärlocher 2016; Jabiol *et al.* 2019). As a result, fungal decomposers should theoretically privilege N and/or P immobilisation when those nutrients are limited in the detrital resource they decompose, and mineralisation should occur only when those nutrients are in sufficient amounts, following Ecological Stoichiometry predictions (Daufresne and Loreau 2001). Surprisingly, few studies have looked at the balance between immobilisation and mineralisation of N and P during litter decomposition mediated by microbial decomposers in freshwater (e.g. Cheever, Kratzer and Webster 2012), and data on the role of available N:P ratios on the intensity and the temporal dynamics of these two processes are scarce.

In this study, we were interested in the effects of available N:P ratios and fungal diversity on the amounts and temporal dynamics of N and P immobilisation and mineralisation during alder

(*Alnus glutinosa*) leaves decomposition. For this purpose, we tested the decomposition process ensured by 5 common aquatic hyphomycetes (AH) taken individually and together in mixed cultures, along a gradient of 8 N:P ratios with a constant concentration of N-NO_3^-, and a decreasing concentration of P-PO_4^{3-}. We hypothesised that (1) fungal biomass increases along the P gradient until reaching a certain N:P ratios where N becomes limiting, (2) this N:P ratio would be dependent on each individual fungal strain or the mixture of those strains. Also, (3) P-PO_4^{3-} uptake, N-NO_3^- immobilisation and N mineralisation (in the form of NH_4^+) would depend on the P gradient, and 4) the net N mineralisation would only occur after an acute phase of NO_3^- immobilisation. Temporal dynamics of fungal biomass as well as those of N and P uptakes, and NH_4^+ releases were also assessed on the fungal mixed culture, after 3 different decomposition durations.

2. Materials and Methods

2.1. Material

Alder (*Alnus glutinosa*) leaves were collected during autumn 2019 in the riparian zone of the La Maix stream, a 2nd order headwater stream located in the Vosges mountains, northeast France (latitude 48°29’2.56″N, longitude 7°4’10.75″E). Nets were hanged 1 m above ground to collect falling leaves and avoiding a contact between leaves and soil. Leaf litter was retrieved at a 1- or 2-weeks maximal interval. Leaves were air dried at room temperature in the lab, then stored prior to use. Leaves were moisturised before being cut with a cork borer into discs of 12 mm Ø. When cutting, central veins were avoided, and discs were centred on secondary veins. 40 sets of 15 leaf discs were weighted to deduce an average dry weight of a single disc, which was 4.82 mg (mass before leaching).

The 5 aquatic hyphomycetes (AHs) used for the leaf disc decomposition experiment were *Articulospora tetracladia* (ARTE), *Clavariopsis aquatica* (CLAQ), *Heliscus lugdenensis* (HULU), *Tetracladium marchalianum* (TEMA), and *Tricladium spelendens* (TRSP) previously isolated in our lab from different forested headwater streams. Small pieces (25 mm^2) of mycelium coming from colonies' fringes growing on agar plates (Malt Agar with 20 g L^{-1} of agar and 10 g L^{-1} of malt extract) were cut and put into Erlenmeyer flasks with 30 ml of sterilised distilled water. Spores production was induced by putting the flasks under agitation at 12 °C for no longer than 72 h. After filtration of an aliquot of spore suspension on nitrocellulose filters (Millipore MF™ 5.0 µm SMWP02500), spore densities were evaluated for each species through counting under optic microscope after Trypan Blue (0.05 %, in 60 % lactic acid) staining (Bärlocher 2020).

2.2. Experimental setup

Culture solutions were prepared using a medium derived from the COMBO mineral medium (Kilham *et al.* 1998), and modified to obtain a gradient of 8 different levels of P while maintaining a constant quantity of N, thus creating a gradient of dissolved N:P ratios. The final media contain 0.001 M of $CaCl_2 \cdot 2H_2O$, $MgSO_4 \cdot 7H_2O$, $NaHCO_3$, Na_2SiO_3 and H_3BO_3, 67.36 mg L^{-1} of KNO_3 (or 9.33 mg L^{-1} of N) and either 10, 5, 2.5, 1, 0.4, 0.16, 0.064 or 0.0256 mg L^{-1} of $P\text{-}PO_4^{3-}$. achieved from a mixed solution of KH_2PO_4 and K_2HPO_4 (3.85:6.15 v/v, for keeping pH close to 7). The molar N:P ratios obtained for the final culture media were 0.4 (R1), 0.8 (R2), 1.7 (R3), 4.2 (R4), 10 (R5), 26 (R6), 66 (R7), and 164 (R8). Note that NO_3^- was the only source of mineral N in our media, in order to be able to quantify the N mineralised by fungal activity under the form of NH_4^+. Subsamples of the initial culture media were conserved at 4 °C for further chemical analyses of PO_4^{3-}, NH_4^+ and NO_3^-.

To ensuring the fungal colonisation step, leaf discs were separated into 1 set of 200, 5 sets of 400 and 2 sets of 600 discs, in adequate-sized-Erlenmeyer flasks and submerged in MilliQ ultrapure water (MQ water), and then sterilised by autoclaving (120 °C, 30 min). After cooling down, discs were rinsed twice with clean sterilised MQ water, then kept in fresh MQ water at 4 °C until experimental setup. We assume that most of the soluble carbon and nutrient of leaf discs were eliminated at this stage, and the average mass for a single disc after this step is 4.79 mg (99.3 % of the initial mass before leaching) (as described in Danger *et al.* 2013).

To ensure all leaf discs were colonised under homogeneous conditions, all leaf discs were inoculated before the main experiment. Water in each set of leaf discs was drained and replaced with COMBO mineral solution without any N nor P source. Each set of 400 discs was inoculated with 1000 spores with each of the 5 AH species. Each of the 2 sets of 600 discs was inoculated with 300 spores of each of the 5 AH species, resulting in a total of 1500 spores for the Mix culture – ensuring a similar total number of spores per leaf disc in single species and in the Mix treatment. The colonisation took 8 days under agitation at 12 °C. The set of 200 leaf discs followed the same treatment but was not inoculated with any spore and served as control.

After the colonisation, each set of discs was rinsed with sterilised MQ water, then 14 discs were added to individual 100 ml Erlenmeyer flask containing 28 ml of the culture media with one of the N:P ratios. In total, 24 flasks (3 replicates for each N:P ratio, 1 sampling date at 40 days) were prepared with leaf discs colonised with each of the 5 AH species and 72 flasks (9 replicates in total for each N:P ratio, with 3 replicates stopped on 3 sampling dates – at 13, 26, and 40 days) were prepared with leaf discs colonised with the Mix treatment. 8 control flasks were also prepared with uncolonised leaf discs (one for each N:P ratio without replicate). All flasks were then incubated at 15 °C under agitation and in the dark. Each flask contains in average, a total of 67.5 mg (mass before leaching) of leaf discs.

2.3. Sample collection and chemical analyses

For comparing the effects of N:P ratios in culture media and the effects of AH diversity on N and P immobilisation and mineralisation, all samples of single strains and a set of 3 replicates of the Mix treatment (containing a mixture of the 5 AH strains) were collected after 40 days of experiment. In order to understand temporal dynamics of N and P immobilisation and mineralisation, additional samples of the treatment were also collected after 13 and 26 days of experiment (3 replicates per N:P ratio per date). Partially decomposed leaf discs were immediately rinsed with deionised water then frozen at -20 °C before being freeze-dried prior to analyses. Culture media were collected and stored at 4°C for a maximum of 24 hours before analyses.

Leaf disc mass losses were measured from 8 freeze-dried discs to the nearest 0.1 mg and after subtracting fungal mycelium biomass as measured through ergosterol quantification. Ergosterol content was analysed from 4 of the freeze-dried discs by following a standard method (Gessner 2020), and total N and P on discs were quantified on the other 4 freeze-dried discs, previously ground with a bead beater. For N quantification, 1 mg of samples aliquot powder was encapsulated in tin capsules and analysed with a CHN elementary analyser (Carlo Erba NA2100). For total P quantification, 1 mg sample powder was first mineralised in a solution of NaOH (0.1 N) and $Na_2S_2O_8$ (29.75 g L^{-1}), autoclaved at 120 °C for 2 hours. Then, P concentrations were measured from the digested liquid with the molybdate blue colorimetric method (NF EN ISO 6878) using a spectrophotometer. Concerning culture media, NO_3^-, NH_4^+ and PO_4^{3-} concentrations were measured after each sampling date (13 and 26 days for the Mix, and 40 days for all treatments). Concentrations of NO_3^- were determined with ion chromatography (Dionex ICS 3000, column AS11-HC), and concentrations of NH_4^+ and PO_4^{3-} were quantified with colorimetric methods (NF ISO 7150, NF EN ISO 6878) using a spectrophotometer.

Fungal biomass was estimated from ergosterol measurement. Ergosterol was extracted from leaf discs and measured with HPLC following a standard protocol (Gessner 2020). To avoid using a single conversion factor from the literature (Gessner and Chauvet 1993; Brosed, Jabiol and Gessner 2017) and increase the accuracy of mycelium biomass estimations in our study, we choose to measure species specific conversion factors for each of our 5 AH species. Briefly, each AH strain ergosterol to biomass conversion factor was obtained by extracting this compound from pure mycelium of the 5 AH strains previously grown in liquid media (as in Danger and Chauvet 2013). Mycelium was rinsed, freeze-dried, and ergosterol was extracted and analysed using the same ergosterol quantification protocol as the one used for leaf discs. AH strain specific conversion factors are 5.2, 5.2, 1.8, 6.1, and 8.9 (µg ergosterol per mg of dry mycelium) for ARTE, CLAQ, HULU, TEMA, and TRSP, respectively. Consequently, individual strain biomass was estimated with corresponding conversion factor. For the Mix treatment, we assumed a positive correlation between ergosterol and DNA concentration for each strain (Baudy *et al.* 2019), and we have applied the specific conversion factor for each strain proportionally used the relative proportion of each strain obtained by specific real-time PCR (see below).

2.4. Strain specific primer pairs and probes design for real-time PCR

One of the aims of this study was also to evaluate the impact of dissolved N:P ratios on species assemblages in the mixture, hypothesising that species with different stoichiometric optimal ratios would be selected along the N:P gradient. To reach this goal, we had to quantify, as accurately as possible, the relative abundance of each strain on leaf discs in the Mix treatment. For this purpose, we developed real-time PCR assays targeting ITS region specific to our strains using TaqMan probes.

First, we sequenced ITS regions of our 5 AH strains. For this, REDExtract-N-Amp™ Plant PCR Kit protocol (Sigma Aldrich) was applied for each strain's DNA extraction individually from pieces of mycelium on malt-agar plate (0.25 cm²) and PCR amplification using universal ITS1-ITS4 primers (covering ITS1, 5.8S and ITS2). The amplification mix was prepared in 25 µl with: 0.5 µl of Dimethyl sulfoxide (DMSO); 0.25 µl of 0.3 % bovine serum albumin (BSA); 12.5 µl of REDExtract-N-Amp PCR ReadyMix; 0.6 µl of each primer (10 mM); 9.55 µl of DNA-free distilled water and 1 µl of template DNA (or distilled water for negative control). 35 cycles of amplification at 54 °C (annealing temperature) were performed. These PCR products were then sent to Eurofins Genomics for Sanger sequencing, and taxonomic affiliation of the 5 AH strains was confirmed by BlastN (NCBI, Schoch *et al.* 2020).

Table II 1. Primer pairs (targeting ITS region) and specific TaqMan probes used for real-time PCR of the five AH strains.

Name	Sequence
Articulospora tetracladia	
Forward	AGGCACCAATACCAAGCG
Reverse	GCCCTGTGGTATTCCGCA
Probe	[6-FAM]-CTTGATGGGTTGAAATGA-[MGBNFQ]
Clavariopsis aquatica	
Forward	GAGAGGCTTAATGCAAGGAGGTA
Reverse	AATTCATTGGCAGCCGGTAT
Probe	[6-FAM]-ACTGGATCGTGACACA-[MGBNFQ]
Heliscus lugdunensis	
Forward	CCGAGGTCAACCTTTCAGAAGT
Reverse	TGTAGCTTCCTCTGCGTAGTAGCA
Probe	[6-FAM]-GCTTTCCAGTGCGA-[MGBNFQ]
Tetracladium marchalianum	
Forward	GTTCTGGCGAGTGTCCATCA
Reverse	GCTGTCAGGCTCTAAGCGTAGTAA
Probe	[6-FAM]-GTGTCTGTAGCGAGAGAG-[MGBNFQ]
Tricladium spelendens	
Forward	CCTGTAGCGAGAAGATTT
Reverse	CCTGTTCGAGCGTCATTATA
Probe	[6-FAM]-TGCCCAAGACCCAG-[MGBNFQ]

Specific PCR primers (ITS region) and TaqMan® probes (Eurofins Genomics) were then designed (Table.II.1) based on Baudy *et al.* (2019) with adaptations to our strains (based on strain ITS sequences, see above). TaqMan® probes contain the fluorescent reporter dye 6-carboxyfluorescein (6-FAM) on the 5' end and the non-fluorescent quencher (MGBNFQ) on the 3' end. Primers and probes were tested for their specificity on each strain in a crossover

manner for strain specific real-time quantitative PCR (qPCR). Total DNA was then extracted from 2 leaf discs of the Mix treatment cultures at each sampling date using DNeasy PowerSoil Kit (Qiagen) and following the manufacturer's protocol. qPCR reactions were prepared in 20 µl volume consisted of 10 µl iTaq Universal Probe Supermix (BioRad), 2 µl of each primer (940nM final concentration), 0.5 µl of probe (260 nM final concentration), 0.4 µl of 3 % BSA, 0.2 µl of DMSO, 0.08 µl of T4gp32 (MP Biomedicals), 3.82 µl of sterile MilliQ water and 1 µl of template DNA, ten-time dilutions (from 10^8 to 10^2 copies μl^{-1}) of standard plasmids prepared as described in Cébron *et al.* (2008), or sterile DNA-free water for negative control. The qPCR assays were performed using CFX96 apparatus (BioRad) running a 2-step amplification protocol (50 cycles with denaturation for 30s at 95 °C and hybridisation, extension, and fluorescence acquisition for 30 s at 60 °C). Data for each AH strain were expressed as % of total gene copy number of the 5 stains, allowing the comparison of the relative abundances of each strain on the leaf discs on each sampling date of the Mix treatment. Note that strain specific PCR was only performed for the Mix treatment but not for the treatments with strains individually.

2.5. Statistical analysis

All statistical analyses were carried out with the "stats" package in R software v 4.2.1 (R Core Team 2022) using R Studio (RStudio Team 2022). To test the effects of AH species and N:P ratios on fungal biomass, leaf disc decomposition as well as nutrient dynamics – both on leaf litter and in the culture medium, analyses of variance (ANOVA) and Kruskal-Wallis (when data did not meet ANOVAs assumptions) was applied. To quantify nutrient dynamics on leaf discs, net N and P uptakes were calculated as the absolute quantities of N and P (in mg) gained (if > 0) or lost (if < 0) on leaf discs by subtracting to each N and P quantification, on each date and for each ratio, the N and P contents measured on control leaf discs. These data were then

analysed using ANOVA to evaluate the effects of AH strains, water N:P ratios, and their interactions. *P*-value < 0.05 were considered as the significance threshold for all analyses.

3. Results

3.1. Individual strain and their mixed culture after 40 days

After 40 days of decomposition, there were no significant differences in alder leaf disc mass loss among the 8 N:P ratios for a given AH strain or the Mix (one-way ANOVA, all $P > 0.05$). In contrast, leaf disc mass loss was affected by the strain species, and this effect was dependent on the N:P ratio (Significant strain × N:P ratio interaction, Figure.II.2a). The mass loss of alder leaf discs ranged between 18 % (TRSP) and 33 % (HULU) of their initial mass (before leaching), and reached 24 % for the Mix treatment, which was not significantly different from what was observed for TRSP, ARTE and CLAQ.

Fungal biomass was dependent on both N:P ratios, strains (Kruskal-Wallis, between ratios $P < 0.001$; between strains $P < 0.001$, Figure.II.2b), and the interaction between both factors ($P < 0.001$). For HULU and TRSP, mycelium biomass was maximised at ratio R1 (ca. 0.4, low N:P ratio) and gradually decreased with increasing ratio, while it was maximised between R2 (0.8) and R4 (4.2) for others. The minimal fungal biomass measured was at ratios R6 (26) to R8 (164) for all strains, with values ranging between 1.2-12.8 mg g^{-1}, and even below the detection limit for HULU at R7 (66).

There was initially 9.33 mg L^{-1} of $N\text{-}NO_3^-$ in each flask. After 40 days of decomposition, for ARTE, CLAQ, HULU, and the Mix, almost the totality of initially added N was no longer detectable from R1 (0.4) up to R3 (1.7) (to R4 (4.2) for CLAQ), while for TEMA and TRSP there was still 0.5 mg L^{-1} of $N\text{-}NO_3^-$ remaining at these ratios. From R4 (4.2) to R8 (164), the remaining $N\text{-}NO_3^-$ increase regularly along the increasing N:P ratios. Analyses did not reveal

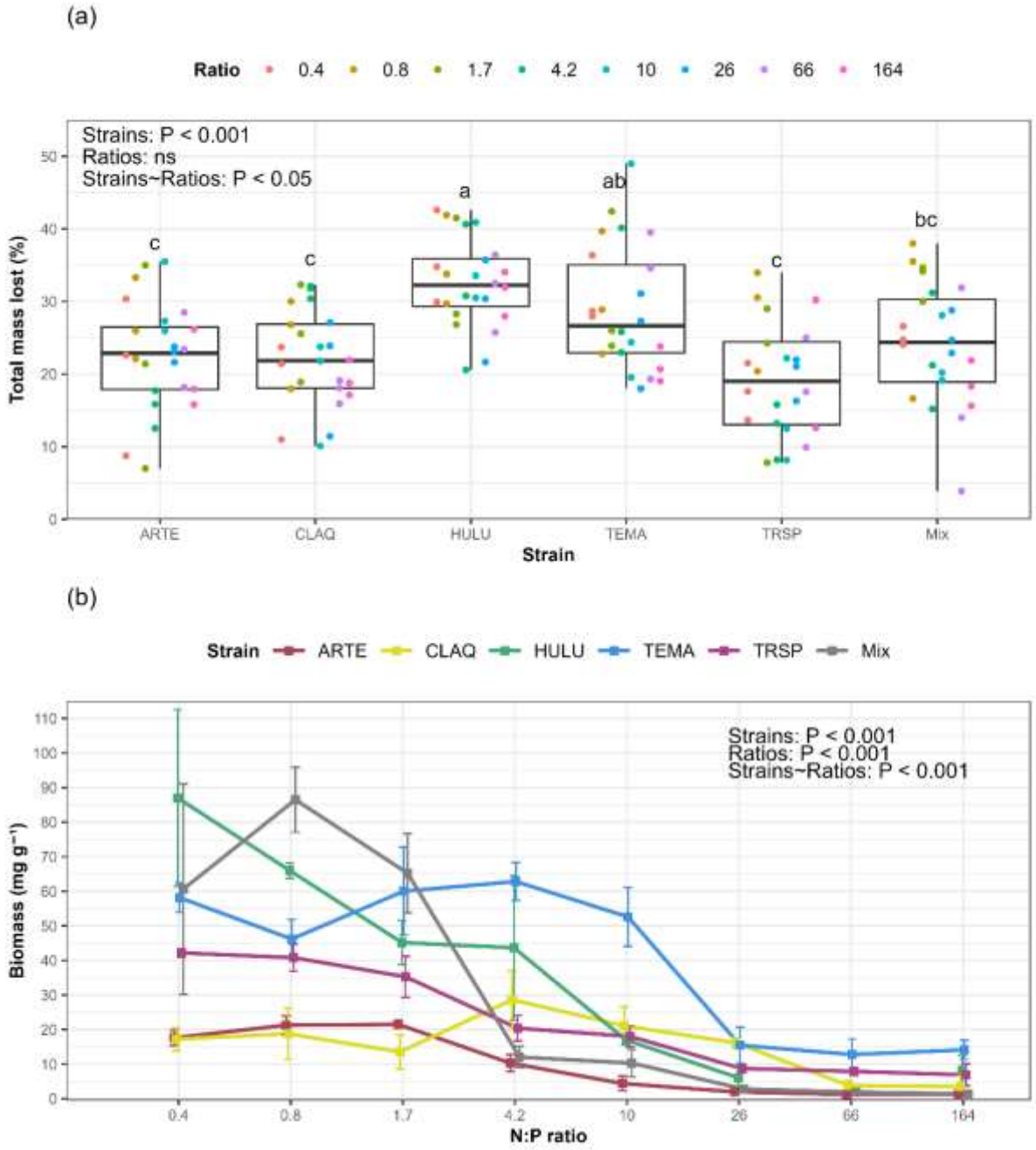

Figure II 2. (a) Leaf mass losses observed after 40 days of decomposition. (b) Fungal biomass measured on leaf discs.

(a) These values were calculated in comparison with initial leaf discs mass and after subtracting the measured fungal biomass of each replicate. *P*-values from ANOVA analyses. **(b)** calculated with strain specific ergosterol to biomass conversion factors. Mean values (n=3) ± SE The missing point for HULU at R7 (66) was due to ergosterol values under detection limits. *P*-values correspond to the results of Kruskal-Wallis tests.

any significant difference between strains concerning the remaining NO_3^- (Kruskal-Wallis, P = 0.8), while differences were significant between ratios (Kruskal-Wallis, $P < 0.001$; Wilcox, $P < 0.05$ except between R1 (0.4), R2 (0.8), and R3 (1.7) with each other). The differences were

also significant between combinations of strains and ratios (Kruskal-Wallis, $P < 0.001$), especially for CLAQ, which always led to lower remaining concentrations than other strains for a same ratio (Figure.II.3a).

At the beginning of the experiment, there was no $N\text{-}NH_4^+$ in the culture medium in order to quantify N mineralisation without any bias: the presence of $N\text{-}NH_4^+$ was only due to the metabolic activities of fungi. After 40 days of decomposition, $N\text{-}NH_4^+$ release was only detected at very low quantity (< 0.01 mg L^{-1}). The effect of N:P ratios, strain type, and their combinations all had significant influences on NH_4^+ releases (Kruskal-Wallis, all $P < 0.001$).

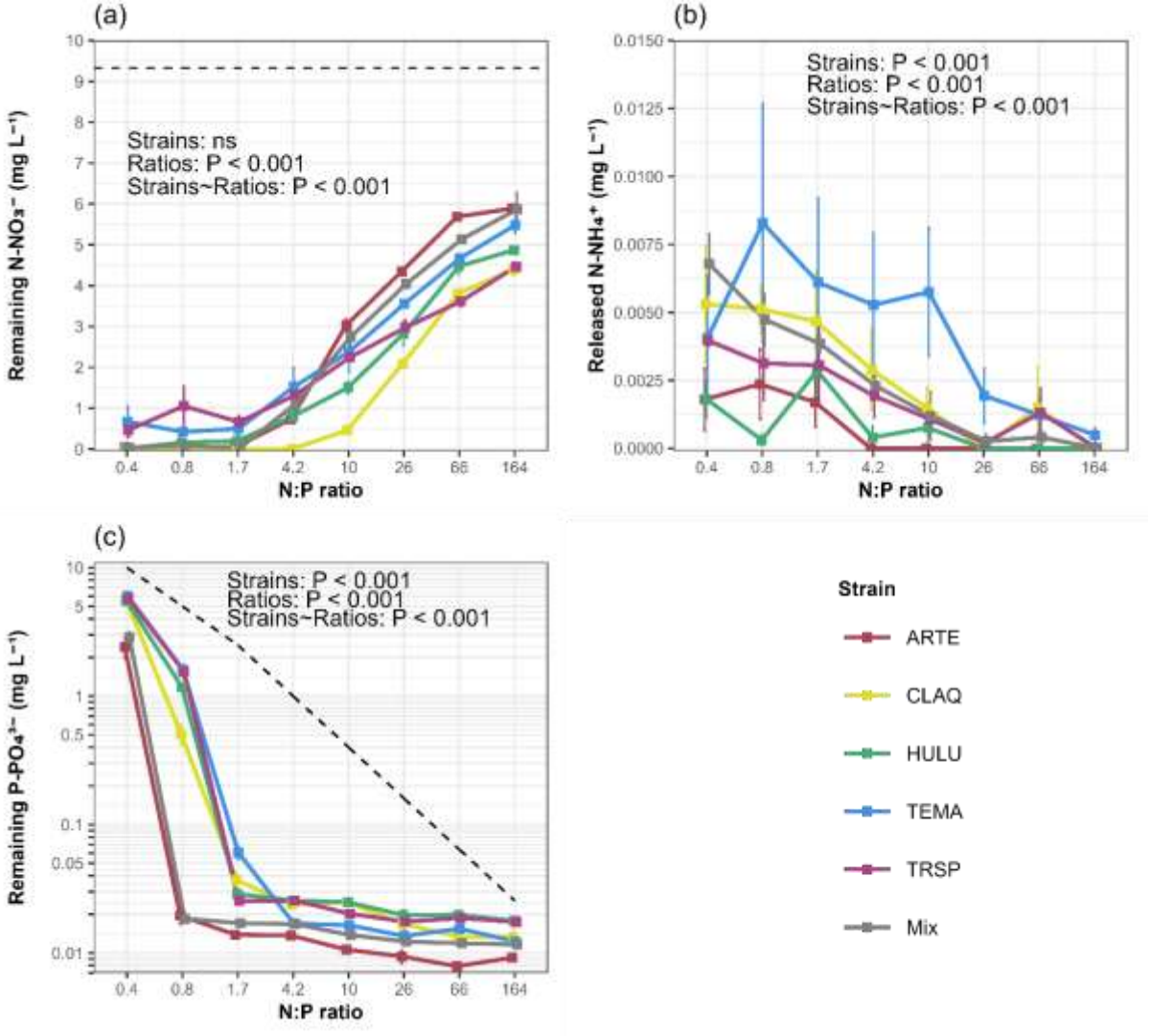

Figure II 3. (a) Remaining $N\text{-}NO_3^-$, (b) released $N\text{-}NH_4^+$ and (c) remaining $P\text{-}PO_4^{3+}$ for each of the 5 AH strain and the Mix treatment, across N:P ratios. Dashed lines in panels **(a, c)** show the starting quantities of N and P at each ratio. Mean values (n=3) ± SE. *P*-values from Kruskal-Wallis.

Most of them (except for HULU) were negatively related to the N:P ratios, with the highest releases occurring at the lowest N:P ratios (0.4 and 0.8) (Figure.II.3b).

The initially added quantities of $P\text{-}PO_4^{3-}$ in each flask ranged from 10 mg L^{-1} to 0.0256 mg L^{-1} from R1 (0.4) to R8 (164). The quantities remaining in the media at the end of the experiment showed similar profiles for all strains along the N:P ratio gradient. Generally, there were between a maximum of 2.5 mg L^{-1} and 7 mg L^{-1} left in the media at the end of the experiment for the lowest N:P ratio (0.4). Then, the P quantities drop dramatically to reach quite invariable minimum values along the N:P gradient. For ARTE and the Mix treatment, remaining PO_4^{3-} already reached their minimal values at R2 (0.8), while these minimal values were reached at R3 for CLAQ, HULU, and TRSP, and at R4 (4.2) for TEMA. The minimal quantities left in the culture media remained constant between 0.008 mg L^{-1} at R2 (0.8)/R3 (1.7) and 0.04 mg L^{-1} at higher N:P ratios. The differences were significant between ratios, strains, and between all strain-ratio pairs (Kruskal-Wallis, all $P < 0.001$, Figure.II.3c).

Net N and P uptakes on leaf discs were calculated as the absolute quantities gained (if > 0) or lost (if < 0) on leaves during decomposition. Net N uptakes were globally negative (-0.11 mg when averaging all treatments), but with mostly positive values for the lowest N:P ratios and negative values at higher N:P ratios (Kruskal-Wallis, between ratios $P < 0.05$ with significant differences shown in Figure.II.4a). Uptake was also different between strains ($P < 0.001$). Leaves colonised by HULU had on average the lowest N uptake quantities (-0.26 mg) across ratios. There were no significant interactions between strains and the N:P ratios on the net N uptake ($P > 0.05$). Net P uptakes were globally positive (Figure.II.4b) and were maximal for R1 (0.4) and R2 (0.8) - remaining all under 0.2 mg - then decreasing significantly along the N:P ratio gradient and even becoming slightly negative for the highest N:P ratios (Kruskal-Wallis, $P < 0.001$). Analyses also revealed strong significant interactions between AH strains and the medium N:P ratios on net P uptake ($P < 0.001$). Again, leaves colonised with HULU strain

exhibited the lowest net P uptake (between 0 and 0.1 mg) at each ratio compared with other strains. However there was no significant difference between strains ($P > 0.05$).

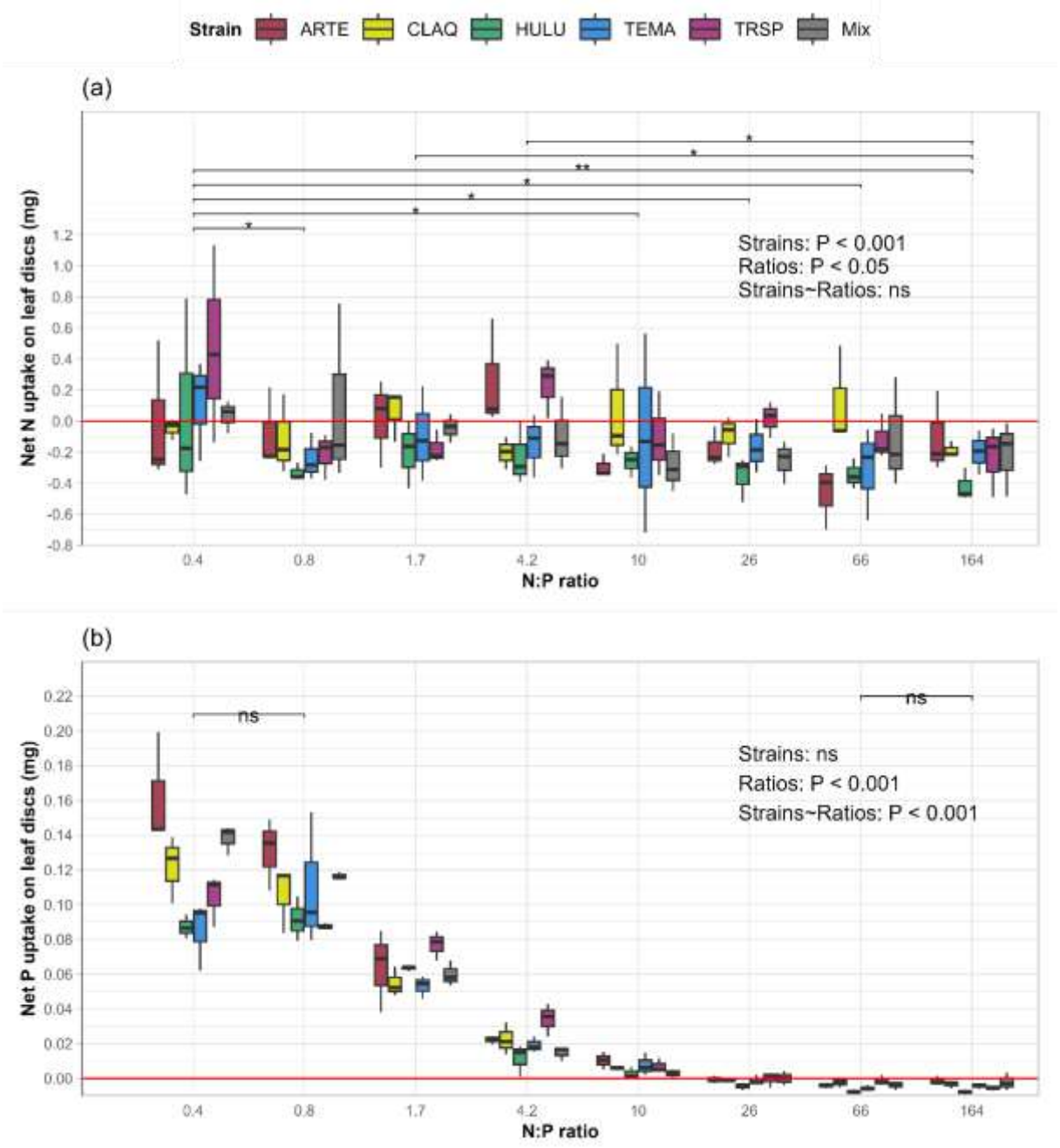

Figure II 4. Net quantities of N (a) and P (b) uptakes on leaf discs.

Baseline 0 in red was set as the N or P quantities on discs of the control group. *P*-values from Kruskal-Wallis.

3.2. Temporal dynamics of the decomposition process using the Mix treatment

Mass losses were not dependent on N:P ratios, we thus analysed all data for each sampling date together. The average total mass losses for all ratios taken together, after 13 days, 26 days and

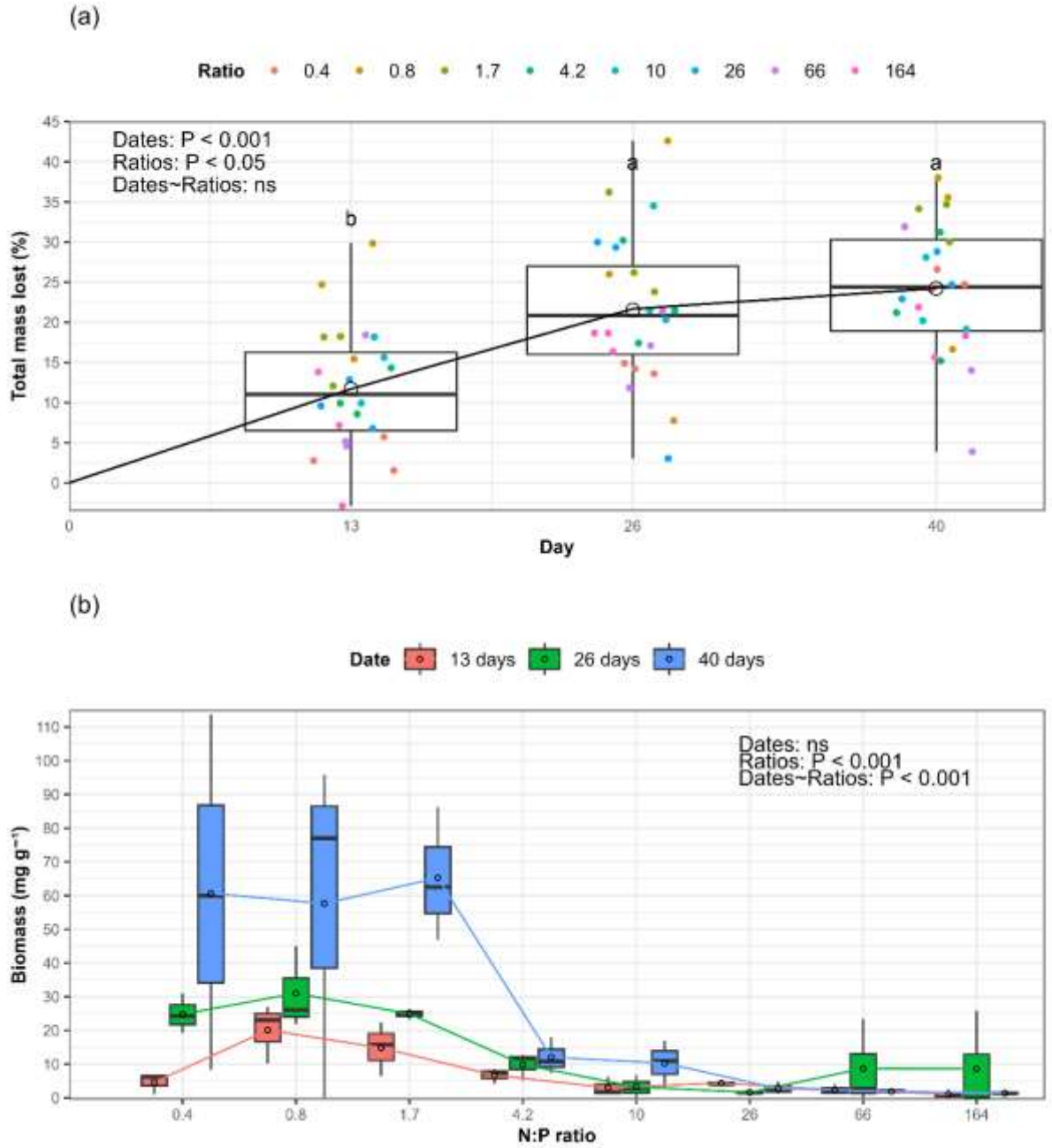

Figure II 5. (a) Temporal dynamics of leaf mass loss measured on leaf discs colonised by a mixture of 5 AH species. (b) Fungal biomass measured on leaf discs.

(a) These values were calculated in comparison with initial leaf discs mass and after subtracting the measured fungal biomass of each replicate. *P*-values from ANOVA analyses. **(b)** Calculated with strain specific ergosterol to biomass conversion factors and following the proportion of each strain from strain specific real-time PCR results (Figure.II.6). Mean values (n=3) ± SE. *P*-values correspond to the results of Kruskal-Wallis tests.

40 days were 12 %, 22 % and 24 %, respectively. Leaf mass loss significant increased between 13 days and 26 days but remained stable between 26 and 40 days (one-way ANOVA, $P < 0.001$; Figure.II.5a). Fungal biomass depended on both N:P ratios (Kruskal-Wallis, $P < 0.001$) and their combinations with sampling date ($P < 0.001$), but not solely on the date ($P > 0.1$). Biomass was significantly higher among ratios R1 (0.4) and R3 (1.7) from 13 to 40 days, while there was no more significant difference between dates from R4 (4.2) to R8 (164) (Figure.II.5b).

Strain specific qPCR revealed significant differences in the sum of ITS copy numbers between N:P ratios (Kruskal-Wallis, $P < 0.001$, Figure SII 1), between sampling date ($P < 0.05$), and between their combinations ($P < 0.001$). TEMA was the dominant strain followed by ARTE, while CLAQ was weakly detected or not detected at all (Figure.II.6). Each strain's individual copy number, except for CLAQ, was also significantly different between ratios (one-way

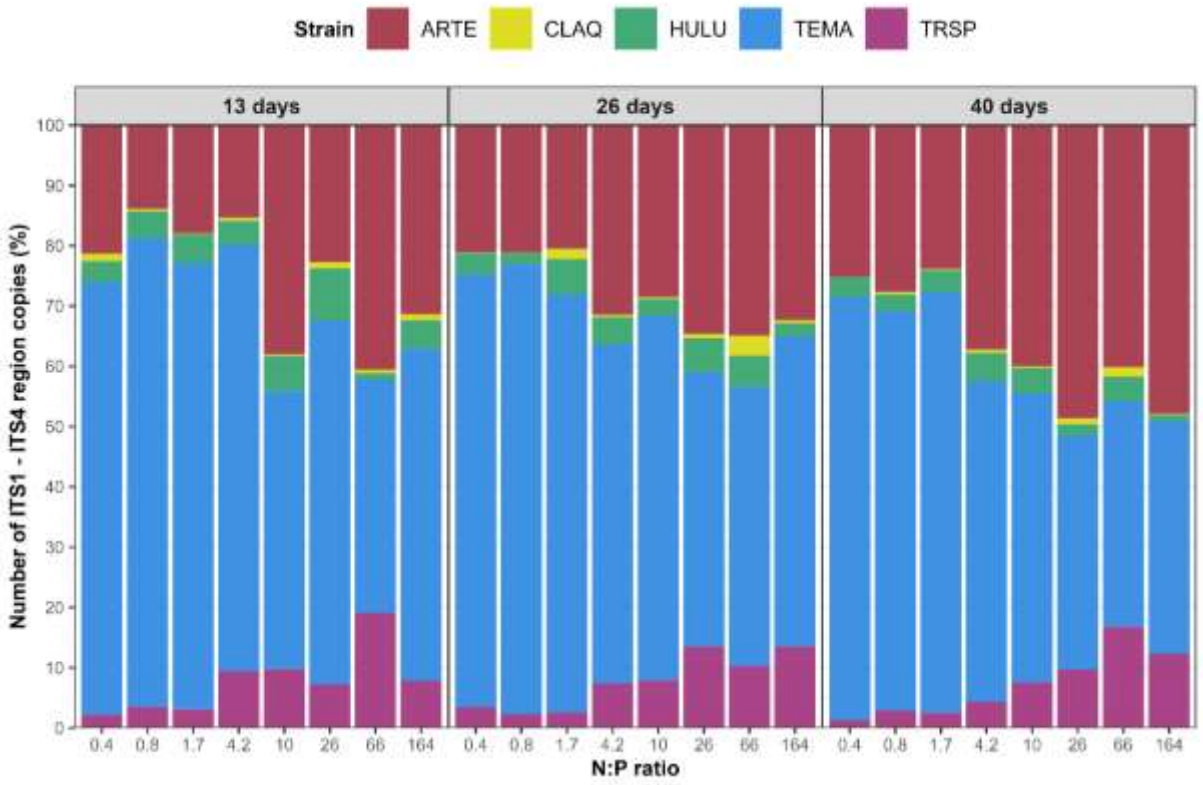

Figure II 6. Real-time PCR quantification of ITS gene copy numbers of the 5 AH strains present across N:P ratios in the Mix treatment at each sampling date (13, 26 and 40 days).

ITS gene copy numbers in the percentage of the total copy numbers (sum of the 5 strains). Total copy numbers follow the same patters across N:P ratios as for the fungal biomass (Figure.SII.1).

ANOVA, all $P < 0.05$, except for CLAQ $P > 0.05$) and sampling dates (all $P < 0.05$, except for CLAQ and HULU $P > 0.05$).

The remaining quantities of $N\text{-}NO_3^-$ and $P\text{-}PO_4^{3-}$ after each date significantly differed between ratios (Kruskal-Wallis, both $P < 0.001$), but analyses revealed no significant differences between the different dates on these parameters (both $P > 0.1$). From R1 (0.4) to R3 (1.7), no $N\text{-}NO_3^-$ remained in the culture after 13 days. From R4 (4.2) to R7 (66), the remaining $N\text{-}NO_3^-$ increased with the medium N:P ratio until it reached a maximum at R7 (66) and R8 (164) with about 5.5 mg of $N\text{-}NO_3^-$ remaining (Figure.II.7a). The quantity of remaining $P\text{-}PO_4^{3-}$ drastically

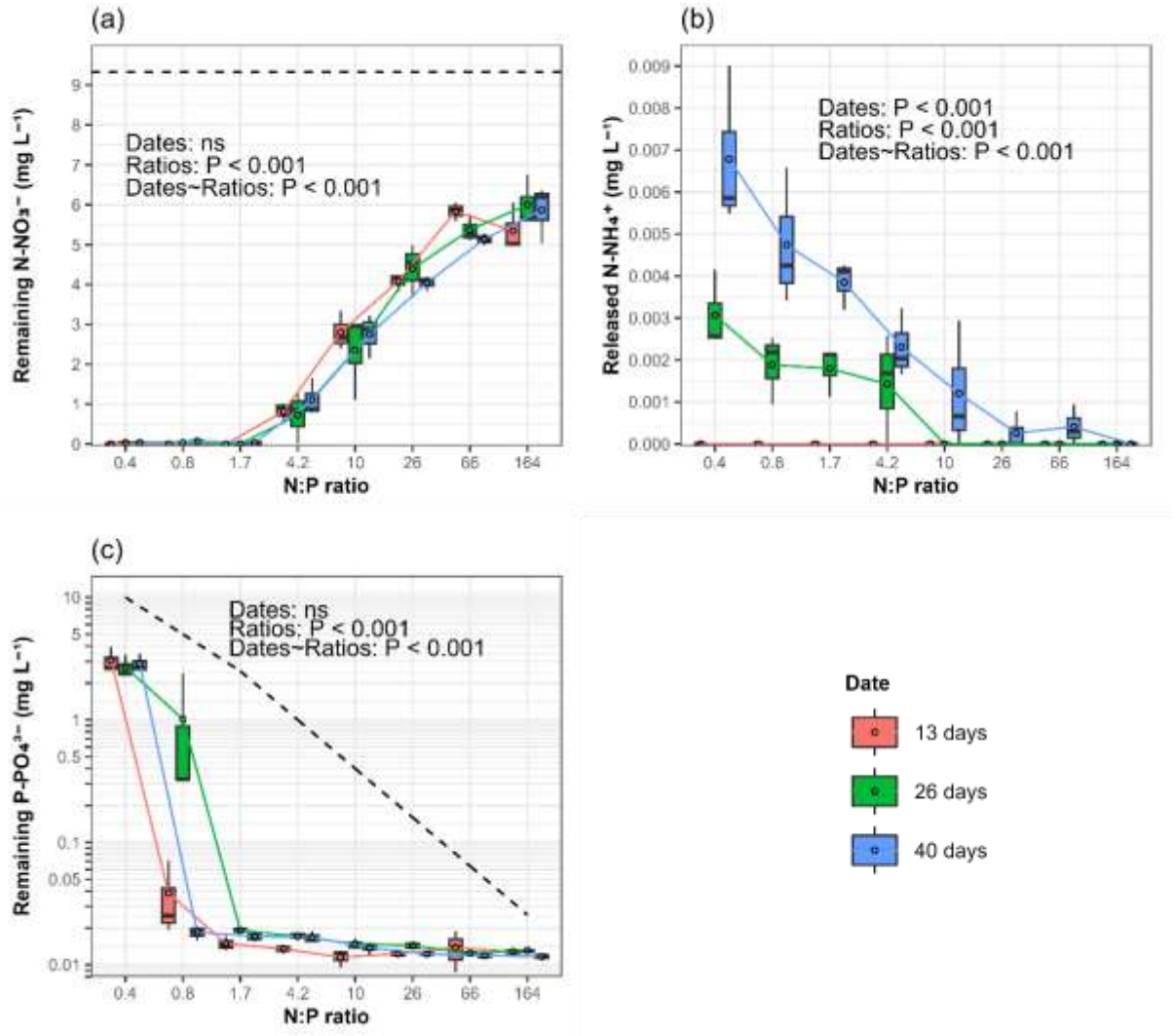

Figure II 7. (a) Remaining $N\text{-}NO_3^-$, (b) released $N\text{-}NH_4^+$ and (c) remaining $P\text{-}PO_4^{3+}$.

For each strain across N:P ratios during leaf litter decomposition. Dashed lines in panels (a, c) show the starting quantities of N and P at each ratio. Mean values (n=3) ± SE. *P*-values from Kruskal-Wallis tests.

decreased from R1 (0.4) to R2 (0.8), then stabilised between 0.01 mg and 0.02 mg for R3 (1.7) to R8 (164) (Figure.II.7c). The released N-NH_4^+ was only detected at very low quantity (lower than 0.01 mg L^{-1}), amounts of NH_4^+ depending on both the N:P ratios (Kruskal-Wallis, $P < 0.001$) and the sampling date ($P < 0.001$), and their combinations ($P < 0.001$). N-NH_4^+ was only detected after 26 days up to R5 (10) and after 40 days through all tested ratios, and the quantity decreased with rising ratios (Figure.II.7b).

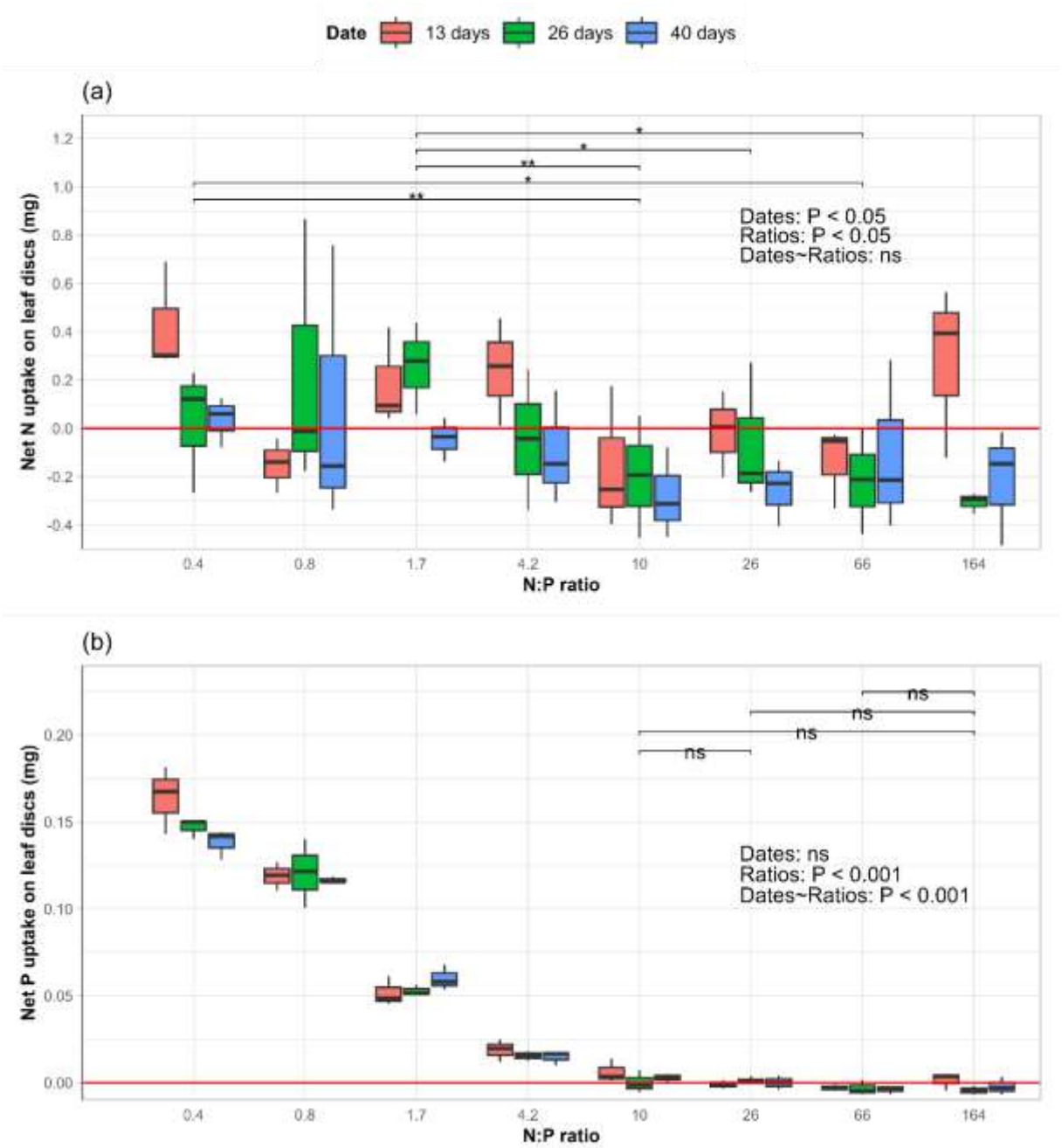

Figure II 8. Net quantities of N (a) and P (b) uptakes on leaf discs.

Baseline 0 was set as the N or P quantities on discs of the control group. *P*-values from Kruskal-Wallis tests.

Net N uptakes were mostly above zero at low N:P ratios and decreased slowly becoming often negative at high N:P ratios (Figure.II.8a). The ranges of net N uptake quantities were quite variable, and analyses revealed only weak significant differences between ratios (Kruskal-Wallis, $P < 0.05$) but significant changes with time ($P < 0.05$), net N uptake systematically decreased during the leaf litter decomposition process (from 13 to 40 days). Net P uptakes were strongly dependent on N:P ratios ($P < 0.001$) but there was no significant difference between values obtained at different sampling dates ($P > 0.05$). In contrast, analyses revealed a significant interaction between ratios and sampling date ($P < 0.001$), P uptake progressively reduced with time in the R1 condition but stayed almost stable throughout leaf litter decomposition for the other N:P ratio tested. The net uptake quantities across ratios were mostly above zero, with a range between 0 and 0.18 mg (Figure.II.8b).

4. Discussion

The main goals of our studies were to understand in more depth the impacts of dissolved N:P ratios on leaf litter decomposition, nutrient immobilisation vs. mineralisation patterns, and the structure of fungal decomposers communities. In this experiment, we choose to manipulate a large N:P gradient by using a constant N-NO_3^- input in culture media and adding an increasing amount of PO_4^{3-}. Microbial growth and activity were thus supposed to shift from a P limitation for the highest N:P ratios (up to 164) to an N-limitation for the lowest N:P ratios (down to 0.4). Microbial activity was thus expected to increase along the P addition gradient (i.e. when decreasing the N:P ratio) then stabilising due to a shift in the limiting element (Danger *et al.* 2008). While fungal biomass globally followed these predictions, i.e. increasing when reducing the media N:P ratios, leaf litter mass loss was unexpectedly unaffected by the P-gradient. However, in a metanalysis, Ferreira *et al.* (2015) already observed such an effect of P concentration on leaf litter decomposition, this effect was even magnified when N and P were

added together. These results also contrast with the observation of Gulis *et al.* (2017) which suggested that only dissolved N was responsible of increasing fungal growth and biomass production and that P availability only controls fungal biomass elemental composition. This result might be at least partly due to the fact that leaf litter decomposition was only observed on a single date and that even if final mass losses are close from each other, temporal dynamics of decomposition might have differed between N:P treatments. Leaf litter decomposition indeed follow asymptotic dynamics – as it can be seen in our experiment in the Mix treatment, Figure.II.5a - and differences are necessarily reduced between treatments when getting closer to the asymptote. Nevertheless, the stimulation of fungal biomass production with P addition tends to indicate that fungal growth was certainly limited, up to a point, by P-availability.

Interestingly, despite the absence of significant dissolved N:P ratio effect on leaf litter decomposition, leaf mass loss measured after 40 days was significantly affected by AH species. HULU and TEMA led to the highest leaf mass losses, the mixture of the 5 selected strains led to intermediate decomposition, and ARTE, CLAQ and TRSP led to the lowest decomposition. This result adds to the previous observations that AH species can differ in their abilities to decompose leaf litter (e.g. Suberkropp, Arsuffi and Anderson 1983), even if these differences remain limited – at least for the quite labile leaf litter species chosen in this study, degradation abilities being certainly more pronounced on more refractory materiel (e.g. Butler and Suberkropp 1986). Also, assembling the different species (Mix treatment) did not increase leaf litter decomposition as often thought to be the case in biodiversity-ecosystem functioning predictions (Gessner *et al.* 2010), rather slightly reducing it. Dang *et al.* (2005) manipulating AH diversity in a laboratory experiment also failed to demonstrate any diversity effect on the decomposition process, but their results mainly showed a reduction of the variability of this process along the diversity increase gradient. Other studies showed that different communities can lead to similar decomposition rates (e.g. Ferreira and Chauvet 2012), confirming such

functional redundancy between taxa. Note that while considered for long as a prerequisite for species coexistence, species functional complementarity might not always be mandatory to maintain species diversity. Competition and predation can also represent mechanisms favouring functionally redundant and coexisting taxa in communities (Haraldsson and Thébault 2023). This might especially be the case for fungal communities which remain diversified despite apparently highly functional redundancy between taxa.

Response of fungal biomass to P gradient were also significantly different between AH species and also between species and their assemblage. Two species (HULU and TRSP) saw their biomass increase monotonically when increasing P availability, whereas others reached a plateau or even decreased for the lowest N:P ratios after reaching a maximal biomass at intermediate N:P ratios. This bell-shaped relationship was especially visible for the Mix treatment with a maximal biomass observed at R2 (0.8), and for CLAQ and TEMA with a maximal biomass reached at R4 (4.2). These differences between taxa might be seen as different optimal ratios for fungal biomass production. Güsewell and Gessner (2009) followed by Wang *et al.* (2022) (chapter IV) already observed such bell-shaped relationships for intermediate N:P ratio, either for fungal communities biomass or for decomposition rates. Differences in fungal species optimal ratios might represent a trait of interest since it could play a role in the degree of nutrient limitations of each taxon and potentially their competitiveness in natural communities. In our study, bell-shaped relationships of leaf mass loss were not evidenced after 40 days, but we cannot exclude that such relationships occurred on earlier dates, before decomposition rates get close to asymptotic values.

As expected, large nutrient immobilisation preceded nutrient mineralisation. Phosphorus and nitrogen immobilisation followed expectations along the N:P gradient, PO_4^{3-} being totally immobilised – even disappearing from the culture medium - at high N:P values then being progressively accumulated in fungal biomass as luxury consumption, leading to litter P-

enrichment proportional to dissolved P initially available in the culture medium. In parallel, NO_3^- was almost totally immobilised by aquatic hyphomycetes for the lowest N:P ratios (i.e. when N became limiting along the N:P gradient) while NO_3^- was still available in culture media above R3 (1.7) for Mix treatment, HULU, and ARTE or above R4 (4.2) for CLAQ. Interestingly, TEMA and TRSP were unable to totally deplete the culture media in NO_3^-, suggesting that threshold concentrations for immobilising nitrates might differ between these species and the other ones tested. It would be interesting to test if these two species are less competitive than the other ones in natural communities when growing in very low nitrate concentrations.

In average, after 40 days of decomposition, leaf litter lost N, meaning that N losses exceeded N immobilisation. Despite this general trend, N uptake was significantly affected by both AH species and by the N:P ratio. In particular, HULU led to significantly higher net N release while TRSP led to lower net N release. Other taxa and the Mix treatment led to more variable and intermediate N uptakes over the 40-day period. This result might be at least partly explained by the different N:P requirements of fungal taxa, HULU being for example the only fungal species that did not exhibit any clear shift from N to P limitations along the N:P gradient. In contrast, TRSP was among the two species that left some dissolved NO_3^- available in the low N:P culture media at the end of the experiment, probably revealing lower N requirements. N uptake was also largely dependent upon the dissolved N:P ratio, this parameter remaining positive or null for the lowest N:P ratios (0.4-1.7) while it progressively declining for leaf litters decomposed under the highest N:P ratios (66-164). This observation may probably be because less N was immobilised due to stronger P limitations of fungal growth. In general ecology literature, decomposers are seen as net mineralisers, i.e. organisms that will ultimately lead to a net release of mineral elements from plant litter, this one being at the basis of mutualistic relationships between decomposers and primary producers (e.g. Harte and Kinzig 1993). Along our N:P gradient, we expected that N mineralisation to only occur in the less N limiting conditions (high

N:P ratios). In our experiment, there was initially no $N\text{-}NH_4^+$ in the system, meaning that any $N\text{-}NH_4^+$ detected was the result of fungal decomposing activity (N mineralisation). Despite the majority of $N\text{-}NO_3^-$ at low N:P ratios had been removed from the system (presumably incorporated and transformed by AH into other forms of N), the concentrations of detected $N\text{-}NH_4^+$ remained very low, meaning that whatever the N:P ratio tested, fungal mediated N mineralisation under the NH_4^+ form remained limited. Also, contrary to expectations, $N\text{-}NH_4^+$ release clearly followed the gradient of P, not the shift in nutrient limitation. NH_4^+ release was rather related to fungal biomass, suggesting more of an N release related to a general fungal activity rather than to a release of excess N compared to fungal requirements. Also, nutrient uptake calculations suggest that a non-negligible amount of N loss is mainly done under organic forms since N uptake was in average negative, and since inorganic N forms ($N\text{-}NH_4^+$ and $N\text{-}NO_3^-$, $N\text{-}NO_2^-$ being below detection limits in our microcosms) were not sufficient to explain these N losses. These organic forms might be organic molecules released by fungal activity during leaf litter decomposition and/or directly corresponding to the amount of N released under the form of exoenzymes. All these results question the general assumptions of stoichiometric models where stoichiometric imbalance is considered as the main driver of nutrient mineralisation (Daufresne and Loreau 2001).

Our experiment using AH mixture allowed us to investigate the temporal dynamic of litter decomposition and, more originally, those of nutrient immobilisation and mineralisation. The decomposition speed of litter by the AH assemblage significantly slowed down after 26 days. In parallel, fungal biomass significantly increased between each sampling date, at least for the lowest N:P ratios, i.e. when P was no more the limiting element. This result slightly contrasts with the observation of Gulis *et al.* (2017) who proposed that only N was controlling fungal growth, P being stored as luxury consumption when present in excess in the medium. As already observed for phytoplankton, the response of fungi – both in terms of stoichiometry, growth, and

activity - might be largely dependent on the nature and the degree of nutrient limitation (Danger *et al.* 2007b). Another important observation on the dynamic of nutrient immobilisation is that it occurred very quickly, and both $N\text{-}NO_3^-$ and PO_4^{3-} concentrations had reached their minimum already after 13 days. This observation agrees with the results of Danger *et al.* (2013) who obtained maximal nutrient immobilisation on microbial preconditioned leaf litter after 3 days. These immobilised nutrients might then be used by fungi and/or stored under other forms in fungal biomass. Future studies will require to specifically investigate these storage forms and the way they are used.

Finally, our study allowed to investigate the impacts of time and nutrient ratios on the taxonomic structure of our fungal assemblage. TEMA was the dominant taxon in the assemblage for the lowest N:P ratios, whereas the proportion of ARTE and TRSP tended to increase for the highest N:P ratios. The structure of the assemblages was already stabilised after 13 days since variations with time were very limited. The dominance of ARTE was somehow predictable from the observations on the single species treatment, ARTE leading to the highest decomposition rates as well as producing the highest biomass for the lowest P availability. Also, HULU, which led to high decomposition rates for the lowest N:P ratios remained at very low proportions in the assemblage. This species was the only one being apparently always P-limited all along the P-gradient. In contrast, no observation carried out on single species treatment allowed us to understand why ARTE – one of the taxa that produced the lowest biomass and led to the lowest leaf mass loss – was so abundant in the assemblage, especially for the highest N:P ratios. Fungal competitiveness might thus not only be driven by their stoichiometric traits but also by other traits that deserves to be described. Using a multi-trait approach on AH might be essential to disentangle all the determinants of their dominance on different leaf litters.

5. Conclusion

To conclude, despite strong stoichiometric responses to the dissolved N:P ratio (differences in fungal growth and nutrient immobilisation abilities), leaf litter decomposition was similar after 40 days. The study of leaf litter decomposition by fungal assemblages at different days indicated that N:P gradients might have effects on the temporal dynamics of this decomposition, not on the final result of this decomposition. Nutrient imbalances might thus delay leaf litter decomposition but not its final intensity. Also, contrary to what is commonly thought, mineralisation by fungal of leaf litter might be far less pronounced to what is commonly thought and detritivores (feeding on decomposing leaf litter and excreting nutrients in excess; Elser and Urabe 1999) might play a great role in the remineralisation process in ecosystems, this process being also certainly strongly affected by the elemental composition of the resources. Finally, despite stoichiometric traits evidenced on single AH species partly explained species dominance in the Mix treatment, these traits failed to explain the importance of some taxa in the assemblage. These observations pave the way for further research on the determinants of fungal community structure and the development a large trait-based approach applied to AH.

CHAPTER III

Cellulose Decomposition by Fungal and Bacterial Decomposers Depends on Both Ratios and Gradient of N and P

In the previous chapter, an artificial assemblage of aquatic hyphomycetes (AH) did not increase the decomposition efficiency of leaf litter decomposition compared to that of individual AH strains. Yet, in natural decomposer communities, AH diversities are generally higher than 5 species and other decomposers are likely to be present. In this third chapter, we wanted to compare litter decomposition carried out by different assemblages of microorganisms (AH alone, bacteria alone, bacteria + AH, and a natural community of decomposers including both fungi and bacteria) and investigate the role of available N:P ratios on species interactions and on litter decomposition.

Abstract

Plant litter is generally considered as a low-quality resource rich in refractory carbon and poor in nitrogen (N) and phosphorus (P). To balance their nutrient requirements, decomposers must acquire extra nutrients from their environment while decomposing plant litter. Aquatic hyphomycetes (AH) generally exhibit higher C:N and C:P ratios as well as specific enzymes activities than bacteria, which has been proposed as a strategy with which AH could outcompete bacteria during litter decomposition, at least during the first steps of this process. Previous studies suggest that the response of decomposers to N or P might depend on the availability of each other, but these responses were not symmetric. Environmental N:P ratios and the absolute amounts of N and P are thus expected to impact the coexistence of AH and bacteria and result in different decomposition intensities. To answer these questions, we measured decomposition of cellulose discs by 4 different decomposer communities [AH alone (H); bacteria alone (B), bacteria + AH (BH); a natural community (NC) of decomposers including both fungi and bacteria] under two nutrient gradients: one with a constant level of N and varying concentrations of P, the other one with a constant level of P and varying concentrations of N.

Along the P-constant N:P gradient, H and NC have the highest optimal N:P ratio and efficiency for cellulose decomposition. When the P supply is constant, a lack or an excess of N slows down cellulose decomposition rate by all tested communities. In contrast, when the supplied N is constant, both the lack or the excess of P seems to limit the decomposition efficiency of B. When AH are present in a community, cellulose decomposition remained almost unaffected by P-availability, probably due to extremely high P-use efficiency and P-remobilisation capacities of AH. Further analyses on the species present in the different communities should help to understand in more depth how much N:P ratios affected interspecific competition in decomposer communities.

Key words:

Optimal N:P ratios, N:P gradient, decomposer community, bacteria, aquatic hyphomycetes, cellulose decomposition, interaction

1. Introduction

Small streams and rivers often depend on allochthonous plant litter as the main carbon and energy source to maintain their ecological functions (Wallace *et al.* 1999). Aquatic hyphomycetes (AH) and heterotrophic bacteria are the main decomposers of this detritus, but their relationships with each other are complex. Previous studies of the interactions between bacteria and AH during decomposition have often led to conflicting results: some studies showed that microbial activity and growth are improved when bacteria and fungi co-occur (e.g. Bengtsson 1992), other showed mainly antagonistic interactions (Romaní *et al.* 2006) or positive impacts of fungi on bacterial development, bacteria taking advantage of fungal extracellular enzyme activities (Romaní *et al.* 2006a) or through fungal-induced increases in the accessibility of the leaf matrix for bacteria (De Boer *et al.* 2005). One way to explain these divergent results is to look into the stoichiometric requirements (often nitrogen and phosphorous) of bacteria and AH (Gulis and Suberkropp 2003b). Stoichiometric requirements have long been proposed as main drivers of plant community structures (Tilman 1982; Miller *et al.* 2005) and more recently for animals (zooplankton: Elser *et al.* 1998; aquatic macroinvertebrates: Beck *et al.* 2023). Transposition of such approaches to microbial communities is more complicated since knowledge of stoichiometric traits of microorganisms is reduced (e.g. Godwin and Cotner 2018 for bacteria; Danger, Gessner and Bärlocher 2016 for fungi) and since temporal dynamics of species replacements in microbial communities can be quick in comparison with the decomposition process they ensure (Danger *et al.* 2008). To date, enrichment of either N, P or both elements have been shown to enhance litter decomposition (Ferreira *et al.* 2015b) but such studies did not necessarily look at the composition of the decomposer communities involved, and it is therefore difficult to interpret the impacts of these diverse nutrient enrichments.

AH are a polyphyletic group of fungi that commonly appear on plant litter in streams and rivers(Bärlocher 1992). Because of their capacity to penetrate the surface and grow underneath large pieces of substrates with their hyphae, AH can have access to nutrients which are otherwise unavailable for bacteria (Gulis and Suberkropp 2003b). AH are also well adapted to decompose complex carbon compounds such as cellulose and lignin. Bacteria, on the other hand, are omnipresent and abundant in freshwater ecosystems. They are highly competitive for assimilating dissolved organic matter (DOM) and inorganic nutrients and break down simple organic compounds.

Plant litter is mostly considered as a low-quality resource, rich in structural carbon (cellulose and lignin) but depleted in essential nutrients (Cross *et al.* 2005). To balance their nutrient requirements, microbial decomposers must generally acquire extra nutrients from their environment to be able to decompose litters with C:nutrient ratios. In headwater streams, leaf litter decomposition is generally initiated by AH and followed by bacteria at a later stage (Baldy, Gessner and Chauvet 1995). From a stoichiometric viewpoint, this observation may be related to the fact that AH has on average higher C:N and C:P ratios than bacteria, these ratios being closer to those of their plant litter resource (Danger *et al.* 2016). Investigating cellulose mass loss by natural microbial communities along a supplied N:P ratio gradient, Güsewell and Gessner (2009) evidenced "bell-shaped" curves, suggesting that intermediate N:P ratios might optimise leaf litter decomposition. Their study also showed that lower N:P ratios mainly promoted bacterial development whereas high N:P ratios mainly promoted fungi (Güsewell and Gessner 2009). In the Ecological Stoichiometry framework, this result agrees with the Growth Rate Hypothesis (GRH, Elser *et al.* 2000, 2003). GRH states that organisms' growth rates should correlate with their P demand – and thus goes with lower N:P ratios – due to higher demand for ribosomal RNA which are among the most P-rich molecules in cells (Elser *et al.* 2000; Hessen *et al.* 2007). Additionally, given the nature of N and P implications in microbial

biomass, it is safe to suggest that P allocated to rRNA (and other P rich molecule, for example ATP) may have shorter half-life compared to N-rich proteins which, once synthesised, will be less available on short terms for other purposes (Belle *et al.* 2006; Pedersen *et al.* 2011). As a result, different microbial N:P optimal ratios are expected to be related to large differences in the tolerance to a P and N limitations.

Environmental N:P ratios (in both detritus and the water column) would thus be expected to impact bacterial and fungal coexistence, as well as the processes these microorganisms ensure, namely leaf litter decomposition and nutrient immobilisation inside microbial biomass. In addition, due to known distinct abilities for microorganisms to immobilise dissolved N and P from their environment (Chapters I and II of this thesis; Gulis and Suberkropp 2003b; Gulis *et al.* 2017), microorganisms response to N:P gradient would be expected to depend on the nature of the gradient, i.e. if the gradient of N:P ratios is obtained through an increase of dissolved P concentration with constant N (as in the Chapter II of this thesis), through an increase of N with constant P, or through changes in both N and P (as in Güsewell and Gessner 2009 or Gulis *et al.* 2017). In particular, Gulis *et al.* (2017) recently proposed that P availability has no effect on fungal biomass but strongly affects litter stoichiometry while dissolved N greatly affects fungal growth but not fungal stoichiometry. To test these hypotheses, we measured decomposition of cellulose (a simplified analogue of leaf litter) by 4 different decomposer communities: a natural bacterial community, an assemblage of 4 common AH species, a mixture of both the natural bacterial community and the assemblage of 4 AH species, and a natural stream microbial community. To test stoichiometric hypotheses, this experiment was carried out under two nutrient gradients: one with a constant level of N and varying concentrations of P, the other one with a constant level of P and varying concentrations of N. We aimed to answer the following questions: (1) Will we obtain similar “bell-shaped” curves of cellulose mass loss under both types of N:P gradients? (2) Will the decomposition differ between bacterial, fungal, and mixed

communities and this as a function of the N:P gradients? (3) Would optimal N:P ratios for cellulose decomposition depend on the nutrient gradient type and the community involved? In our experiment, both nutrient gradients formed the same 10 different N:P ratios with one intermediate ratio sharing the same N and P concentrations for both gradients. After six months of cellulose decomposition, we measured the cellulose mass losses, and final N and P quantities present on cellulose as proxies of decomposers' N and P requirements.

2. Materials and Methods

2.1. Microcosm design

The experiment was carried out in a microcosm system with 2 gradients of 10 N:P ratios to test 4 combinations of microbial decomposers. The microcosm setup was adapted from that of a previous study (Güsewell and Gessner 2009). Briefly, in a 100 mm diameter Pyrex Petri dish with lid, 50 g of gravel was covered by a fine nylon mesh (250 µm), and 7 cellulose discs (25 mm diameter paper filter; Whatman) were placed on top of the mesh. The average mass of 7 discs was 313.2 mg. The gravel was previously sieved to 2 mm, washed, dried, and burned at 500 °C for 5 h to remove all traces of organic matter. The nylon mesh can still allow nutrient access but is used to prevent gravel particles from sticking onto cellulose discs which could eventually hinder precise cellulose weighting at the end of the experiment. The cellulose discs were the sole carbon source in microcosms and were used as a simplified analogue of leaf litter which allows to precisely control the nutrient (N and P) ratios in each microcosm. Each Petri dish was wrapped individually in aluminium and autoclaved at 120 °C for 2 h to be sterilised.

2.2. Nutrient solution and N:P ratios

Nutritive solutions were prepared with 12.6 mg L^{-1} $NaHCO_3$, 24.0 mg L^{-1} H_3BO_3, 28.4 mg L^{-1} $Na_2SiO_3 \cdot 9H_2O$, 36.8 mg L^{-1} $CaCl_2 \cdot 2H_2O$, and 37.0 mg L^{-1} $MgSO_4 \cdot 7H_2O$ (Kilham *et al.* 1998). Nitrogen (50 % N-NH_4^+ and 50 % N-NO_3^-), and phosphorous (P-PO_4^{3-}) were added individually to the nutritive solution at different concentrations to form 2 gradients: the first gradient (N-constant) was with 100 mg L^{-1} of N and with 2.5 10^{-1} to 10^3 mg L^{-1} of P, and the second gradient (P-constant) was with 10 mg L^{-1} of P and with 1 to 4 10^3 mg L^{-1} of N. Both gradients formed 10 identical N:P (molar) ratios from R1 to R10: 0.05, 0.12, 0.29, 0.72, 1.8, 4.5, 11, 28, 70, and 176. The ratio R6 (4.5) was common to both gradient types and had the same N and P concentrations (100 mg L^{-1} and 10 mg L^{-1}, respectively). All solutions were prepared with MilliQ ultrapure water and were sterilised by autoclaving. Nutrient solution (20 ml) with the appropriate N:P ratio was added into each microcosm. There were 3 replicates for each ratio of each gradient.

2.3. Decomposer inoculum preparation

The 4 combinations of decomposer communities tested were as follows: a natural community with both aquatic hyphomycetes and bacteria (**NC**), a natural bacteria community without fungi (**B**), an artificial mix of 4 aquatic hyphomycete strains (**H**), and a natural bacteria community mixed with the 4 aquatic hyphomycete strains (**BH**). Except for the artificial mix of aquatic hyphomycetes (see below), the natural microbial inoculum was obtained by inducing fungal spores and bacteria development on leaf litter. Briefly, leaf litter (mixture of hazel *Corylus avellana*, alder *Alnus glutinosa*, and hornbeam *Carpinus betulus*) was put in nylon mesh (500 µm) bags and colonised in La Maix stream (latitude 48° 29’2.56 ″ N, longitude 7° 4’10.75 ″ E) in early spring 2019. The colonised litter bags were collected and brought back

to the lab after 2 weeks as well as stream water. Leaf litters were then put into Erlenmeyer flasks with stream water, incubated with gentle agitation at 18 °C for 48 h for spore production and bacteria development. The inoculum for **NC** was obtained by collecting the supernatant with extra care not to bring any suspended particle. A portion of the supernatant was filtered (Microfiber filter paper Whatman GF/C, 1.2 µm) to remove fungal spores and prepare the inoculum of natural bacterial community (**B**). To obtain the mix of fungal spores (**H**), we used 4 strains of aquatic hyphomycetes (*Articulospora tetracladia*, *Heliscus lugdenensis*, *Tetracladium marchalianum*, and *Tricladium splendens*, later named ARTE, HELU, TEMA, and TRSP, respectively) from laboratory fungal collection. Conidia or each strain were produced by putting small pieces of mycelium-coming from cultures (grown on malt agar solid medium) in sterilised water with agitation at 18 °C for 3 days. The number of spores was estimated under a microscope after filtration on 5 µm nitrocellulose filter and coloration with Trypan blue (0.05 % in 60 % lactic acid). Spores of each strain were then mixed equally to obtain a suspension of ca. 500 total spores per ml. A total of 40 ml of this conidia suspension was mixed with an equal volume of bacterial inoculum to obtain the inoculum of **BH**. Finally, 1 ml of inoculum was equally distributed onto the whole 7 cellulose discs of each microcosm. There were in total 240 microcosms prepared (2 gradients ×10 N:P ratios × 4 types of inoculum × 3 replicates). The microcosms were incubated in the dark at 14 °C for 6 months.

2.4. Cellulose mass loss

Partially decomposed cellulose discs were retrieved individually and stored at – 80 °C before being freeze-dried and weighted to the nearest 0.1 mg. From 4 discs of each replicate, individual cellulose disc mass losses were calculated by subtracting the mass of the discs to the average initial mass of a single disc (44.6 mg). In total, we have obtained 12 measurements for each tested condition (3 replicate per condition × 4 discs weighted).

2.5. N and P content measurement

For total N analysis, 1.5 mg of each sample powder was put into a tin capsule (Säntis Analytical SA7698110). Masses were weighted to the nearest 1 µg using a microbalance. Samples were analysed using a CHN elementary (Carlo Erba NA 2100). For total P quantification, samples followed an alkaline digestion step first to reduce all organic phosphates, then P was quantified with the molybdate blue colorimetric method (NF EN ISO 6878).

2.6. Statistical analyses

Statistical analyses were done with R using RStudio (R Core Team 2022; RStudio Team 2022). N:P ratios were log transformed prior to analyses. Analyse of variance (ANOVA) or Kruskal-Wallis (when ANOVA assumptions were not respected) were applied. When *P*-value was < 0.05, we considered the differences as significant. When cellulose mass loss followed a biphasic trend (symmetric bell-shape curve, Figure.III.1) along the log transformed N:P gradient, we fitted the data to an adapted version of a Gaussian-type model with four parameters (Larras *et al.* 2018):

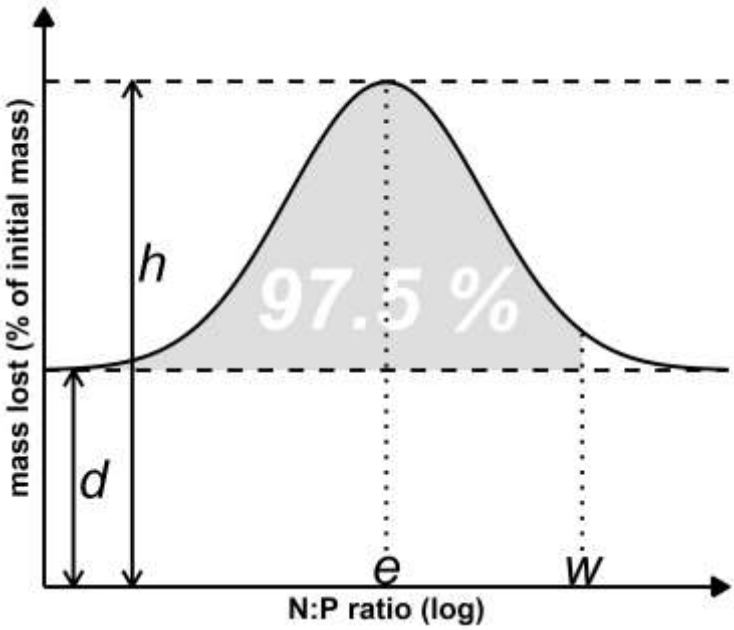

Figure III 1. Representation of the Gaussian model.

h is the maximal mass loss, *d* is the minimal mass loss, *w* (> 0) is the maximal effective N:P ratio, and *e* (> 0) is the optimal N:P ratio.

$$y = (h - d)exp\left(-2\left(\frac{x - e}{w - e}\right)^2\right) + d$$

where *y* is the cellulose mass loss in percentages, *x* is the N:P ratio transformed in log, *h* is the maximal mass loss (the height of the curve peak), *d* is the minimal mass loss which is assumed to be constant for extremely low and extremely high N:P ratios, *w* (> 0) is what well called the maximal effective N:P ratio, it the turning point below which there is 97.5 % cumulative mass loss from the level if *d*, and beyond which the additional mass loss over *d* is negligible, and *e* (> 0) is the log-transformed N:P ratio which corresponds to the maximal mass loss. Confidence intervals at 95% (95% CI) were calculated for each parameter calculated from this equation to evaluate significant differences.

3. Results

Decomposition of cellulose discs ranged from less than 5 % to 65 % of their initial dry mass (Figure.III.2). With the N-constant gradient, mass losses did not show "bell-shaped" curve along the N:P ratios, with the exception of the bacterial community (**B)** which had a maximal

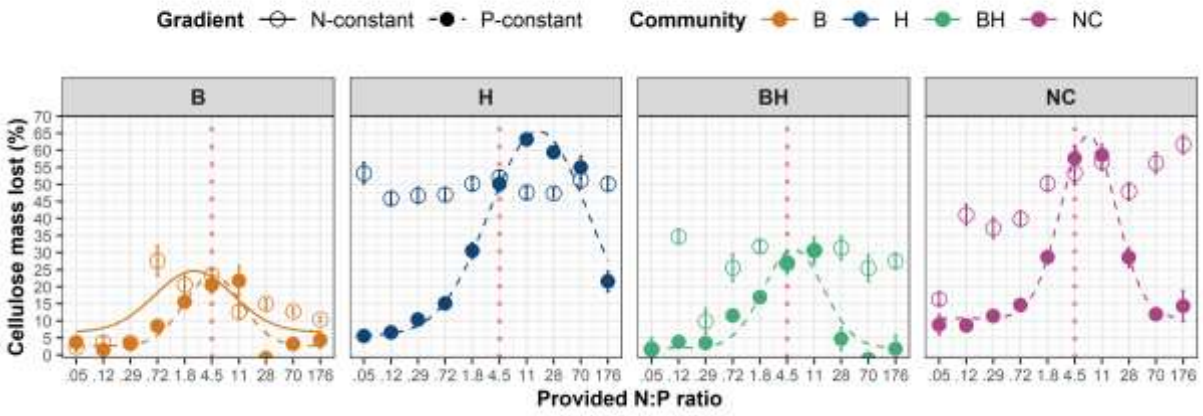

Figure III 2. Cellulose mass loss.

Average cellulose disc mass losses (%) after 6 months. Comparison between the two nutrient gradients (empty circles are for N-constant gradient and plain circles are for P-constant gradient) for each of the four tested communities (B-bacteria; BH-bacteria and 4 aquatic hyphomycetes; H-4 aquatic hyphomycetes; NC-natural community including bacteria and a wide range of aquatic hyphomycetes). *X-axis* for provided N:P ratios is log-transformed but shown in the molar ratios. Points show measured mass losses (n = 12 ± SE), and when applicable, curves show the mass losses calculated by the Gaussian model. Red dotted line is the N:P ratio R6 with equal N and P concentrations in both nutrient gradients.

mass loss of around 25 % at N:P ratio of 1.8 (R5). Natural microbial communities (**NC)** and the AH assemblage (**H)** lost twice as much mass as communities **B** or the mixture between AH strains and bacteria (**BH)**. On the other hand, with the P-constant gradient, mass losses of all 4 tested community types showed "bell-shaped" responses along the N:P ratios. For the same nutrient gradient, mass losses were significantly different depending on community type, N:P ratios, and their combinations (Kruskal-Wallis, all $P < 0.001$). For the same community type, mass losses were also significantly different depending on the type of nutrient gradient (all $P < 0.001$).

For all mass losses that exhibited a "bell-shaped" response along the N:P gradient (i.e. all communities of the P-constant gradient, and the **B** community of the N-constant gradient), values of four parameters deduced from Gaussian model describing mass loss curves and their confidence intervals (CI 95 %) were estimated (Figure.III.3). With the P-constant, N:P gradient, minimal and maximal mass losses (parameter *d* and *h*, respectively) were both higher for communities **NC** and **H**. Community **H** had the highest optimal N:P ratio (parameter *e*) value (ca 17), which was more than doubled when compared to that of the three other communities. Treatment **H** also had the highest maximal effective N:P ratio (parameter *w*) value (ca. 89) while the values for the other three communities were around ca. 15. For the **B** community, minimal mass loss was slightly higher with the N-constant N:P gradient than with the P-constant N:P gradient, while they shared a similar maximal mass loss. The optimal N:P ratio with the N-constant N:P gradient was significantly lower than that with the P-constant gradient. The maximal effective N:P ratios with both gradients were comparable, with values around ca. 10.

The final N quantities (per g of cellulose, including microbial biomass, Figure.III.4a) for both nutrient gradients were significantly different between communities, N:P ratios and their interaction (Kruskal-Wallis, all $P < 0.05$). Final N variations mainly followed the initial N

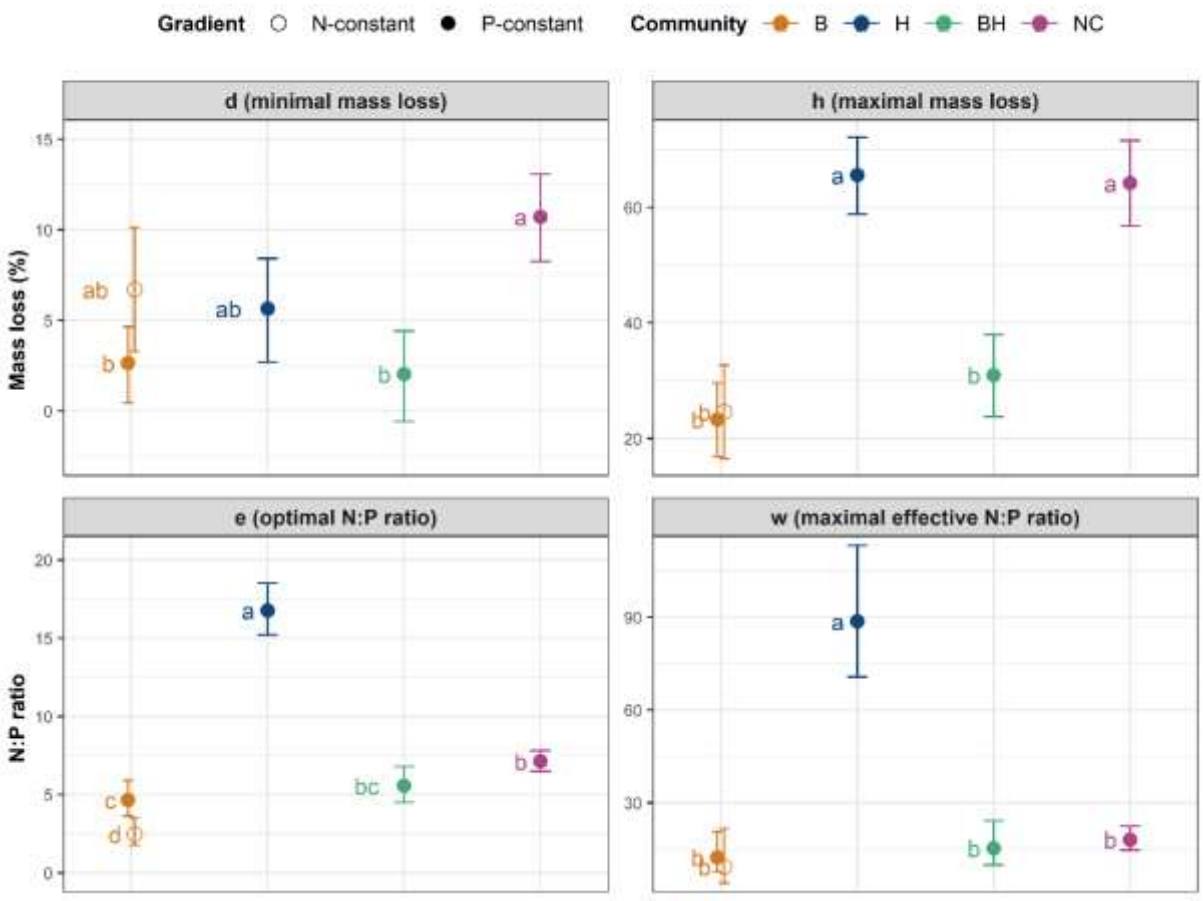

Figure III 3. Graphic representations of each parameter estimated by the Gaussian model. When the mass loss result showed a "bell-shaped" curve, the results were fitted using the model to calculate the four parameters. Each parameter is an estimation (± 95% CI). Notice that the ranges of *y-axes* are different for each panel.

availabilities. There were less variations in N quantity with the N-constant N:P gradient (between 1 and 8 mg g^{-1}) than with the P-constant N:P gradient (from 1 mg g^{-1} at low N:P ratios up to 26 mg g^{-1} at high N:P ratios). For each community type, final N quantities were significantly different between the two gradient types for the **B** community, between N:P ratios for **H** and **NC** communities, and between the combinations of gradients and ratios for all four communities.

Similarly, the final P quantities measured on cellulose discs for both nutrient gradient types were also significantly different between communities (Figure.III.4b), N:P ratios, and their interaction (Kruskal-Wallis, all $P < 0.05$). Final P quantities also followed the initial P

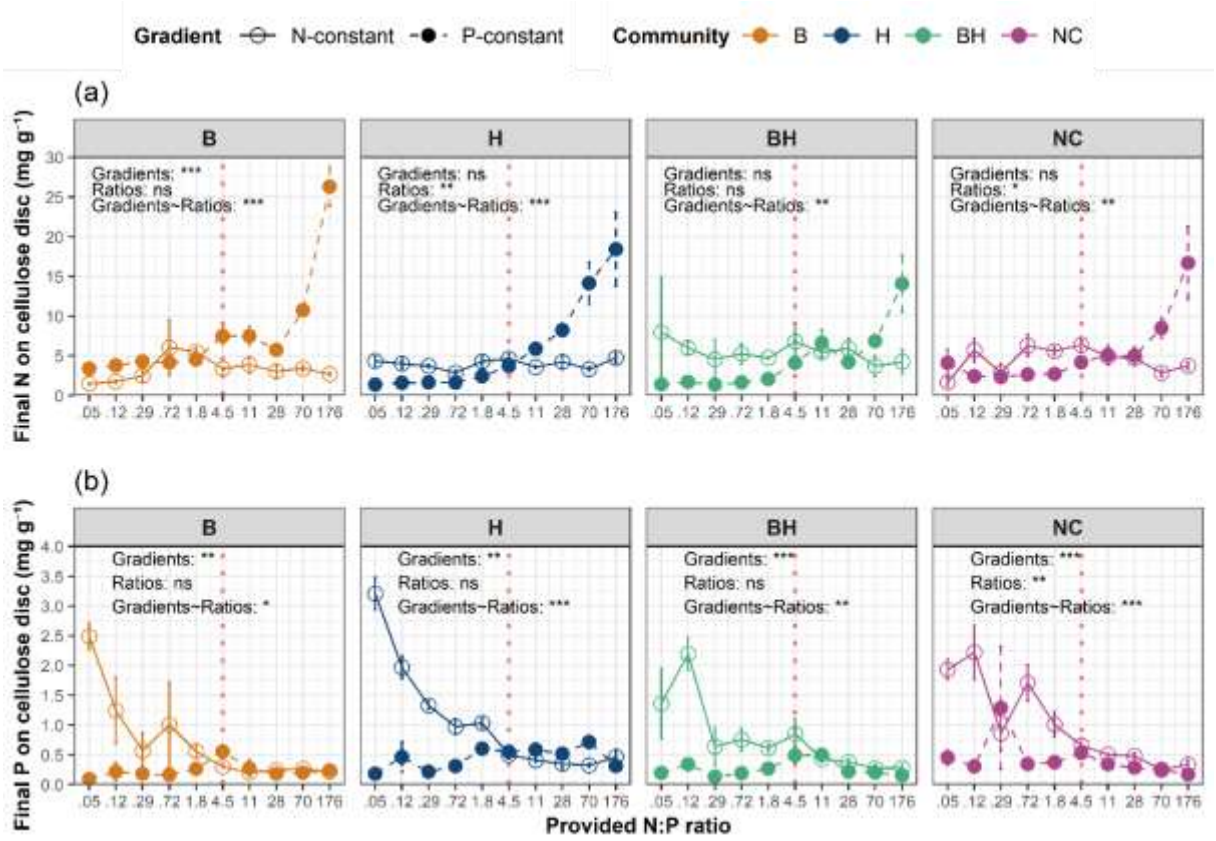

Figure III 4. (a) Final N and (b) final P on cellulose discs.

Values expressed in mg per g of cellulose (dw) for the 4 microbial communities and the two N:P gradient tested. Red dotted line is the N:P ratio R6 with equal N and P concentrations in both nutrient gradients.

availabilities. The variations were smaller with the P-constant N:P gradient (between 0 and 0.6 mg g^{-1}) than with the N-constant N:P gradient (between 0 and 3.3 mg g^{-1}). For each community type, final P quantities were significantly different between gradient types, and the combinations of gradients and ratios. The difference was only significant between ratios for the **NC** community.

Final N:P ratios on cellulose discs positively correlated with the initial N:P ratios in microcosms (Figure.III.5). For cellulose decomposed under both nutrient gradient types, final N:P ratios on discs were higher at each provided ratio under the P-constant N:P gradient, final ratios were also generally higher than the provided N:P ratios when the latter were low, and *vice versa*. The transition where ratio on disc equals to provided ratio occurred at R6 (4.5) (Figure.III.5a). With the N-constant N:P gradient, ratios on cellulose disc increased up to R6 and stabilised afterward;

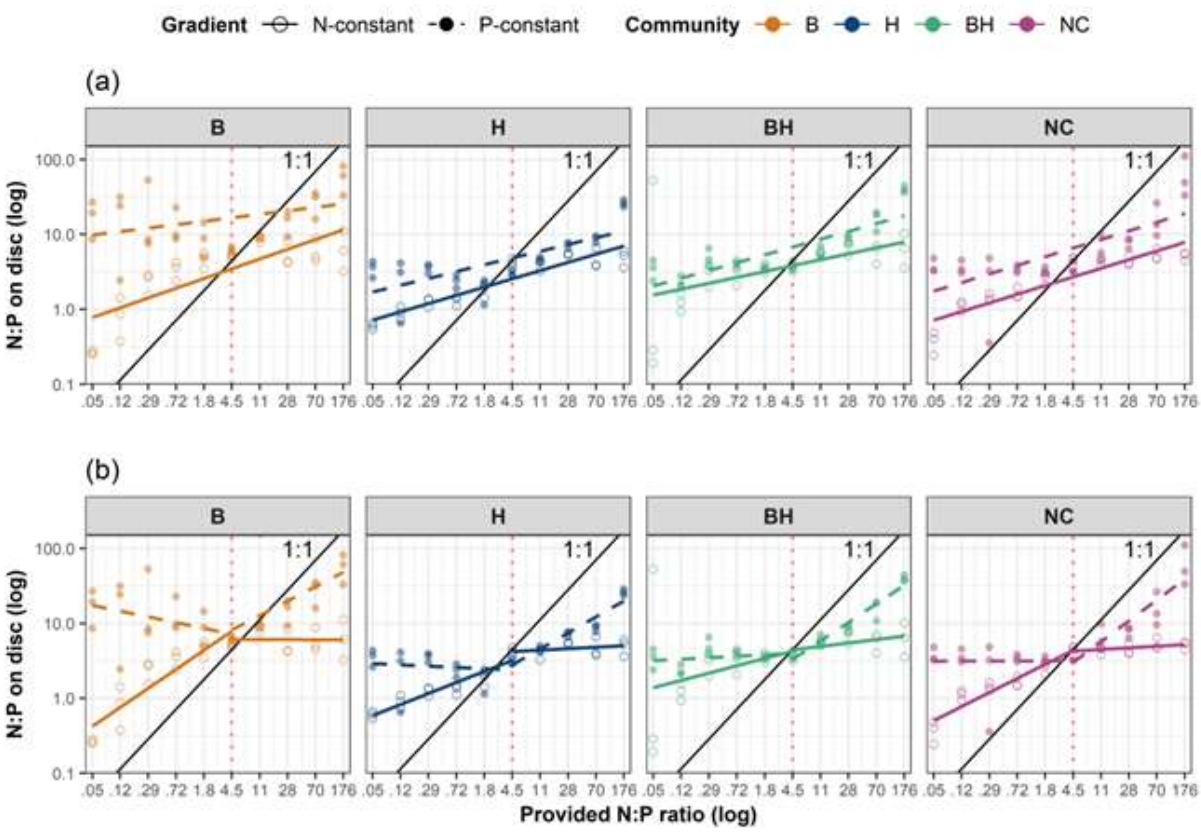

Figure III 5. Final N:P ratio on cellulose discs for the 4 microbial communities and the two N:P gradient tested.

(a) Linear regressions from R1(0.05) to R10 (176). **(b)** Linear regressions under R6 (⩽ 4.5) and over R6 (⩾ 4.5). Red dotted line is the N:P ratio R6 (4.5) with equal N and P concentrations in both nutrient gradients. Black diagonal 1:1 line is where final N:P on cellulose discs equals to the provided N:P ratios in the medium.

With the P-constant N:P gradient, the final ratios were almost constant up to R6, and steadily increased afterward (Figure.III.5b). Because of the bi-phasic observations, degree of homoeostasis (*1/H*) were calculated between R1 to R6 (N:P ≤ 4.5), and between R6 to R10 (N:P ≥ 4.5) for the four communities and the two nutrient gradients. *1/H* is the slope of the linear regression between log-transformed of both final N:P ratios on cellulose discs and provided N:P ratios (Table.III.1). For all tested communities, most decomposers showed higher plasticities when provided N:P ≤ 4.5 for the N-constant gradient, and when provided N:P ≥ 4.5 for the P-constant gradient. The degrees of homoeostasis of each community across the whole range of provided N:P ratios were similar for both nutrient gradients (between 0.2 and 0.29),

with the exception for the community **B** which had a higher degree of homoeostasis (ca 0.33) under the N-constant gradient, and a much lower degree (ca 0.12) under the P-constant gradient.

Table III 1. Degree of homoeostasis of microbial decomposers under different nutrient gradients.

1/H is the slope of linear regression between log (final N:P cellulose discs) and log (provided N:P). Values of 1/H are between 0 and 1, a value close to 0 indicates that the community is homoeostatic. r^2 is the Pearson correlation coefficient. "***" When P < 0.001, "**" when P < 0.05, "ns" when P > 0.05.

N:P	1/H	r^2	P
NC			
N-constant	**0.29 [0.24, 0.34]**	**0.82**	***
≤ 4.5	0.47 [0.38, 0.57]	0.88	***
≥ 4.5	0.054 [-0.004, 0.11]	0.24	ns
P-constant	**0.29 [0.18, 0.39]**	**0.54**	***
≤ 4.5	0.0019 [-0.18, 0.19]	0.00003	ns
≥ 4.5	0.7 [0.5, 0.9]	0.81	***
BH			
N-constant	**0.2 [0.07, 0.33]**	**0.26**	**
≤ 4.5	0.25 [-0.12, 0.61]	0.11	***
≥ 4.5	0.12 [-0.02, 0.25]	0.22	ns
P-constant	**0.26 [0.23, 0.32]**	**0.7**	***
≤ 4.5	0.05 [-0.04, 0.14]	0.083	ns
≥ 4.5	0.62 [0.52, 0.72]	0.93	***
B			
N-constant	**0.33 [0.14, 0.31]**	**0.64**	***
≤ 4.5	0.64 [0.48, 0.79]	0.83	***
≥ 4.5	-0.0023 [-0.16, 0.16]	0.00007	ns
P-constant	**0.12 [0.19, 0.33]**	**0.11**	**ns**
≤ 4.5	-0.19 [-0.43, 0.04]	0.16	ns
≥ 4.5	0.48 [0.14, 0.83]	0.42	***
H			
N-constant	**0.28 [-0.01, 0.24]**	**0.87**	***
≤ 4.5	0.37 [0.3, 0.44]	0.88	***
≥ 4.5	0.048 [-0.04, 0.14]	0.098	ns
P-constant	**0.23 [0.23, 0.42]**	**0.53**	***
≤ 4.5	-0.043 [-0.2, 0.11]	0.022	ns
≥ 4.5	0.54 [0.44, 0.63]	0.92	***

4. Discussion

In our study, we have found that, for all tested communities along the P-constant N:P gradient, cellulose mass loss exhibited "bell-shaped" curves as described by Güsewell and Guessner (2009). This result indicates cellulose decomposition rates had increased with the increasing dissolved N quantities, until it reached a certain N:P ratio that was unique to each community. At this ratio, utilisation of both N and P were optimised. The decomposition rate decreased, however, after the optimal ratio, suggesting a shifted limitation from N to P and a negative impact of this nutrient imbalance on decomposers activity. Among the studied communities, the community **H**, corresponding to an artificial mixture of 4 AH strains, had both the highest optimal and effective N:P ratios. This result is consistent with previous observations (Güsewell and Gessner 2009), fungi N:P being generally higher than that of bacteria (Danger, Gessner and

Bärlocher 2016). Bacteria have indeed generally high P requirements in order to ensure their fast growth (Danger *et al.* 2007b) while fungi are able to grow with extremely low amounts of P (Danger and Chauvet 2013; Grimmett *et al.* 2013). Aquatic hyphomycetes are thus expected to dominate bacteria in decomposers' communities under high N:P conditions. It could also help to explain that fungi are able to decompose plant litter in extremely low P conditions (e.g. in chapter II of this thesis) but also decompose plant litter that is almost totally P-depleted (litter with N:P > 100 in Hladyz *et al.* 2009).

Communities **NC** and **H** both generated the highest mass loss of cellulose. When fungi were removed from the **NC**, the **B** community alone led to about only 1/3 of the maximal cellulose mass loss observed in NC. This result clearly shows that fungal communities were the main driver of cellulose decomposition under our experimental conditions. This result confirms what is generally thought about the preponderant role played by aquatic fungi in leaf litter decomposition occurring in streams, bacteria being generally less efficient to decompose this recalcitrant material (Baldy, Gessner and Chauvet 1995; Gulis and Suberkropp 2003b). Interestingly, when the community **B** was associated to the community **H**, the resulting **BH** community exhibited maximal mass losses similar to those observed with the community **B** alone. The presence of the 4 AH strains did not restore cellulose decomposition rate to its maximum value observed with the community **H** alone. This negative effect of bacteria on AH development and activity suggests that competition may have occurred between both microbial populations. In this case, bacteria certainly dominated the microbial community and overtook fungi. As a consequence, the cellulose decomposition capacity of the whole community was brought down. With their faster growth rates compared to fungi, bacteria were shown to be able to take advantage of the more advanced fungal decomposition machinery, absorbing soluble compounds processed by fungal enzymes, and deprive fungi from its carbon and nutrient sources (De Boer *et al.* 2005). To verify this assumption, it will be interesting to measure the

relative abundance of bacteria and fungi at the end of our experiment in the community **BH** (work currently in progress). Another explanation may stand in the competition that could have occurred during the leaf litter colonisation process. Mille-Lindblom *et al.* (2006) already shown that negative effects of bacteria on fungi can be avoided if fungi are given an opportunity to establish before inoculation of bacteria. Even small reductions in fungal conidia germination capacities may largely impact the outcome of such interaction experiments.

With the N-constant N:P gradient, cellulose mass loss by the community **B** was the only one that exhibited a "bell-shaped" response of cellulose decomposition, with mass losses ranging from 5 % to 22 % of initial mass and maximal effective N:P ratio (10 %) comparable to the same community under the P-constant N:P gradient. The optimal N:P ratio that maximised decomposition was statistically significantly lower than the one obtained with the same community under the P-constant gradient. However, both ratios remained in comparable ranges (ca 2 to 5). On the other hand, communities **BH**, and **H** seemed to have had somehow constant cellulose decomposition rates despite N:P ratios were strongly imbalanced at the upper and lower parts of the N:P gradient. Decomposition remained high for the lowest P availabilities, confirming that decomposers (at least fungi, not bacteria alone) are able to live with extremely low amount of P and might be able to recycle and/or remobilise their internal P very efficiently. In contrast to expectations, community **NC** even showed increasing decomposition rates of cellulose as N:P ratios went higher. This observation seems puzzling as it suggests negative effect of the P quantity in the medium on cellulose decomposition rate, this observation contradicting previous studies (Ferreira *et al.* 2015b). A second observation is that when bacteria were present in a decomposer community (**B**, **BH,** and **NC**), cellulose mass losses were much lower than that from the pure fungal community (**H**) at the lowest N:P ratios where P was in excess. This result suggests that too much dissolved P in the microcosm may have had a negative effect on bacterial decomposers. A hypothesis is that P excess might be directly toxic

to bacterial development (Lorencová *et al.* 2012). A second hypothesis is that, since the inoculum of **NC**, **B**, and **BH** was issued from natural environment, only particles larger than fungal spores have been filtered out, and any particles smaller than bacteria cells were still present. Among these particles, bacteriophages using bacteria as hosts may have proliferated in our microcosms. Phage replication process demands high amounts of P-rich RNA and/or DNA (Weigel and Seitz 2006). High P availabilities could thus have increased decomposers mortality, as already observed for metazoans (Frost, Ebert and Smith 2008). Further studies will be required to test this hypothesis, but protocols already exist to quantify bacteriophage abundance (e.g. Panec and Sue Katz 2016).

Final N and P quantities on cellulose discs for both nutrient gradients followed the initial N and P availabilities in the microcosms. At first glance, this result was not surprising since pure cellulose was almost depleted in both nutrients. As decomposers develop on the leaves, all the dissolved nutrients they have immobilised would be eventually accumulated on the decomposing material. However, although the level of both N and P found on cellulose discs were comparable for all 4 tested communities under our test conditions, the level of cellulose decomposition was shown to be different between the tested communities. The high mass loss of cellulose by community **H** might not only be due to the high decomposition efficiency of fungi, but it might also be because the community **H** was an artificial construct from pure fungal strains. This community with reduced diversity would also release them from competitive pressure with presumably less negative interaction with each other. As pointed out earlier, the other 3 communities could contain other uncontrolled variables – such as other microorganisms - which might affect microbial decomposers efficiency of processing cellulose. Nevertheless, despite the decomposer communities composition (bacteria, fungi, or both), our observations highlighted a functional redundancy of different decomposer communities as they all ensure nutrient immobilisation and decomposition.

Finally, our experiment also allowed to compare the elemental homoeostasis of the different communities. Overall homoeostasis across the whole range of provided N:P ratios for all tested communities were under 0.33 which indicates that under the tested conditions, all communities were quite homoeostatic (Persson *et al.* 2010). This means that the community as a whole had a great ability to maintain the balance between both nutrients. This result contrasts with the theoretical predictions and the experimental results previously obtained on bacterial communities (Danger *et al.* 2008). Species replacements along nutrient gradients were indeed expected to optimise nutrient use and ensure non-homoeostasis at the community level. However, looking at the final N:P ratios of cellulose discs, there was clearly a slope shift between stoichiometric values found under and over the provided ratio R6 (4.5), meaning that at this ratio, the limiting factor was certainly close to shift from N to P (co-limitation ratio, as in Danger *et al.* 2007). However, the result of this change depended on the nutrient gradient type. For the N-constant N:P gradient, decomposer communities were relatively less homoeostatic under the provided ratio of 4.5, and in reverse, for P-constant gradient, they were less homoeostatic over the provided ratio of 4.5. As already observed for primary producers (Danger *et al.* 2007), the way nutrients are used and stored by decomposers might thus at least partly depend on the nature of the limiting nutrient as well as on the intensity of the nutrient imbalance.

5. Conclusions

Overall, under our experimental conditions, the fungal assemblage (H) and the natural decomposer community (NC) have the highest optimal N:P ratio and efficiency for cellulose decomposition. Cellulose decomposition rate is known to depend on both nutrient gradient and supplied nutrient ratios (Güsewell and Gessner 2009). In our study, when the supply of P is constant, a lack or an excess of N slows down cellulose decomposition rate by bacteria, fungi,

or both. When the supplied N is constant, however, both the lack or the excess of P seems to limit the decomposition efficiency of bacteria-only community. In contrast, when fungi are present in a community, the lack of P does not affect the community's efficiency of cellulose decomposition, probably due to extremely high P-use efficiency of fungi. If our results are generalisable to freshwater streams under natural conditions, depending on litter nutrient content and the decomposer community, shifts of N:P ratios (common at a global scale, Peñuelas *et al.* 2017) but also the nature of the element that is mainly changed (N or P) could largely determine the consequences on litter decomposition. Extending these laboratory results to field observations should give interesting insights on the understanding of changes in nutrient availability on the functioning of streams.

CHAPTER IV

Towards the use of decomposer optimal N:P ratios to predict the response of decomposer communities to environmental stressors

Results of the previous chapters showed that using adapted N:P gradients, it was possible to evidence optimal N:P ratios for litter decomposition, and that these ratios might differ between decomposer species (AH taxa) or taxonomic groups (bacteria vs. fungi). Previous results also showed that these optimal ratios might impact the functional role of decomposers (decomposition efficiency and nutrient immobilisation/mineralisation balance). In this last chapter, we wanted to investigate if environmental stressors (namely metal pollution and temperature variation) were prone to alter the N:P ratios maximising plant litter decomposition.

CHAPTER IV

Part 1

Nitrogen to phosphorus ratio shapes the bacterial communities involved in cellulose decomposition and copper contamination alters their stoichiometric demands

Ziming Wang, Aurélie Cébron, Vincent Baillard, Michael Danger

Published on FEMS Microbiology Ecology

DOI: 10.1093/femsec/fiac107

Abstract

All living organisms have theoretically an optimal stoichiometric nitrogen:phosphorus (N:P) ratio below and beyond which their growth is affected but data remain scarce for microbial decomposers. Here, we evaluated optimal N:P ratios of microbial communities involved in cellulose decomposition and assessed their stability when exposed to copper Cu(II). We hypothesised that (1) cellulose decomposition is maximised for an optimal N:P ratio, (2) copper exposure reduces cellulose decomposition and (3) increases microbial optimal N:P ratio, (4) N:P ratio and copper modify the structure of microbial decomposer communities. We measured cellulose disc decomposition by a natural inoculum in microcosms exposed to a gradient of N:P ratios at three copper concentrations (0, 1 and 15 µM). Bacteria were most probably the main decomposers. Without copper, cellulose decomposition was maximised at an N:P molar ratio of 4.7. Contrary to expectations, at high copper concentration, the optimal N:P ratio (2.8) and the range of N:P ratios allowing decomposition were significantly reduced and accompanied by a reduction of bacterial diversity. Copper contamination led to the development of tolerant taxa probably less efficient in decomposing cellulose. Our results shed new lights on the understanding of multiple stressor effects on microbial decomposition in an increasingly stoichiometrically imbalanced world.

Key words:

N:P ratio, metal contamination, ecological stoichiometry, nutrient immobilisation, nutrient mineralisation, bacterial diversity, microbial decomposer

1. Introduction

Decomposition is the biological process that leads to mass reduction and transformation of dead organic matter (Gessner *et al.* 2010). It is a ubiquitous process and a fundamental link in the biogeochemical cycles of elements and central for ecosystem functioning. Plant litter decomposition is a complex process controlled simultaneously by intrinsic factors, environmental factors and abundance and diversity of biological actors (Gessner *et al.* 2010; Bani *et al.* 2018). Some heterotrophic microorganisms, including both fungi and bacteria, form the functional group of microbial decomposers which are the main actors of decomposition (Gessner, Chauvet and Dobson 1999). Among the environmental factors likely to impact the plant litter decomposition process, nutrient availability in the surrounding environment of the litter plays a crucial role (Güsewell and Verhoeven 2006; Güsewell and Gessner 2009; Woodward *et al.* 2012). Plant litter is generally nutrient depleted (Moore *et al.* 2004), and microbial decomposers must balance their nutrient requirements through the consumption of mineral elements coming from their environment (a process called nutrient immobilisation: Daufresne & Loreau, 2001; Harte & Kinzig, 1993). When these requirements are satisfied, these organisms are able to efficiently decompose plant litter, converting it into their biomass. At the same time, they also release inorganic carbon through their respiration and nutrients through their exoenzymatic activities, these elements being considered as recycled back into ecosystems (inorganic carbon and nutrient releases correspond to the mineralisation process: Harte and Kinzig 1993). Several reviews clearly confirmed the stimulating effects of nutrient enrichment on decomposition rates (Ge *et al.* 2013; Ferreira *et al.* 2015b; Zhang *et al.* 2018), suggesting the idea that a balanced nutrient availability which allows the microorganisms to optimally fulfil their nutrient demand should be beneficial for maximising their decomposition activity. A precise knowledge of the elemental requirement of microbial decomposers is thus an essential

prerequisite for predicting the speed and intensity of litter decomposition as well as nutrient and carbon releases.

In the ecological stoichiometry framework, the imbalance between consumer requirements and elements availability is often referred to as "stoichiometric constraints" (Sterner and Elser 2003a). Among all the necessary chemical elements that ensure living organism growth, nitrogen (N) and phosphorus (P) are generally the most commonly considered. N is one of the main components of amino acids (proteins), and P is, among others, a fundamental component of nucleic acids (DNA and RNA). Litter decomposition is frequently controlled by N and P availability in the medium (Woodward *et al.* 2012). For microbial decomposers, the overall litter and environmental N:P ratio may therefore be a potential indicator for determining whether the N or P might be limiting for microorganisms growth and activity, at least during the early stage of decomposition when carbon availability is not limiting (Tessier and Raynal 2003).

While the specific optimal elemental ratios have long been studied in plants (e.g. Tilman 1985) and animals (e.g. Frost *et al.* 2006), data are far less available for microorganisms. Using natural microbial inoculum, Güsewell and Gessner (2009) shown that cellulose and plant litter decomposition were maximised at intermediate available N:P ratios, these ratios corresponding to optimal N:P ratios for the decomposition process at the community level. Changes in the available N:P ratios also resulted in altered balance between microbial decomposers, as shown by changes in the bacteria to fungi ratio along their N:P gradient. From a stoichiometric viewpoint, such changes in community structure could result from competitive exclusion and the selection of species based on their optimal nutrient requirements along the N:P availability gradient (Danger *et al.* 2008). Thus, based on microbial nutrient requirements, the relative N to P availability should, at least partly, determine community structure and composition.

Concerning the decomposition process, these species replacements are expected to maximise nutrient uptake and reduce variations in litter decomposition efficiency (Fanin *et al.* 2013).

Giving the importance of microbial optimal nutrient ratios for the decomposition process and community structures, understanding the response of these optimal ratios to environmental stressors might be of particular interest. If multiple environmental stressors impact microbial diversity, plant litter decomposition may be affected (Niyogi *et al.* 2009; Gessner *et al.* 2010; Ferreira *et al.* 2015a; Tolkkinen *et al.* 2015). Both nutrient availability (Falkowski *et al.* 2000) and ratios (Elser *et al.* 2009; Peñuelas *et al.* 2013) can be problematic for ecosystem functioning due to changes in nutrient balance. Metal contamination is another major recurrent stressor. Metals have long been shown to reduce plant litter decomposition rates in lands (Berg *et al.* 1991) and in streams (Duarte *et al.* 2008). The number of litter-colonising fungus decreases in presence of high metal concentrations (Solé *et al.* 2008). Microbial activity is lower in metal polluted environments (Niyogi *et al.* 2009). Copper (Cu) represents a classical model of metallic contaminant. This metal is still actively used in agriculture, resulting in its accumulation in soils and leaching into surface water ecosystems. Cu has been largely studied and is known to alter microbial community structures (Wakelin *et al.* 2010; Keiblinger *et al.* 2018) and affect litter decomposition (Fernández *et al.* 2015).

In this study, using Cu as a model of contaminant, we investigated its impact on the optimal elemental N:P ratios for cellulose decomposition by microbial decomposers. We hypothesised that (H1) cellulose decomposition rate reaches its maximum at an optimal N:P ratio; (H2) high Cu concentration reduces the overall cellulose decomposition rate; (H3) due to increased N-demand for detoxification and reduced microbial growth, the optimal N:P ratio increases under higher Cu contamination, and (H4) both N:P ratio and the presence of Cu interactively affect the composition of microbial decomposer communities. Since natural plant litter nutrient content is often variable (Cornwell *et al.* 2008), pure cellulose, representing a part of plant cell

walls, was used as a model carbon substrate to control N and P quantities, as successfully used in the past (Hopkins *et al.* 1990; Chew, Obbard and Stanforth 2001; Güsewell and Gessner 2009). To test our hypotheses, we quantified the decomposition of cellulose discs by a natural inoculum of microbial decomposers in microcosms under laboratory-controlled conditions. Decomposition was followed along a gradient of available N:P ratios in liquid culture media and under three concentrations of dissolved Cu: 0 µM, 1 µM and 15 µM. After 79 days of incubation, we measured the mass loss of the cellulose discs, the quantities of N and P immobilised on the discs by microbial decomposers, and we analysed the abundance and diversity of the microbial decomposers.

2. Materials and Methods

2.1. Microbial inoculum preparation

Leaves (mainly beech) were collected in 2015, by using suspended filets around trees (1 m above ground) in the forest near the Maix stream in the Vosges Mountains (latitude 48° 29'2.56″ N, longitude 7° 4'10.75″ E). In early 2018, eight litterbags (500 µm mesh size) each containing 5 g of leaves (dry weight) were submerged in the same stream to allow bacterial and fungal colonisation. The bags were retrieved after 14 days along with samples of stream water. Leaf litter contained in the bags were gathered. Microbial inoculum was prepared by putting 20 g (fresh weight) of leaf litter in 5 L Erlenmeyer flasks with 1 L of fresh stream water, incubated under gentle agitation and aerobic condition for 48 hours at 18 °C. After the incubation, water was separated from large litter debris by passing through a sieve (1 mm mesh size) and was left at 4 °C to decant for 2–3 hours before collecting the supernatant. This microbial inoculum was stored for less than 24 hours at 4°C prior its use for the experiment.

The initial number of fungal spores and bacteria was determined on aliquots of the inoculum. Fungal spores were counted under an optical microscope, inoculum was fixed with formaldehyde (2 %) and stained with Trypan blue (0.05 %) before being filtered (Millipore MF™ 5.0 µm SMWP02500). Bacteria were counted through DAPI (1 µg ml^{-1}) staining after filtration (Whatman Nucleopore Track-Etch membrane 25 mm, 0.2 µm). Seven images were taken using an epifluorescence microscope (Nikon C-HGFIE equipped with a DS-Qi1Hc CCD camera) and were analysed using a NIS-Elements BR software (Nikon). Although we planned to have a mixed inoculum, the microcosms were largely inoculated with bacteria (ca 9.6 × 107 bacteria per microcosm) and no fungal spores but with a few mycelia fragments (see discussion).

2.2. Microcosm preparation

The microcosms were prepared under sterile condition, following the model from a previous study (Güsewell and Gessner 2009). In a plastic Petri dish (Ø 90 mm) containing 50 g of river sand and covered by a nylon mesh (250 µm porosity), five cellulose discs of Ø 22 mm were placed (Figure.IV.S1). The river sand was sieved (< 2 mm), washed, dried, and burned at 450 °C for over four hours to sterilise and remove all traces of organic material. The cellulose discs were cut out from cellulose paper filter (Whatman ashless 110 mm, GE), sterilised, and were used as the only carbon source for microorganisms. The total cellulose dry mass introduced into each microcosm was 181.5 ± 5.7 mg (36.3 ± 1.2 mg per disc).

Each microcosm was filled with 18.5 ml of a sterilised COMBO mineral medium containing 36.8 mg L^{-1} $CaCl_2 \cdot 2H_2O$, 37.0 mg L^{-1} $MgSO_4 \cdot 7H_2O$, 12.6 mg L^{-1} $NaHCO_3$, 28.4 mg L^{-1} $Na_2SiO_3 \cdot 9H_2O$ and 24.0 mg L^{-1} H_3BO_3 (Kilham *et al.* 1998). Nitrogen (N), phosphorous (P) and copper (Cu) were also included but with different concentrations to obtain desired N:P ratios and Cu contamination levels.

Seven N:P ratios (molar) were created by varying the amount of both N and P in each medium using NH_4NO_3 for N, and a mixture of KH_2PO_4 and K_2HPO_4 (3.85/6.15 v/v, for pH 7) for P. The seven N:P ratios were 1.2, 3.7, 11, 33, 100, 300 and 898 with a global supply level of 0.75 [geometric mean of N and P mass in mg for all N:P ratios, i.e. in a microcosm, $[(m_N \times m_P)^{0.5} = 0.75$, see Güsewell and Gessner 2009]. Three Cu contamination levels (0, 1 and 15 µM) were tested by adding $CuSO_4 \bullet 5H_2O$ to each medium. The initial concentrations of N, P and Cu were verified. N and P reached at least 86.4 % of their nominal values, which made the practical N:P ratios vary between 93.9 % and 97.5 % of the theoretical values. Measured copper concentrations were 0.69 ± 0.06 µM and 13.33 ± 0.83 µM for the media containing 1 and 15 µM respectively.

A total of 21 conditions (seven N:P ratios × three [Cu]) were tested. Each condition was replicated in five microcosms. Additionally, controls without inoculum were included.

The inoculation was done by dispensing 300 µl of freshly prepared and well-homogenised inoculum directly onto each cellulose disc (1.5 ml per microcosm). The microcosms were then placed in dark boxes and kept in an incubator at 18 °C. A water tray was placed in each box to maintain humidity and avoid media evaporation. Humidity of each microcosm was monitored every two weeks during the incubation period. If necessary, water levels were adjusted with MilliQ ultrapure sterile water. Since we were interested in early stages of cellulose decomposition, we initially planned to stop the experiment when ca. 35-50% of detritus mass loss was reached. At day 79, some of the cellulose discs were becoming almost transparent suggesting an advanced stage of decomposition, thus we decided to stop the experiment. Each cellulose disc was collected and conserved individually. To take into account potential heterogeneity between discs in each microcosm, the purpose of each disc was decided randomly. Two discs were freeze-dried and used for cellulose mass loss calculation, one of them was then

used for total N and P quantification and the other one was kept for ergosterol extraction. A third disc was used for DNA extraction, and the last two discs were stored at -20 °C as backup.

2.3. Mass loss, ergosterol and N P content

Cellulose mass loss was determined by weighting the two freeze-dried discs to the nearest 0.1 mg. Subsequently, one of the discs was used to analyse total N and P content (70 samples, seven N:P ratios × four replicates for [Cu] 0 µM, and seven N:P ratios × three replicates for [Cu] 1 µM and 15 µM). Those discs were reduced into fine powder using Ø 3 mm, clean, steel grinding balls and a bead beater (Mixer Mill, Retsch MM301). Between 1.5 and 2.0 mg of powder was put into tin capsules (Säntis Analytical SA7698110) and used to analyse the total N quantity by an elementary analyser (Carlo Erba NA 2100). The total P quantity was analysed by first digesting 2.0 to 2.5 mg of the powder in 10 ml of NaOH (0.1 M) and Na2S2O8 (0.125 M) for two hours at 105 Pa (1 bar) 120 °C. After cooling, P was measured on the digested solutions using molybdate blue colorimetric method at 880 nm (ISO 6878:2004). The second freeze-dried disc was used to determine ergosterol content (estimation of fungal biomass). During inoculum preparation and incubation, absence of fungal spores and development has been noted, Real-Time qPCR of fungal 18S rRNA genes also resulted low copy numbers (see below). To confirm this result, only one replicate per condition (21 samples) was extracted and analysed for ergosterol, confirming the extremely low abundance of active fungi. Ergosterol extraction and HPLC analyse followed a standard protocol (Gessner 2005). Briefly, the cellulose disc was placed into a KOH/methanol (8 g L^{-1}) solution overnight at 4 °C, then heated at 80 °C during 30 min for extraction. The extracts were loaded into SPE cartridges (Oasis HLB 30 µm Extraction Cartridge). Ergosterol was eluted in 1.4 ml isopropanol and stored at -20 °C until HPLC analyses. Extractions were carried out in a series of 12 with 11 samples and a positive control with known concentration of HPLC grade ergosterol (>95 %, Sigma Life

Science). HPLC analyses were assured by Chromaster Hitachi (Pump 5110, Autosampler 5210, UV Detector 5410), using LiChrospher RP18 column (LiChroCART 250-4 HPLC cartridge, Merck), equipped with a column thermostat set at 33 °C (Jetstream 2 plus).

2.4. Molecular analyses (DNA extraction, qPCR, NG-sequencing, OTU analyses)

Total genomic DNA was extracted from one disc of each microcosm (65 samples, seven N:P ratios × three [Cu] × three replicates plus two replicates of the initial inoculum), using the PowerSoil DNA Isolation Kit (MO BIO), and following the manufacturer protocol. Between 3 and 7 ng μl^{-1} of total DNA (measured with a Shimatzu spectrophotometer equipped with a Traycell tank) were recovered from each cellulose disc.

Real-Time qPCR targeting the 16S and 18S rRNA genes (bacteria and fungi, respectively) were performed as described in Cébron *et al.* (2008) and Thion *et al.* (2012). The number of 16S and 18S rRNA gene copies was used to estimate bacterial and fungal relative abundances. The primer pairs used were 968F (5'-GAACGCGAAGAACCTTAC-3') and 1401R (5'-CGGTGTGTACAAGACCC-3') for bacterial 16S rDNA (Nübel *et al.* 1996) and Fung5F (5'-GTAAAAGTCCTGGTTCCCC-3') and FF390R (5'-CGATAACGAACGAGACCT-3') for fungal 18S rDNA (Smit *et al.* 1999; Vainio and Hantula 2000). The amplification mix was prepared in 20 µl with: 10 µl 2× iQ SyberGreen Supermix (Bio-Rad); 0.8 µl of each primer (10 µM); 0.4 µl of 3 % bovine serum albumin (BSA); 0.2 µl of dimethyl sulfoxide (DMSO); 0.08 µl of T4 bacteriophage gene-32 product (QBiogene); 6.72 µl of DNA-free distilled water and 1 µl of template DNA or distilled water (negative control) or ten-time dilutions of standard plasmids from 108 to 101 copies μl^{-1}). The amplification programmes used for Real-Time qPCR were as follows: 95 °C for 5 min, 40 cycles with 20 s at 95 °C, 20 s at the primers specific annealing temperature (56 °C and 50 °C for 16S and 18S rDNA, respectively), 30 s at 72 °C

and 5 s measurement of SYBR® Green I signal at 82 °C or 80 °C (for 16S and 18S rDNA, respectively), followed by a melting curve analysis from 50 °C to 95 °C.

For bacterial 16S rRNA gene amplicon-sequencing, the primer pair used for the first-step PCR were 341F (5'-CCTACGGGAGGCAGCAG-3'; Muyzer, de Waal and Uitterlinden 1993) and 787R (5'-GGACTACNVGGGTWTCTAAT-3'; Caporaso *et al.* 2011), each attached to an adaptor for a second PCR. The amplification mix was prepared for 50 µl final volume with: 10 µl 5× HF Buffer; 1 µl of dNTP (10 mM); 0.25 µl of dimethyl sulfoxide (DMSO); 0.1 µl of T4 bacteriophage gene32 product (QBiogene); 1.5 µl of $MgCl_2$ (50 mM); 1 µl of each primer (10 µM); 33.05 µl of DNA free distilled water; 0.1 µl of Phusion polymerase (Thermo Scientific) and 2 µl of DNA samples (or distilled water for negative control). 30 cycles of amplification at 56 °C annealing temperature were performed. These first-step PCR products containing unpurified DNA were then sent to Microsynth (Next Generation Sequencing Department, Microsynth AG, Switzerland) for the second-step PCR and MiSeq 2 × 250 bp paired-end sequencing (Illumina).

A total of 4 443 671 paired-end reads from the 65 samples (accessible on SRA-NCBI database under BioProject accession number PRJNA820766) were obtained. Paired-end sequences were processed for quality filtering and clustered into operational taxonomic unit (OTU) at 97 % using Mothur (v1.44.3; Schloss *et al.* 2009) and following MiSeqSOP (first access date: 14 December 2020; Kozich *et al.* 2013). Taxonomy was assigned using SILVA ssu132 database. Singletons and sequences not affiliated to bacteria were removed. The final dataset comprised 1 896 248 sequences ranging from 4576 to 81 348 sequences per sample. Finally, the dataset was rarefied to the lowest number of sequences per sample (i.e. 4576 reads/sample, see Figure.IV.S2 for rarefication curves) to compare the diversity of 2219 OTUs (including data from the initial inoculum). By doing so, we had sufficient sequencing depth and statistical power to compare between conditions although some OTUs had been excluded. Alpha diversity

was expressed by calculating Chao1 richness and Shannon diversity indices (Hill *et al.* 2003) using Mothur (v1.44.3; Schloss *et al.* 2009).

2.5. Statistical Analyses

All modelling and statistical analyses of our results were carried out with R software (v4.1.0; R Core Team 2022). The N:P ratios were log transformed prior to all analyses.

We assume the cellulose mass loss caused by microbial decomposers follows a biphasic tendency (symmetric "bell-shape" curve) alongside the log transformed gradient of N:P ratios. For this reason, the cellulose disc mass loss data was fitted using a Gaussian type model with four parameters:

$$y = (h - d)exp\left(-2\left(\frac{x - e}{w - e}\right)^2\right) + d$$

Where *y* is the cellulose disc mass loss in percentages, *x* is the log-transformed value of N:P ratio, *h* is the maximum *y* value which is the height of the curve peak (i.e. the maximal mass loss), *d* is the mass loss for very low and very high N:P ratios (i.e. the minimal mass loss which is considered to be constant regardless of the N:P ratio), *w* (> 0) is a shape parameter which controls the width of the "bell", it is the N:P ratio below which the mass loss reaches 97.5 % of *d*. It can also be seen as the highest N:P ratio beyond which the additional mass loss over *d* is negligible. Finally, *e* (> 0) is the value of *x* which corresponds to the maximum *y* value, it is the log of the N:P ratios where the maximal mass loss can be observed. (Figure .IV.1a adapted from Larras *et al.* 2018)

Two-way analysis of variance (ANOVA) was used to evaluate the effect of N:P ratio, [Cu] and their interaction on cellulose mass loss, and immobilised N and P quantities. In case of a *P-value* lower than 0.05, Tukey HSD *post-hoc* tests were performed to determine which

treatments differ significantly from others. When ANOVA was inapplicable, nonparametric Kruskal-Wallis test followed by Wilcoxon-Mann Whitney *post-hoc* test was applied. Levene's test was applied to verify homogeneity of variance between conditions. The linear correlations between cellulose mass loss and OTU numbers, Chao1 or Shannon indices of all three Cu contamination levels were obtained by calculating the Pearson's correlation coefficient. Levene's test was from "car" R package (v3.0-13; Fox and Weisberg 2019), other tests were from the "stats" package (v4.2.0; R Core Team 2022).

The beta diversity based on Bray-Curtis dissimilarity was represented using non-metric multidimensional scaling (NMDS) analysis with two dimensions using the "metaMDS" function of the "vegan" R package (v2.5-7; Oksanen *et al.* 2020). The differences in community composition between each level of [Cu] were tested by permutational multivariate analysis of variance (PerMANOVA) with 999 permutations using the "adonis2" function.

In an attempt to identify bacterial taxa that stand out the most under contrasted treatments, indicator species were analysed. The indicator values (IndVal < 1) of OTUs were calculated using the "multipatt" function of the "indicspecies" package (v1.7.9; de Cáceres, Legendre and Moretti 2010). We used the group-equalised IndVal (IndVal.g) index to find OTUs that were proportionally more likely to be present at a group. By limiting the index between 0.7 and 1 as done previously by other studies (Demircan *et al.* 2018), we can focus on the most relevant OTUs. The higher the value, the more likely an OTU was abundant in that group. Based on result similarities of bacterial diversities and cellulose decomposition at different N:P ratios and [Cu] (see results section), we have decided to merge these results into four groups: 0 and 1 µM of [Cu] were grouped together as "low Cu (CL)" and the group of 15 µM as "high Cu (CH)", we omitted all the samples of N:P ratio of 33 as it is an intermediate ratio and then grouped the three lower ratios together and the three higher ratios together (as "RL" and "RH", respectively), thus forming four groups: CLRL, CLRH, CHRL and CHRH. The indicator species analysis

was performed with 9999 permutations on the rarefied dataset of 1603 OTUs (excluding data from the initial inoculum).

3. Results

3.1. Cellulose disc mass loss – Optimal N:P ratio

Cellulose discs lost up to 30 % of their initial dry mass. Mass losses depended on [Cu] (ANOVA, $F = 62.365$, $P < 0.001$) and supplied N:P ratio ($F = 108.317$, $P < 0.001$), with a significant interaction ($F = 3.652$, $P < 0.001$). Figure.IV.1b shows the mean values of empirical mass losses (points) and the statistical models (curves). For all three Cu contamination levels, the maximal mass loss occurred at the supply ratio of 3.7 and the minimal mass loss occurred at ratios greater than 100. For lower [Cu] (0 and 1 µM of Cu), the minimum mass loss was about 10 % while it was as low as about 2 % for the group of 15 µM. Values of each parameter and their confidence intervals (CI, 95 %) were extracted from models. Optimal N:P ratios (parameter *e*, Figure.IV.1c) decreased with increasing [Cu]. The CI showed that the optimal N:P ratios for 0 and 15 µM of Cu (4.7 and 2.8, respectively) differed significantly from each other. Minimal mass losses (parameter *d*, Figure.IV.1d) showed no difference between 0 and 1 µM of Cu (8.0 % and 8.3 %, respectively) but both were significantly different from that of 15 µM (1.5 %). On the other hand, the maximal mass losses (parameter *h*, Figure.IV.1e) between all three groups were not significantly different from each other (28.6 %, 25.3 % and 23.9 % for 0, 1 µM and 15 µM of Cu, respectively), the value tended to decrease with increasing [Cu]. Although the maximal effective N:P ratio (parameter *w*, Figure.IV.1f, N:P ratio beyond which the mass loss is minimal and stays constant) values were not significantly different among the three Cu contamination levels, they were reduced from 102.4 to 33.6 between 0 µM to 15 µM of Cu.

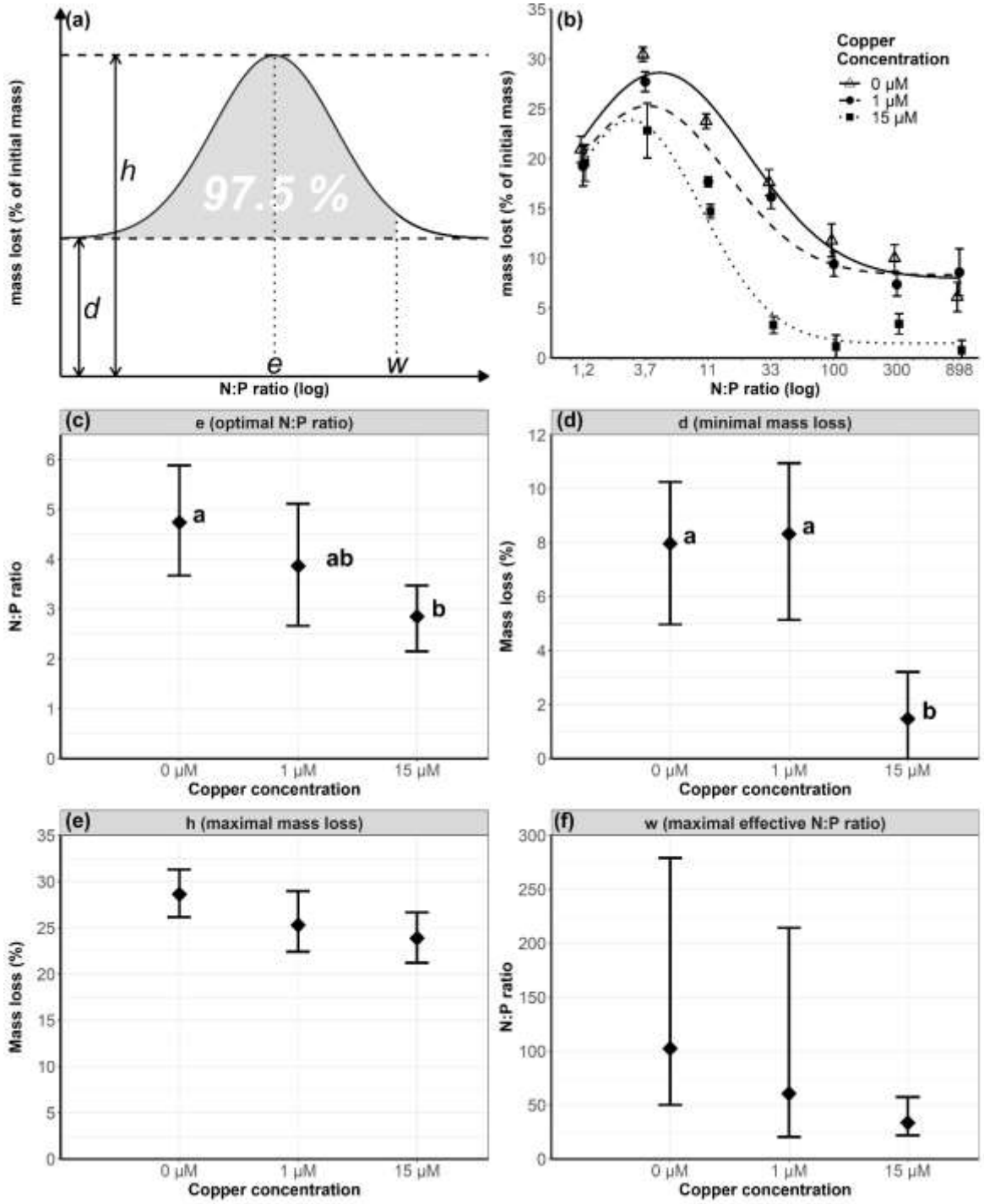

Figure IV 1. (a) Schematic representation of the Gaussian model. *x-axis* is the log transformed N:P ratios; *y-axis* is the mass loss. ***d*** is the minimal mass loss; ***h*** is the maximal mass loss; ***e*** is the optimal N:P ratio for the maximal mass loss; ***w*** is the maximal effective N:P ratio less than which there are 97.5 % of cumulative mass loss from the level of ***d*** (grey area). **(b) Cellulose mass losses**. Cellulose disc mass losses after 79 days calculated in the percentage of the average initial mass (36.3 mg) minus the average 3 % loss of the controls without inoculum. *x-axis* for provided N:P ratios is log-transformed but shows as the molar ratio for reading convenience. Curves show mass loss calculated by the Gaussian model. **(c, d, e, f) Graphical representation of each parameter estimated by the Gaussian model for all three tested copper concentration levels.** The error bars show the 95 % confidence interval (CI) for each estimation.

3.2. Immobilised N and P quantities on cellulose discs

The quantity of immobilised N was independent of [Cu] (ANOVA, F = 1.301, $P = 0.28158$), but varied with provided N:P ratio (F = 12.477, $P < 0.001$) and showed a significant interaction (F = 3.308, $P = 0.00147$) (Figure.IV.2a). The variation was non-linear and the difference (Δ = Max. – Min.) was greater for samples without Cu (0.24 mmol g^{-1}) compared to the one with 1 µM and 15 µM of Cu (0.11 mmol g^{-1} and 0.13 mmol g^{-1}, respectively). Since the global average of immobilised N was around 0.17 mmol g^{-1}, the percentage of provided N that has been immobilised decreased significantly with increasing N:P ratio (Kruskal-Wallis, $X^2 = 62.998$, $P < 0.001$) (Figure.IV.2b). The quantity of immobilised P was lower at 15 µM [Cu] ($X^2 = 8.5283$, $P = 0.01406$) and decreased with increasing N:P ratio ($X^2 = 38.221$, $P < 0.001$) (Figure.IV.2c). As a result, the percentage of provided P that has been immobilised increased significantly with increasing N:P ratio ($X^2 = 44.306$, $P < 0.001$) and lower with [Cu] ($X^2 = 6.8641$, $P = 0.03232$)

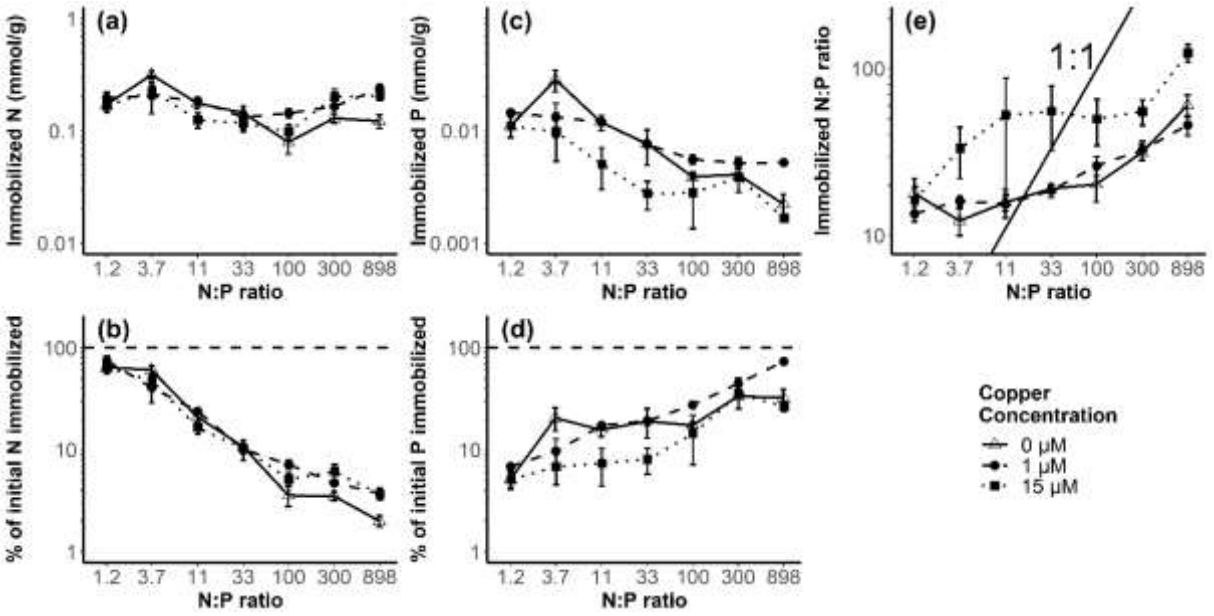

Figure IV 2. N and P immobilised on cellulose discs for three copper concentrations in relation to the provided N:P ratio.

(a, c) millimoles of N and P immobilised per gram of final cellulose dry mass; **(b, d)** percentage of provided N and P immobilised on the disc; **(e)** immobilised N:P ratio, the 1:1 line shows the immobilised N and P in proportion to the provided ratio. Error bars show the standard deviation of 4 replicates for 0 copper, and 3 replicates for 1 µM and 15 µM copper. x-axis for provided N:P ratios is log-transformed but shows as the molar ratio for reading convenience.

(Figure.IV.2d). As a proxy of the microbial N:P ratio, the ratio of immobilised N:P ranged from 12 to 125, with a 10-fold increase with increasing of the provided N:P ratio and up to 3-fold at the higher [Cu]. The condition with 15 µM of Cu showed a greater intra-replicate variation and higher immobilised N:P ratios compared to the 0 and 1 µM of Cu (Figure.IV.2e).

3.3. Identification of the cellulose decomposition actors

The relative abundance of bacteria and fungi was estimated through qPCR quantification of 16S and 18S rRNA genes. The relative proportion of bacteria to fungi (Figure.IV.3) was not changed by N:P ratios (X^2 = 1.8853, P = 0.9299) but significantly decreased 10 folds with increasing [Cu] (X^2 = 42.229, P < 0.001). Abundance of bacterial 16S was about 10^3 to 10^5 times higher than that of fungi. The 16S rRNA gene copies stayed relatively constant (10^6 to 10^7 copies μl^{-1}) among the provided N:P ratios (X^2 = 12.733, P = 0.04748) and [Cu] (X^2 = 3.943, P = 0.1392). The number of 18S rRNA gene copies was not influenced by N:P ratios (X^2 = 1.2234, P = 0.9757), but increased with [Cu] from 102 to 104 copies μl^{-1} (X^2 = 46.624, P < 0.001) (See Figure.IV.S3). The ergosterol assays also confirm the low abundance of fungi since ergosterol was detected only on 2 out of 21 samples analysed (0.08 and 0.20 µg ml^{-1} compared to at least 4.15 µg ml^{-1} for positive controls, which correspond to 7.1 and 26.4 µg g^{-1} of cellulose disc). All these results indicated that cellulose discs were mainly colonised by bacterial communities confirming our visual observations made during incubations (no fungal mycelium development on cellulose disc surface).

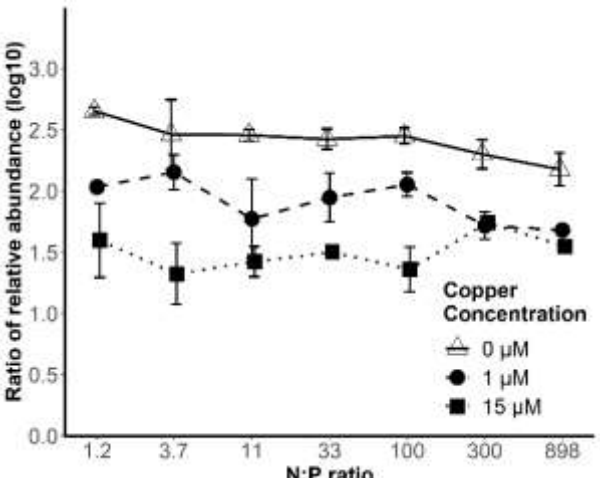

Figure IV 3. Ratio between bacterial 16S and fungal 18S rRNA gene copies.

x-axis for provided N:P ratios is log-transformed but shows as the molar ratio for reading convenience. For the abundances of 16S and 18S rRNA, see Figure.IV.S3.

3.4. Bacterial community diversity

Since bacteria were dominant, only bacterial community diversity was assessed through 16S rDNA sequencing. Alpha-diversity indices are shown in Figure.IV.S4. The Chao1 index indicated that the mean bacterial species richness decreased with increasing N:P ratio (X^2 = 14.126, P = 0.04898) and with increasing [Cu] (X^2 = 48.128, P < 0.001). The Shannon index showed that the bacterial diversity stayed relatively constant for all tested [Cu] (F = 5.079, P < 0.001). For bacterial communities exposed to 0 and 1 µM [Cu], the diversity index values were lower for high N:P ratio indicating the emergence of very abundant taxa. Higher variability in Shannon diversity indices was observed with increasing [Cu] (Levene's Test, F = 6.4451, P < 0.001) indicating a higher intra-replicate heterogeneity.

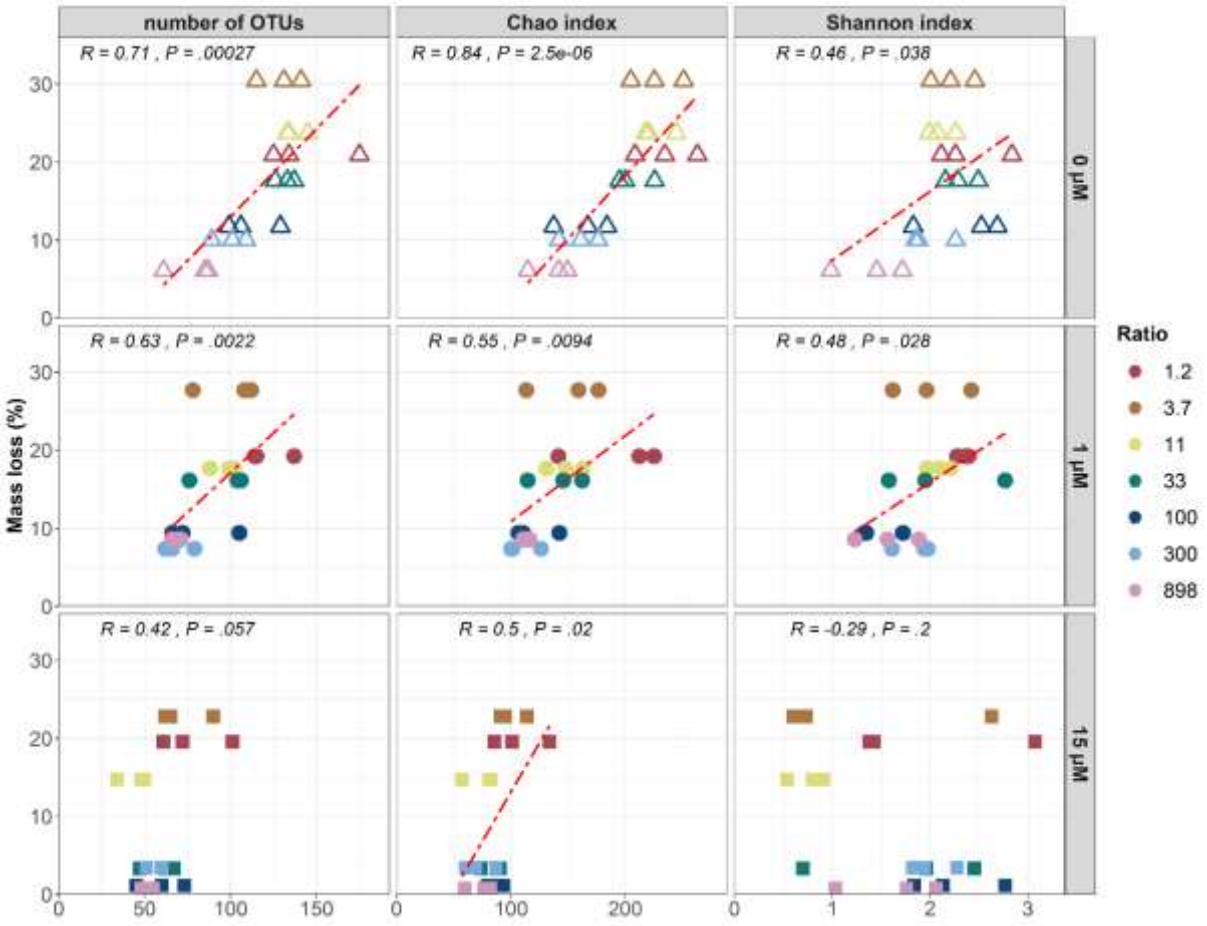

Figure IV 4. Linear correlation between mass losses and numbers of OTUs, Chao or Shannon indices of three Cu contamination levels.

Linear correlations between cellulose mass loss and OTU numbers, Chao1 richness or Shannon diversity indices of all three Cu contamination levels are shown in Figure.IV.4. For 0 and 1 µM of Cu, cellulose mass loss was positively correlated with the OTU number, Chao1 index and

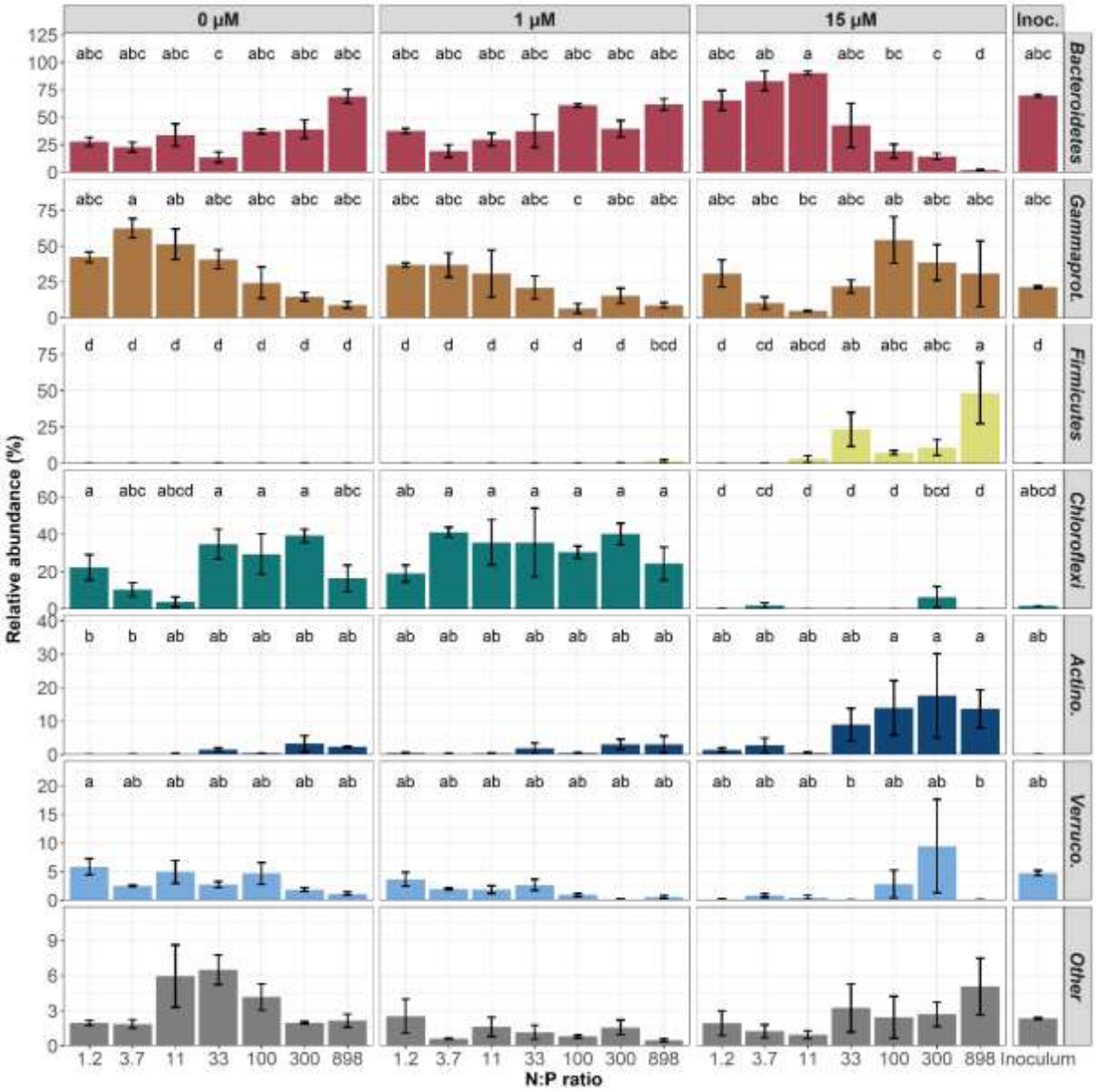

Figure IV 5. Bacterial diversity for all three levels of copper contamination and the inoculum.

Gammaprot.: *Gammaproteobacteria* (class). The rest are shown at phylum level. *Actino.*: *Actinobacteria*, *Verruco.*: *Verrucomicrobia*. Values are the mean abundance of replicates (n =3, for inoculum n = 2). Error bars show the standard deviation between replicates. Letters show significance groups, there is no significant differences between relative abundances in "Other". "Other" groups all OTUs with a relative abundance less than 10 % in any of the replicates. The phyla in the "Other" group are: *Armatimonadetes*, BRC1, *Clamydiae*, *Cyanobacteria*, *Deinococcus-Thermus*, *Dependentiae*, FBP, *Fibrobacteres*, *Hydrogenedentes*, *Lentisphaerae*, *Nitrospirae*, *Planctomycetes*, *Spirochaetes*, unclassified bacteria and *Proteobacteria* (none *Gammaproteobacteria*).

Shannon index. For 15 µM Cu, similar correlation was found between cellulose mass loss and Chao1 index, but no correlation was found with OTU number and Shannon index. The variation in richness was minimal compared to that of the mass loss.

The bacterial taxonomic diversity for each condition is shown in Figure.IV.5 as the relative abundance of the five major phyla and the major *Proteobacteria* class (i.e. *Gammaproteobacteria*) representing more than 10 % of the sequences. The relative abundance of each phylum was significantly different between N:P ratios and between [Cu]. The bacterial communities from conditions with 0 and 1 µM of [Cu] were dominated by either *Gammaproteobacteria* at lower N:P ratio, by *Bacteroidetes* at higher N:P ratio or by *Chloroflexi* regardless of the N:P ratio. In the microcosms with the higher [Cu] (15 µM), the bacterial community was dominated either by *Bacteroidetes* at lower N:P ratio, or by *Gammaproteobacteria*, *Firmicutes* and *Actinobacteria* at higher N:P ratio. *Actinobacteria* and *Firmicutes* were stimulated in condition with 15µM of Cu (Wilcoxon-Mann Whitney test, P <0.001 for both phyla). The relative proportion of *Chloroflexi* decreased at the higher [Cu] (P < 2e-16).

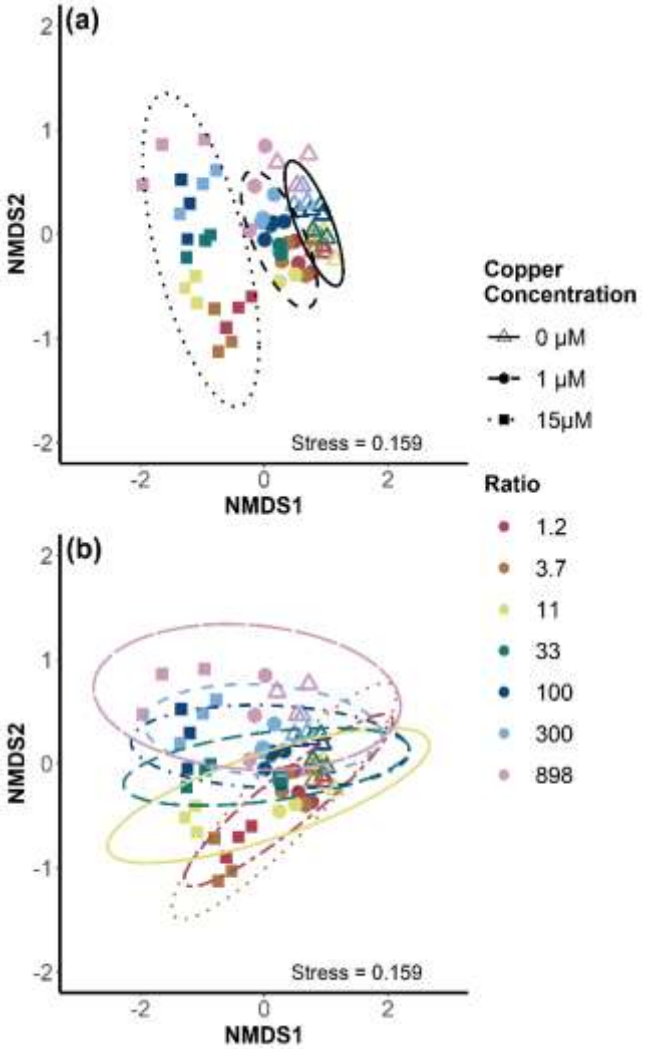

Figure IV 6. OTU based beta diversity in NMDS using Bray-Curtis dissimilarity index.

(a) beta diversity for all tested [Cu]; **(b)** beta diversity for all tested N:P ratios. Ellipses show the 95 % confidence interval.

Beta diversity of the communities developing in all the tested conditions was

shown through NMDS analyses (Figure.IV.6). Samples were clearly separated (first dimension, NMDS1) based on the [Cu] (Figure.IV.6a). A higher variability among samples exposed to 15 µM of Cu was observed compared to 0 and 1µM of Cu. A shift in the community composition was highlighted according to the N:P ratios mainly for samples exposed at higher [Cu] (separation on the second dimension NMDS2; Figure.IV.6b). PerMANOVA analyses confirmed the significant difference of the community composition between each of the three [Cu] ($F = 10.795$, $P = 0.001$), while the difference was lower but also significant between each of the seven N:P ratios ($F = 1.365$, $P = 0.024$).

The results of indicator species analysis with indicator values are shown in Figure.SIV.5. The reasons behind our decision of merging the conditions into four groups are, firstly bacterial diversities with 0 and 1 µM of [Cu] were similar compared to that of 15 µM of [Cu], and secondly cellulose decomposition at N:P ratios lower than 33 at different [Cu] varied compared to that at ratios higher than 33 which stayed constant. For the group CLRL (low copper, low ratios), there were 11 indicators of which four *Bacteroidetes*, three *Gammaproteobacteria* and four *Verrucomicrobia*. For the group CLRH (low copper, high ratios), there were two indicators of which one *Bacteroidetes* and one *Gammaproteobacteria*. For the group CHRL (high copper, low ratios), there were nine indicators of which seven *Bacteroidetes*, one *Gammaproteobacteria* and one *Verrucomicrobia*. For the group CHRH (high copper, high ratios), there were ten indicators of which one *Bacteroidetes*, four *Gammaproteobacteria*, one *Firmicutes*, and four *Actinobacteria*. The analysis also revealed 15 indicator species related to the combination of groups CLRL and CLRH, which is equivalent to the group with low copper (CL). And finally, four indicator species for the groups of CHRL and CHRL, which is the equivalent to the group with high copper (CH). For the group CL, there were five *Bacteroidetes*, three *Gammaproteobacteria*, five *Chloroflexi* and one *Verrucomicrobia*. For the group CH,

there were three *Bacteroidetes* and one *Gammaproteobacteria*. More detailed information can be found under Figure.SIV.5.

4. Discussion and conclusion

4.1. General observations

Cellulose decomposition was maximised at an optimal N:P ratio with, or without copper contamination. Copper contamination had no significant effect on the maximal decomposition rate around the optimal N:P ratio but had strongly reduced the range of the ratio in which cellulose decomposition can occur. These changes were followed by large shifts in bacterial community compositions. Bacteria sensitivities toward the contaminant and the relative N:P availability in environment can both select particular taxa within a bacterial decomposer community.

Despite the use of a natural microbial inoculum, fungal spores were not present in our inoculum, and fungi hardly developed in our microcosms. Some possible explanations might be that we have collected the leaf bags at a late stage of decomposition. During inoculum preparation, partially decomposed leaves were reduced into small pieces instead of staying intact as we usually get while inducing fungal spores. This observation is consistent with the common assumption that bacteria only become abundant at a later stage on small leaf litter fragments (Sinsabaugh and Findlay 1995). The decantation step we applied in the inoculum to limit the risk of introducing leaf litter fragments in our microcosms might also have participated in the absence of fungal spores. Finally, aquatic hyphomycetes that were expected to be present in our inoculum generally require very high levels of oxygen to maintain their activity (Medeiros, Pascoal and Graça 2009) and our microcosms, leading to the development of a few anaerobic taxa (see section 4.2), were certainly not perfectly adapted for ensuring their development. As

a result, bacteria were largely dominant under all tested conditions, and we ultimately decided to focus on bacterial communities for taxonomic analysis.

4.2. Stoichiometric demand of microbial decomposers for cellulose decomposition

In our study, cellulose decomposition was largely controlled by ratios of dissolved inorganic N and P in the medium. As predicted by our first hypothesis (H1), the decomposition rate reached its maximum at a dissolved N:P ratio of 4.7. At this particular N:P ratio, N and P availabilities were certainly co-limiting microbial activity allowing an optimal decomposition of the carbon substrate. The occurrence of such a bell-shaped response of cellulose decomposition had already been observed by Güsewell and Gessner (2009), by using a natural microbial inoculum containing both bacteria and fungi. At the same nutrient supply level, they have found an optimal mass N:P ratio for cellulose decomposition of 15 (33 molar ratio), which is higher than the optimal N:P ratio found in our study. Meanwhile, the same authors also found that bacterial development was maximised at lower environmental N:P ratios than for fungal development. In our study, microbial communities were largely dominated by bacteria, and the low optimal N:P ratio we observed might be explained by this dominance. Bacteria and fungi have different nutrient requirements, yet both are found to be flexible. This flexibility is the result of differences in cellular contents and processes between bacteria and fungi (Godwin and Cotner 2018; Camenzind *et al.* 2020, 2021). The differences in nutrient requirements between bacteria and fungi can directly affect their competitive abilities and dominance on different substrates (Danger, Gessner and Bärlocher 2016).

In the absence of Cu contaminant, significant cellulose mass losses were observed throughout the whole N:P ratio range tested, even when the medium was extremely depleted in P (high N:P ratio). Mass loss was always above 8 %. This result suggests that even though the

decomposition rate was reduced outside the optimal N:P ratio of the given microbial decomposer community, this process was never fully stopped. Nevertheless, it was not possible to follow decomposition kinetics using a single sampling date. The next step will be to verify if stoichiometric imbalances would mostly slow down the decomposition process or if this process would eventually stop due to nutrient unavailability.

Although the average quantity of N immobilised on cellulose disc stayed at a relatively constant level around 0.17 mmol g^{-1} of dry cellulose disc, N immobilisation was not linear along the gradient of N:P ratios tested. The quantity of N immobilised was maximised at the optimal N:P ratio for cellulose decomposition and minimised at the N:P ratio where the minimal decomposition rate occurred. The portion of N immobilised increased when the ratio was low. This result agrees with that of Güsewell and Gessner (2009), showing that decomposers were more efficient at immobilising N when it was the most limiting element. The quantity of P immobilised followed a similar profile as cellulose decomposition rate, i.e. a bell-shaped response, P immobilisation was maximised at an N:P ratio of 3.7. The proportion of total P immobilised increased when N:P ratios were high, suggesting the decomposers immobilise P more efficiently when it is the limiting element. This observation, however, contrasts with the previous observations of Güsewell and Gessner (2009). A possible explanation could be related to the very low abundance of fungi in our study, since fungi are known to be able to store large amounts of extra P as polyphosphates when P is not limiting (Beever and Burns 1981).

Interestingly, bacterial species richness dropped significantly for the highest N:P ratio, where cellulose decomposition rate slowed down to its minimum. As already observed in previous studies (e.g. Leflaive *et al.* 2008; Lemmel *et al.* 2019), our results evidenced positive correlations between the intensity of microbial functions and the diversity: cellulose mass losses were significantly and positively related to bacteria OTU numbers, Chao1 richness and Shannon diversity indices. This suggests that only a few bacterial taxa are capable of surviving

in environment with highly imbalanced N and P, and these species are probably less efficient in decomposing cellulose under high N:P ratios. When looking more specifically to the taxa present along the N:P gradient, we found that the relative abundance of *Gammaproteobacteria* was strongly related to cellulose decomposition efficiency, these being more abundant around the optimal N:P ratio. Bacteria from this class probably carried out most of the decomposition in our study. Even if we cannot exclude the possibilities that certain bacteria with low abundances can also be very actively involved in decomposition. Although *Gammaproteobacteria* are still present at higher N:P ratios, their abundance decreased in favour of *Chloroflexi* and Bacteroidetes which became dominant. Among *Chloroflexi*, *Anaerolineae* was the dominant class. Although the ecological role of the *Anaerolineae* members remains unclear, these bacteria have been shown to exhibit cellulolytic activities (Hug *et al.* 2013; Xia *et al.* 2016). The detection of these strict anaerobic bacteria suggests that despite the absence of total water immersion, parts of the cellulose discs could have ended up in anaerobic conditions. For the highest N:P ratio, Bacteroidetes represented up to 75 % of total abundance. Verrucomicrobia was shown to be less abundant yet consistently present throughout all the N:P ratios. A recent study has argued a possible under estimation of its abundance due to methodological biases (Chiang *et al.* 2018). All these findings confirm partially our fourth hypothesis (H4) that N:P ratio strongly contributes to the composition of active bacterial communities. Even though the functional redundancy among bacterial decomposers could ensure basal cellulose decomposition, the activities of these different active taxa at different N:P ratios were not equally efficient.

4.3. Stoichiometric demand for cellulose decomposition in the presence of copper

In the presence of Cu in the microcosms, the overall cellulose decomposition remained unchanged in the presence of copper when N:P ratios were close to microbial stoichiometric optimal requirements, whatever the copper concentration tested. For the highest Cu concentration (15 µM of Cu), cellulose mass loss was significantly reduced when deviating from this optimal ratio. This observation partly confirms our second hypothesis that high Cu concentration would reduce cellulose decomposition rates (H2) and is consistent with previous studies investigating copper effects on leaf litter decomposition (Roussel, Chauvet and Bonzom 2008; Ferreira *et al.* 2016) and alter the structure of bacterial decomposer community (Duarte *et al.* 2008). This result might be due to direct Cu toxicity which has long been evidenced for both bacteria and fungi (e.g. Dupont, Grass and Rensing 2011).

Contrary to our expectation (see hypothesis H3), the optimal N:P ratio for maximal cellulose decomposition rate decreased with raising Cu concentration. Cu at low concentrations is known to be an essential microelement (Cervantes and Gutierrez-Corona 1994), metal-transporting-proteins which regulate multiple metal homoeostasis (including Cu) are naturally present on bacterial membranes to regulate intracellular metal concentrations. Cu(II) ion appears to be less toxic than Cu(I), as we introduced Cu(II) from CuSO4, bacteria were exempt from synthesising Cu(I)-detoxification-proteins (Ladomersky and Petris 2015), which would have required more N. Cu(II) export, on the other hand, does not require synthesising additional transporters, but mainly relies on existing ATP-dependent proteins to actively relocate Cu outside the cell membrane (Ma, Jacobsen and Giedroc 2009). A stronger increase in energetic requirements (and thus in P-rich molecules, such as ATP) than in the production of N-rich detoxification proteins might be a plausible explanation of why the optimal N:P ratio for decomposition had decreased.

Our results also highlighted that the minimal cellulose mass losses under high Cu contamination (close to 0 %) were significantly lower than those of control and low Cu contamination treatment (which always remained above 8 %, whatever the N:P ratio tested). In other words, rather than keeping a slow but non-zero rate of decomposition, high Cu contamination arising concomitantly with N:P ratios higher than 33 had led to a total stop of cellulose decomposition. As pointed out by Peñuelas *et al.* (2013), anthropic input of N into the biosphere is excessively higher than that of P, creating an increasingly imbalanced environmental N:P ratio, This N:P imbalance alone had already affected the life histories of microorganisms and other life forms (Elser *et al.* 2009). In case of high Cu contamination, it could take the decomposition process to halt and effectively stop carbon turnover. Our findings suggest that human-induced global nutrient imbalances might lead to exacerbated responses of microbial processes in presence of contaminants.

Copper reduced the richness of the bacteria community at each N:P ratio even at the lowest level test. For the highest copper concentration, the effect of N:P ratios over bacterial richness was minimised, suggesting a higher selective pressure of Cu rather than N:P balances on bacterial communities. Cellulose decomposition blocked in both high N:P and high copper conditions could be partly explained by the elimination, or at least a decrease in abundance of certain cellulolytic taxa that are sensitive to high Cu concentrations, and their replacement (with similar abundance) by Cu-tolerant taxa (Indicator species: *Flavobacterium*, *Nitrosospira*, *Pseudomonas*, *Aeromonas*, *Variovorax*, *Paenibacillus* and *Nocardiaceae*) probably less efficient or even incapable of decomposing cellulose. The positive correlations between cellulose mass losses and OTU numbers, richness and diversity of the bacterial community observed in control and low Cu conditions almost disappeared in the presence of 15µM of copper. This means that in the most contaminated conditions, the community richness had little to do with cellulose mass loss, which suggests a shift in the community composition and taxa

replacements. As shown that *Bacteroidetes* dominance were replaced by *Gammaproteobacteria*, Firmicutes and *Actinobacteria* from low to high N:P ratio. Different indicator species were also identified under different situations. All these observations confirm our hypothesis (H4) that the contaminant and the N:P ratio in the environment interactively control microbial community structure, with large consequences on their functions and activities (i.e. cellulose decomposition).

5. Conclusion

Bacteria were the main decomposers in our study. Without copper contamination, cellulose decomposition was maximised at an N:P molar ratio of 4.7. Both N and P immobilisation by bacterial decomposers were more efficient when these elements were the limiting ones. Bacterial species diversity and richness dropped at high N:P ratios (when P was limited) but the community as a whole maintained a basal level of cellulose decomposition.

Overall, the lowest Cu concentration tested had little to no negative effect over bacterial decomposer communities, their taxonomic compositions, their N and P stoichiometric demands, and their capacity to decompose cellulose. In contrast, at the highest Cu concentration tested, the composition of bacterial communities was drastically reshaped, which had significantly reduced the optimal N:P ratio for cellulose decomposition to 2.8, and negatively affected the global cellulose decomposition efficiency in the most stoichiometrically imbalanced conditions (the highest N:P ratios). In this study, we focused on cellulose decomposition, but other microbial functions could be simultaneously affected and would require further studies. For example, Cu has been shown to inhibit bacterial glucose utilization, or nitrifiers and denitrifiers metabolic activities (Ochoa-Herrera *et al.* 2011). To conclude, the current increased imbalance between N and P availabilities on Earth, which correspond to a major parameter of global change, might lead to unexpected interactions with other stressors, in turn largely impacting

microbial functions. Our results shed the light on a potentially important and understudied environmental problem that could have large repercussions on ecosystem functioning worldwide.

Funding

This work was supported by the French National Research Agency through ANR project "StoichioMic" (ANR 18 CE32 0003 01).

Acknowledgement

We are grateful to Mr Q. Bachelet for fields and technical support, to Mr P. Rousselle for conducting chemical analyses, and to three anonymous reviewers for their constructive comments on an earlier draft of this manuscript.

Conflict of Interest

The authors declare no conflict of interest.

CHAPTER IV

Part 2

Decomposer optimal N:P ratios for decomposition affected by temperature variation

(Preliminary results)

Do stoichiometric demands of decomposer communities depend on temperature? (Draft)

Temperature has long been proposed as a key environmental factor that controls leaf litter decomposition dynamic, and this response has been shown to interact in a complex way with nutrient availability (Fernandes *et al.* 2014; Martínez *et al.* 2014; Gossiaux *et al.* 2020). Studying the relationship between decomposer's optimal nutrient ratios for decomposition and the temperature might be a way to understand in more depth these interactions. For this purpose, we carried out a similar experiment than in Wang *et al.* (2022) but following decomposition of the cellulose discs under 5 distinct temperatures. All other experimental setups, conditions, and analyses were identical to that of the experiment with copper. The only difference was that instead of having 3 copper concentrations, the incubations were done in distinct climatic chambers at 9 °C, 12 °C, 15 °C, 18 °C, and 21 °C. Because higher temperature accelerates metabolic activities, incubation durations were adapted to each temperature in order to reach visually a similar stage of cellulose decomposition. The incubation durations were 142 days for 9 °C, 121 days for 12 °C, 100 days for 15 °C, 79 days for 18 °C, and 58 days for 21 °C.

Cellulose discs had lost between 0.005 % and 0.02 % of their initial dry mass per degree-day (Figure.IV.7). Cellulose mass losses depended on N:P ratios (two-way ANOVA, $P < 0.001$), temperatures ($P < 0.001$), and the interactions between these two factors ($P < 0.001$). For all tested temperatures, maximal cellulose mass losses occurred between N:P ratios 3.7 et 11. Results from our statistical model were given with 95 %

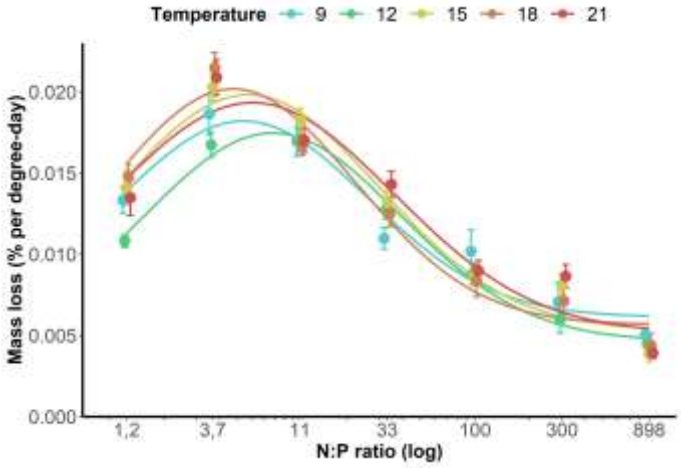

Figure IV 7. Cellulose mass losses per degree-day. In % of the average initial mass (36.3 mg) minus the average 3 % loss of the control group without inoculum.

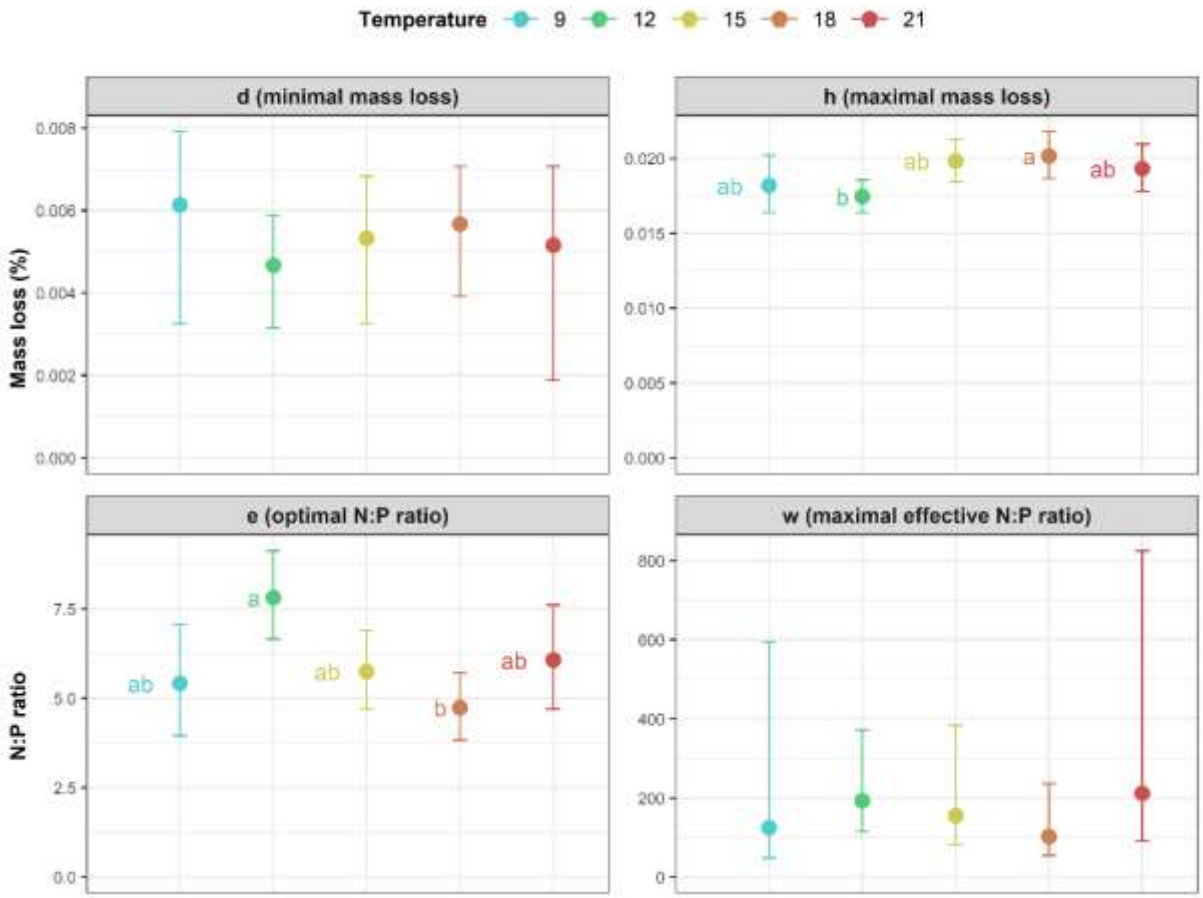

Figure IV 8. Representations of each parameter estimated by our Gaussian model.

confidence intervals (CI) (Figure.IV.8). Minimal mass losses (parameter *d*) were not different between temperatures, but maximal mass losses (parameter *h*) were significantly different between temperatures, with the lowest decomposition (0.0175 % degree-day^{-1}) occurring at 12 °C and the highest (0.02 % degree-day^{-1}) at 15 °C. Optimal N:P ratios for cellulose decomposition (parameter *e*) were significantly different between 12 °C (ca. 7.5, for the highest) and 18 °C (ca. 5, for the lowest). Meanwhile, maximal effective N:P ratios (parameter *w*, from which the mass loss equals to minimal mass loss) showed no significant difference between temperatures.

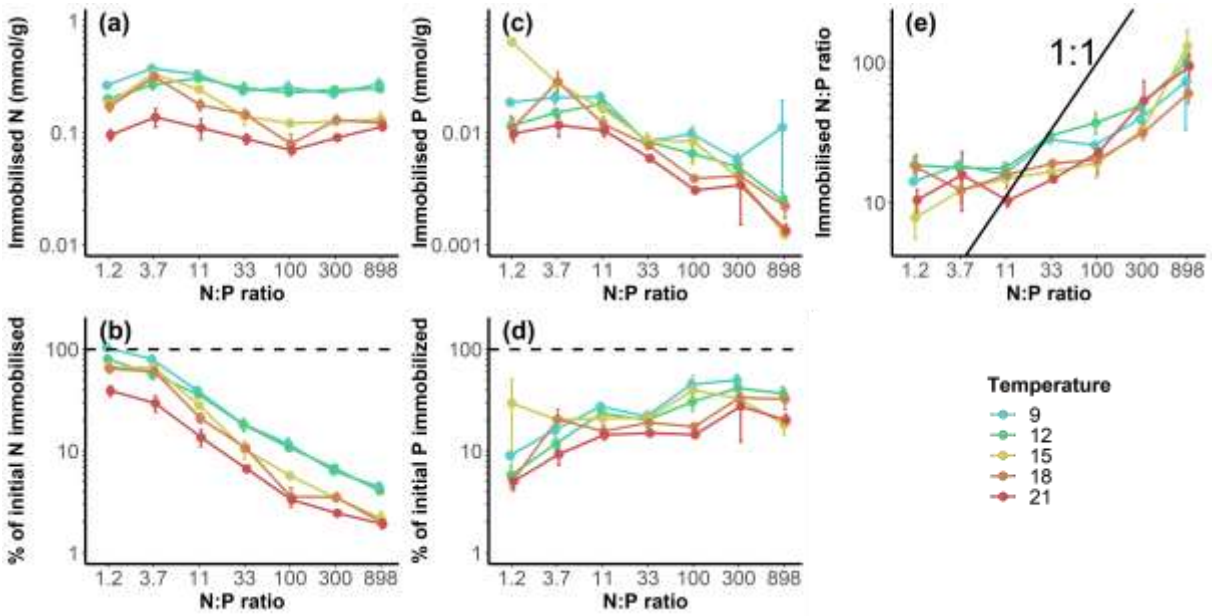

Figure IV 9. N and P immobilised on cellulose disc for five temperatures in relation to the supplied N:P ratios.

Immobilised N quantities on partially decomposed cellulose discs (Figure.IV.9a) depended on both N:P ratios, temperatures, and interactions of both factors (two-way ANOVA, all $P < 0.001$). The proportion of initial N immobilised (Figure.IV.9b) were only affected by N:P ratios (Kruskal-Wallis, $P < 0.001$). Immobilised P quantities (Figure.IV.9c) were only affected by N:P ratios ($P < 0.001$), and % of initial P immobilised (Figure.IV.9d) depended on both N:P ratios and temperatures (both $P < 0.001$). The ratios of immobilised N:P on cellulose (Figure.IV.9) were only affected by N:P ratios ($P < 0.001$).

The relative abundances of bacteria and fungi were estimated with qPCR quantification of bacterial 16S and fungal 18S rRNA genes. Bacterial abundances (Figure.IV.10a) were not affected by N:P ratios (Kruskal-Wallis, $P = 0.133$) but were different between temperatures ($P < 0.001$). Fungal abundances (Figure.IV.10b) were different between N:P ratios and temperatures (two-way ANOVA, both $P < 0.05$). The ratios between bacterial and fungal abundance (Figure.IV.11) were not affected by N:P ratios (Kruskal-Wallis, $P = 0.19$) but differed with temperature ($P < 0.001$).

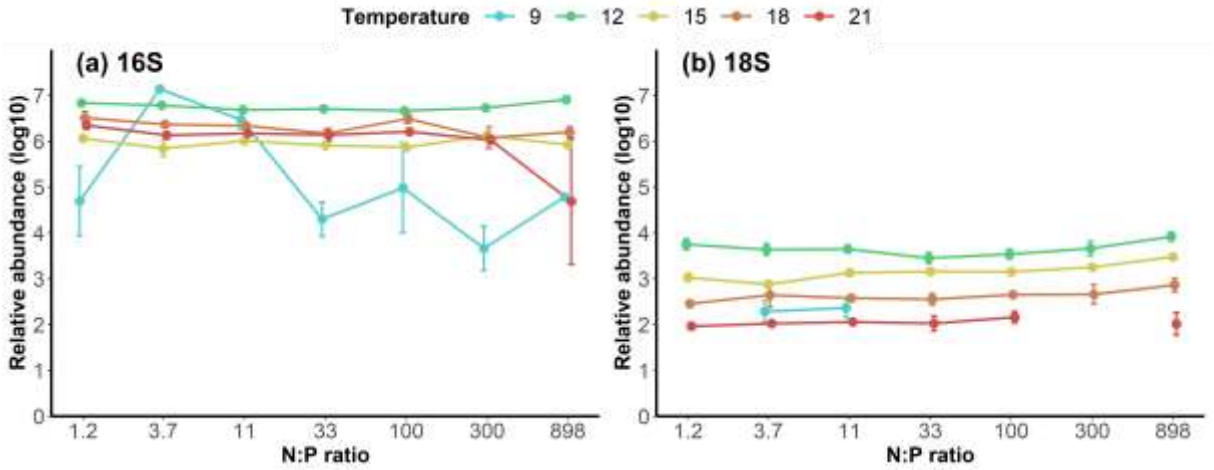

Figure IV 11. Relative abundances of bacterial 16S and fungal 18S rRNA gene copies. Missing points for 18S copies were due to undetectable signal from qPCR. Analyses for samples of 9 °C were done separately from analyses of other samples.

Analyses of bacterial community richness and diversity are not yet finalised, but we have a general overview of the 5 major taxa (Figure.IV.12). Overall, *Gammaproteobacteria* was the most abundant taxa, followed by *Bacteroidetes* and *Chloroflexi*. Generally speaking, the abundance of each taxa seems to be dependent on both N:P ratios and temperatures. For example, *Gammaproteobacteria* seems to be promoted at lower temperatures and lower N:P ratios, in contrast, *Bacteroidetes* seems to be more adapted to higher N:P ratios and not affected by temperatures. *Chloroflexi* seems to be promoted at higher temperatures.

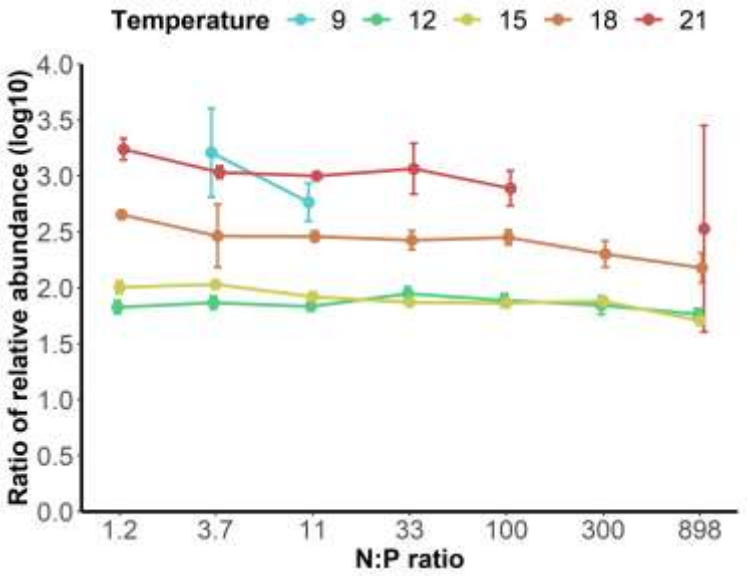

Figure IV 10. Ratios between bacterial 16S and fungal 18S rRNA gene copies.

These results will certainly have to be analysed more thoroughly for any definitive conclusion, but cellulose decomposition intensity does not seem to be significantly affected by changes of

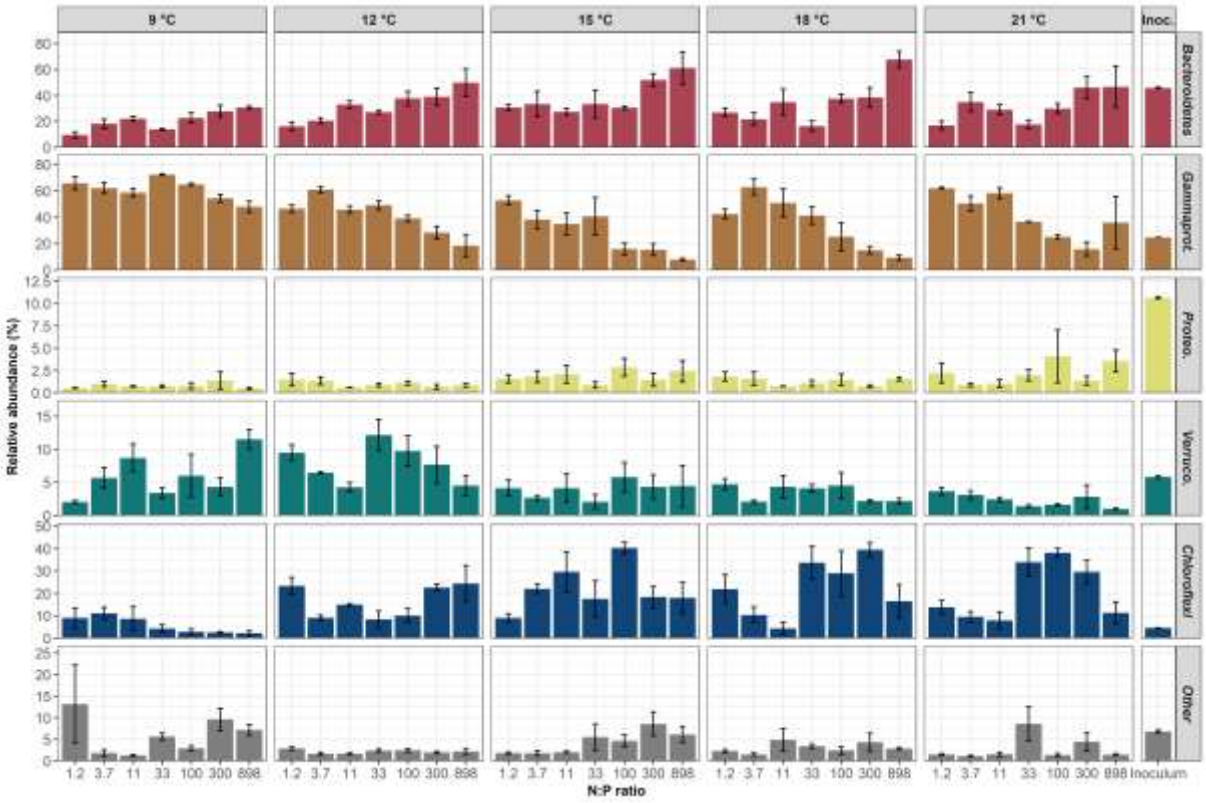

Figure IV 12. Bacterial community abundance shown with the five major taxa.

temperature and the effects of supplied N:P ratios were more pronounced. Temperatures seem to have a non-unidirectional impact on the optimal N:P ratios for cellulose decomposition. Note that in this experiment decomposer communities were mostly represented by bacteria, and those observations could have been different if aquatic hyphomycetes were present. Future studies of this subject are certainly necessary.

As a brief description of these preliminary results, N:P ratios maximising leaf litter decomposition significantly differed with temperature but not in a simple way, optimal N:P ratios being higher at 12°C, minimal at 18°C and intermediate for the 3 other temperatures. Previous studies investigating the effects of temperature on optimal N:P of the crustacean herbivore, *Daphnia magna*, also showed non-linear responses to temperature (Ruiz *et al.* 2020; Laspoumaderes *et al.* 2022). Understanding the observed response of microorganisms optimal N:P ratios would deserve further studies, but it does not seem to depend on shifts in community

assemblages. These responses might rather depend on changes in nutrient use efficiencies and microbial N:P requirements with the temperature-induced increase in microbial metabolism.

Analyses for bacterial community richness and diversity were not yet finalised; but we have a general overview of the 5 major taxa (Figure.IV.12, statistical analysis will be done in the future.). Overall, *Gammaproteobacteria* was the most abundant taxa, followed by *Bacteroidetes* and *Chloroflexi*. Generally speaking, the abundance of each taxa seems to be dependent on both N:P ratios and temperatures. For example, *Gammaproteobacteria* seems to be promoted at lower temperatures and lower N:P ratios, in contrast, *Bacteroidetes* seems to be more adapted to higher N:P ratios and not affected by temperatures. And *Chloroflexi* could be promoted at higher temperatures.

These results will certainly have to be analysed more thoroughly for any definitive conclusion, but cellulose decomposition intensity does not seem to be significantly affected by changes of temperature and the effects of supplied N:P ratios were more pronounced. Temperatures seem to have a non-unidirectional impact on the optimal N:P ratios for cellulose decomposition.

General Discussion and Outlook

This thesis explores the role of aquatic hyphomycetes (AH) and heterotrophic bacteria from freshwater ecosystems as plant litter decomposers, with the main aim of developing a stoichiometric trait-based approach to studying microorganisms response to global changes, such as nutrient availability variations but also presence of contaminants or temperature variations. We characterised the elemental plasticity of several AH strain individually or in artificial assemblages, and some more complex decomposer communities (including natural bacterial communities). We have highlighted the consequences of stoichiometric imbalances on nutrient immobilisation and mineralisation processes. We have also identified some impacts of copper contamination and temperature variations (as examples of stressors caused by global changes) on decomposers' elemental plasticity and potential ecological consequences. Combining the results of the different experiments carried out in this work allows drawing some general conclusions on the mechanisms involved in decomposers responses to nutrient imbalances and propose some new questions and perspectives for future work.

1. Stoichiometric traits for microorganisms: Which traits and at which scale?

According to Violle *et al.* (2007), a trait corresponds to any morphological, physiological or phenological characteristic of an organism that is able to impact its fitness (through its effects on growth, reproduction and/or organisms' survival). Following this definition, Meunier *et al.* (2017) proposed several traits that could be related more or less closely to stoichiometry, in particular organism's elemental ratios, homoeostasis, as well as nutrient assimilation and recycling capacities have been proposed. However, these reflexions remain easier for metazoans than for microorganisms. For microorganisms, the two traits that we focused on in this thesis were species optimal nutrient ratios and species degree of homoeostasis. While studies in microbial elemental composition are increasingly available in scientific literature,

data specifically characterising stoichiometric traits of individual species are lacking. Similar to plants (Tilman 1985), we expected that each aquatic hyphomycete (AH) species to have its own optimal N:P ratio. Our results indeed indicated that different AH species (represented by one strain each) had slightly different responses (in terms of biomass production) along the N:P gradient tested. Some species clearly showed a shift in nutrient limitation along the dissolved N:P ratios where biomass increase reached a plateau when P get to a certain amount) while others (HULU in particular) showed no asymptotic trend with no shift in nutrient limitation despite the large range of N:P ratios tested. Species thus seem to differ in their optimal N:P ratios and, in the same line as for plants, one could have expected that these traits represent a major selecting factor explaining species dominance in a community (Tilman 1982; Miller *et al.* 2005). Yet, despite these differences, optimal N:P ratios were unable to explain all the differences observed in the relative abundances of AH species in artificial assemblages. This observation means that the use of stoichiometric traits alone might be insufficient to predict the outcome of competitive interactions in fungal communities. In contrast, adding stoichiometric traits to the list of traits already available for fungi (Crowther *et al.* 2014; Abrego, Norberg and Ovaskainen 2017) could be a promising way to answer this important question in microbial ecology.

Another question that arises after these different experiments is: can we imagine using a microbial community response as a "trait" for predicting the impact of stressors on ecosystem processes (here, decomposition of plant litter)? As previously underlined, the definition of a trait is a characteristic that can be measured on a single organism (Violle *et al.* 2007). Yet, for microorganisms, considering the response of a community as a whole when investigating ecosystem processes could make sense. Following this train of thought, the N:P ratios maximising litter decomposition measured by Güsewell and Gessner (2009) or in chapters II and IV of this thesis could be seen as "community traits" and which could be directly used for

predicting the intensity and the dynamic of plant litter decomposition (see Wang *et al.* 2022, i.e. chapter IV). Even if the use of this "community traits" goes far beyond the classical definition of traits, it deserves to be questioned for microbial communities that can commonly exhibit species replacements in shorter times than the whole process they ensure (plant litter decomposition as an example). This would at least make sense when studying ecological processes – but not community structure – as the main endpoint of the study.

2. Growth strategies and elemental plasticity of AH

We have found in chapter I, that the four AH taxa studied (ARTE, HULU, TEMA, and TRSP) adapt their growth strategy accordingly under different nutrient conditions. The most common strategy is to trade off mycelium density with growth size in order to cover a larger surface under a same amount of time (a surface similar to those observed under more balanced nutrient conditions but with a lower mycelium density). This explorer strategy can be interpreted as a way to maximise the chances to find a nutrient rich resource close by. The second strategy, which was only observed once among the four tested taxa, is to grow both faster and denser under the most ideal nutrient condition (with balanced and abundant nutrients). This way of development may allow covering and acquire more available nutrients in their environment, which can grant a competitive advantage to the AH when facing other microorganisms.

Our results from chapter I have also added evidence to the elemental plasticity of AH when facing P gradients (as by Danger and Chauvet 2013; Gulis *et al.* 2017), but concerning the plasticity of N – which is not consensual in the literature (e.g. Danger and Chauvet, 2013 found N plasticity but not Gulis *et al.* 2017) – seems to be taxa dependent. Among the four taxa tested, TRSP indeed showed a highly variable N content in its biomass while for ARTE and HULU, N contents remained quite stable whatever the N availability found in the culture medium. This

particular trait would deserve special attention to understand why it occurs, and how the taxa showing N plasticity accumulate this element and in what form.

Another interesting result is about the effect of mycelium age on fungal plasticity. As fungi grow actively from the tips of their mycelia, younger mycelia generally followed a strict homoeostasis (with constricted N:P ratio in biomass). In contrast, older mycelia were more plastic, as they were less active in their metabolic activities, as a result, old biomass N:P ratios reflect more of that of their environment. In Ecological Stoichiometry Theory, the Growth Rate Hypothesis (GRH; faster growth correlate with high P demands, thus low N:P ratios in biomass) is an important concept. In our studies, GRH failed to apply to the young mycelia but apparently applied to the older ones (chapter I). This negative relationship observed between overall mycelium growth rate and the N:P ratio of old mycelium might thus be more likely due to a nutrient storage in older mycelium than to a particular investment in ribosomal RNA. Developing future studies dedicated to the understanding of the molecular and biochemical determinants of old and young mycelium elemental composition should represent an important next step.

3. Being plastic, but why?

Another important question that this thesis was unable to totally solve is why microbial decomposers – AH in particular have such plastic in their elemental composition. One common assumption is that nutrient storage would be useful to prevent potential nutrient shortage. This would give a competitive advantage for taxa populating habitats where nutrients are susceptible to vary rapidly (Mason-Jones *et al.* 2022). In our studies, we were unable to relate mycelium nutrient richness with its capacity of faster growth in nutrient-depleted media (chapter I). This study could be further completed by other studies where both mycelium biomass growth and radial growth are investigated, but visual observation of culture plates did not reveal any large

difference in this aspect. Since this hypothesis has not been confirmed, alternative hypotheses may be proposed. Two hypotheses appear to be plausible, although both of them will have to be investigated further. First, storing excess nutrients could reduce the risk of toxicity associated with excessive accumulation of some compounds in fungi environment (as already proposed for metals for example, Cecchi *et al.* 2017). Another explanation is that by depleting essential nutrients – such as N and P – from their environment, fungi would limit the competition by other organisms which require same nutrients. While rarely studied, this strategy has already been proposed theoretically as a strategy used by organisms to outcompete their competitor with higher nutrient demands (de Mazancourt and Schwartz 2012) —In particular bacteria. Bacteria are known to have an extremely high demand in P to satisfy their growth requirements (e.g. Danger *et al.* 2007). And because of their high surface-to-volume ratio, bacteria are generally considered as better competitors than bigger osmotrophic organisms for absorbing dissolved resources from their environment. This idea was first proposed by Currie and Kalff 1984 for bacteria-plant interactions but could also be extended to bacteria-fungi interactions. This way of fungi outcompeting high-nutrient-requiring bacteria through a rapid nutrient immobilisation would be a complementary strategy to the one commonly proposed (production of antibacterial molecules). Nevertheless, the physiological benefits and costs for fungi to store extra N and P in their biomass remain to be further studied.

4. Decomposition by AH does not equal to mineralisation by AH

A common assumption about the role of decomposers in ecosystems is that they are the main drivers of nutrient mineralisation from decomposing organic matter (Harte and Kinzig 1993; Daufresne and Loreau 2001). In reality, our results showed that it might not be that simple. In chapter II, we used $N\text{-}NO_3^-$ as the sole source of N for AH to decompose alder leaf litter under a gradient of dissolved N:P ratios created by varying the $P\text{-}PO_4^{3-}$ concentrations. Since no N-

NH_4^+ was introduced into the systems, any trace of NH_4^+ would be a direct result of mineralisation by AH activities. By monitoring the final N-NO_3^- and N-NH_4^+ concentrations, we have shown that NO_3^- was almost totally immobilised by AH at the lowest N:P ratios (where N was limited), but still available in culture media at higher N:P ratios (where N was in excess). Our results showed that N-NH_4^+ was released in very low concentrations in the medium. NH_4^+ release was rather related to fungal biomass, which clearly followed the gradient of P, but not to the shift in nutrient limitation. NH_4^+ releases suggested more of an N release related to a general fungal activity rather than to a release of excess N compared to fungal requirements. With a negative net N uptake, we suspect that a part of the N-NO_3^- that disappeared from the water column and from leaf litter has been released as other organic forms of N (e.g. exoenzymes and other proteins). In that case, we suspect that detritivores feeding on decomposing leaf litter might take a bigger role in nutrient remineralisation process in ecosystems through their excretion (Consumer-Driven Nutrient Recycling; Elser and Urabe 1999).

5. Decomposition by fungi and bacteria depends on the type of nutrient gradient

In chapter III, we showed that an artificial community of AH and a natural decomposer community (containing at least both AH and bacteria) were most efficient on cellulose decomposition than bacteria alone, and both had the highest optimal N:P ratio for maximising the decomposition process. Communities with bacteria alone had the lowest cellulose decomposition efficiency, and lower optimal N:P ratios compared to fungi. However, this response was largely dependent upon the type of nutrient gradient.

In both chapter II and chapter III, we have designed our N to P gradients by keeping the quantity of one of the elements constant while varying the other, and the results of litter decomposition

carried out by different decomposers communities differed depending on the choice of the gradient. When tested under an N-constant N:P gradient (i.e. a gradient of P), both fungal communities in chapter II and in chapter III exhibited a constant decomposition efficiency across several environmental N:P ratios. In contrast, when tested under a P-constant N:P gradient, in chapter III, all tested communities exhibited variation in their decomposition efficiency across the tested N:P ratios, with higher efficiency under intermediate ratios (between ca 1.8 to 28) and lower efficiency under low and high ratios (with litter mass losses across tested N:P ratios showing a "bell-shaped" curve, as in Güsewell and Gessner 2009). This curve was also observed in chapter IV with a gradient design of varying simultaneously N and P quantities while keeping a constant global quantity of both elements (a constant geometric mean of N and P, $(m_N \times m_P)^{0.5} = 0.75$, see chapter IV). These observations, mainly due to the different use of N and P by fungi (see discussion of chapter III), highlight the importance of considering the type of nutrient gradient used when explaining differences of litter decomposition caused by N:P ratios. To our knowledge, this point has never been considered when studying effects of dissolved N:P ratio in ecosystems, either in experimental conditions (e.g. in Demi *et al.* 2020 where authors manipulated *in situ* the N:P ratio of 5 streams) nor in observational studies (e.g. Beck *et al.* 2021). Yet, it could largely affect the results of experiments and their explanations. This should be kept in mind for further investigations of N:P effects on litter decomposition and more widely ecosystem functioning.

6. Stoichiometric traits under stress

Stoichiometric traits under stress could only be evaluated for bacteria. In the experiment testing the effect of copper and temperature, aquatic hyphomycetes did not develop. Despite these experimental hazards, we were able to study the response of bacterial communities, but it will

certainly be interesting to evaluate the response of more diversified communities with both bacteria and fungi.

In chapter IV, we have found that the optimal N:P ratio for cellulose decomposition by bacterial decomposers decreased significantly from 4.7 without copper (Cu) contamination to 2.8 with 15 µM of Cu contamination in the media. While not affecting the maximal cellulose decomposition efficiency at the optimal ratio – which was already an important result – the minimal decomposition measured (outside the optimal ratio) with Cu contamination was drastically reduced to only 18 % of the minimal decomposition observed without contamination. Bacterial diversity was also negatively affected by Cu. In chapter IV, we have discussed how a human induced, disproportional N input into the environment (which is common after human activity; Elser *et al.* 2009; Peñuelas *et al.* 2013) coupled with a Cu contamination could effectively impact detritus carbon turnover in ecosystems. Here, we want to add another possible explanation of why an insufficient P supply (rather than an excess N availability) can be the problem. Given the implication of P in multiple cellular functions (i.e. building blocks for DNA, RNA, and ATP), we could expect a general shrinkage of P plasticity and a reduction of optimal N:P ratios for decomposition in presence of other metal contaminants. In addition, Cu has been shown to decrease oxygen utilisation in *E. coli* (Domek *et al.* 2011) which could also be the case for other bacteria found in our decomposer community. As a result, viability and activity of aerobic bacteria were reduced and probably allowed less efficient, anaerobic species to proliferate (see chapter IV, Figure. 5). As for contaminants, temperature variation was also able to significantly alter optimal N:P ratios for leaf litter decomposition (se info box following chapter IV). Combining these different results, we are confident that investigating nutrient optimal ratios for leaf litter decomposition (taking into account the nature of the N:P gradient, cf. point 5. above) in presence of different stressors might be an efficient way to investigate the interactive effects of nutrient addition and environmental stressors, which

remain a big challenge in ecological sciences (Cross *et al.* 2015). This would be especially important since nutrient availability is largely altered across Earth due to human activities (Elser *et al.* 2009; Peñuelas *et al.* 2013).

7. Phosphorus – too much or not enough of a good thing, is a bad thing.

Polyphosphate (polyP) is an important biopolymer that is present in all types of organisms, including bacteria. PolyP protect cells by shielding proteins against oxidative stresses (Rao, Gómez-García and Kornberg 2009; Gray *et al.* 2014) which, in our case, could have occurred through Cu toxicity (chapter IV). A lack of sufficient inorganic P supply, as was the case for our experiment with high N:P ratios, could lead to insufficient synthesis of polyP in bacteria thus leading to a reduced activity (cellulose decomposition). On the other hand, an excess of P might have negative effect on activities ensured by bacteria (chapter III). Cellulose decomposition efficiency by communities in presence of bacteria (alone or with fungi and other microscopic entities) under P excess condition was low compared to that ensured by a pure AH community. Hypotheses were made in an attempt to explain this result regarding the potential presence of other non-investigated entities (e.g. bacteriophages) in chapter III. Another explanation of these results would be that P excess can be toxic to bacterial development. A recent study has linked excess phosphate (PO_4^{3-}) uptake to a disrupted cytoplasmic magnesium (Mg^{2+}) homoeostasis which inhibits protein synthesis in bacteria (Bruna *et al.* 2021). Fungi, on the other hand, were found to be able to acquire and store an excess amount of P ("luxury consumption"). While it has not been directly proved for AH yet, AH are most likely to share a similar P uptake and storage mechanism with other non-aquatic fungi. For example, a eukaryote polyP kinase was first identified in vacuoles of the yeast *Saccharomyces cerevisiae* (Hothorn *et al.* 2009). Homolog proteins have recently been characterised in some arbuscular

mycorrhizal fungi and is believed to be implicated in modulating cellular ATP and polyP levels (Nguyen, Ezawa and Saito 2022). By regulating polyP synthesis from inorganic P in the vacuole, fungi could precisely control the concentration of intracellular inorganic P concentration to avoid intoxication when P is in excess, and provide a stable supply when P is limiting. Again, this hypothesis remains to be tested.

8. Improvement and perspective for future research

In chapter I, in the experiment where we measured fungal growth under different nutrient conditions, we have used the cellophane membrane to physically separate mycelium from its substrate. By doing this, we were able to easily collect mycelium without worrying about separating mycelium from its agar medium (which is complex and need solid medium heating, as in Camenzind *et al.* 2021, and one cannot exclude the possibility that heating alters mycelium elemental composition). However, we have found that fungi are also able to break down the cellophane membrane, it just takes them more time (How much? And does it differ from one species to another? This remains to be tested). Once passed under the cellophane membrane, mycelium starts to grow inside the agar. This phenomenon could be problematic for the measurement of colony radial growth – instead of growth in a 2-dimension surface, colony grow in a 3-dimensional space. If the global growth rate stays constant, from the moment when the mycelium breaks through the cellophane, their radial growth speed might slow down, as the colonies redirect their energy for growth to the less restricted and more nutrient rich agar matrix (at least on the upper part, where oxygen is abundant). As a result, measuring the colony size could lead to underestimations of the overall fungal growth rate. A group of researchers have used a polyvinylidene difluoride membrane on agar plates for easy collection of mycelia (Lange, Müller and Peiter 2014), this type of membrane can be an interesting candidate for future experiments. Although it can be time consuming, characterising the growth strategy and

elemental plasticity of a larger number of aquatic hyphomycete species individually will certainly be beneficial for our understanding of their stoichiometric requirements.

The identification of aquatic hyphomycetes still strongly relies on the morphological identification of their spores. Yet with the current advance of molecular tools, genetic information of AH in database is still limited (Malosso and Schoenlein-Crusius 2022) compared to that for terrestrial fungi, and to our knowledge only 1 taxon—*Clavariopsis aquatica* had its genome entirely sequenced and annotated (Heeger *et al.* 2021). It is without a doubt that more efforts will have to be put into acquiring genomic data of AH taxa to better understand their genetic material, their specific functions, highlight the presence of various pathways and thus identify species-specific functional traits. This will be beneficial for researchers to link experimental observations with physiological evidence with the help of molecular tools. As an example, we are planning to generate biomass of *C. aquatica* grown under different nutrient supply levels to evaluate the physiological response of this AH strain at the transcriptomic and proteomic levels and test recent findings on fungal polyP synthesis (Hothorn *et al.* 2009; Nguyen, Ezawa and Saito 2022). Only this strain could be used because for omics data analyses we need to have correctly annotated genome. We hope to be able to identify any differences in, for example, RNA and protein profiles between those different nutrient levels. Those results will certainly provide us with new intel and help us to understand the recurring question of this thesis—What is the mechanism for inorganic P uptake in aquatic hyphomycetes?

Appendix

1. Supplementary Material for chapter II

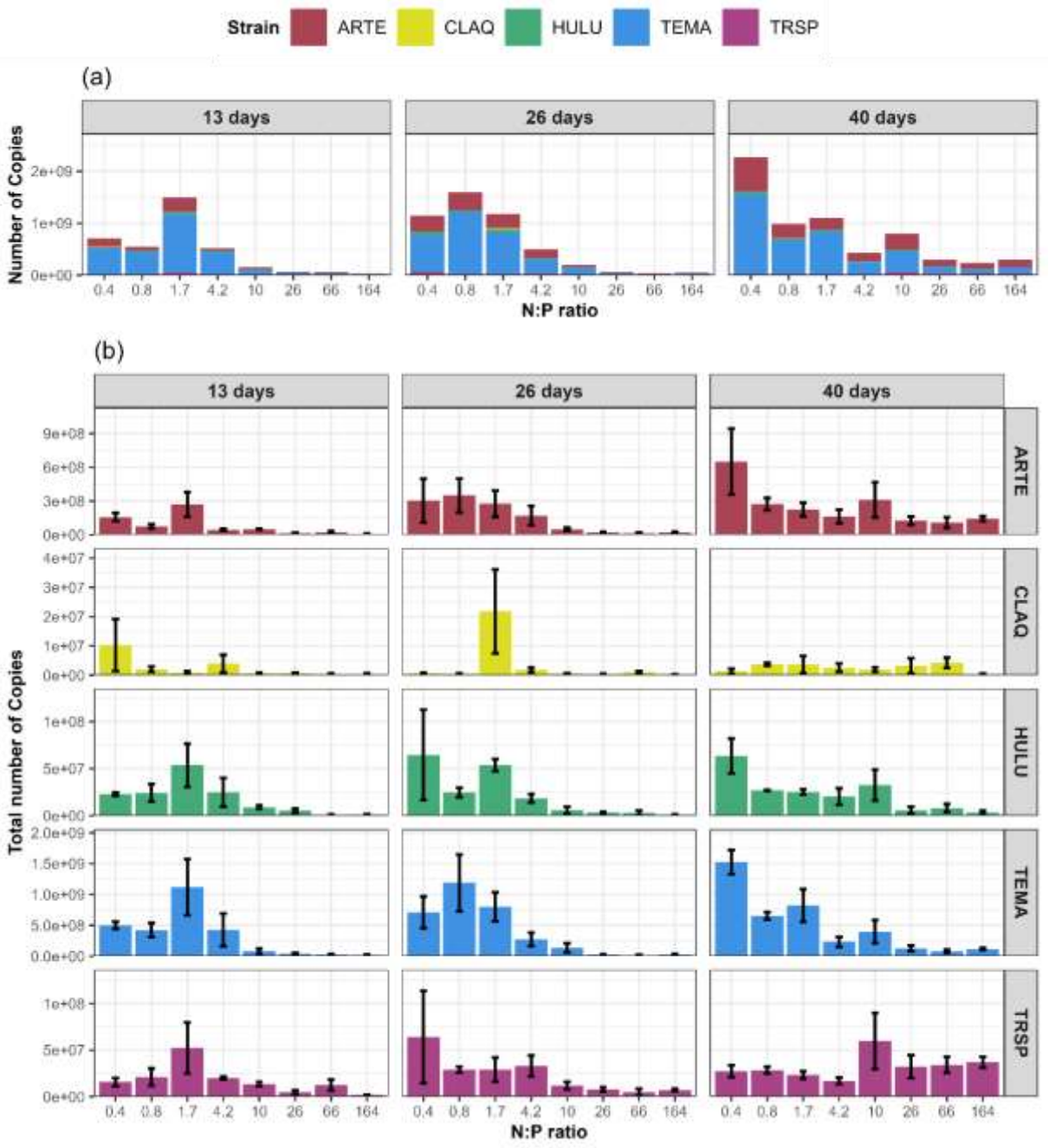

Figure SII 1. (a) Real-time PCR quantification of total ITS gene copy numbers of the 5 AH strains present across N:P ratios in the Mix treatment along time (after 13, 26 and 40 days). Strain specific qPCR revealed significant differences in the sum of ITS copy numbers between N:P ratios (Kruskal-Wallis, $P < 0.001$), between durations ($P < 0.05$), and between the combinations of both factor ($P < 0.001$). **(b) Each strain's individual copy number.** Except for CLAQ, Copy numbers were significantly different between ratios (one-way ANOVA, all $P < 0.05$, except for CLAQ $P > 0.05$) and sampling dates (all $P < 0.05$, except for CLAQ and HULU $P > 0.05$).

2. Supplementary Material for chapter IV

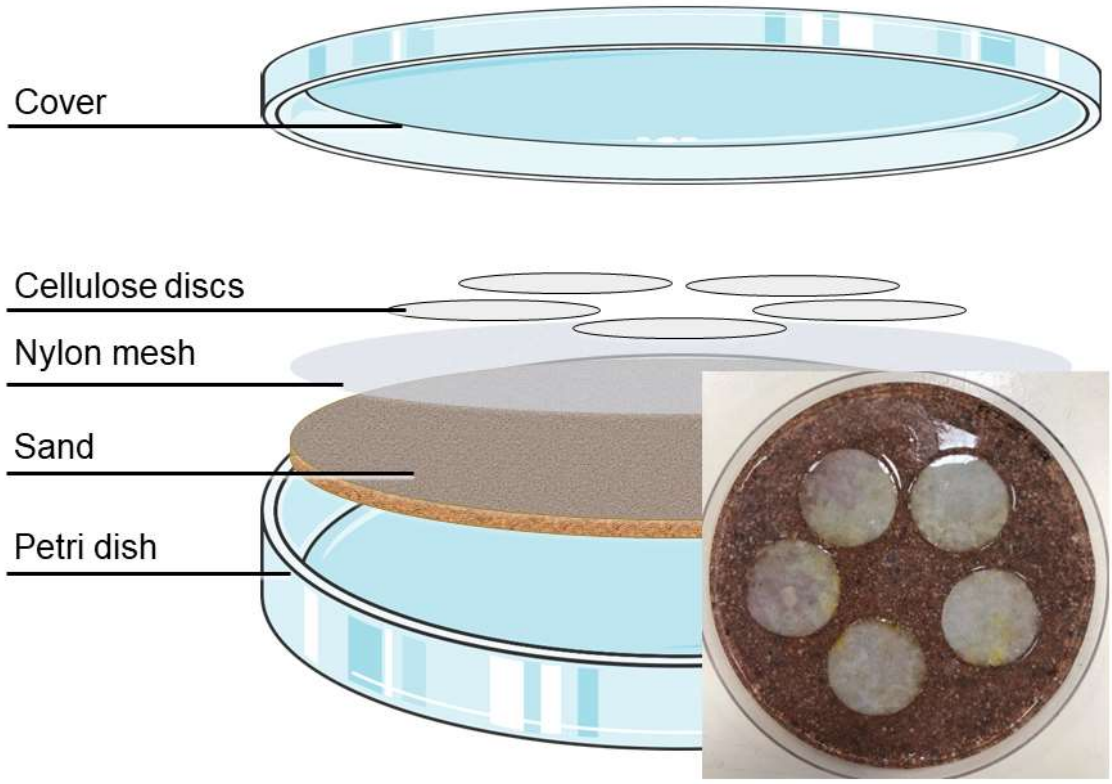

Figure SIV 1. Schematic representation of the microcosm setup.

The sand acts as a support to keep the discs stay moisturised but not submerged in the liquid culture solution. The picture at the bottom right shows an actual microcosm during the experiment. Petri dish artwork used here is from Servier Medical Art.

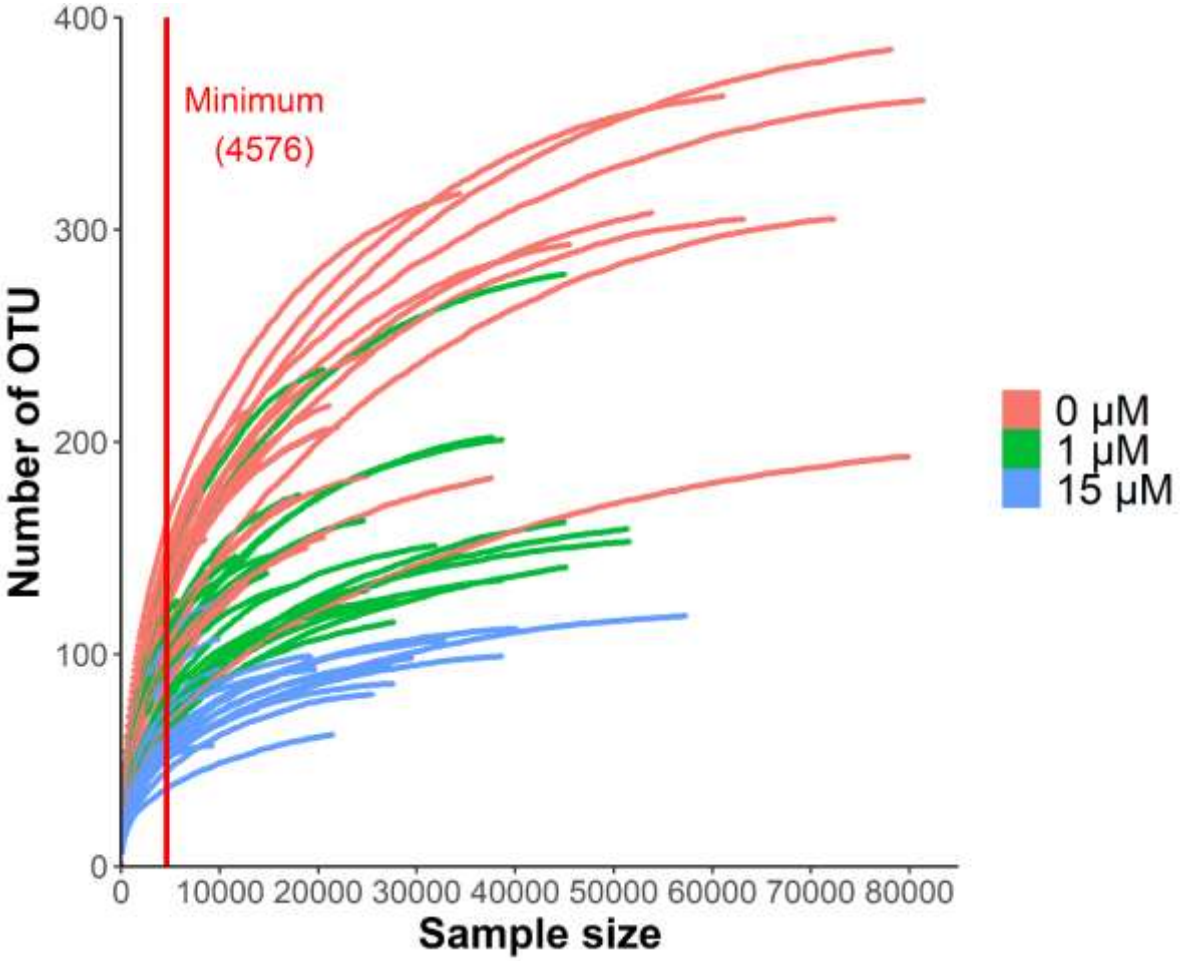

Figure SIV 2. Rarefication curve of all samples.
The dataset was rarefied to the minimum of 4576 sequences which allow us to have sufficient sequencing depth and statistical power to compare between conditions.

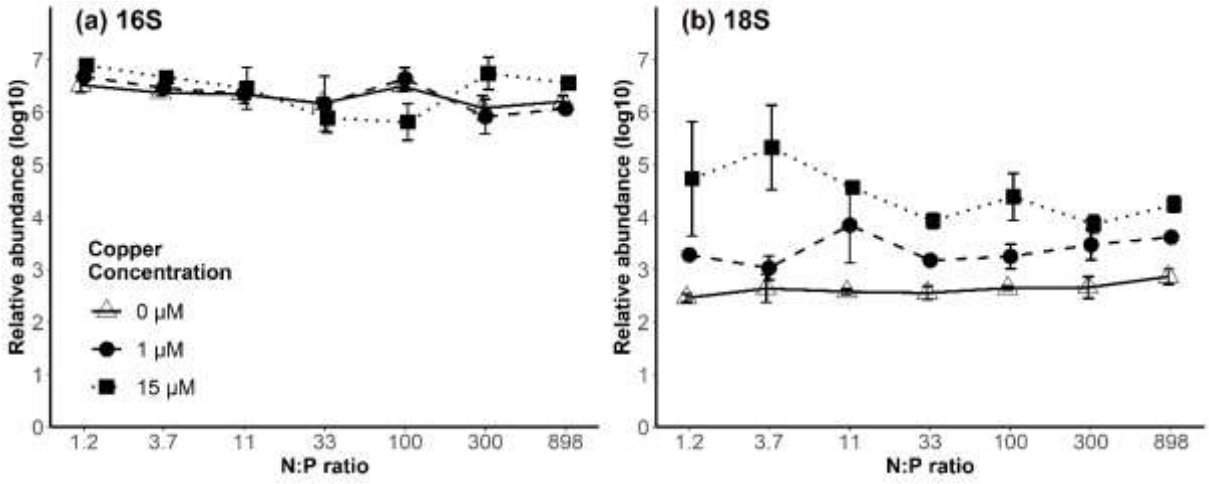

Figure SIV 3. Relative abundance of bacterial 16S and fungal 18S rRNA gene copies.
x-axis for provided N:P ratios is log-transformed but shows as the molar ratio for reading convenience.

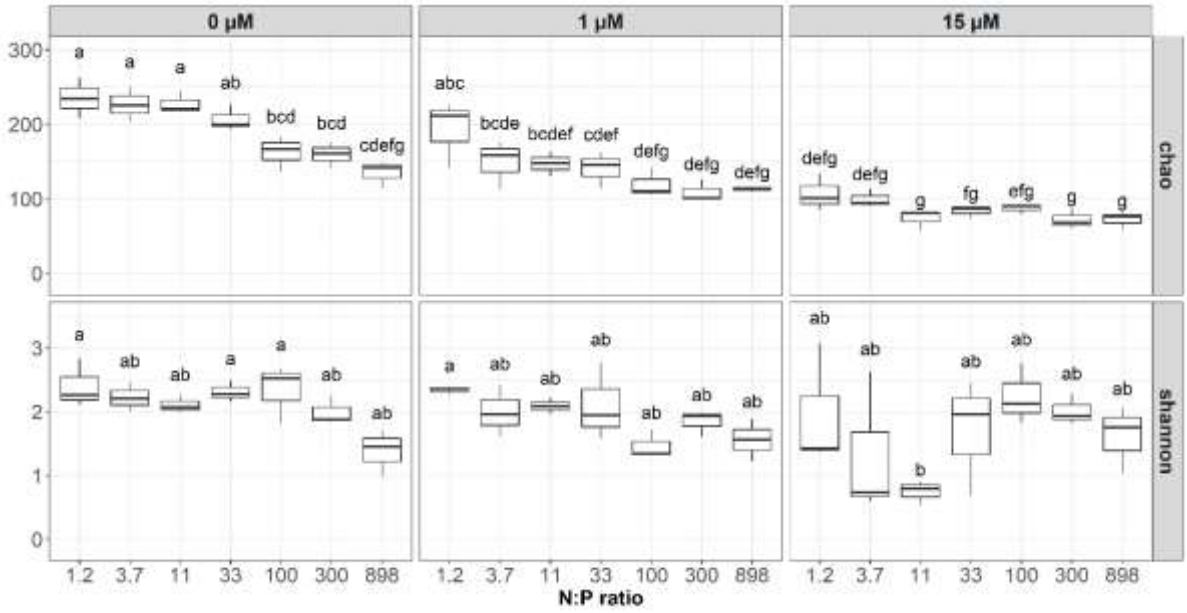

Figure SIV 4. Comparison of alpha diversity indices at different copper concentration group.

chao: Chao1 richness index; Shannon: Shannon diversity index.

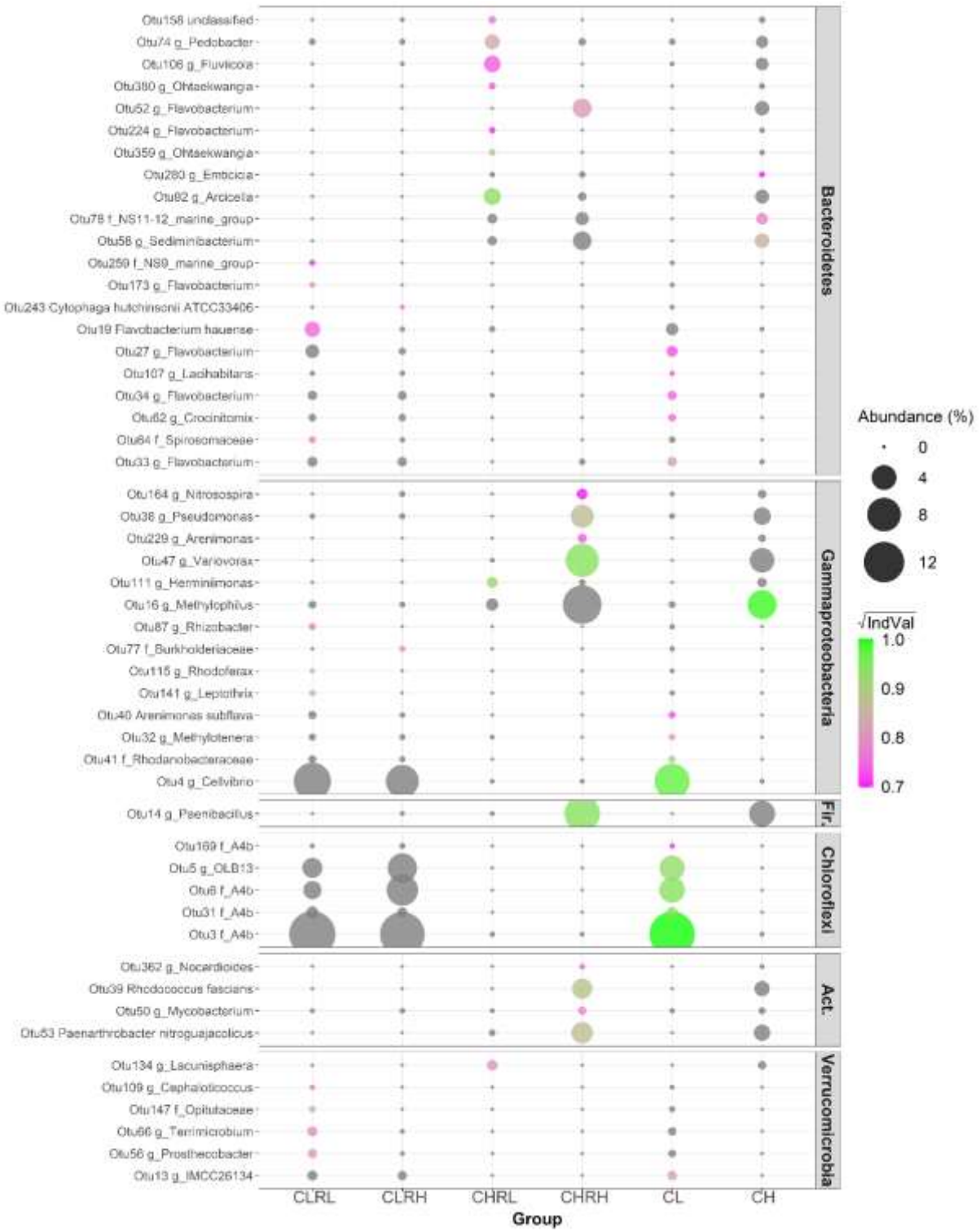

Figure SIV 5. Indicator species with indicator values > 0.7.

CLRL: low copper, low ratios; CLRH: low copper, high ratios; CHRL: high copper, low ratios; CHRH: high copper, high ratio; CL: low copper, all ratios and CH: high copper, all ratios. Fir.: Firmicutes. Act.: Actinobacteria.

We researched for indicator species responding to low or high Cu concentration and to low and high N:P ratios. The results of indicator species analysis with indicator values higher than 0.7 are shown. For the group CLRL (low copper, low ratios), 11 indicators (4 *Bacteroidetes* members of which 2 *Flavobacterium*, 3 *Gammaproteobacteria* belonging to *Burkholderiales* order and 4 *Verrucomicrobia* members of which 2 belonging to *Opitutacea* familly) were identified. For the group CLRH (low copper, high ratios), 2 indicators (1 *Bacteroidetes* belonging to *Cytophaga* and 1 *Gammaproteobacteria* belonging to *Burkholderiacea*) were identified. For the group CHRL (high copper, low ratios), 9 indicators (7 *Bacteroidetes* members of which 3 *Cytophagales*, 2 *Flavobacteriales* and 1 *Sphingobacteriales*, 1 *Gammaproteobacteria* belonging to *Herminiimonas* and 1 *Verrucomicrobia* belonging to *Lacunisphaera*) were identified. For the group CHRH (high copper, high ratios), 10 indicators (1 *Bacteroidetes* belonging to *Flavobacterium*, 4 *Gammaproteobacteria* belonging to *Nitrosospira*, *Pseudomonas*, *Aeromonas* and *Variovorax*, 1 *Firmicutes* belonging to *Paenibacillus*, 4 *Actinobacteria* members of which 2 belong to *Nocardiaceae*) were identified. The analysis also revealed 15 indicators related to low copper (CL: CLRL and CLRH groups) condition: 5 *Bacteroidetes* members of which 3 belong to *Flavobacterium*, 1 to *Crocinitomix* and 1 to *Lacihabitans*, 3 *Gammaproteobacteria* members with the dominance of a *Cellvibrio* member, 5 *Chloroflexi* belonging to the putative family A4B, and 1 *Verrucomicrobia*. Finally, 4 indicators related to high copper (CH: CHRL and CHRH groups) condition were identified: 3 *Bacteroidetes* members belonging to *Cytophagia* and *Chitinophagia* classes and 1 *Gammaproteobacteria* member affiliated to *Methylophilus*.

There is almost no information in the literature about the stoichiometric demand and Cu resistance of those identified taxa, but the information we found about their cellulose decomposition capacity tends to agree with our results. Since cellulose was the unique carbon source, taxa identified at low copper and low ratios (CLRL group) suggest mostly their capacity

of cellulose decomposition and potentially their demands on low N:P ratios. Similarly, taxa identified at low copper high ratios (CLRH) suggest their capacity of surviving a highly imbalance N:P ratio which probably limited their cellulose decomposition capacities. For example, *Cytophaga* are known to use cellulose, (Lynd *et al.* 2002; Krishna and Mohan 2017). Other indicator species identified at low copper and whatever the ratio (CL) also showed some well know cellulose decomposing taxa (e.g. *Flavobacterium*, *Cellvibrio*). *Anaerolineae* (phylum of *Chloroflexi*) has also been detected. They are strict anaerobic bacteria their abundance suggests that despite the absence of total water immersion, at least the bottom of the cellulose discs could have ended up in anaerobic conditions such as biofilm formation. Although the ecological role of the *Anaerolineae* members remains unclear, these bacteria have been shown to exhibit cellulolytic activities (Hug *et al.* 2013; Xia *et al.* 2016). Taxa identified at high copper low ratios (CHRL) may suggest some cellulose decomposing taxa are also Cu resistant, whilst those identified at CHRH would be resistant at both highly imbalance N:P ratios and high copper concentration. For example, *Paenibacillus*, *Nocardiodes*, *Rhodococcus*, *Mycobacterium* and *Paenarthrobacter* are capable of cellulose degradation (Ho, di Lonardo and Bodelier 2017; Yadav and Dubey 2018), but seemed to have a very low decomposition activity. Moreover, *Paenibacillus* are also shown to have a certain heavy metal biosoption ability (Prado Acosta *et al.* 2005) which might reduce the overall Cu toxicity to the whole bacterial community. *Actinobacteria* are also known for their resistance to Cu (Polti *et al.* 2014). The significant increase in abundance of *Actinobacteria* at high Cu and high N:P ratios might be explained by the absence of dominant, Cu-sensitive cellulolytic bacteria. Previous study has speculated an upregulation of their cellulolytic activity under excess N (Ho, di Lonardo and Bodelier 2017), yet our results contradict their suggestion.

References

Abrego N, Norberg A, Ovaskainen O. Measuring and predicting the influence of traits on the assembly processes of wood-inhabiting fungi. *Journal of Ecology* 2017;**105**, DOI: 10.1111/1365-2745.12722.

Alexander RB, Boyer EW, Smith RA *et al.* The role of headwater streams in downstream water quality. *J Am Water Resour Assoc* 2007;**43**:41–59.

Amoatey P, Baawain MS. Effects of pollution on freshwater aquatic organisms. *Water Environment Research* 2019;**91**, DOI: 10.1002/wer.1221.

Arendt JD. Adaptive intrinsic growth rates: An integration across taxa. *Quarterly Review of Biology* 1997;**72**, DOI: 10.1086/419764.

Baldy V, Gessner MO, Chauvet E. Bacteria, Fungi and the Breakdown of Leaf Litter in a Large River. *Oikos* 1995;**74**:93.

Bani A, Pioli S, Ventura M *et al.* The role of microbial community in the decomposition of leaf litter and deadwood. *Applied Soil Ecology* 2018;**126**:75–84.

Bärlocher F. The contribution of fungal enzymes to the digestion of leaves by Gammarus fossarum Koch (Amphipoda). *Oecologia* 1982;**52**:1–4.

Bärlocher F. The role of fungi in the nutrition of stream invertebrates. *Botanical Journal of the Linnean Society* 1985;**91**:83–94.

Bärlocher F. Research on Aquatic Hyphomycetes: Historical Background and Overview. 1992:1–15.

Bärlocher F. Sporulation by Aquatic Hyphomycetes. *Methods to Study Litter Decomposition* 2020:241–5.

Bärlocher F, Chamier A-C, Chandrashekar KR *et al. The Ecology of Aquatic Hyphomycetes*. Bärlocher F (ed.). Berlin, Heidelberg: Springer Berlin Heidelberg, 1992.

Bar-On YM, Phillips R, Milo R. The biomass distribution on Earth. *Proceedings of the National Academy of Sciences* 2018;**115**:6506–11.

Baudy P, Zubrod JP, Röder N *et al.* A glance into the black box: Novel species-specific quantitative real-time PCR assays to disentangle aquatic hyphomycete community composition. *Fungal Ecol* 2019;**42**:100858.

Beaumelle L, De Laender F, Eisenhauer N. Biodiversity mediates the effects of stressors but not nutrients on litter decomposition. *Elife* 2020;**9**:1–40.

Beck M, Billoir E, Floury M *et al.* A 34-year survey under phosphorus decline and warming: Consequences on stoichiometry and functional trait composition of freshwater macroinvertebrate communities. *Science of the Total Environment* 2023;**858**, DOI: 10.1016/j.scitotenv.2022.159786.

Beck M, Mondy CP, Danger M *et al.* Extending the growth rate hypothesis to species development: Can stoichiometric traits help to explain the composition of macroinvertebrate communities? *Oikos* 2021;**130**, DOI: 10.1111/oik.08090.

Beever RE, Burns DJW. Phosphorus Uptake, Storage and Utilization by Fungi. *Adv Bot Res* 1981;**8**:127–219.

Belle A, Tanay A, Bitincka L *et al.* Quantification of protein half-lives in the budding yeast proteome. *Proc Natl Acad Sci U S A* 2006;**103**:13004.

Berg B, Ekbohm G, Söderström B *et al.* Reduction of decomposition rates of scots pine needle litter due to heavy-metal pollution. *Water Air Soil Pollut* 1991;**59**:165–77.

Berg B, McClaugherty C. Initial Litter Chemical Composition. *Plant Litter* 2020a:67–100.

Berg B, McClaugherty C. Changes in Substrate Composition During Decomposition. *Plant Litter* 2020b:101–28.

Besemer K. Biodiversity, community structure and function of biofilms in stream ecosystems. *Res Microbiol* 2015;**166**, DOI: 10.1016/j.resmic.2015.05.006.

De Boer W, Folman LB, Summerbell RC *et al.* Living in a fungal world: Impact of fungi on soil bacterial niche development. *FEMS Microbiol Rev* 2005;**29**:795–811.

Brosed M, Jabiol J, Gessner MO. Nutrient stoichiometry of aquatic hyphomycetes: Interstrain variation and ergosterol conversion factors. *Fungal Ecol* 2017;**29**:96–102.

Bruna RE, Kendra CG, Groisman EA *et al.* Limitation of phosphate assimilation maintains cytoplasmic magnesium homeostasis. *Proc Natl Acad Sci U S A* 2021;**118**, DOI: 10.1073/PNAS.2021370118/-/DCSUPPLEMENTAL.

Butler SK, Suberkropp K. Aquatic Hyphomycetes on Oak Leaves: Comparison of Growth, Degradation and Palatability. *Mycologia* 1986;**78**, DOI: 10.2307/3807432.

de Cáceres M, Legendre P, Moretti M. Improving indicator species analysis by combining groups of sites. *Oikos* 2010;**119**:1674–84.

Camenzind T, Lehmann A, Ahland J *et al.* Trait-based approaches reveal fungal adaptations to nutrient-limiting conditions. *Environ Microbiol* 2020;**22**:3548–60.

Camenzind T, Philipp Grenz K, Lehmann J *et al.* Soil fungal mycelia have unexpectedly flexible stoichiometric C:N and C:P ratios. Liu L (ed.). *Ecol Lett* 2021;**24**:208–18.

Caporaso JG, Lauber CL, Walters WA *et al.* Global patterns of 16S rRNA diversity at a depth of millions of sequences per sample. *Proc Natl Acad Sci U S A* 2011;**108**:4516–22.

Cebrian J. Patterns in the fate of production in plant communities. *American Naturalist* 1999;**154**:449–68.

Cébron A, Norini MP, Beguiristain T *et al.* Real-Time PCR quantification of PAH-ring hydroxylating dioxygenase (PAH-RHDα) genes from Gram positive and Gram negative bacteria in soil and sediment samples. *J Microbiol Methods* 2008;**73**:148–59.

Cecchi G, Roccotiello E, Di Piazza S *et al.* Assessment of Ni accumulation capability by fungi for a possible approach to remove metals from soils and waters. *J Environ Sci Health B* 2017;**52**, DOI: 10.1080/03601234.2017.1261539.

Cervantes C, Gutierrez-Corona F. Copper resistance mechanisms in bacteria and fungi. *FEMS Microbiol Rev* 1994;**14**:121–37.

Chamier A-C, Dixon PA. Pectinases in Leaf Degradation by Aquatic Hyphomycetes: the Enzymes and Leaf Maceration. *Microbiology (N Y)* 1982;**128**, DOI: 10.1099/00221287-128-10-2469.

Chauvet E. Hyphomycètes aquatiques du sud-ouest de la France. *Gaussenia* 1990;**6**:3–31.

Cheever BM, Kratzer EB, Webster JR. Immobilization and mineralization of N and P by heterotrophic microbes during leaf decomposition. *Freshwater Science* 2012;**31**:133–47.

Cheever BM, Webster JR, Bilger EE *et al.* The relative importance of exogenous and substrate-derived nitrogen for microbial growth during leaf decomposition. *Ecology* 2013;**94**:1614–25.

Chew I, Obbard JP, Stanforth RR. Microbial cellulose decomposition in soils from a rifle range contaminated with heavy metals. *Environmental Pollution* 2001;**111**:367–75.

Chiang E, Schmidt ML, Berry MA *et al.* Verrucomicrobia are prevalent in north-temperate freshwater lakes and display class-level preferences between lake habitats. Smidt H (ed.). *PLoS One* 2018;**13**:e0195112.

Conover WJ. *Practical Nonparametric Statistics*. 3rd ed., 1999.

Cornwell WK, Cornelissen JHC, Amatangelo K *et al.* Plant species traits are the predominant control on litter decomposition rates within biomes worldwide. *Ecol Lett* 2008;**11**:1065–71.

Crawford DL, Crawford RL. Microbial degradation of lignin. *Enzyme Microb Technol* 1980;**2**, DOI: 10.1016/0141-0229(80)90003-4.

Cross WF, Benstead JP, Frost PC *et al.* Ecological stoichiometry in freshwater benthic systems: Recent progress and perspectives. *Freshw Biol* 2005;**50**:1895–912.

Cross WF, Hood JM, Benstead JP *et al.* Interactions between temperature and nutrients across levels of ecological organization. *Glob Chang Biol* 2015;**21**:1025–40.

Crowther TW, Maynard DS, Crowther TR *et al.* Untangling the fungal niche: The trait-based approach. *Front Microbiol* 2014;**5**, DOI: 10.3389/fmicb.2014.00579.

Currie DJ, Kalff J. A comparison of the abilities of freshwater algae and bacteria to acquire and retain phosphorus. *Limnol Oceanogr* 1984;**29**, DOI: 10.4319/lo.1984.29.2.0298.

Dang CK, Gessner MO, Chauvet E. Influence of conidial traits and leaf structure on attachment success of aquatic hyphomycetes on leaf litter. *Mycologia* 2007;**99**:24–32.

Danger M. Ecological stoichiometry in detritus-based ecosystems with a special focus on forested headwater streams. 2020;**39**, DOI: 10.23818/limn.39.xx.

Danger M, Arce Funck J, Devin S *et al.* Phosphorus content in detritus controls life-history traits of a detritivore. *Funct Ecol* 2013;**27**:807–15.

Danger M, Chauvet E. Elemental composition and degree of homeostasis of fungi: Are aquatic hyphomycetes more like metazoans, bacteria or plants? *Fungal Ecol* 2013;**6**:453–7.

Danger M, Daufresne T, Lucas F *et al.* Does Liebig's law of the minimum scale up from species to communities? *Oikos* 2008;**117**:1741–51.

Danger M, Gessner MO, Bärlocher F. Ecological stoichiometry of aquatic fungi: current knowledge and perspectives. *Fungal Ecol* 2016;**19**:100–11.

Danger M, Leflaive J, Oumarou C *et al.* Control of phytoplankton–bacteria interactions by stoichiometric constraints. *Oikos* 2007a;**116**:1079–86.

Danger M, Oumarou C, Benest D *et al.* Bacteria can control stoichiometry and nutrient limitation of phytoplankton. *Funct Ecol* 2007b;**21**:202–10.

Daufresne T, Loreau M. Ecological stoichiometry, primary producer-decomposer interactions, and ecosystem persistence. *Ecology* 2001;**82**:3069–82.

Demi LM, Benstead JP, Rosemond AD *et al.* Experimental N and P additions relieve stoichiometric constraints on organic matter flows through five stream food webs. *Journal of Animal Ecology* 2020;**89**, DOI: 10.1111/1365-2656.13197.

Demircan T, Ovezmyradov G, Yıldırım B *et al.* Experimentally induced metamorphosis in highly regenerative axolotl (ambystoma mexicanum) under constant diet restructures microbiota. *Sci Rep* 2018;**8**:1–13.

Descals E. Techniques for Handling Ingoldian Fungi. In: Bärlocher Felix and Gessner MO and GMAS (ed.). *Methods to Study Litter Decomposition: A Practical Guide*. Cham: Springer International Publishing, 2020, 197–209.

Domek MJ, Robbins JE, Anderson ME *et al.* Metabolism of Escherichia coli injured by copper. *https://doi.org/101139/m87-010* 2011;**33**:57–62.

Duarte S, Cássio F, Ferreira V *et al.* Seasonal Variability May Affect Microbial Decomposers and Leaf Decomposition More Than Warming in Streams. *Microb Ecol* 2016;**72**:263–76.

Duarte S, Pascoal C, Alves A *et al.* Copper and zinc mixtures induce shifts in microbial communities and reduce leaf litter decomposition in streams. *Freshw Biol* 2008;**53**:91–101.

Dudgeon D, Arthington AH, Gessner MO *et al.* Freshwater biodiversity: Importance, threats, status and conservation challenges. *Biol Rev Camb Philos Soc* 2006;**81**, DOI: 10.1017/S1464793105006950.

Dupont CL, Grass G, Rensing C. Copper toxicity and the origin of bacterial resistance - New insights and applications. *Metallomics* 2011;**3**:1109–18.

Elser JJ, Acharya K, Kyle M *et al.* Growth rate-stoichiometry couplings in diverse biota. *Ecol Lett* 2003;**6**:936–43.

Elser JJ, Andersen T, Baron JS *et al.* Shifts in lake N: P stoichiometry and nutrient limitation driven by atmospheric nitrogen deposition. *Science (1979)* 2009;**326**:835–7.

Elser JJ, Bracken MES, Cleland EE *et al.* Global analysis of nitrogen and phosphorus limitation of primary producers in freshwater, marine and terrestrial ecosystems. *Ecol Lett* 2007;**10**:1135–42.

Elser JJ, Chrzanowski TH, Sterner RW *et al.* Stoichiometric constraints on food-web dynamics: A whole-lake experiment on the Canadian Shield. *Ecosystems* 1998;**1**, DOI: 10.1007/s100219900009.

Elser JJ, Sterner RW, Gorokhova E *et al.* Biological stoichiometry from genes to ecosystems. *Ecol Lett* 2000;**3**:540–50.

Elser JJ, Urabe J. The stoichiometry of consumer-driven nutrient recycling: Theory, observations, and consequences. *Ecology* 1999;**80**, DOI: 10.1890/0012-9658(1999)080[0735:TSOCDN]2.0.CO;2.

Elton CS. The Animal Community. Huxley JS (ed.). *Animal ecology* 1927:50–70.

Enríquez S, Duarte CM, Sand-Jensen K. Patterns in decomposition rates among photosynthetic organisms: the importance of detritus C:N:P content. *Oecologia* 1993;**94**:457–71.

Esser K, McLaughlin DJ, Spatafora JW. *The Mycota: A Comprehensive Treatise on Fungi as Experimental Systems for Basic and Applied Research: VII Systematics and Evolution Part B 2nd Edition*. Springer Berlin Heidelberg, 2015.

Falkowski P, Scholes RJ, Boyle E *et al.* The global carbon cycle: A test of our knowledge of earth as a system. *Science (1979)* 2000;**290**:291–6.

Fanin N, Fromin N, Buatois B *et al.* An experimental test of the hypothesis of non-homeostatic consumer stoichiometry in a plant litter-microbe system. *Ecol Lett* 2013;**16**:764–72.

Fernandes I, Seena S, Pascoal C *et al.* Elevated temperature may intensify the positive effects of nutrients on microbial decomposition in streams. *Freshw Biol* 2014;**59**, DOI: 10.1111/fwb.12445.

Fernández D, Voss K, Bundschuh M *et al.* Effects of fungicides on decomposer communities and litter decomposition in vineyard streams. *Science of the Total Environment* 2015;**533**:40–8.

Ferreira R, Gaspar H, Gonzalez JM *et al.* Copper and temperature modify microbial communities, ammonium and sulfate release in soil. *Journal of Plant Nutrition and Soil Science* 2015a;**178**:953–62.

Ferreira V, Castagneyrol B, Koricheva J *et al.* A meta-analysis of the effects of nutrient enrichment on litter decomposition in streams. *Biological Reviews* 2015b;**90**:669–88.

Ferreira V, Chauvet E. Changes in dominance among species in aquatic hyphomycete assemblages do not affect litter decomposition rates. *Aquatic Microbial Ecology* 2012;**66**:1–11.

Ferreira V, Koricheva J, Duarte S *et al.* Effects of anthropogenic heavy metal contamination on litter decomposition in streams - A meta-analysis. *Environmental Pollution* 2016;**210**:261–70.

Fierer N, Craine JM, Mclauchlan K *et al.* Litter quality and the temperature sensitivity of decomposition. *Ecology* 2005;**86**:320–6.

Findlay S. Stream microbial ecology. *J North Am Benthol Soc* 2010;**29**:170–81.

Fisher SG, Likens GE. Energy Flow in Bear Brook , New Hampshire : An Integrative Approach to Stream Ecosystem Metabolism Author (s): Stuart G . Fisher and Gene E . Likens Reviewed work (s): Published by : Ecological Society of America Stable URL : http://www.jstor.org/stab. *Ecol Monogr* 1973;**43**:421–39.

Flemming HC, Wuertz S. Bacteria and archaea on Earth and their abundance in biofilms. *Nat Rev Microbiol* 2019;**17**:247–60.

Fontaine S, Mariotti A, Abbadie L. The priming effect of organic matter: A question of microbial competition? *Soil Biol Biochem* 2003;**35**:837–43.

Fox J, Weisberg S. *An {R} Companion to Applied Regression*. Third. Thousand Oaks {CA}: Sage, 2019.

Frost PC, Benstead JP, Cross WF *et al.* Threshold elemental ratios of carbon and phosphorus in aquatic consumers. *Ecol Lett* 2006;**9**:774–9.

Frost PC, Ebert D, Smith VH. Responses of a bacterial pathogen to phosphorus limitation of its aquatic invertebrate host. *Ecology* 2008;**89**, DOI: 10.1890/07-0389.1.

García-Palacios P, Mckie BG, Handa IT *et al.* The importance of litter traits and decomposers for litter decomposition: A comparison of aquatic and terrestrial ecosystems within and across biomes. *Funct Ecol* 2016;**30**:819–29.

Ge X, Zeng L, Xiao W *et al.* Effect of litter substrate quality and soil nutrients on forest litter decomposition: A review. *Acta Ecologica Sinica* 2013;**33**:102–8.

Geraldes P, Pascoal C, Cássio F. Effects of increased temperature and aquatic fungal diversity on litter decomposition. *Fungal Ecol* 2012;**5**:734–40.

Gessner MO. Ergosterol as a Measure of Fungal Biomass. In: Bärlocher F, Gessner MO, Graça MAS (eds.). *Methods to Study Litter Decomposition*. Cham: Springer International Publishing, 2020, 247–55.

Gessner MO, Chauvet E. Ergosterol-to-biomass conversion factors for aquatic hyphomycetes. *Appl Environ Microbiol* 1993;**59**:502–7.

Gessner MO, Chauvet E. Importance of Stream Microfungi in Controlling Breakdown Rates of Leaf Litter. *Ecology* 1994;**75**:1807–17.

Gessner MO, Chauvet E. A case for using litter breakdown to assess functional stream integrity. *Ecological Applications* 2002;**12**, DOI: 10.1890/1051-0761(2002)012[0498:ACFULB]2.0.CO;2.

Gessner MO, Chauvet E, Dobson M. A Perspective on Leaf Litter Breakdown in Streams. *Oikos* 1999;**85**:377.

Gessner MO, Swan CM, Dang CK *et al.* Diversity meets decomposition. *Trends Ecol Evol* 2010;**25**:372–80.

Gessner MO, Thomas M, Jean-Louis AM *et al.* Stable successional patterns of aquatic hyphomycetes on leaves decaying in a summer cool stream. *Mycol Res* 1993;**97**:163–72.

Gibson CA, O'Reilly CM, Conine AL *et al.* Nutrient uptake dynamics across a gradient of nutrient concentrations and ratios at the landscape scale. *Journal of Geophysical Research G: Biogeosciences* 2015;**120**:326–40.

Gilchrist MA, Sulsky DL, Pringle A. IDENTIFYING FITNESS AND OPTIMAL LIFE-HISTORY STRATEGIES FOR AN ASEXUAL FILAMENTOUS FUNGUS. *Evolution (N Y)* 2006;**60**, DOI: 10.1554/05-261.1.

Godwin CM, Cotner JB. What intrinsic and extrinsic factors explain the stoichiometric diversity of aquatic heterotrophic bacteria? *ISME Journal* 2018;**12**:598–609.

Gossiaux A, Rollin M, Guérold F *et al.* Temperature and nutrient effects on the relative importance of brown and green pathways for stream ecosystem functioning: A mesocosm approach. *Freshwater Biology*. Vol 65. 2020.

Gounand I, Daufresne T, Gravel D *et al.* Size evolution in microorganisms masks trade-offs predicted by the growth rate hypothesis. *Proceedings of the Royal Society B: Biological Sciences* 2016;**283**, DOI: 10.1098/rspb.2016.2272.

Graça MAS, Cressa C. Leaf quality of some tropical and temperate tree species as food resource for stream shredders. *Int Rev Hydrobiol* 2010;**95**, DOI: 10.1002/iroh.200911173.

Gray MJ, Wholey WY, Wagner NO *et al.* Polyphosphate Is a Primordial Chaperone. *Mol Cell* 2014;**53**:689–99.

Grimmett IJ, Shipp KN, Macneil A *et al.* Does the growth rate hypothesis apply to aquatic hyphomycetes? *Fungal Ecol* 2013;**6**:493–500.

Groffman PM, Bain DJ, Band LE *et al.* Down by the riverside: Urban riparian ecology. *Front Ecol Environ* 2003;**1**, DOI: 10.1890/1540-9295(2003)001[0315:DBTRUR]2.0.CO;2.

Groffman PM, Boulware NJ, Zipperer WC *et al.* Soil nitrogen cycle processes in urban riparian zones. *Environ Sci Technol* 2002;**36**, DOI: 10.1021/es020649z.

Gulis V, Kuehn K, Suberkropp K. The role of fungi in carbon and nitrogen cycles in freshwater ecosystems. *Fungi in Biogeochemical Cycles* 2006:404–35.

Gulis V, Kuehn KA, Schoettle LN *et al.* Changes in nutrient stoichiometry, elemental homeostasis and growth rate of aquatic litter- associated fungi in response to inorganic nutrient supply. *International Society for Microbial Ecology* 2017;**11**:2729–39.

Gulis V, Marvanová L, Descals E. An Illustrated Key to the Common Temperate Species of Aquatic Hyphomycetes. *Methods to Study Litter Decomposition* 2020:223–39.

Gulis V, Suberkropp K. Interactions between stream fungi and bacteria associated with decomposing leaf litter at different levels of nutrient availability. *Aquatic Microbial Ecology* 2003a;**30**:149–57.

Gulis V, Suberkropp K. Effect of inorganic nutrients on relative contributions of fungi and bacteria to carbon flow from submerged decomposing leaf litter. *Microb Ecol* 2003b;**45**:11–9.

Güsewell S, Gessner MO. N:P ratios influence litter decomposition and colonization by fungi and bacteria in microcosms. *Funct Ecol* 2009;**23**:211–9.

Güsewell S, Verhoeven JTA. Litter N:P ratios indicate whether N or P limits the decomposability of graminoid leaf litter. *Plant Soil* 2006;**287**:131–43.

Haraldsson M, Thébault E. Emerging niche clustering results from both competition and predation. *Ecol Lett* 2023;**00**:1–12.

Hardison EC, O'Driscoll MA, Deloatch JP *et al.* Urban Land Use, Channel Incision, and Water Table Decline Along Coastal Plain Streams, North Carolina1. *JAWRA Journal of the American Water Resources Association* 2009;**45**:1032–46.

Harte J, Kinzig AP. Mutualism and competition between plants and decomposers: implications for nutrient allocation in ecosystems. *American Naturalist* 1993;**141**:829–46.

Heeger F, Bourne EC, Wurzbacher C *et al.* Evidence for lignocellulose-decomposing enzymes in the genome and transcriptome of the aquatic hyphomycete clavariopsis aquatica. *Journal of Fungi* 2021;**7**, DOI: 10.3390/jof7100854.

Hendrickson OQ. Abundance and activity of N2-fixing bacteria in decaying wood. *Canadian Journal of Forest Research* 1991;**21**, DOI: 10.1139/x91-183.

Hessen DO, Jensen TC, Kyle M *et al.* RNA responses to N- and P-limitation; reciprocal regulation of stoichiometry and growth rate in Brachionus. *Funct Ecol* 2007;**21**:956–62.

Hibbett DS, Binder M, Bischoff JF *et al.* A higher-level phylogenetic classification of the Fungi. *Mycol Res* 2007;**111**:509–47.

Hieber M, Gessner MO. Contribution of stream detrivores, fungi, and bacteria to leaf breakdown based on biomass estimates. *Ecology* 2002;**83**, DOI: 10.1890/0012-9658(2002)083[1026:COSDFA]2.0.CO;2.

Hill TCJ, Walsh KA, Harris JA *et al.* Using ecological diversity measures with bacterial communities. *FEMS Microbiol Ecol* 2003;**43**:1–11.

Hillebrand H, Steinert G, Boersma M *et al.* Goldman revisited: Faster-growing phytoplankton has lower N: P and lower stoichiometric flexibility. *Limnol Oceanogr* 2013;**58**, DOI: 10.4319/lo.2013.58.6.2076.

Hladyz S, Gessner MO, Giller PS *et al.* Resource quality and stoichiometric constraints on stream ecosystem functioning. *Freshw Biol* 2009;**54**:957–70.

Ho A, di Lonardo DP, Bodelier PLE. Revisiting life strategy concepts in environmental microbial ecology. *FEMS Microbiol Ecol* 2017;**93**:1–14.

Hopkins DW, Ibrahim DM, O'donnell AG *et al.* Decomposition of cellulose, soil organic matter and plant litter in a temperate grassland soil. *Plant Soil* 1990;**124**:79–85.

Hothorn M, Neumann H, Lenherr ED *et al.* Catalytic core of amembrane-associated eukaryotic polyphosphate polymerase. *Science (1979)* 2009;**324**:513–6.

Hug LA, Castelle CJ, Wrighton KC *et al.* Community genomic analyses constrain the distribution of metabolic traits across the Chloroflexi phylum and indicate roles in sediment carbon cycling. *Microbiome* 2013;**1**:1–17.

Ingold CT. Aquatic hyphomycetes of decaying alder leaves. *Transactions of the British Mycological Society* 1942;**25**:339–417.

Isanta-Navarro J, Prater C, Peoples LM *et al.* Revisiting the growth rate hypothesis: Towards a holistic stoichiometric understanding of growth. *Ecol Lett* 2022;**25**:2324–39.

Jabiol J, Lecerf A, Lamothe S *et al.* Litter Quality Modulates Effects of Dissolved Nitrogen on Leaf Decomposition by Stream Microbial Communities. *Microb Ecol* 2019, DOI: 10.1007/s00248-019-01353-3.

Kassambara A. ggpubr: "ggplot2" Based Publication Ready Plots. 2023.

Kato S, Haruta S, Cui ZJ *et al.* Effective cellulose degradation by a mixed-culture system composed of a cellulolytic Clostridium and aerobic non-cellulolytic bacteria. *FEMS Microbiol Ecol* 2004;**51**, DOI: 10.1016/j.femsec.2004.07.015.

Kearns SG, Bärlocher F. Leaf surface roughness influences colonization success of aquatic hyphomycete conidia. *Fungal Ecol* 2008;**1**:13–8.

Keiblinger KM, Schneider M, Gorfer M *et al.* Assessment of Cu applications in two contrasting soils—effects on soil microbial activity and the fungal community structure. *Ecotoxicology* 2018;**27**:217–33.

Kilham SS, Kreeger DA, Lynn SG *et al.* COMBO: a defined freshwater culture medium for algae and zooplankton. *Hydrobiologia* 1998;**377**:147–59.

Kjøller A, Struwe S, Kjoller A. Microfungi in Ecosystems: Fungal Occurrence and Activity in Litter and Soil. *Oikos* 1982;**39**:391.

Kozich JJ, Westcott SL, Baxter NT *et al.* Development of a dual-index sequencing strategy and curation pipeline for analyzing amplicon sequence data on the miseq illumina sequencing platform. *Appl Environ Microbiol* 2013;**79**:5112–20.

Krishna MP, Mohan M. Litter decomposition in forest ecosystems: a review. *Energy Ecol Environ* 2017;**2**:236–49.

Ladomersky E, Petris MJ. Copper tolerance and virulence in bacteria. *Metallomics* 2015;**7**:957–64.

Lange M, Müller C, Peiter E. Membrane-assisted culture of fungal mycelium on agar plates for RNA extraction and pharmacological analyses. *Anal Biochem* 2014;**453**:58–60.

Larras F, Billoir E, Baillard V *et al.* DRomics: A Turnkey Tool to Support the Use of the Dose-Response Framework for Omics Data in Ecological Risk Assessment. *Environ Sci Technol* 2018;**52**:14461–8.

Laspoumaderes C, Meunier CL, Magnin A *et al.* A common temperature dependence of nutritional demands in ectotherms. *Ecol Lett* 2022;**25**, DOI: 10.1111/ele.14093.

Leflaive J, Danger M, Lacroix G *et al.* Nutrient effects on the genetic and functional diversity of aquatic bacterial communities. *FEMS Microbiol Ecol* 2008;**66**:379–90.

Lemmel F, Maunoury-Danger F, Leyval C *et al.* DNA stable isotope probing reveals contrasted activity and phenanthrene-degrading bacteria identity in a gradient of anthropized soils. *FEMS Microbiol Ecol* 2019;**95**:1–14.

Leroux SJ, Loreau M. Subsidy hypothesis and strength of trophic cascades across ecosystems. *Ecol Lett* 2008;**11**:1147–56.

Leschine SB. Cellulose Degradation in Anaerobic Environments. *Annu Rev Microbiol* 1995;**49**, DOI: 10.1146/annurev.micro.49.1.399.

Li S, Liu W, Gu S *et al.* Spatio-temporal dynamics of nutrients in the upper Han River basin, China. *J Hazard Mater* 2009;**162**, DOI: 10.1016/j.jhazmat.2008.06.059.

Lindeman RL. The trophic-dynamic aspect of ecology. *Ecology*. Vol 23. Ecological Society of Amercia, 1942, 399–417.

López-Mondéjar R, Zühlke D, Becher D *et al.* Cellulose and hemicellulose decomposition by forest soil bacteria proceeds by the action of structurally variable enzymatic systems. *Sci Rep* 2016;**6**:1–12.

Lorencová E, Vltavská P, Budinský P *et al.* Antibacterial effect of phosphates and polyphosphates with different chain length. *http://dx.doi.org/101080/109345292012707544* 2012;**47**:2241–5.

Lynd LR, Weimer PJ, van Zyl WH *et al.* Microbial Cellulose Utilization: Fundamentals and Biotechnology. *Microbiology and Molecular Biology Reviews* 2002;**66**:506–77.

Ma Z, Jacobsen FE, Giedroc DP. Coordination chemistry of bacterial metal transport and sensing. *Chem Rev* 2009;**109**:4644–81.

Makino W, Cotner JB, Sterner RW *et al.* Are bacteria more like plants or animals? Growth rate and resource dependence of bacterial C:N:P stoichiometry. *Funct Ecol* 2003;**17**:121–30.

Malosso E, Schoenlein-Crusius IH. An insight into the study methods of aquatic fungi. *Freshwater Mycology: Perspectives of Fungal Dynamics in Freshwater Ecosystems* 2022:229–46.

Manzoni S, Chakrawal A, Spohn M *et al.* Modeling Microbial Adaptations to Nutrient Limitation During Litter Decomposition. *Frontiers in Forests and Global Change* 2021;**4**, DOI: 10.3389/ffgc.2021.686945.

Mariz J, Franco-Duarte R, Cássio F *et al.* Aquatic hyphomycete taxonomic relatedness translates into lower genetic divergence of the nitrate reductase gene. *Journal of Fungi* 2021;**7**, DOI: 10.3390/jof7121066.

Martínez A, Larrañaga A, Pérez J *et al.* Temperature affects leaf litter decomposition in low-order forest streams: Field and microcosm approaches. *FEMS Microbiol Ecol* 2014;**87**, DOI: 10.1111/1574-6941.12221.

Martinson HM, Schneider K, Gilbert J *et al.* Detritivory: stoichiometry of a neglected trophic level. *Ecol Res* 2008;**23**:487–91.

Mason-Jones K, Robinson SL, Veen GF (Ciska) *et al.* Microbial storage and its implications for soil ecology. *ISME Journal* 2022;**16**:617–29.

de Mazancourt C, Schwartz MW. Starve a competitor: Evolution of luxury consumption as a competitive strategy. *Theor Ecol* 2012;**5**:37–49.

Medeiros AO, Pascoal C, Graça MAS. Diversity and activity of aquatic fungi under low oxygen conditions. *Freshw Biol* 2009;**54**:142–9.

Meunier CL, Boersma M, El-Sabaawi R *et al.* From elements to function: Toward unifying ecological stoichiometry and trait-based ecology. *Front Environ Sci* 2017;**5**, DOI: 10.3389/fenvs.2017.00018.

Mille-Lindblom C, Fischer H, Tranvik LJ. Antagonism between bacteria and fungi: Substrate competition and a possible tradeoff between fungal growth and tolerance towards bacteria. *Oikos* 2006;**113**:233–42.

Miller TE, Burns JH, Munguia P *et al.* A critical review of twenty years' use of the resource-ratio theory. *American Naturalist* 2005;**165**, DOI: 10.1086/428681.

Monroy S, Larrañaga A, Martínez A *et al.* Temperature Sensitivity of Microbial Litter Decomposition in Freshwaters: Role of Leaf Litter Quality and Environmental Characteristics. *Microb Ecol* 2022, DOI: 10.1007/s00248-022-02041-5.

Moore JC, Berlow EL, Coleman DC *et al.* Detritus, trophic dynamics and biodiversity. *Ecol Lett* 2004;**7**:584–600.

Muyzer G, de Waal EC, Uitterlinden AG. Profiling of complex microbial populations by denaturing gradient gel electrophoresis analysis of polymerase chain reaction-amplified genes coding for 16S rRNA. *Appl Environ Microbiol* 1993;**59**:695–700.

Nedeau EJ, Merritt RW, Kaufman MG. The effect of an industrial effluent on an urban stream benthic community: Water quality vs. habitat quality. *Environmental Pollution* 2003;**123**, DOI: 10.1016/S0269-7491(02)00363-9.

Nguyen CT, Ezawa T, Saito K. Polyphosphate polymerizing and depolymerizing activity of VTC4 protein in an arbuscular mycorrhizal fungus. *https://doi.org/101080/0038076820222029220* 2022, DOI: 10.1080/00380768.2022.2029220.

Niyogi DK, Cheatham CA, Thomson WH *et al.* Litter breakdown and fungal diversity in a stream affected by mine drainage. *Fundamental and Applied Limnology* 2009;**175**:39–48.

Nübel U, Engelen B, Felsre A *et al.* Sequence heterogeneities of genes encoding 16S rRNAs in Paenibacillus polymyxa detected by temperature gradient gel electrophoresis. *J Bacteriol* 1996;**178**:5636–43.

Ochoa-Herrera V, León G, Banihani Q *et al.* Toxicity of copper(II) ions to microorganisms in biological wastewater treatment systems. *Science of the Total Environment* 2011;**412–413**:380–5.

Odum E. *Fundamentals of Ecology*. 2nd ed. W. B. Saunders Company, 1959.

Oksanen J, Blanchet FG, Friendly M *et al.* Package "vegan" Title Community Ecology Package Version 2.5-7. *cran.ism.ac.jp* 2020.

Panec M, Sue Katz • D. Plaque Assay Protocols. 2016.

Pascoal C, Fernandes I, Seena S *et al.* Linking Microbial Decomposer Diversity to Plant Litter Decomposition and Associated Processes in Streams. *The Ecology of Plant Litter Decomposition in Stream Ecosystems* 2021:163–92.

Pedersen M, Nissen S, Mitarai N *et al.* The functional half-life of an mRNA depends on the ribosome spacing in an early coding region. *J Mol Biol* 2011;**407**:35–44.

Peñuelas J, Ciais P, Canadell JG *et al.* Shifting from a fertilization-dominated to a warming-dominated period. *Nature Ecology & Evolution 2017 1:10* 2017;**1**:1438–45.

Peñuelas J, Poulter B, Sardans J *et al.* Human-induced nitrogen–phosphorus imbalances alter natural and managed ecosystems across the globe. *Nat Commun* 2013;**4**:2934.

Pérez J, Ferreira V, Graça MAS *et al.* Litter Quality Is a Stronger Driver than Temperature of Early Microbial Decomposition in Oligotrophic Streams: a Microcosm Study. *Microb Ecol* 2021;**82**:897–908.

Persson J, Fink P, Goto A *et al.* To be or not to be what you eat: Regulation of stoichiometric homeostasis among autotrophs and heterotrophs. *Oikos* 2010;**119**, DOI: 10.1111/j.1600-0706.2009.18545.x.

Polti MA, Aparicio JD, Benimeli CS *et al.* Role of Actinobacteria in Bioremediation. *Microbial Biodegradation and Bioremediation* 2014:270–86.

Prado Acosta M, Valdman E, Leite SGF *et al.* Biosorption of copper by Paenibacillus polymyxa cells and their exopolysaccharide. *World J Microbiol Biotechnol* 2005;**21**:1157–63.

Pu G, Tong J, Su A *et al.* Adaptation of microbial communities to multiple stressors associated with litter decomposition of Pterocarya stenoptera. *J Environ Sci (China)* 2014;**26**, DOI: 10.1016/S1001-0742(13)60542-2.

R Core Team. R: A Language and Environment for Statistical Computing. 2022.

Rao NN, Gómez-García MR, Kornberg A. Inorganic Polyphosphate: Essential for Growth and Survival. *https://doi.org/101146/annurev.biochem77083007093039* 2009;**78**:605–47.

Redfield AC. On the proportions of organic derivatives in sea water and their relation to the composition of plankton. *James Johnstone memorial volume* 1934:176–92.

Romaní AM, Fischer H, Mille-lindblom C *et al.* Interactions of Bacteria and Fungi on Decomposing Litter : Differential Extracellular Enzyme Activities. *Ecology* 2006a;**87**:2559–69.

Romaní AM, Fischer H, Mille-Lindblom C *et al.* Interactions of bacteria and fungi on decomposing litter: Differential extracellular enzyme activities. *Ecology* 2006b;**87**:2559–69.

Rosenfeld J, Roff JC. Primary production and potential availability of autochthonous carbon in southern Ontario streams. *Hydrobiologia* 1991;**224**, DOI: 10.1007/BF00006866.

Roussel H, Chauvet E, Bonzom JM. Alteration of leaf decomposition in copper-contaminated freshwater mesocosms. *Environ Toxicol Chem* 2008;**27**:637–44.

RStudio Team. RStudio: Integrated Development Environment for R. 2022.

Ruiz T, Koussoroplis A-M, Danger M *et al.* U-shaped response Unifies views on temperature dependency of stoichiometric requirements. *Ecol Lett* 2020, DOI: 10.1111/ele.13493.

Saccardo PA. Fungi Gallici lecti a cl. viris P. Brunaud, Abb. Letendre, A. Malbranche, J. Therry, vel editi in Mycotheca Gallica C. Roumeguèri. Series II. *Michelia* 1880;**2**:39–135.

Sardans J, Rivas-Ubach A, Peñuelas J. The elemental stoichiometry of aquatic and terrestrial ecosystems and its relationships with organismic lifestyle and ecosystem structure and function: a review and perspectives. *Biogeochemistry* 2012;**111**:1–39.

Schindler MH, Gessner MO, Schindler MH *et al.* Functional Leaf Traits and Biodiversity Effects on Litter Decomposition in a Stream. *Ecology* 2009;**90**:1641–9.

Schloss PD, Westcott SL, Ryabin T *et al.* Introducing mothur: Open-source, platform-independent, community-supported software for describing and comparing microbial communities. *Appl Environ Microbiol* 2009;**75**:7537–41.

Schoch CL, Ciufo S, Domrachev M *et al.* NCBI Taxonomy: A comprehensive update on curation, resources and tools. *Database* 2020;**2020**, DOI: 10.1093/database/baaa062.

Shearer CA, Descals E, Kohlmeyer B *et al.* Fungal biodiversity in aquatic habitats. *Biodivers Conserv* 2007;**16**:49–67.

Sinsabaugh RL, Findlay S. Microbial production, enzyme activity, and carbon turnover in surface sediments of the Hudson River estuary. *Microbial Ecology: An International Journal* 1995;**30**:127–41.

Sinsabaugh RL, Linkins AE, Benfield EF *et al.* Cellulose Digestion and Assimilation by Three Leaf-shredding Aquatic Insects CELLULOSE DIGESTION AND ASSIMILATION BY THREE LEAF-SHREDDING AQUATIC INSECTS1. *Source: Ecology* 1985;**66**:1464–71.

Smit E, Leeflang P, Glandorf B *et al.* Analysis of fungal diversity in the wheat rhizosphere by sequencing of cloned PCR-amplified genes encoding 18S rRNA and temperature gradient gel electrophoresis. *Appl Environ Microbiol* 1999;**65**:2614–21.

Solé M, Fetzer I, Wennrich R *et al.* Aquatic hyphomycete communities as potential bioindicators for assessing anthropogenic stress. *Science of the Total Environment* 2008;**389**:557–65.

Sterner RW, Elser JJ. *Ecological Stoichiometry*. Princeton University Press, 2003a.

Sterner RW, Elser JJ. 3. The Stoichiometry of Autotroph Growth: Variation at the Base of Food Webs. *Ecological Stoichiometry*. Princeton University Press, 2003b, 80–134.

Sterner RW, Elser JJ. 2. Biological Chemistry: Building Cells from Elements. *Ecological Stoichiometry*. Princeton University Press, 2003c, 44–79.

Suberkropp K, Arsuffi TL, Anderson JP. Comparison of degradative ability, enzymatic activity, and palatability of aquatic hyphomycetes grown on leaf litter. *Appl Environ Microbiol* 1983;**46**, DOI: 10.1128/aem.46.1.237-244.1983.

Suberkropp K, Klug MJ. Fungi and Bacteria Associated with Leaves During Processing in a Woodland Stream. *Ecology* 1976;**57**, DOI: 10.2307/1936184.

Swift M, Heal O, Anderson J. *Decomposition in Terrestrial Ecosystems*. University of California Press, 1979.

Tessier JT, Raynal DJ. Use of nitrogen to phosphorus ratios in plant tissue as an indicator of nutrient limitation and nitrogen saturation. *Journal of Applied Ecology* 2003;**40**:523–34.

Thion C, Cébron A, Beguiristain T *et al.* Long-term in situ dynamics of the fungal communities in a multi-contaminated soil are mainly driven by plants. *FEMS Microbiol Ecol* 2012;**82**:169–81.

Tilman D. Resource competition and community structure. *Monogr Popul Biol* 1982;**17**, DOI: 10.2307/4549.

Tilman D. The Resource-Ratio Hypothesis of Plant Succession. *Am Nat* 1985;**125**:827–52.

Tlalka M, Bebber DP, Darrah PR *et al.* Quantifying dynamic resource allocation illuminates foraging strategy in Phanerochaete velutina. *Fungal Genetics and Biology* 2008;**45**, DOI: 10.1016/j.fgb.2008.03.015.

Tlili A, Jabiol J, Behra R *et al.* Chronic Exposure Effects of Silver Nanoparticles on Stream Microbial Decomposer Communities and Ecosystem Functions. *Environ Sci Technol* 2017;**51**:2447–55.

Tolkkinen M, Mykrä H, Annala M *et al.* Multi-Stressor impacts on fungal diversity and ecosystem functions in streams: natural vs. anthropogenic stress. *Ecology* 2015;**96**:672–83.

Vainio EJ, Hantula J. Direct analysis of wood-inhabiting fungi using denaturing gradient gel electrophoresis of amplified ribosomal DNA. *Mycol Res* 2000;**104**:927–36.

Vannote RL, Minshall GW, Cummins KW *et al.* The River Continuum Concept. *Canadian Journal of Fisheries and Aquatic Sciences* 1980;**37**:130_137.

Veresoglou SD, Wang D, Andrade-Linares DR *et al.* Fungal Decision to Exploit or Explore Depends on Growth Rate. *Microb Ecol* 2018;**75**, DOI: 10.1007/s00248-017-1053-4.

Violle C, Navas M-L, Vile D *et al.* Let the concept of trait be functional! *Oikos* 2007;**116**:882–92.

Wakelin SA, Chu G, Lardner R *et al.* A single application of Cu to field soil has long-term effects on bacterial community structure, diversity, and soil processes. *Pedobiologia (Jena)* 2010;**53**:149–58.

Wallace JB, Eggert SL, Meyer JL *et al.* Effects of resource limitation on a detrital-based ecosystem. *Ecol Monogr* 1999;**69**:409–42.

Wang Z, Cébron A, Baillard V *et al.* Nitrogen to phosphorus ratio shapes the bacterial communities involved in cellulose decomposition and copper contamination alters their stoichiometric demands. *FEMS Microbiol Ecol* 2022;**98**, DOI: 10.1093/femsec/fiac107.

Waring RH, Running SW. Forest ecosystems: Analysis at multiple scales. *Forest Ecosystems: Analysis at Multiple Scales* 2007:1–420.

Webster JR, Benfield EF. Vascular plant breakdown in freshwater ecosystems. *Annual review of ecology and systematics Vol 17* 1986;**17**:567–94.

Weigel C, Seitz H. Bacteriophage replication modules. *FEMS Microbiol Rev* 2006;**30**, DOI: 10.1111/j.1574-6976.2006.00015.x.

Whittaker RH. New concepts of kingdoms of organisms. *Science (1979)* 1969;**163**:150–60.

De Wildeman ÉAJ. Notes mycologiques . *Annales de la Société Belge de Microscopie* 1893;**17**.

De Wildeman ÉAJ. Notes mycologiques XVI-XX. *Annales de la Société Belge de Microscopie* 1895;**19**:191–232.

Woodward G, Gessner MO, Giller PS *et al.* Continental-scale effects of nutrient pollution on stream ecosystem functioning. *Science (1979)* 2012;**336**:1438–40.

Xia Y, Wang Y, Wang Y *et al.* Cellular adhesiveness and cellulolytic capacity in Anaerolineae revealed by omics-based genome interpretation. *Biotechnol Biofuels* 2016;**9**:1–13.

Yadav S, Dubey SK. Cellulose degradation potential of Paenibacillus lautus strain BHU3 and its whole genome sequence. *Bioresour Technol* 2018;**262**:124–31.

Zhang T, Luo Y, Chen HYH *et al.* Responses of litter decomposition and nutrient release to N addition: A meta-analysis of terrestrial ecosystems. *Applied Soil Ecology* 2018;**128**:35–42.

Zhao RL, Li GJ, Sánchez-Ramírez S *et al.* A six-gene phylogenetic overview of Basidiomycota and allied phyla with estimated divergence times of higher taxa and a phyloproteomics perspective. *Fungal Divers* 2017;**84**, DOI: 10.1007/s13225-017-0381-5.

Extended Abstract (Fr)

À l'échelle globale, les eaux douces ne représentent en volume que 2,8 % des eaux mondiales. Outre le fait que l'eau douce est une ressource précieuse pour l'Homme, lui fournissant de l'eau potable, les cours d'eau sont surtout les habitats d'une faune très diversifiée. Malheureusement, les activités humaines menacent cette ressource, notamment par la pollution de l'eau. Les polluants provenant de l'agriculture, de l'industrie et des zones urbaines, sont directement ou indirectement apportés aux cours d'eau et contiennent entre autres de grandes quantités d'azote, de phosphore et d'éléments métalliques, provoquant ainsi l'eutrophisation et l'intoxication des écosystèmes aquatiques. La réduction de la qualité de l'eau peut avoir un impact significatif sur les communautés d'organismes aquatiques : sur leur densité, leur diversité et la structure des réseaux trophiques, entraînant une dégradation du fonctionnement de l'écosystème d'eau douce. La production primaire et la décomposition des détritus (matière organique végétale) sont les deux processus à la base des réseaux trophiques qui régissent le fonctionnement de ces écosystèmes. Toute altération de ces processus essentiels peut donc entraîner des conséquences importantes pour les écosystèmes.

La décomposition de la matière organique végétale est un processus biologique qui permet le recyclage de la matière organique morte. La biomasse d'origine végétale est faiblement transférée vers les niveaux trophiques supérieurs (herbivore), ce qui fait qu'une grande quantité de biomasses végétales n'est pas consommée et se retrouve dans un réservoir de matière organique morte. La litière végétale est principalement composée de cellulose, d'hémicellulose, de lignine et d'une variété de composés phénoliques, de sucres simples, d'acides aminés et d'acides gras. Le processus de décomposition est complexe et son efficacité dépend de la nature (origine, composition) de la litière végétale, des conditions physico-chimiques du milieu, ainsi que de l'abondance et de la diversité des agents biologiques (décomposeurs). Les organismes

décomposeurs sont des microorganismes, champignons et les bactéries hétérotrophes qui produisent des exoenzymes spécifiques pour décomposer les divers composés organiques constituants les litières végétales. La décomposition de la litière végétale est ainsi l'une des voies principales de flux d'énergie-étape essentielle dans les cycles biogéochimiques des éléments, et c'est un processus fondamental du fonctionnement des écosystèmes. Dans les écosystèmes d'eau douce, la litière végétale peut représenter la principale source d'énergie et de nutriments à la base de leur fonctionnement, en particulier dans les cours d'eau forestiers de tête de bassin versant où plus de 90 % de l'énergie provient de la décomposition de la matière organique allochtone (végétation riparienne).

La stœchiométrie écologique étudie l'équilibre des éléments chimiques dans les interactions trophiques. L'étude des ratios de carbone, d'azote et de phosphore dans les organismes vivants aide à comprendre leurs besoins élémentaires et comment la qualité des aliments influence les processus écologiques. Alors que les consommateurs ont souvent une homéostasie plus restreinte que leurs ressources, des déséquilibres surviennent lorsque la composition élémentaire des ressources ne répond pas aux besoins des consommateurs. Par exemple, l'hypothèse du taux de croissance (The Growth Rate Hypothesis, GRH) suggère que le développement rapide d'un organisme est positivement corrélé à sa demande en phosphore. Cependant, des études publiées soutiennent ou contredisent cette hypothèse. En ce qui concerne les champignons et les bactéries qui sont les décomposeurs de la litière végétale, les connaissances concernant leur stœchiométrie et leurs besoins élémentaires restent limitées.

Ces travaux de thèse visent à étudier les ratios élémentaires optimaux des décomposeurs microbiens et leur influence sur le processus de décomposition. Bien qu'il soit connu, que les décomposeurs aient besoin d'immobiliser des nutriments inorganiques depuis leur milieu pour équilibrer leurs besoins stœchiométriques afin de pouvoir décomposer la litière végétale appauvrie en nutriments. Les ratios optimaux d'éléments spécifiques pour les espèces et les

communautés de décomposeurs restent largement inconnus. Des études récentes ont montré que les communautés des décomposeurs microbiens adaptent leurs besoins stœchiométriques à celle de leurs ressources. En effet, des changements dans la disponibilité des nutriments dans les ressources induiraient des modifications dans la structure des communautés de décomposeurs (variation d'abondance entre espèces ou remplacement des espèces par d'autres) dont la fonction de décomposition resterait assurée grâce à la redondance fonctionnelle. Par conséquent, comprendre les facteurs qui influencent les besoins des décomposeurs microbiens en nutriments, et comment ces facteurs peuvent être affectés par les changements environnementaux est crucial pour prédire l'intensité et la vitesse de la décomposition microbienne de la litière végétale.

L'anthropisation, l'ensemble des activités humaines, exerce une pression sur les écosystèmes et notamment les milieux aquatiques continentaux d'eau douce, essentiels pour bon nombre de services écosystémiques (épuration, production alimentaire, eau potable…). De multiples facteurs de stress environnementaux, tels que les changements dans l'utilisation des terres (usage), la transformation des cours d'eau (captages, artificialisation, canaux…), la sécheresse, les inondations, l'augmentation de la température et l'apport de contamination multiple par lessivage des sols ou rejets urbains et industriels, peuvent affecter les processus de décomposition de la litière et la diversité microbienne. Il a été montré que les agents de stress chimiques, tels que les métaux (par exemple cuivre et zinc), peuvent entraîner une diminution de la diversité microbienne et réduire les taux de décomposition de la litière. En revanche, bien que cruciale pour prédire les conséquences des changements globaux induits par l'homme sur le fonctionnement des écosystèmes, notre compréhension de l'impact des facteurs de stress sur les ratios optimaux microbiens reste très limitée.

Cette thèse explore le rôle des hyphomycètes aquatiques et des bactéries dans les écosystèmes d'eau douce en tant que décomposeurs de la litière végétale, en mettant l'accent sur le

développement d'une approche basée sur les traits stœchiométriques pour étudier notamment la réponse de ces microorganismes aux changements globaux. Les objectifs de recherche sont (1) de caractériser la plasticité élémentaire des décomposeurs, (2) de mettre en évidence les conséquences des besoins stœchiométriques des décomposeurs sur la dynamique (l'immobilisation et la minéralisation) des nutriments et (3) d'identifier les impacts de certains paramètres du changement global (pollution métallique, variation de température) sur la plasticité des décomposeurs et les conséquences écologiques. Quatre hypothèses sont proposées autour de ces objectifs

[H1] Chaque espèce de décomposeur a un ratio N:P optimal, ce qui permettrait de prédire la structure de la communauté de décomposeurs à un rapport N:P environnemental donné.

[H2] Au-dessus et en dessous de la valeur optimale du ratio N:P, la communauté microbienne en question sera limitée par un seul élément, les activités microbiennes (telles que la croissance de biomasse et la décomposition) seront ralenties et il y aura une accumulation de l'élément non limitant dans la biomasse microbienne et/ou dans le milieu.

[H3] Par une réduction de diversité microbienne, la présence d'un contaminant modifierait la plasticité élémentaire de la communauté, conduisant à des gammes plus étroites de co-limitations par N et par P des processus microbiens et à une immobilisation réduite des nutriments

[H4] Une hausse de la température augmenterait le taux de croissance microbienne, et par conséquent diminuerait le ratio N:P optimisant la décomposition.

Ce manuscrit commence par une introduction générale basant sur une recherche bibliographique des études réalisées. Il se poursuit avec une partie dédiée aux méthodologies et techniques appliquées aux différentes expérimentations, puis 4 chapitres explorant les différentes hypothèses décrites ci-dessus avec une complexité croissante des communautés de

décomposeurs étudiées. Dans le chapitre I, nous avons caractérisé les traits stœchiométriques et la plasticité de quatre souches d'hyphomycètes aquatiques, en nous concentrant sur les variations en fonction de l'âge du mycélium, des espèces et des impacts potentiels de cette plasticité sur leur croissance. Le chapitre II s'est concentré sur la dynamique entre l'immobilisation et la minéralisation des nutriments lors de la décomposition des feuilles d'aulne le long d'un gradient N:P, par un assemblage artificiel d'hyphomycètes aquatiques. Dans le chapitre III, nous avons augmenté la complexité des décomposeurs impliqués en ayant à la fois des communautés bactériennes et fongiques. Nous avons étudié leur capacité à décomposer la cellulose sous 2 gradients de nutriments différents. Enfin, dans le chapitre IV, nous avons examiné l'effet d'une contamination du cuivre et de la température le long d'un gradient N:P disponible sur la décomposition, en nous demandant si d'autres stresseurs environnementaux provoqueraient des effets similaires et comment l'adaptation et l'évolution des décomposeurs peut jouer un rôle à long terme.

Les résultats d'études expérimentales menées en conditions contrôlées dans cette thèse ont permis de confirmer la large plasticité élémentaire de la biomasse fongique, tant à l'échelle individuelle qu'à l'échelle de l'assemblage/communauté. Cette plasticité est apparue plus importante pour le phosphore (P) que pour l'azote (N), et l'immobilisation des nutriments s'est produite rapidement (observée pour le P inorganique après 18 h d'ajout de nutriments). En évaluant la décomposition de la litière de feuilles le long des gradients N:P, les communautés de décomposeurs comprenant les hyphomycètes aquatiques — mais pas les bactéries seules — ont pu maintenir des intensités élevées de décomposition même à des teneurs en P extrêmement faibles et lorsque N était suffisant, suggérant des capacités élevées des hyphomycètes aquatiques à remobiliser leur P interne. De plus, la quantification de l'abondance relative des espèces dans les assemblages des hyphomycètes aquatiques a suggéré que les traits stœchiométriques individuels participaient à la distribution des espèces le long du gradient N:P,

mais qui n'étaient pas suffisants pour expliquer entièrement les structures des assemblages. Contrairement aux assomptions générales et bien qu'elle soit liée au gradient N:P disponible, la minéralisation des nutriments (c'est-à-dire la libération nette de nutriments inorganiques de la litière) est restée limitée, mais le processus d'immobilisation des nutriments était dominant, du moins pendant la durée de nos expériences. Enfin, les contaminants et la variation de température ont pu modifier de manière significative les ratios N:P optimaux pour la décomposition par les décomposeurs. Ces résultats suggèrent des impacts importants — et potentiellement prédictible — de ces facteurs de stresses environnementaux sur l'intensité et la dynamique de la décomposition microbienne de la litière végétale. Les résultats de ces travaux confirment que la combinaison de traits stœchiométriques avec d'autres traits écologiques et biologiques permettrait certainement de comprendre plus en profondeur le processus de décomposition et sa réponse aux changements globaux.

Abstract

Decomposition of plant litter is one of the most important processes driving ecosystem functioning, it is the main energy and nutrient source in forested headwater streams. Any impairment of this process can have significant consequences for nutrient cycling. Decomposers, including aquatic hyphomycetes (AH) and heterotrophic bacteria, play a central role in decomposition, but their stoichiometric requirements and elemental plasticity remain understudied. While decomposers require inorganic nutrients to balance their stoichiometric requirements when breaking down nutrient-depleted plant litter, the specific optimal elemental ratios for species and communities of decomposers remain largely unknown.

Results of different experimental studies carried out in controlled conditions first allowed to confirm the wide elemental plasticity of fungal biomass, both at the individual and at the assemblage/community scales. This plasticity appeared greater for phosphorus (P) than for nitrogen (N), and nutrient immobilisation occurred very quickly (observed for inorganic P after an 18h of nutrients addition). When evaluating leaf litter decomposition along N:P gradients, decomposer communities containing AH – but not bacteria alone – were able to maintain the decomposition process at high levels even at extremely low P contents and when N was sufficient, suggesting high capacities of AH to remobilise their internal P. Also, quantification of species relative abundances in AH assemblages suggested that individual stoichiometric traits participated to species distribution along the N:P gradient but were not sufficient to entirely explain assemblage structures. Contrary to common assumptions, while related to available N:P gradient, nutrient mineralisation (i.e. net release of inorganic nutrients from plant litter) remained limited, and nutrient immobilisation was the dominant process, at least for the duration of our experiments. Finally, both contaminants and temperature variations were able to significantly change the optimal N:P ratios for litter decomposition by decomposer communities, suggesting large – and potentially predictable – impacts of these stressors on the intensity and the dynamic of microbial decomposition of plant litter in ecosystems. All the results from these studies confirm that combining stoichiometric traits with other ecological and biological traits would certainly allow our understanding in depth, the decomposition process, and its response to global changes.

Résumé

La décomposition de la litière végétale est un processus fondamental de l'écosystème et la principale source d'énergie et de nutriments dans les cours d'eau. Toute altération de ce processus peut entraîner des conséquences importantes sur le cycle des nutriments. Les décomposeurs, y compris les hyphomycètes aquatiques (HA) et les bactéries hétérotrophes, jouent un rôle central dans la décomposition, mais leurs exigences stœchiométriques et leur plasticité élémentaire restent peu étudiées. Alors que les décomposeurs ont besoin de nutriments inorganiques pour équilibrer leurs besoins élémentaires lors de la décomposition de la litière végétale appauvrie en nutriments, les ratios élémentaires optimaux spécifiques pour les espèces et les communautés de décomposeurs restent largement inconnus.

Les résultats d'études expérimentales menées en conditions contrôlées ont permis de confirmer la large plasticité élémentaire de la biomasse fongique, tant à l'échelle individuelle qu'à l'échelle de la communauté. Cette plasticité est apparue plus importante pour le phosphore (P) que pour l'azote (N), et l'immobilisation des nutriments s'est produite rapidement (observée pour le P inorganique après 18 h d'ajout de nutriments). En évaluant la décomposition de la litière de feuilles le long des gradients N:P, les communautés de décomposeurs comprenant les HA — mais pas les bactéries seules — ont pu maintenir des intensités élevées de décomposition même à des teneurs en P extrêmement faibles et lorsque N était suffisant, suggérant des capacités élevées des HA à remobiliser leur P interne. De plus, la quantification de l'abondance relative des espèces dans les assemblages de HA a suggéré que les traits stœchiométriques individuels participaient à la distribution des espèces le long du gradient N:P, mais qui n'étaient pas suffisants pour expliquer entièrement les structures des assemblages. Contrairement aux assomptions générales et bien qu'elle soit liée au gradient N:P disponible, la minéralisation des nutriments (c'est-à-dire la libération nette de nutriments inorganiques de la litière) est restée limitée, mais le processus d'immobilisation des nutriments était dominant, du moins pendant la durée de nos expériences. Enfin, les contaminants et la variation de température ont pu modifier de manière significative les ratios N:P optimaux pour la décomposition par les décomposeurs. Ces résultats suggèrent des impacts importants — et potentiellement prédictible — de ces stresseurs sur l'intensité et la dynamique de la décomposition microbienne de la litière végétale. Les résultats de ces travaux confirment que la combinaison de traits stœchiométriques avec d'autres traits écologiques et biologiques permettrait certainement de comprendre plus en profondeur le processus de décomposition et sa réponse aux changements globaux.

· 学 无 止 境 ·